6-2003

Hydrogeological and Geophysical Studies on AI Jaww Plain, AI Ain Area, U.A.E.

Hind Saif Ali AI-Nuaimi

United Arab Emirates University
Faculty of Graduate Studies

Hydrogeological and Geophysical Studies on Al Jaww Plain, Al Ain Area, U.A.E.

By
Hind Saif Ali Al-Nuaimi

A Thesis Submitted to

Faculty of Graduate Studies
United Arab Emirates University

In the Partial Fulfilment of the Requirenments for the of M. Sc. Degree in

Water Resources

Faculty of Graduate Studies
United Arab Emirates University
June 2003

United Arab Emirates University
Faculty Of Graduate Studies

Thesis Title

Hydrogeological and Geophysical Studies on Al Jaww Plain, Al Ain Area, U.A.E.

Author's Name

Hind Saif Ali Al-Nuaimi

Supervisors

No.	Name	Position
1	Dr. Ahmed El-Sayed El-Mamoudi	Associate Professor of Geophysics, Geology Department, Faculty of Science, United Arab Emirates University
2	Prof. Mohsen Sherif	Professor of Water Resources, Civil and Environmental Engineering Department, College of Engineering, United Arab Emirates University
3	Dr. Tareq Al-Zabet	Assistant Professor of Hydrogeology, Geology Department, Faculty of Science, United Arab Emirates University

Thesis of Hind Saif Ali Al-Nuaimi
Submitted in Partial Fulfillment for the Degree of
Master of Science in Water Resources

Chair of Examination Committee
Dr. Ahmed El Mahmoudi, Associate Professor
Geology Department

External Examiner
Prof. Ole Bernt Lile, Professor of Applied Geophysics
Petroleum Engineering and Applied Geophysics Department
Norwegian University of Science and Technology, Norway

Internal Examiner
Dr. Fares Howari, Assistant Professor
Geology Department

Dean of Graduate Studies
Dr. Hadef Rashed Al-Owais

United Arab Emirates University
2002/2003

DEDICATION

To

The Memory of My Father

My Mother

My Brothers .. My Sisters

ACKNOWLEDGMENT

Praise be to ALLAH (GOD), the Lord of the world, who has blessed me with countless blessings in my life. Most important are the true love, full understanding, and endless support of my family. He has blessed me with more than sufficient life, health and energy to carry out this study. My trust and believe in ALLAH have been, and will always remain, inspiriting my life.

I would like to express my deepest gratitude and indebtedness to my ***Mother, Brothers*** *and* ***Sisters*** *for their continuous moral support throughout my life. Their love and support have always been overwhelming.*

Sincere thanks are due to Dr. Ahmed El Mahmoudi, Associate Prof. of Geophysics, Faculty of Science, UAE University. He suggested the topic and provided much of his time to guide the work in its various phases. His discussions were constructive. His patience and guidance are very much appreciated.

I am indebted to Prof. Mohsen Sherif, Professor of Water Resources, College of Engineering, UAE University. His supervision, scientific discussions, and critical review of the manuscript were quite important.

Dr. Tarek Al Zabet, Assistant Professor of Hydrogeology, Faculty of Science, UAE University, reviewed some parts of the thesis.

Dr. Reyad Al-Mehedeb, Vice Dean of Faculty of Engineering and Coordinator of the Water Resources Graduate Program, UAE University, is acknowledged for providing the administrative support throughout the duration of the study.

Mr. Hamdi Kandil, Remote Sensing and GIS laboratory, is acknowledged for his help in drafting the figures. He assisted in the preparation of the final version of the thesis. Mr. Gaber Latif and Mr. Ayman El Say prepared some Figures. Thanks are due to. Dr. Hassan Garamon and Dr. Amir Gabr for their kind help in field activities. Dr. Othman Abdlghany provided the figure for the stratigraphic description of the study area. Thanks are also due to all the staff of the Geology Department, UAE University for their kind support and help during the progress of this work.

The data were provided by the National Drilling Company (NDC), Water and Electricity Department (WED) and Department of Civil Aviation (Abu Dhabi International Airport). Their support, through providing the data, is appreciated.

The members of the examination committee provided many constructive remarks which have added to the quality of the study.

Finally, special thanks are due to my sincere friends, Miss Moza Al Shamsei and Miss Muna Al-Hammadi whom have been a source of encouragement and inspiration. They have always been there for advice and support whenever and wherever needed. Their true love and sincere friendship have added another pleasure to my life.

ABSTRACT

In the last few decades, the United Arab Emirates has witnessed a remarkable development in the various aspects of life. Such fast development imposes a tremendous pressure on natural resources including water. Despite the severe shortage in the natural water resources, the per capita water consumption in the UAE is among the highest consumption rates of the world.

UAE depends on conventional and non-conventional water resources to meet its ever-increasing water demands. Groundwater is one of the most important conventional water resources in UAE, in general, and Al Ain area, in particular.

The focus area of the current study is **Al-Jaww Plain.** It lies in the eastern part of Al-Ain city and is bounded by Oman Mountains range in the east and Jabal Hafit in the west. It represents one of the main plains at Al-Ain and occupies an area of about 500 km^2.

The spatial extent and petrophysical characteristics of the Quaternary aquifer at Al Jaww Plain and the bedrock are the primary factors controlling storage and movement of groundwater. Information about the aquifer geometry in space, petrophysical parameters, hydrology and drainage basins network are vital to understand the flow regime, recharge mechanism and the boundary conditions of the hydrogeological system.

This study is devoted to the investigation of the water potentiality and quality at Al Jaww Plain. It defines the hydrogeological parameters of Al Jaww Plain using different techniques. To that end, detailed geophysical and hydrogeological investigations were conducted.

The results of this study provide quantitative and qualitative assessment for the groundwater resources in Al Jaww Plain. These results could be used by other researchers, concerned authorities and decision makers to outline future plans for groundwater development in this area.

Keywords: Al Jaww Plain, Al Ain groundwater, Assessment, Hydrochemistry, water quality, Geophysics, DC Resistivity, Time Domain Electromagnetic, Wireline well logging.

TABLE OF CONTENTS

LIST OF TABLES

LIST OF FIGURES

ABBREVIATIONS

mm	Millimeter
cm	Centimeter
m	Meter
km	Kilometer
asl	Above sea level
UTM	Universal Transverse Mercator
MCM	Million Cubic Meters
NDC	National Drilling Company
μmhos	micromohs per centimetres
°C	Degree Centigrade
ppm	part per million
BH	Borehole
TDS	Total Dissolved Solids
EC	Electrical Conductivity
ha	Hectare=10,000 Square Meters
Ω-m	Ohm meter
RSC	Residual Sodium Carbonate
WED	Water & Electricity Department
epm	equivelant per milliliter
DC	Direct Current
VES	Vertical Electrical Sounding
TDE	Time Domain Electromagnetic
S.P	Self Potential
R_w	Resistivity of formation water
R_{mf}	Resistivity of the mud filtrate
R_t	true resistivity
φ	porosity
F	tortuosity
Δt's	the travel times (in microsecond)
ρ	resistivity
GWP	Ground Water Project
TH	Total Hardness
SAR	Sodium Adsorption Ratio
pH	Hydrogen Ion Concentration

Chapter I

INTRODUCTION

CHAPTER ONE

INTRODUCTION

1.1 General Outline

In the last few decades, the United Arab Emirates has witnessed a remarkable development in the various aspects of life. The standard of living in the different emirates has been elevated. Agricultural, industrial and commercial activities were developed. Such fast development imposes a tremendous pressure on natural resources including water.

UAE depends on conventional and non-conventional water resources to meet the ever-increasing water demands. Groundwater is considered as one of the most important water resources in UAE. Under present climatic condition the groundwater is not recharged. Therefore, groundwater levels are declining and its quality is deteriorating due to the increase of the total dissolved salts, seawater intrusion in the coastal areas and saline water upconing in the inland areas where saline water horizons exist below fresh water horizons.

Al Ain area, in the east of the Emirate of Abu Dhabi, is characterized by its good supply of fresh water fom Oman Mountains to the east. Al Jaww Plain is regarded as one of the most important aquifers with fresh groundwater. This thesis aims to evaluate the various aspects of Al Jaww Plain to assess water potentiality, quality and define its hydrogeological parameters using different techniques.

In this chapter a review of the water resources in UAE, in general and in Al Ain area, in particular, is presented.

1.2 Physical Setting and Climatic Conditions

The United Arab Emirates lies in the southeastern part of the Arabian Peninsula between Latitudes 22° 40' and 26° 00' N and Longitudes 51° 00' and 56° 00'E. It is bounded from the north by the Arabian Gulf, on the east by the Sultanate of Oman and the Gulf of Oman and on the south and the west by the Kingdom of Saudi Arabia (Fig. 1.1). The total area of the United Arab Emirates is about 77,700 km^2.

The UAE is characterized by a dry and long hot summer and a short mild winter. It is exposed to the oceanic effects of the Arabian Gulf and the Indian Ocean. Humidity is always relevant to the coastal zone and it decreases inland as the sea losses its influence. The rainfall is usually higher in the northeastern parts and lower in the southwest.

Fig. (1.1) Arabian peninsula and location of the United Arab Emirates.

High evaporation rates occur when high temperature, low humidity and long hours of sunshine combined together. The wind speed is low most of the year, yet sometimes winds may be strong due to the passage of weather systems. Mist and fogs occur in winter while dust storms commonly occur during summer (Ministry of Communications, 1996).

The UAE lies across the tropic of cancer. It receives the highest solar radiation in June and the lowest in December. The maximum solar radiation is on June 21 where the sun appears directly overhead giving an angle of incidence of the sun rays of 90°. In December 21 the incidence of the sun rays falls to 43° 06', therefore the lowest insulation level is received (Garamoon, 1996).

The sky is cloudy most of the year, however, an extensive cloud cover is encountered in February and March while the least cloud cover is found in June and November. The average annual hours of sunshine in UAE is 10 hours per day; in May sunshine hours increase to 11.5 hours while in December they decrease to reach 8.4 hours (Al-Shamsei, 1993).

The mean annual temperature in UAE is constant through out the country but there are some variations especially through the eastern mountains where the mean temperature is 25° C. The hottest month is July and the coldest month is January. The average temperature from May to September is 40° C. The monthly average temperature is 25° C between November and March (Garamoon, 1996 and Rizk, 1999).

The relative humidity in UAE reaches its maximum value during the November-March period and its minimum value in May. In general the relative humidity is higher in the coastal area than in the interior area. The humidity decreases from 60% in Abu Dhabi to 45% in Al Ain and to 25% in Liwa (Garamoon, 1996).

The UAE faces two types of wind speed, the winter depression which descend the Arabian Gulf from the north and northwest and the summer monsoonal low which is developed over Rub Al Khali (Rizk, 1999).

According to (Al-Shamsei, 1993) the wind speed over the country can be considered light to moderate. The annual mean wind speed is less than 18.5 kilometres per hour (kph) and it decreases from north-northwest to south-southeast.

Along the eastern coast, the wind speed is stronger than the interior. The coastal areas are subject to local sea breeze and have a different wind regime. In general the highest wind speed is observed at Gabal Danna in March and the lowest is occurred at Kalba in September (Rizk, 1999).

The evaporation rate is relatively high all over the UAE. The western coast has the lowest annual average pan evaporation (between 7.5-8 mm/day). The eastern coast has higher evaporation rate, (between 9-9.5 mm/day) due to the high wind speed. In the eastern mountain, western gravel plain and desert foreland the evaporation ranges between 10-11 mm/day. Evaporation rate in the western and the southwestern desert regions is the highest and may reach 12mm/day.

The average evapotranspiration (ET) value in UAE changes from one location to the other. In northern parts of UAE the annual average (ET) reaches 1909 mm. The monthly minimum value is 80 mm in January and the maximum monthly value is 262 mm in July. The monthly average value is 164 mm.

In central UAE, the annual average (ET) reaches 2124 mm. The monthly minimum (ET) is 83 mm in January and the monthly maximum is 285mm in July. The monthly average (ET) is 177 mm. In general, annual (ET) in UAE ranges between 1909 mm and 2124 mm. The minimum value can be observed along the eastern coast while the maximum value can be observed in interior parts. ET is generally higher during summer.

1.3 Water Resources in UAE

Because of the serious deficit of water resources, the United Arab Emirates relies on non-conventional water resources, including desalinated water and treated wastewater. Conventional water resources include seasonal floods, springs falajes and groundwater. However, the conventional water resources do not support the freshwater demands in the country. A large part of the fresh water demand is met by desalinated water. Table (1.1) summarizes the conventional and non-conventional water resources in UAE (Rizk, 1999).

Table (1.1). Summary of conventional and non-conventional water resources in UAE (after Rizk, 1999).

a) Conventional Resources (million cubic meters per year)

Resource	Existing	Potential	In use	Source
Seasonal Floods	125	125	125	Al Asam,1996
Perennial Springs	3	6	3	Rizk and El Etr,1997
Seasonal Springs	22	40	---	*MAF, 1998
Falajes	20	40	20	Rizk, 1998
Aquifer Recharge	120	120	120	Khalifa,1995
Groundwater	---	---	880	*MAF, 1998

b) Non-Conventional Resources (million cubic meters per year)

Resource	Existing	Potential	In use	Source
Desalinated water	---	—	694	[+]MEW, 1998
Reclaimed water	150	—	150	Hamouda,1995

*MAF=Ministry of Agriculture and Fisheries

[+]MEW= Ministry of Electricity and Water

1.3.1 Conventional water resources

The conventional water resources in UAE include seasonal floods, springs, falajes, and groundwater. There are no perennial surface water resources in UAE such as rivers or lakes. However, a few numbers of springs and several falajes provide a limited renewable supply of water. In general, rainfall increases toward the north and east and decreases in the south and west. Estimates of the total annual volume of rainfall ranges from 700 to 1480 million m^3. About 10% of this amount recharges the groundwater every year (70 to 148 m^3) with an average of 120 million m^3 (Khalifa, 1995). Convential water resources are discussed hereafter.

Seasonal floods

Flash floods are always encountered in desert areas. Flash floods occur in the eastern region in association with strong, short lasting, rain storms. Large amounts of rainwater move on land surface as surface water runoff because of the low porosity and permeability of the prevailing igneous and metamorphic rocks. This flow starts usually near the water divide and moves toward the Gulf of Oman in the east or desert in the west. On the other hand, the western region is dry and lacks surface runoff due to low rainfall (40 mm/year), high natural evaporation (3360 mm/year), scarce vegetation cover, and high porosity and permeability of dune- forming sands dominating this area.

Topographic maps, aerial photographs, and satellite images show that the mountain range of the eastern region has 70 drainage basins, 58 of them are within UAE. The catchment areas of these basins vary between 5 km^2 (Wadi Dhednah, Al Fujeirah) and 500 km^2 (Wadi Al Bih, Ras Al Khaimah), (Fig. 1.2). Some large wadis may witness more than one runoff event every year, others may have surface runoff once every several years and the rest of the wadis may remain dry for longer periods.

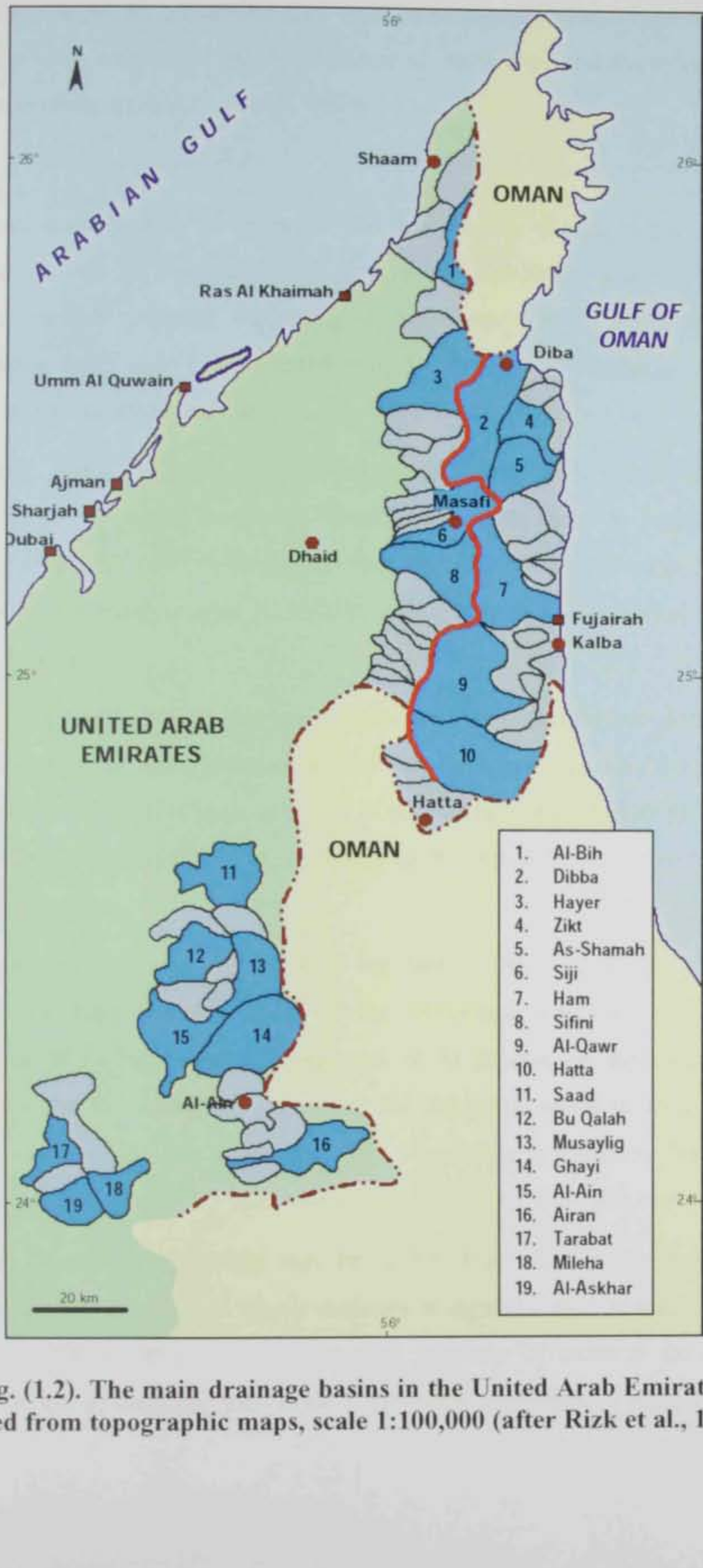

Fig. (1.2). The main drainage basins in the United Arab Emirates, traced from topographic maps, scale 1:100,000 (after Rizk et al., 1997).

A large volume of water is now being harvested by 35 dams with a total storage capacity of 75 million m^3. In addition to their roles in protection against flood and recharging. These dams have been constructed by the Ministry of Agriculture and Fisheries and there are several others dams under construction (Rizk, 1999).

Springs

Springs are considered to be important historical sources of fresh water. In the area of dry and arid climate with no permanent river they provide reasonable amounts of water which can be used for various purposes. According to Mayboom (1966), spring is defined as a groundwater outcrop but Todd (1980) defined it as a "concentrated discharge of groundwater appearing at the surface as a flow current".

The springs water may contain dissolved minerals and gases and is usually found at temperatures close to the mean annual air temperatures, even close to boiling. Mineralized springs, usually associated with faulting and fracturing, have been developed as tourist or recreational sites as, for example, Ain Al Faydah and Ain Khatt in the United Arab Emirates (Alsharhan et al., 2001).

The UAE springs seem to discharge from local and intermediate groundwater flow-systems (Rizk and El-Etr, 1997). Mineralized and thermal springs have a therapeutic value. In UAE, several springs, (Fig. 1.3), such as Khatt (Ras Al Khaimah), Maddab (Al Fujairah) and Bu Sukhanah or Ain Al Faydah (Al Ain) belong to this category and have been utilized as recreational and tourist sites.

The Khatt springs are located about 13 km east of Diba and 15 km south of Ras Al Khaimah, within the hard limestone rocks of the Musandum Formation. Siji spring lies at about 50 km west of Al Fujairah and 75 km east of Al Sharjah, on the contact between the ophiolite sequence and the western gravel plains. Bu Sukhanah spring is about 4 km west of Jabal Hafit, and south of Al Ain town (Fig. 1.3). According to El-Shami (1990), the spring issues from Miocene gypsum and clay layer through thin Quaternary loose sediments.

The water discharged by springs may be derived from aquifers in virtually any part of the stratigraphic column; however in many instances it depends upon rainfall recharge and in the absence of rainfall a spring may dry up. The presence of recharge dams may have a stabilizing effect on springs discharge; such as for of Siji spring, (Alsharhan et al., 2001).

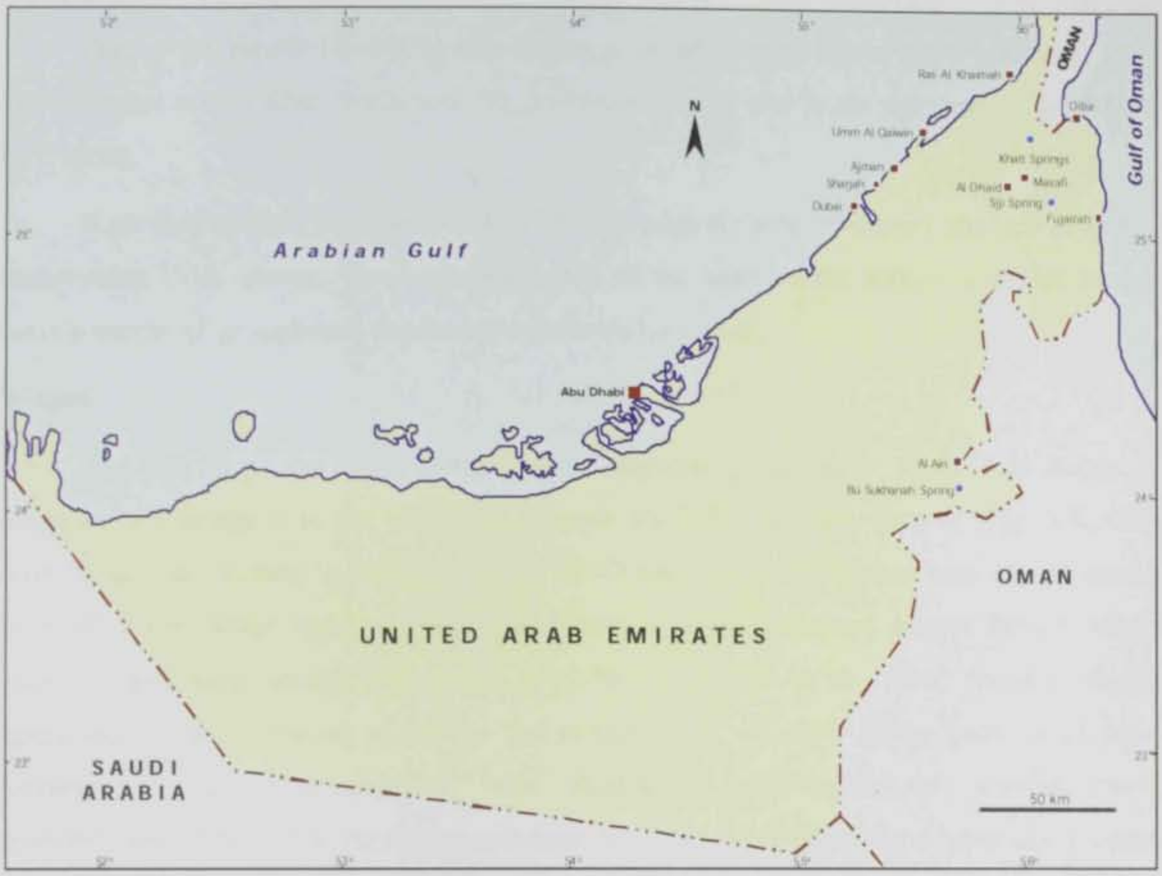

Fig. (1.3) Location map of the main towns and springs in UAE.

Rizk and El Etr (1997) studied the relationship between rainfall events and discharge of permanent springs based on the records at Khatt, Al Fujairah, Siji and Bu Sukhanah meteorological stations in the period from 1984 to 1991. They reported that Bu Sukhanah spring has the highest discharge ($2.50x10^6$ m^3/yr) whereas Siji spring has the lowest discharge ($0.06x10^6$ m^3/yr).

During the period 1984-1991 the discharge of all springs shows wide variations, with a net increase in the Khatt south and Bu Sukhanah springs and a net decrease in the Khatt North spring.

High temperature water (about 40 C°) represents the most important physical property characterizing UAE springs. This high temperature of the water of the springs is related to the deep circulation of groundwater or presence of radioactive source.

Falajes

The falaj is a man made stream which intercepts groundwater at the foot slopes of mountains and brings it to the surface at a lower level for irrigation purpose (Fig. 1.4). The word "Falaj", or A falaj in Arabic, means the division of an ownership into shares among those who have water rights. A falaj also means a distinct irrigation system through which water is distributed among individuals who have a right to it. Until recently, falajes represented the main arteries of life in the eastern UAE. At their outlets palm oases have flourished, permanent communities were established, and agricultural activities were developed upon their water. At the present time, many of UAE falajes have gone dry because of the low rainfall and excessive groundwater pumping; however, several falajes are still flowing and feeding the same, but larger, palm oases. Despite their limited amount, falaj waters are renewable resources which originate from rainfall. The UAE falajes lie in the eastern region, between Longitudes 55° 00' and 56° 30' E and Latitudes 24° 00' and 26° 00' N, (Fig. 1.5), covering an area of about 40,000 km^2 (Rizk, 1998).

The Ministry of Agriculture and Fisheries monitors and manages over 40 active falajes (Fig. 1.5). These falajes are confined to the Northern Oman Mountains in the United Arab Emirates and the gravels plains flanking these mountains from the east and west. The falaj lengths range from 0.5 km (e.g., Falaj Khatt at Ras Al Khaimah) to about 15 km (e.g., Falaj Al Daudi at Al Ain) (Alsharhan et al., 2001).

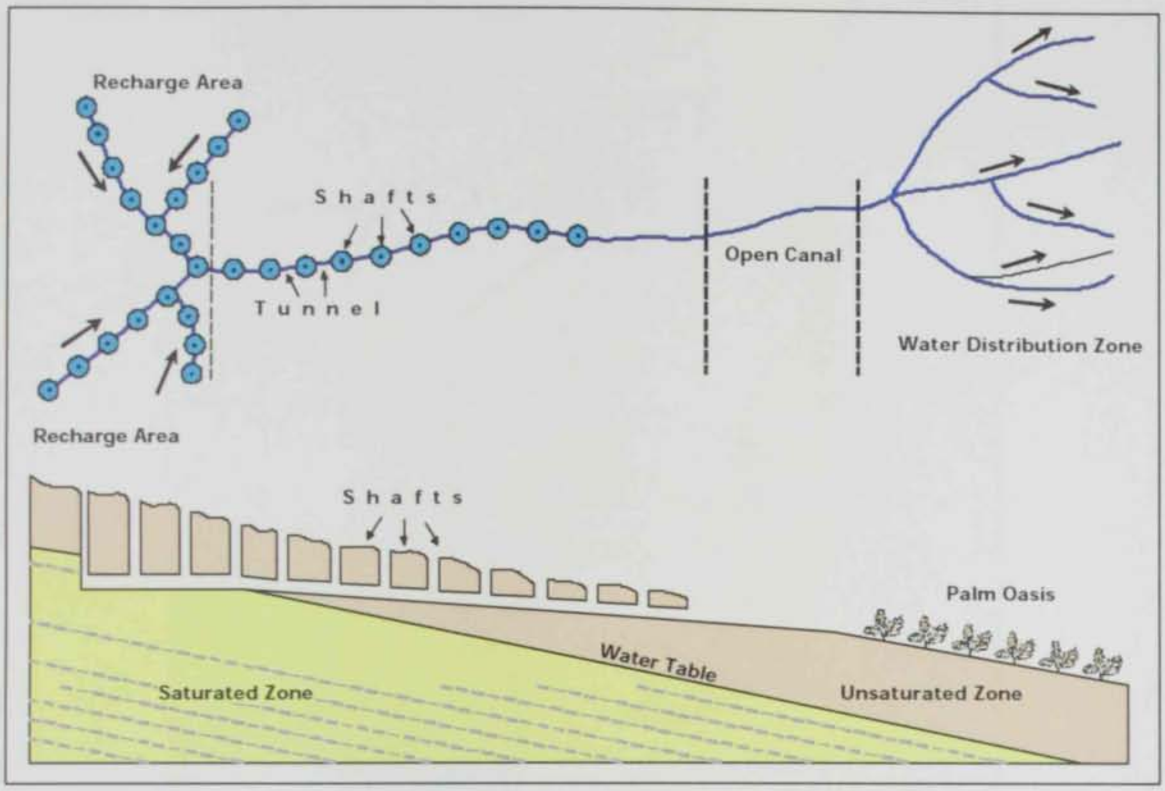

Fig. (1.4) Map view and a vertical cross section of a falaj (Modified from UAE National Atlas, 1993).

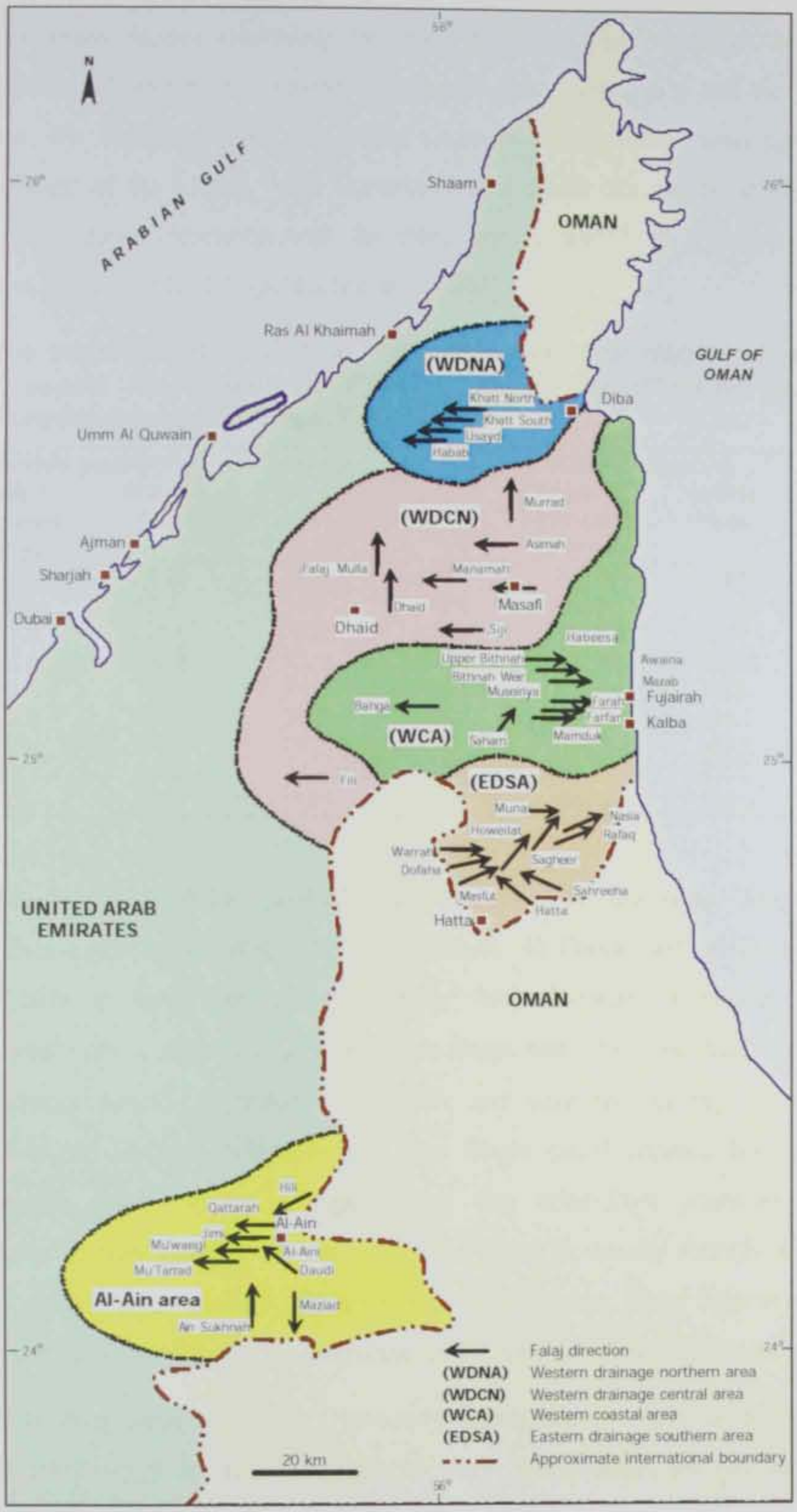

Fig. (1.5) Location map of the falajes in the United Arab Emirates. The lengths of arrows represent falaj lengths (modified after Rizk, 1998).

There are many factors controlling the falaj discharge which include the location of the main well, nature of aquifer, the amount of seepage from tunnel side and the main annual rainfall. However, the discharge from the falajes depends mainly upon mean annual rainfall. The annual discharge of the United Arab Emirates falajes which are predominantly of the Al Gheli type, shows a direct correlation with the mean annual rainfall on the Eastern Mountain Ranges and gravel plains, Table (1.2) (Alsharhan et al., 2001).

Table (1.2). The mean annual rainfall on the eastern mountain range and gravel plain, and the total annual falaj discharges (Mm^3/yr) during the 1978-1995 period in the United Arab Emirates (after Al Sharhan et al., 2001).

Year	Rainfall (mm/yr)		Discharge (10^6 m^3)	Year	Rainfall (mm/yr)		Discharge (10^6 m^3)
	Eastern Mountains Range	Gravel Plain			Eastern Mountains Range	Gravel Plain	
1978	94.3	73.3	18.8	1987	191.9	153.0	28.7
1979	75.6	60.4	18.2	1988	262.3	188.0	29.2
1980	160.6	137.5	17.9	1989	70.3	79.4	23.2
1981	110.8	100.2	21.1	1990	230.8	184.2	22.4
1982	339.7	283	31.2	1991	81.4	80.6	16.9
1983	353.9	225.9	26.2	1992	198.3	105.7	13.5
1984	46.1	27.2	26.3	1993	189.9	184.1	15.0
1985	32	30.5	18.4	1994	40.9	33.7	9.0
1986	75.9	61.3	14	1995	284.4	185.0	16.5

Alsharhan et al., (2001) reported that according to discharge, falajes could be classified into three types locally designated as Al Gheli, Al Daudi, and Al Hadouri types. Al Daudi falajes have a large groundwater supply and maintain a permanent discharge throughout the year with a little change in their discharge rate. Al Gheli falajes carry seasonal water with discharge directly dependent on rainfall, and may become dry when the rainfall ceases. In contrast Al Hadouri falajes or Al Aini falajes could produce hot water as their discharge is directly related to the springs. Where they arise from limestone they provide good quality water. If they emerge from ophiolites the water is usually strongly alkaline and is connected with deep artesian aquifers, draining water which rises along fissures and fractures. The Al Hadouri (Maddah in Fujairah), Bu Sukhanah (in Al Ain) belong to this category.

Due to the over pumping of the Quaternary during the last three decades the aquifer's hydraulic head has lowered at an average rate of 1m/yr. As a result, the Mu'Tarrad, Maziad, and Jimi falajes went dry in 1977, 1982 and 1983, respectively.

Al Aini and Al Daudi falajes in the Al Ain area are still active due to the continuous maintenance, extension, and pumping of groundwater into their channels (Rizk, 1998).

Groundwater

Aquifers provide the major supply of potable fresh water in the Gulf area. Because neither the amount nor the quantity of groundwater produced in the Gulf States satisfy the ever-increasing demands for water, desalination plants were established since 1970. Also during the rainy seasons, some rain and flood water are retained behind dams to recharge shallow aquifers (Alsharhan et al., 2001).

The aquifers of the UAE are discussed by Rizk et al., (1997), Ministry of Agriculture and Fisheries (1986a&b) and by Bakhit (1998). More details about the different types of aquifers are presented in chapter four.

1.3.2 Non conventional water resources

During the last three decades, a rapid development has occurred in the different sectors in the United Arab Emirates. The population has experienced a rapid improvement in the standard of living. These factors have disturbed the balance between the water demand and the available water resources. Non-conventional water resources such as desalination of seawater and treated wastewater were therefore introduced.

Desalination water

Desalination plants in the United Arab Emirates operate based on shared production of electricity and drinking water. Low-capacity plants apply the reverse osmosis technique. Advancement in water desalination techniques has reduced the production costs of water from 8 Dirham for 1 m^3 in 1980 to 4 Dirham in 1995. However, its usage in irrigation is still uneconomical. Due to the large investment required in water desalination project, the water price for the consumer has to be re-evaluated. The use of a solar energy as an alternative source of energy in water desalination should be considered in the Arabian Gulf (Alsharhan et al., 2001).

Two main types of desalination processes are available commercially: distillation processes and membrane processes. The most important distillation methods are multi-stage flash distillation and multi-effect distillation. Both of them involve the evaporation of saline feed water and its condensation back into fresh water, leaving dissolved substances in the waste brine.

Water desalination in UAE started since 1973 in Abu Dhabi at an annual production rate of 7.0 million m^3, reaching 33 million m^3 in 2001. Since 1974, over thirty desalination plants have been built in UAE. Most of the plants are located on the coast or on islands, although small number of units are located inland, such as Al Burayrat (Ras Al Khaimah) and As Surrah (Umm Al Quwein), where brackish groundwater is desalinated.

The number of desalination plants in UAE increased from one station at Abu Dhabi in 1976 to 65 stations in the 1995, with each Emirates having at least one desalination plant. The daily production of desalinated water in the Abu Dhabi Emirate, jumped from 12.5 thousand m^3 in 1969 to 90 thousand m^3 in 2001.

Treated wastewater

Water is scarce resource in United Arab Emirates. Therefore, every drop of water must be used in an economically feasible manner so that no higher quality water is used for a purpose that can tolerate a lower quality. As a substitute for freshwater in agriculture and industry, treated wastewater has an important role to play in water resources management in UAE.

The annual treated sewerage water in UAE is 80 Million m^3, and it is used in irrigation of public parks and development of green areas along the streets and in the roundabouts of major cities. The total discharge of sewage treated water reached about 175 Million m^3 in the year 2000. The sewerage water is treated primarily, secondary and tertiary. Tertiary treated wastewater could be used in the irrigation because poisons and heavy minerals would be removed. The sewage water could be used for industrial development, groundwater recharge. (Alsharhan et al., 2001).

There are four sewage treatment plants in the United Arab Emirates in Abu Dhabi, Dubai, Al Ain, and Al Sharjah. The first sewage treatment plant was constructed in Abu Dhabi during 1973 with a daily capacity of 4,000 m^3. The capacity of the plant reached 120,000 m^3/day in 1994. The Al Aweir plant in Dubai has a daily capacity of 110,000 m^3. These plants provide primary, secondary (biological treatment), and tertiary (advanced) treatments. The latter makes the quality of produced water suitable for reuse in irrigation.

Table (1.3) summarizes the treated-sewage water compared with the water quality criteria for irrigation. It could be seen that the produced water is suitable for irrigation, as it does not contain heavy metals. Chlorinating the treated sewage during the tertiary treatment kills germs and microorganisms that are health hazardous.

Table (1.3). Tertiary treated wastewater characteristics in UAE for reuse in irrigation (after Hamouda, 1994).

Parameter (mg/l)	Major treated plants (1993)			Water quality criteria for irrigation
	Abu Dhabi	Dubai	Al Ain	
Biological Oxygen Demand	1.2	2.2	2.7	10
Chemical Oxygen Demand	2.4	49.1	15	75
Suspended Solids	3	1.5	6.3	8
NH_3- N	1.1	1.3	1.4	1
NO_3- N	11	20	13.2	20
PH	6.8	6.7	7.9	6-8
Conductivity	2800	2140	1600	750-2000
Total Dissolved Solids	1950	1356	1042	1500
Chloride		524	320	40-200
Sulphate		104	135	100-380
Phosphate		12.6	10.9	23
Calcium		39		
Magnesium		36		
Sodium Adsorption Ratio		15		<10
Total Coliform (MPN/100 ml)	90			<100
Fecal Coliform (MPN/100 ml)		<2	<2	<2

The economic feasibility for the treatment of sewage water and its usage depends on many factors, such as the cost of treatment and the degree of required treatment in comparison to the cost of producing an alternative water source for the same usage. The cost of producing one m^3 of desalinated water is 4 UAE Dirham, whereas the cost of producing one m^3 of treated sewage water is 2 Dirham. However, important questions still remain about the degree of treatment of sewage water for irrigation, possible use of treated sewage water, and the possibility of chemical and biological pollution to the plants, soils and groundwater. In addition one should consider the possible health hazards associated with the use of sewage treated water in irrigation. In order to avoid the consequences, safe treatment process should be applied. Such a process should enable the development of clean water that have no pollutants. Periodical analysis and field studies should be conducted to spread the safety of the use of sewage water for irrigation and to educate the community on how to avoid any adverse effect and health risks associated with the application of treated wastewater.

1.4 Water Resources in Al Ain Area

Al Ain area is located in the east of the Emirate of Abu Dhabi, near the international border with the Sultanate of Oman (Fig. 1.3). It is the administrative centre of Abu Dhabi. It has a supply of surface and subsurface water drainage from the Oman Mountain to the east. It is regarded as one of the most ancient oasis of the Arabian Peninsula and is cultivated with palm trees which depend mainly on the shallow wells. Al Ain area is located within an arid belt and is characterized by low rainfall and high evaporation. Al Ain city lies on an alluvial plain, which forms the northwest extension of Al Jaww plain. There are some large wadis covering Al Ain area like Wadi Al Ain, Wadi Towayya and Wadi Al Jimi (Fig. 1.6).

Conventional water resources in Al Ain include surface water such as (springs, falajes, seasonal floods) and groundwater. A brief discussion on the water resources in Al Ain area is presented hereafter.

1.4.1 Surface water

Due to the distribution of the arid region and despite the absence of permanent surface stream, Al Ain area has better ephemeral surface water resources as compared to the rest of the country.

Rizk (1999) calculated the minimum annual rainfall that can produce surface runoff on the drainage basins of the Al Ain area which is of about 75 mm in the Oman Mountains and 90 mm in Jabal Hafit. The annual average runoff volume ranges from 0.25 million cubic meters (MCM) in southwest Al Ain to 3.00 MCM in the northeast. The average annual runoff for the 1981-1991 period ranges from 5 mm in southwest of Al Ain to 20 mm in the northeast. The percentage of rainfall as runoff varies between 3% in Jabal Hafit basins and 18% in the basins of the Oman Mountains. Based on the values of the infiltration rate and length of overland flow, Wadi Sidr of the Oman mountains and Wadi Ain Al Faydah of Jabal Hafit have the highest flood potential, while Wadi Muraykhat and Wadi Al Ain West have the lowest flood potential (Rizk, 1999).

1.4.2 Springs

The only spring which is available in Al Ain is Al Ain Al Faydah (Ain Bu Sukhanah) which is located 15 km south of Al Ain area and 2 km west of Jabal Hafit (Fig. 1.3). The spring represents a discharge area of a deep water source which found its way up through one of several thrust faults dissecting the area. In 1991, the discharge of the Bu Sukhanah was estimated to be 2.5 million m^3 of brackish water. The water temperature is about 39 °C and the spring outflow has a negative correlation with the local rain indicating that the spring receives its discharge from Oman Mountains further east (Rizk and El Etr, 1997). Ain Bu Sukhanah represents resort with a therapeutic capability because of its high temperature and high contents of sulphur. Moreover, its water can be used to grow the palms trees because palms are high tolerance crops.

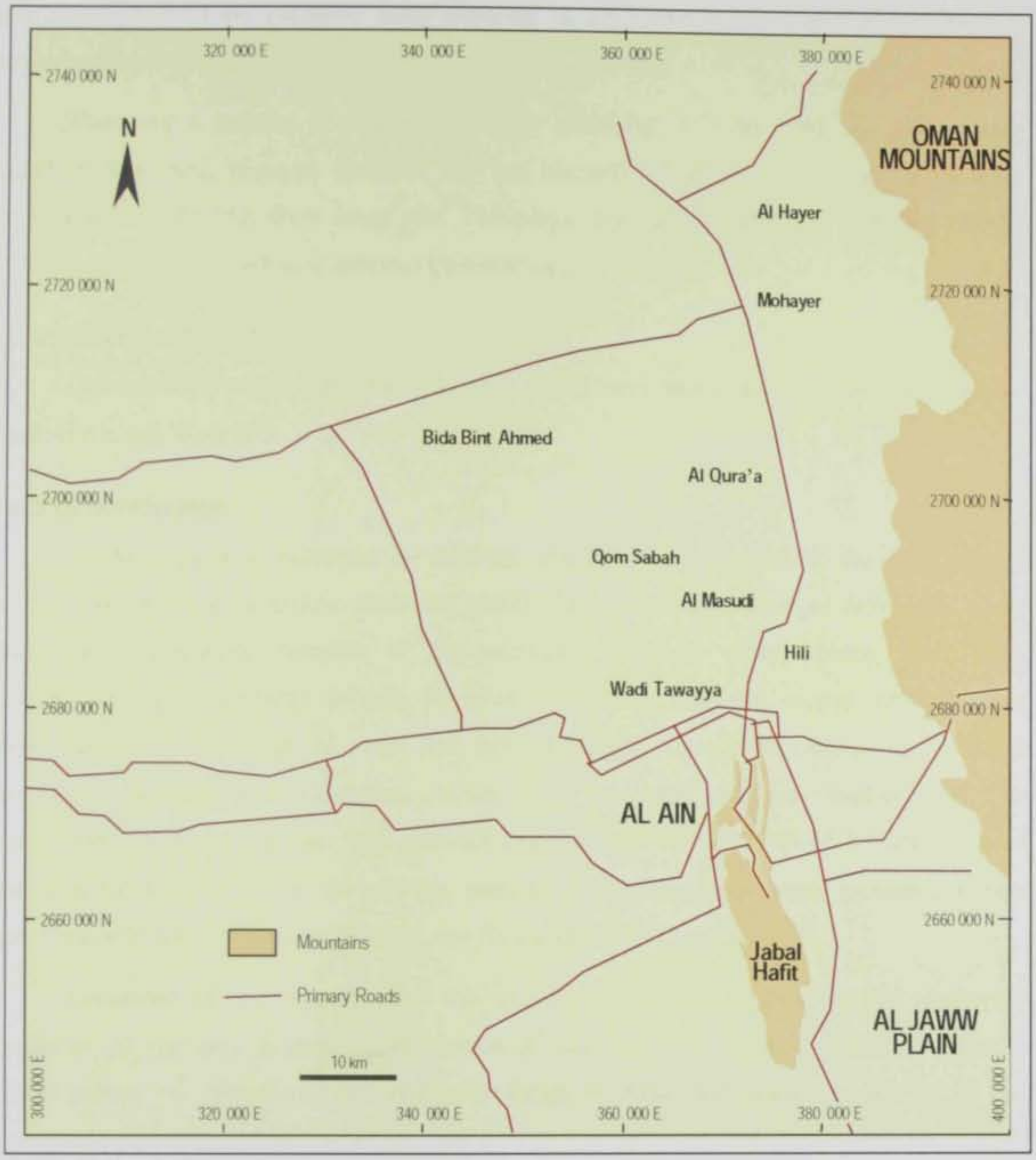

Fig. (1.6) Location map of Al Jaww Plain, Al Ain area, UAE.

1.4.3 Falajes

The falajes in Al Ain are open channels used to collect groundwater to the oasis and palm farms. Due to the excessive water pumping in the recent years, a decline in the water level was encountered.

There are a number of falajes in Al Ain area (Fig. 1.7). In 1984 five falajes were ceased to flow (Jimi, Mutarad, Qattarah, Hili and Maziad). All of these falajes except Maziad are located near the Hili draw down area. Nowadays, two falaj systems (Al Aini and Daudi) are active. Both of them are supplemented by water supply wells (Fig. 1.8).

1.4.4 Seasonal floods

Garamoon (1996) reported that the main wadis carry water at Al Ain area are Selimi, Wadi Al Ain and Wadi Shik.

1.4.5 Groundwater

Al Ain aquifer is recharged by different sources. It is recharged by the infiltration of the precipitation in the interdune areas and gravel plains. It is also recharged from Jabal Hafit where the precipitations percolate in the permeable limestone rocks forming Jabal Hafit. Another sources of recharge include irrigation return flow, upward vertical recharge from deeper rocks and infiltration of water lost from the leaky water transmission lines, although very small quantities (U.S Geological Survey,1993). The most important aquifers in Al Ain area is the Quaternary aquifer. The northern dune aquifer and Jabal Hafit aquifer are good reservoirs for fresh water. Al Jaww Plain receives fresh water through the groundwater flow from the northern Oman Mountains to the east (Garamoon,1996).

Garamoon (1996) reported that the total storage of fresh water in the Quaternary aquifer in Al Ain area is about 2,600 million m^3 and the total storage of brackish water is 18,000 million m^3. Therefore, the combined storage of fresh and brackish water in Al Ain area is estimated as 20,600 million m^3.

Gibb and Partners (1970) stated that the decline of groundwater level started since 1966. However, the decline was about 2 m in areas with heavy groundwater pumping for irrigation date palm. Since 1970, the abstraction of groundwater in Al Ain area has increased excessively, mainly through wells equipped with mechanical pumps. The Water and Electricity Department (WED) and the Agriculture and Fisheries Department (AFD) of the Municipality are the main consumers for water in Al Ain.

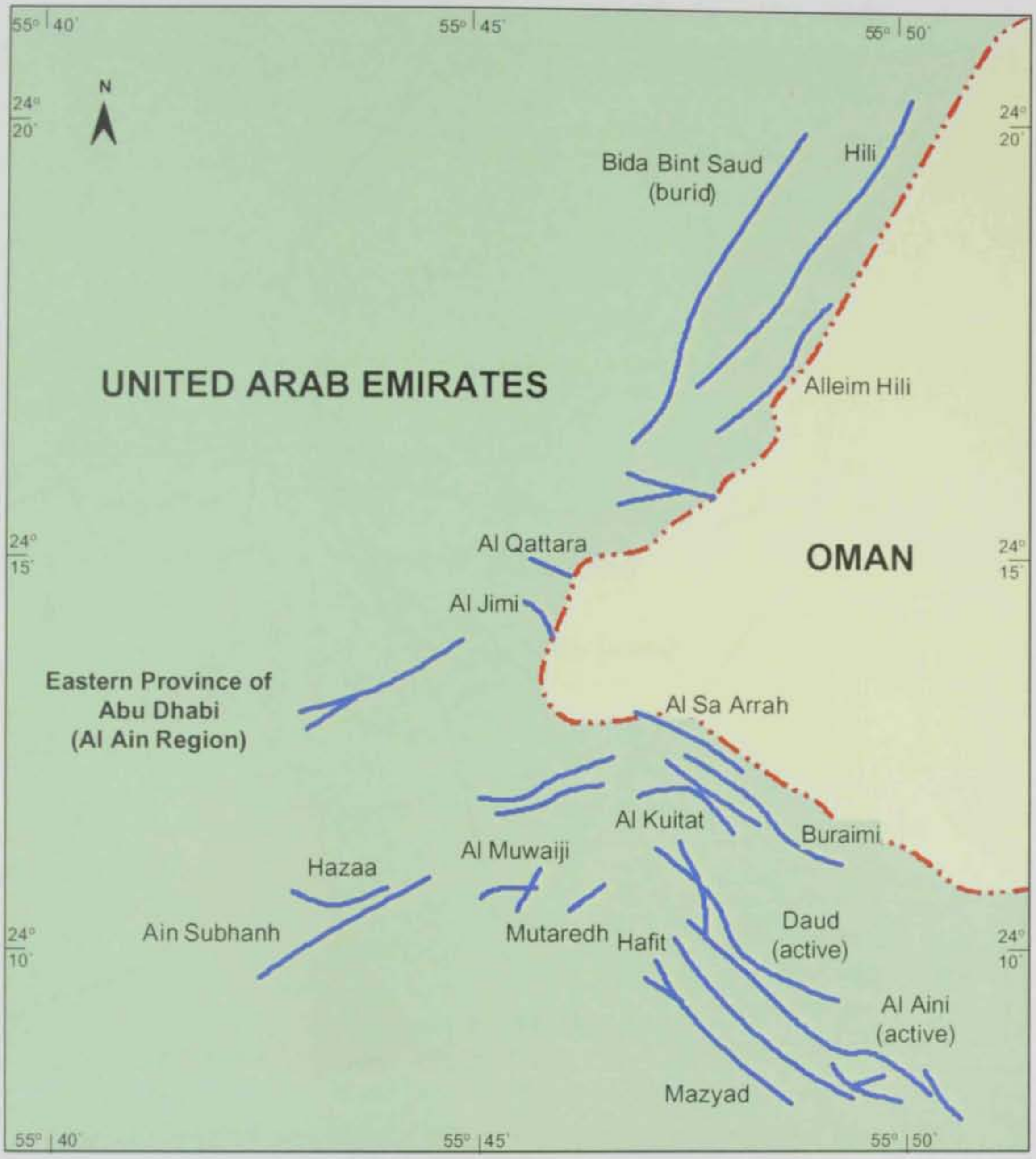

Fig. (1.7) Location map of the falajes in the Al Ain area, United Arab Emirates (after Rizk, 1998).

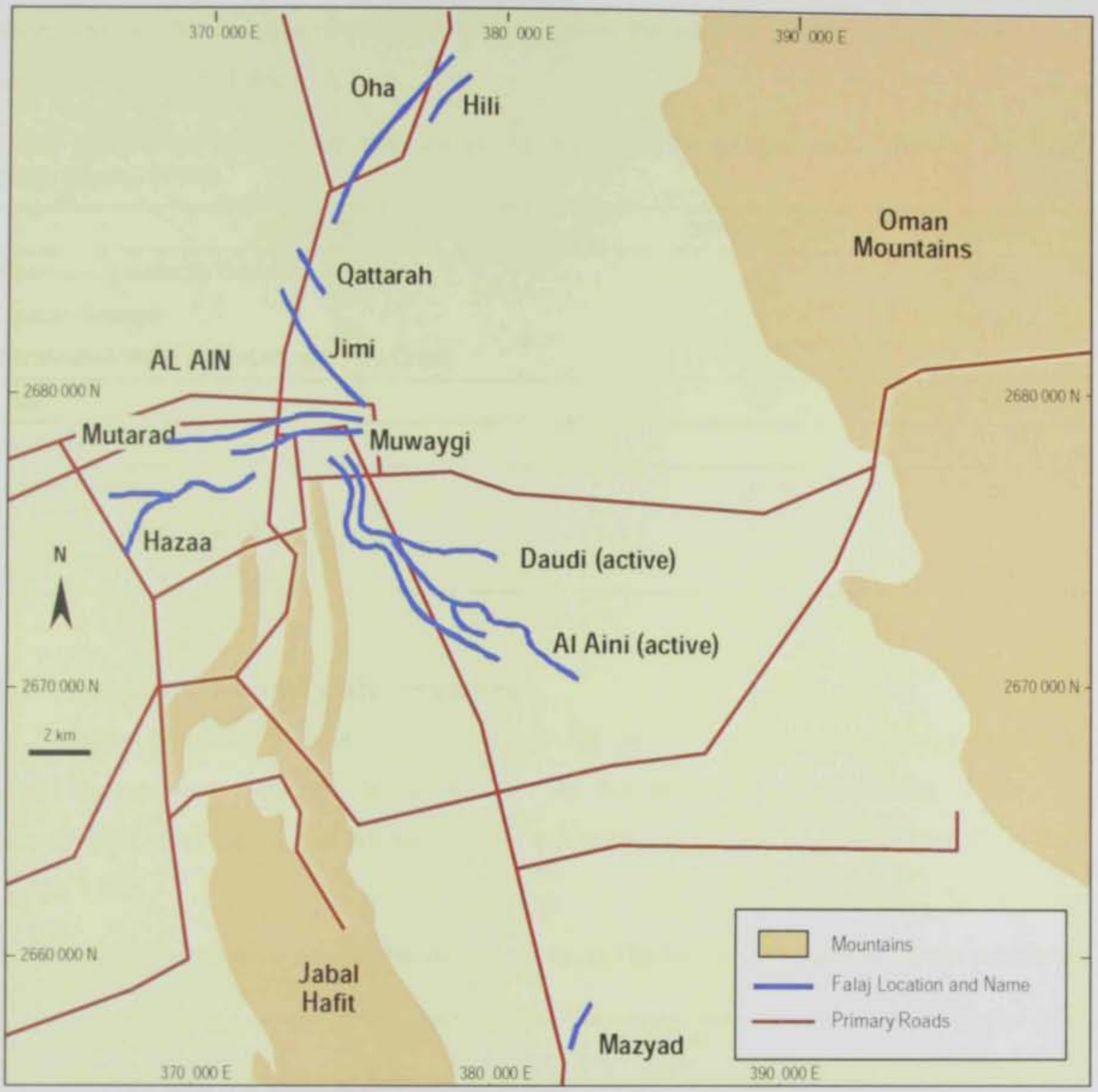

Fig. (1.8) Location and types of active falajes in Al Ain area (after Rizk, 1998).

The WED utilizes exclusively the fresh water only but the AFD uses both fresh and brackish waters.

Hyde (1992) reported an increase of 27% and 80% in fresh and brackish water usage, respectively in Al Ain area during 1985-1991 period. He summarized the water balance in Al Ain area as given in (Table 1.4).

Table (1.4). The 1989 water balance in Al Ain area, in million cubic meters per year (after Hyde, 1992).

SOURCE	Million m^3/yr	Percent
Water and Electricity Department Wells	33	52.4
Treated Sewage	7	11.1
Desalinated Water Imported from Abu Dhabi	23	36.5
Total	63	100
Uses		
Public Supply	31.5	50
Municipal Supply (Watering)	31.5	50
Total	63	100

1.4.6 Non conventional water resources

Non-conventional water resources in Al Ain area include desalinated water from Abu Dhabi Emirate and recycled wastewater from Al Ain treatment plant in Zaker. Table (1.5) lists the total water use in the Al Ain area, in the years 1990, 2000 and the predicted for 2010 (Hyde, 1992).

Table (1.5). Total water use in the Al Ain area, in the years 1990, 2000 and the predicted for 2010 (after Hyde, 1992).

Source	Years					
	1990		2000		2010	
	Million m^3/yr	percent	Million m^3/yr	percent	Million m^3/yr	percent
WED Wells	28	60	28	44.4	28	35
Treated Sewage	19	40	35	55.6	52	65
TOTAL	47	100	63	100	80	100
USE						
Public Supply	40	51.9	68	62.1	103	67.3
Municipal Watering	37	48.1	43	38.8	50	32.7
TOTAL	77	100	111	100	153	100
BALANCE	-30		-48		-37	

Al Ain receives about 16 million gallons of desalinated water per day. This water is used to meet the rapid increase in the fresh water demand. This amount of desalinated water is expect to be double after the construction of Al Taweilah desalination plant .

The treated wastewater which is produced from Al Ain treatment plant is used mainly for irrigating parks and gardens located in and around Al Ain area. About 7 million gallon per day is currently produced. The capacity of the plant is expected to reach 30 million gallons per day.

1.5 Aim of Study

The future development in Al Ain area depends mainly on the availability and sustainability of the groundwater resources. The Quaternary aquifer is the most promising and economic source for the groundwater supply in Al Ain Area. Al Jaww Plain lies in the eastern part of Al Ain city and receives a considerable share of Abu Dhabi's fresh water resources.

The present work aims at studying the main geomorphologic units and their effect on groundwater occurrence. The hydrogeological conditions prevailing in Al Ain area are investigated. The groundwater occurrences, movements and fluctuations, along with the different hydraulic parameters of the main aquifers are discussed. One of the main goals of this study is the hydrogeochemical assessment of the Quaternary aquifer. The groundwater resources, origin, recharges, discharges and potentiality are evaluated.

The groundwater is defined through the geological data identified from different wells and through geoelectric resistivity and electromagnetic investigations. Wire line logging analyses of some available data are used to define the petrophysical properties relevant to hydrogeology, hydrogeological, and hydrochemical setting. The implications of this study toward the sustainable use of groundwater resources in Al Ain area are addressed.

Chapter II

GEOLOGY OF AL AIN AREA

GEOLOGY OF AL AIN AREA

The study area, Al Jaww Plain, is located in Al Ain area. A brief discussion about the geology of Al Ain, in general, with emphasis on the geological elements that affect its hydrogeology is presented in the following sections. These geological elements comprise geomorphology, stratigraphy, geometry and distribution of geologic units along with the structural deformation affecting the hydrogeology of these units.

2.1 Location of Al Ain

Al Ain lies east of Abu Dhabi Emirate, near the border with the Sultanate of Oman and at the western margin of the northern Oman Mountains (Fig. 1.3). It is one of the largest and most ancient oases of the Arabian Peninsula due to the plentiful supply of fresh groundwater from the Oman Mountains to the east.

Although Al Ain is located within the arid desert belt of the world, it is characterized by relics of integrated drainage net that was formed as a result of the prevalence of humid climate during the Quaternary. The net drains externally towards the west (Al Ain region). Rapid development is taking place in the city both in agriculture and housing.

2.2 Geomorphology of Al Ain Area

The geomorphology of Al Ain area was studied by several investigators (e.g. Hunting, Geology and Geophysics, 1979; Abou El-Enin, 1993; Al-Shamsei, 1993; UAE National Atlas, 1993; Garamoon, 1996 and Baghdady, 1998). The geomorphic units in Al Ain area are classified as mountains, gravel plains, drainage basins, sand dunes, interdune areas and inland sabkhas (Figs. 2.1 and 2.2). These units are presented hereafter.

2.2.1 Mountains

The main mountains in Al Ain area are Jabal Hafit, Jabal Moundassah, Jabal Malaqet, Jabal Al-Oha and Jabal Rawdah. Jabal Hafit is one of the most prominent features of Al Ain area. It is located southeast of Al Ain at lat 24° 02' - 24° 13' N and long 55° 44' - 55° 49' E (Figs. 2.1 and 2.2). Hunting Geology and Geophysics (1979) and Abou El-Enin (1993) reported that Jabal Hafit is a Tertiary anticlinal structure plunging southeasterly in Oman and northwesterly in the United Arab Emirates. Jabal Hafit has approximately a length of 29 km

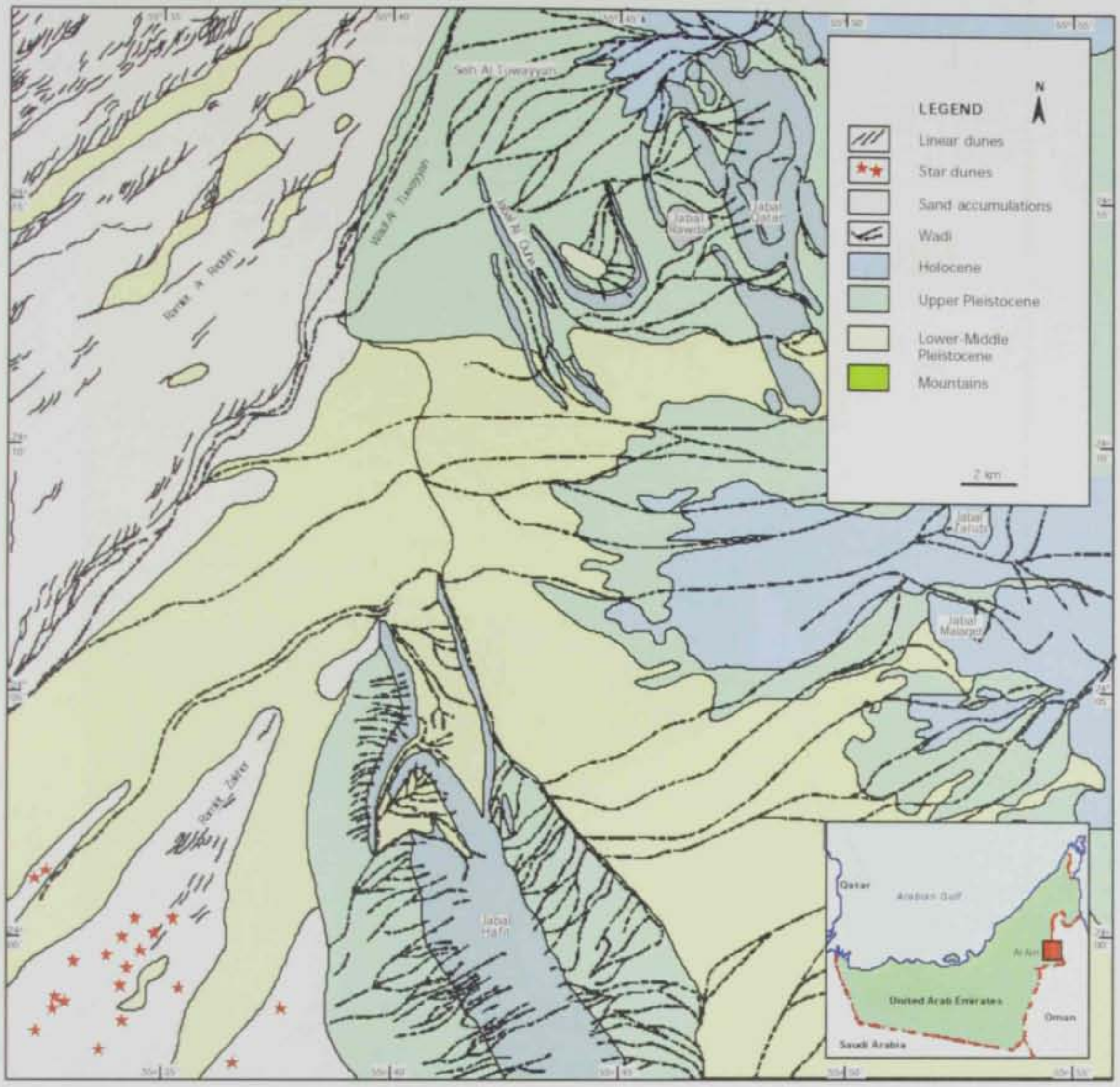

Fig. (2.1) Geomorphology of Al Ain region (after the National Atlas of United Arab Emirates, 1993).

Fig. (2.2) Physiographic subdivisions of eastern study area.

and width of 5 km. It reaches a maximum elevation of about 1160 m above the sea level. The rocks forming Jabal Hafit are almost composed of limestone and dolomite (Rus Formation).

The mountain has a whale-back form with beds dipping down to the east and west along the two fold limbs. North of the core, limestones and marls of the lower and middle intervals of the Dammam Formation (Middle to Upper Eocene) are eroded forming a low-lying area of small hills enclosed between ridges of the Asmari Formation (Lower to Middle Oligocene). The eastern limb of Jabal Hafit is characterized by slumps because of high dip values in addition to the presence of rather alternating with limestone.

The marls of the overlying Middle Eocene Dammam Formation are less resistant to erosion leading to the fmation of two wadies known as Wadi Tarabat to the east and Wadi Al Nahayan to the west. These marls form a low-lying area with small hills between the resistant Oligocene ridges. The resistant Oligocene limestone forms two Cuestas known as East Cuesta and West Cuesta. The beds of the east Cuesta dip at about 70° E and an elevation of 320 m above sea level whereas those of the west Cuesta are gently dipping at about 29° W and an elevation of 460 m above sea level.

Jabals Malaqet and Mundassah are parts of the northern Oman Mountains and located approximately 17 km east of Jabal Hafit (Fig. 2.1). They form asymmetrical anticlinal structures (Warrak, 1987). Each of the eastern limbs represents the main part of the exposures, while the western limbs are represented by disconnected strike ridges. The rocks forming these two Jabals are composed of serpentinized predotite (in the cores), conglomerates and carbonates of Late Cretaceous age, overlain by marls and carbonates of Paleocene to Early-Middle Eocene age (Hamdan and El-Deeb, 1990).

Jabal Al Oha lies about 8 km northeast of Al Ain City (Fig. 2.1). It consists of three NW-SE parallel hogback ridges of about 10 km length. The ridges represent fault repetition of the western limb of the horseshoe-shaped southerly-plunging anticline of Jabal Huwayah exposed immediately to the east of Jabal Al Oha, further east.

Jabal Al Oha succession attains a total thickness about 85 m, and is of Late early to Late Maastrichtian age. It is divided into a lower unit that consists of gray to green mudstone to shale of Qahlah Formation, and 3 m thick unit of red-colored chert pebble conglomerate and is overlain by white limestone of Simsima Formation.

Jabal Rawdha is a plunging anticlinal located at the western end of the Hatta shear zone. It consists of ridge of Hawasina limestones which are unconformably overlain by Upper

Cretaceous -Tertiary carbonate cover. This cover is folded into open symmetrical fold trending axes.

2.2.2 Gravel plains

Two gravel plains terminate the eastern part of Al Ain area; one fringes the Oman Mountains and the second fringes Jabal Hafit. The first fringe reaches its maximum development in the study area of Al Jaww Plain which is located between Jabal Hafit and the Oman Mountains (Hunting Geology and Geophysics, 1979).

The main features of the gravel plains are low-relief piedmonts that slope gently westward away from the western margin of the Oman Mountains. The term piedmont is applied as a general term for an alluvial plain associated with a variety of landforms, such as alluvial fans, wadies, and associated terraces, or for erosional bedrock surface (piedmont) thinly mantled by alluvium (U.S. Geological Survey, 1993).

Surface drainage on the piedmonts and alluvial fans subdivisions is generally channalized in wadis with variable flow patterns, through most systems exhibit complexly braided channel morphologies (Menges and Woodward in U.S. Geological Survey, 1993).

2.2.3 Drainage basins

There are two systems of drainage basins in Al Ain area; one is related to the northern Oman Mountains and the second belongs to Jabal Hafit (Fig. 1.2).

Drainage basins of the Oman Mountains

The drainage pattern of the Oman Mountains is generally dendritic; as it is typical of massive igneous rocks forming these mountains. However, some areas due to the faulting, have more rectangular patterns, with long stream segments trending at about N 60° to 70° W, parallel to the northwesterly fault trend common through the Ophiolite (Fig. 2.3a). In the west of Al Ain area there is some tendency for rectangular drainage in the faulted parts of the sedimentary sequence. In Al Jaww Plain, the dendritic pattern (Fig. 2.3b) usually changes to braided pattern where the slope decreases in Al Jaww Plain (Fig. 2.3c). The main reasons for the variation in the drainage pattern are either deformation, or decrease in slope (Al-Shamsei, 1993).

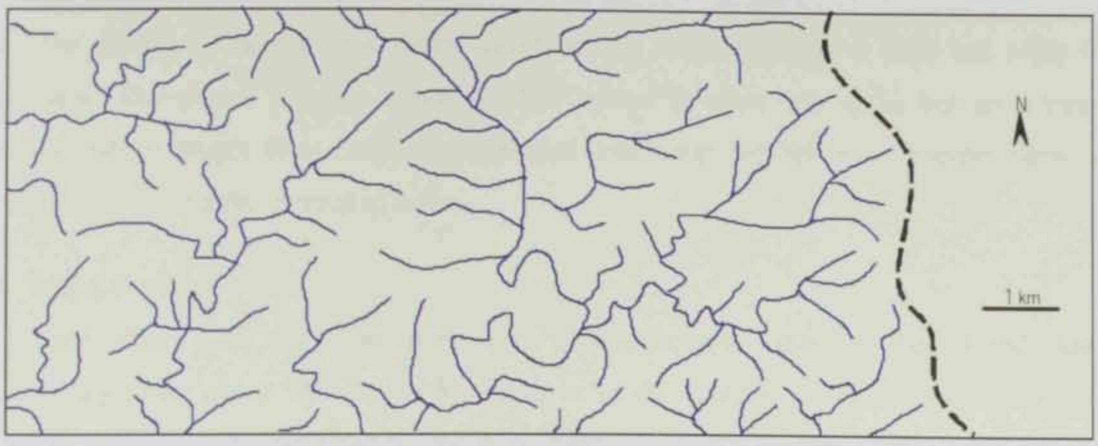

a) Rectangular dendritic pattern in the ophiolitic sequence

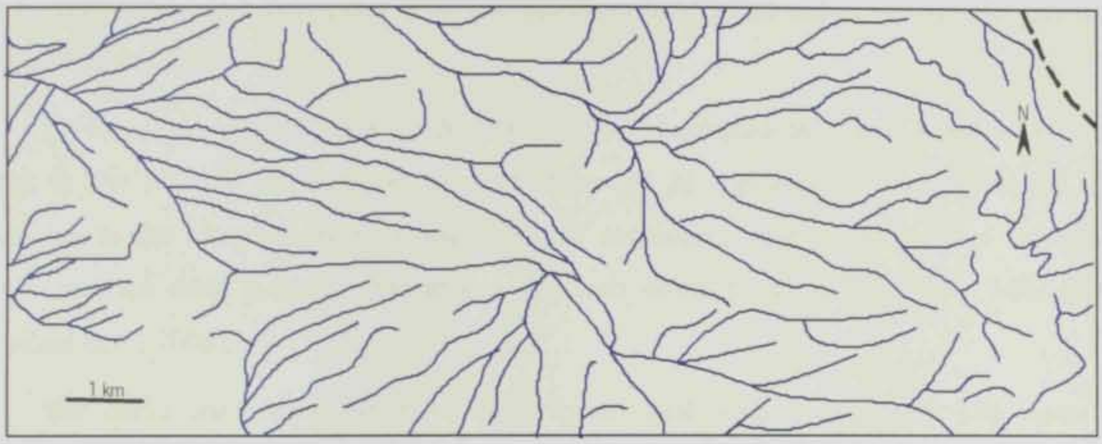

b) Dendritic drainage in the sedimentary rocks

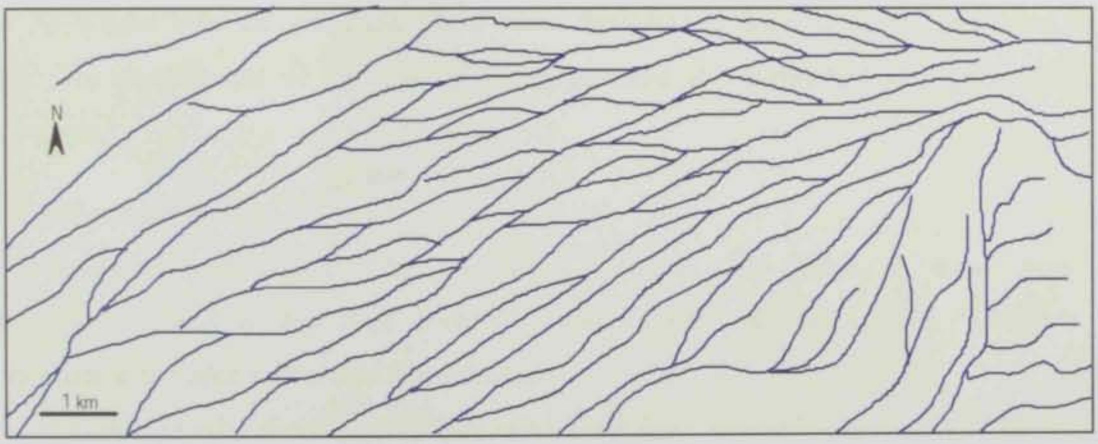

c) Braided drainage pattern in Al Jaww Plain

Fig. (2.3) Drainage pattern in Al Jaww Plain area (after Al -Shamsei 1993).

Drainage basins of Jabal Hafit

The drainage pattern of this system occurs in the west of Al Jaww Plain and south of Al Ain area. The overall drainage pattern of this system is rather sub radial but on a basin scale. The pattern ranges from dendritic to braided with some parallel or rectangular patterns especially in the structurally-controlled areas.

2.2.4. Sand dunes

Sand dunes are the most dominated geomorphologic units in the United Arab Emirates; they cover about 75% of the surface area of the country. The northern and western parts of Al Ain area are dominated by the dune fields (Fig. 2.1). Embabi (1991) attributed the regional and local variations in type and pattern of sand dunes to the variations in the wind regime, sand supply and local relief. The two dominant dune types within Al Ain area are the linear and the star dunes.

Northern and western parts of Al Ain area are dominated by linear dunes which are located in the NE-SW direction. In the east region of Al Ain area the dune is darker and denser due to the contributions from the ophiolitic succession, whereas at the west region of Al Ain area the dune is lighter due to the carbonate debris which derived from Jabal Hafit (Abu-Zeid et al., 2000).

Star dunes are radially symmetrical, pyramidal sand accumulations with slip faces on arms that radiate from the high central parts of the mound. In the southeastern part of Al Ain area star dunes, exist near Al Wagan associated with the E-W barchanoid and linear ridges. Near Al Wagan area the star dunes show more development because of the increasing sand supply. The development of this type of dunes increases in environment with multidirectional wind regime.

2.2.5 Interdune areas

Interdune areas occupy the low lands between sand dunes. In these areas the groundwater is shallow and high content of fine grained sediments exist. Therefore the groundwater in this area is favorable for agriculture.

2.3 Stratigraphy

Al Ain area is covered by a rock sequence ranges from Cretaceous to Quaternary (Figs. 2.4, 2.5 & 2.6). The following is a brief discussion of this sequence.

fig(2.4)

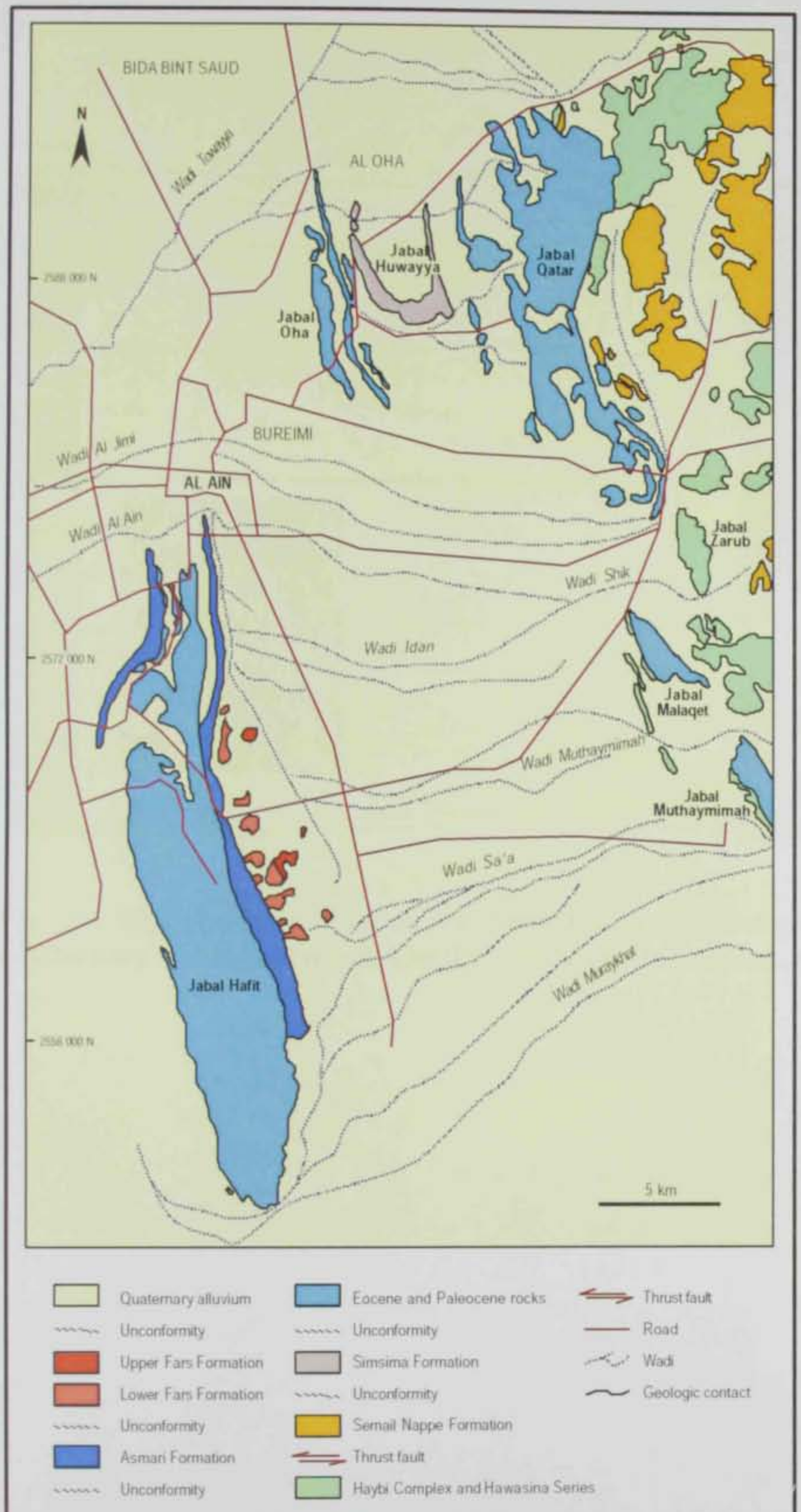

Fig. (2.4) Geology of Al Ain area (modified from Hunting Geology and Geophysics, Ltd., 1979; Warrak, 1987).

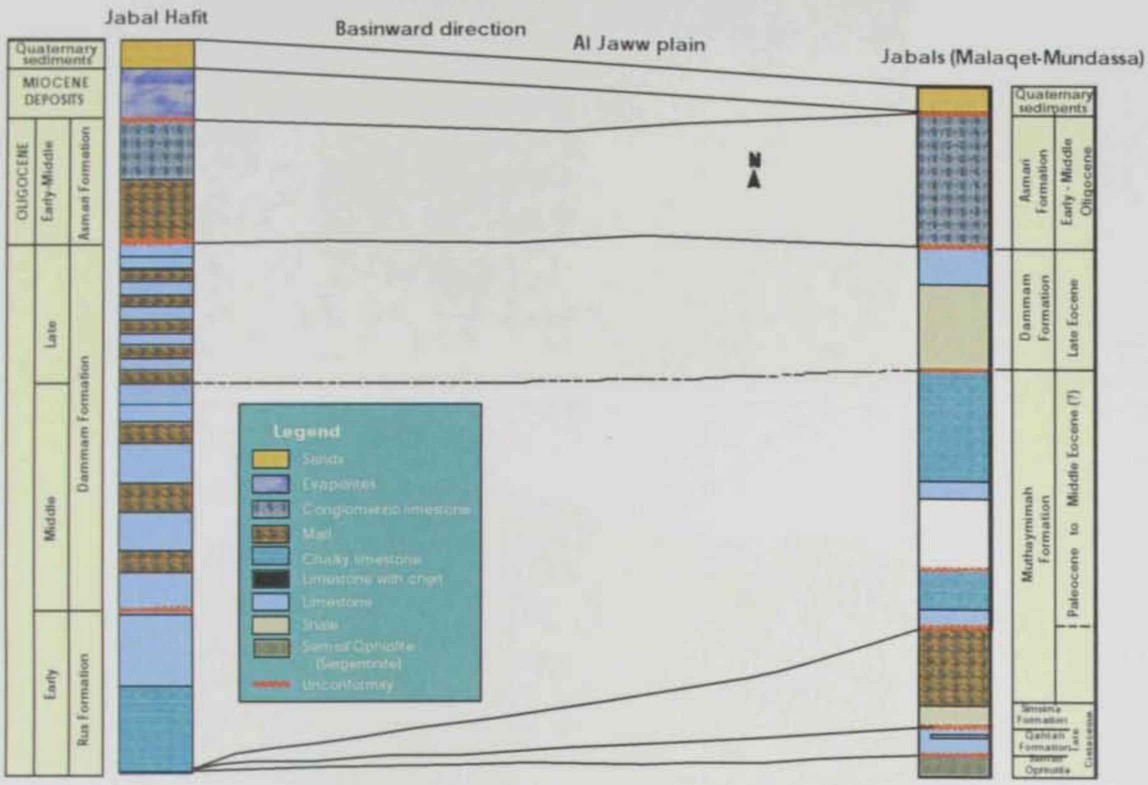

Fig. (2.5) Stratigraphic description and correlation of the identified Cretaceous/Tertiary rock units surrounding the study area (Abdelghany, in prep.).

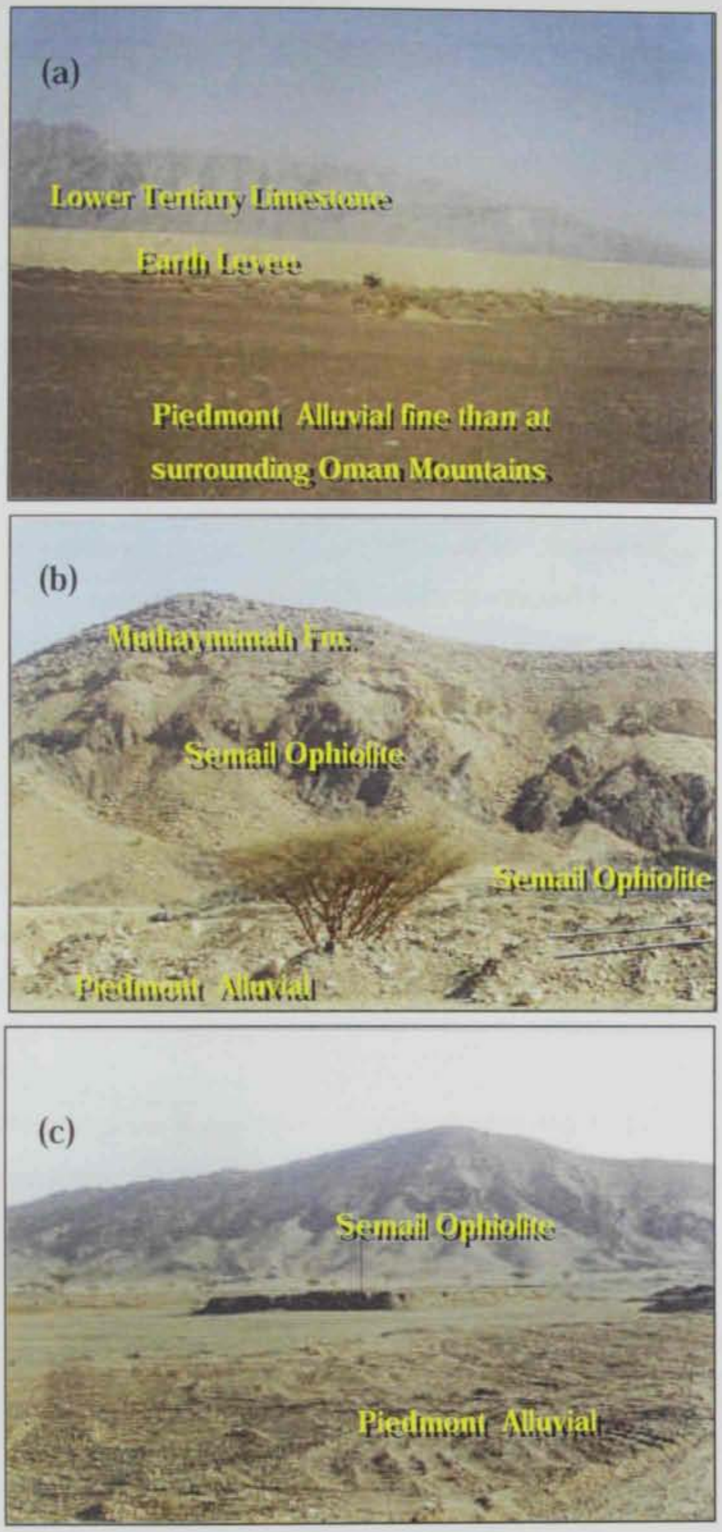

Fig. (2.6) Photos showing Jabal Hafit (a) to the west of Al Jaww Plain and Jabal Muthaymimah (b,c) to the east of Al Jaww Plain.

a) The Upper Cretaceous

According to Hamdan and Anan (1993), the Upper Cretaceous sequence includes (from base to top): Semail Ophiolites, Qahlah Formation, Simsima Formation and Fiqa Formation. The Semail Ophiolites are pre-Maastrichtian serpentine and serpentinized predotite. They represent the oldest exposed rocks in Al-Ain area where they form the base of Jabal Malaqet and Jabal Moundassah in its eastern side. The Qahlah Formation consists of red to yellow unfossiliferous clast-supported conglomerates composed of rounded clasts of serpentinized predotite derived from the Semail Ophiolites. Hunting Geology and Geophysics (1979) and Warrak (1987) indicated that Qahlah Formation is in fact Haybi and Hawasina suite which structurally underlies the Semail Ophiolites.

Simsima Formation is composed of medium-to thick-bedded shallow marine bioclastic limestones with rudists, corals and echinoids. It disconformably overlies the Qahlah Formation (Hamdan and Anan, 1993). In the northern and middle sections of Jabal Moundassah, however, the Simsima Formation unconformably overlies the Semail Ophiolites and was given by Hunting Geology and Geophysics (1979) the informal name Simsima Limestone.

The Fiqa Formation is represented by tongues in Jabal Moundassah and consists of light grey to buff thinly-bedded pelagic marls and calcareous shales with creamy to orange nodular to flaggy argillaceous limestone interbeds.

b) The Paleocene

The Paleocene sequence is separated from the underlying Upper Cretaceous sequence by a regional unconformity with local conglomerate at its base. It is represented by the Muthaymimah Formation. Hamdan and Anan (1989) and Hamdan and El-Deeb (1990) described this unit as the Pabdeh "equivalent" Formation. Nolan et al., (1990) formally named this unit the Muthaymimah Formation and assigned it to the Late Paleocene-Early Middle Eocene. This unit is exposed in Jabal Malaqet and Jabal Moundassah. It consists of shale, marl and argillaceous limestone with conglomerate interbeds.

c) The Eocene

Whittle and Alsharhan (1994) considered the Eocene sequence to include the Rus Formation and Dammam Formation. The Rus Formation (Lower Eocene) is composed of fossiliferous dolomitic limestone with thin argillaceous limestone (Tle_1) grading upward to well-bedded nodular limestone (Tel_2). The formation constitutes the core of Jabal Hafit anticline where it has unexposed base. The Dammam Formation (Middle to Upper Eocene) unconformably overlies the Rus Formation (Hamdan and Bahr, 1992). It constitutes most of the outcrops of Jabal Hafit and is made up of fossiliferous marl and limestone interbeds. Hunting Geology and Geophysics (1979) gave informal designations for this formation; namely: TIe_3 to TIe_6.

d) The Oligocene

According to Whittle and Alsharhan (1994) the Asmari Formation ranges in age from Middle to Late Oligocene. It is composed upwardly of silty marl (TIe_7), bioclastic nodular limestone (TIo_1), and interbedded bioclastic limestone and marl (TIo_2). The formation constitutes the east and west cuestas of Jabal Hafit which extend north of Wadi Tarabat and Al Ain Cement Factory respectively. At the western cuesta, the upper and lower contacts of the Asmari Formation are covered by alluvium.

e) The Miocene

The Miocene succession unconformably overlies the Asmari Formation (Whittle and Alsharhan, 1994). It is low-lying and located at the eastern flank of Jabal Hafit as nterbeds of gypsum and clay (Tm_1) and gypsiferous clay (Tm_2).

f) The Quaternary

Quaternary age deposits cover most of Al Ain area and consist of near-surface and surficial sediment of mixed alluvial, eolian, and, locally, sabkha (evaporatic origins). These units collectively form a relatively thin veneer that overlies most older rocks with varying degrees of structural discordance. In the following section, Quaternary deposits in the study area of Al Jaww Plain are discussed. The Quaternary alluvium will also be elaborated in chapter four as it constitutes the principle water-bearing lithostratgraphic unit.

2.4 Geology of Al Jaww Plain

Al Jaww Plain is an especially large (15 km) wide and prominent piedmont situated east and southeast of the city of Al Ain between the Oman Mountains and Jabal Hafit. It consists of gently inclined gravelly materials transported by wadis dissecting the northern Oman Mountains. The plain is transversed by numerous wadis such as Wadi Shik, Al Ain, and Muraykhat. Al-Shamsei (1993) identified three alluvial fans within plain; namely: the Zarub fan in the north, the Moundassah fan in the middle and the Ajran fan in the south.

Al Jaww Plain is mostly covered with the Quaternary deposits. Hunting Geology and Geophysics (1979) recognized five sediment types. They are broadly contemporaneous and represent different facies of deposits being formed by present-day processes.

(i) Aluvial deposits (Qg)

Alluvial deposits occur beneath the piedmont plains fringing the Oman Mountains and Jabal Hafit. The grain size of these deposits ranges from boulder gravel and conglomerate in the east part to fine sand and silt where wadis disappear in the sand dune to the west. A typical section through the alluvium of Al Jaww Plain consists of pebbles and cobbles of gabbros, serpentine, limestone and chert set in a fine-grained cement of carbonate silt. At some localities, the clastic matrix is absent and the pebbles are either uncemented or loosely held together by coarse-grained recrystallised calcite. These rocks are both porous and permeable and make excellent aquifers. The deposits are crudely bedded and contain impresistent lenses of cross-laminated sand. Around Jabal Hafit the clastics are composed entirely of limestone.

Towards Al Ain town and further west the gravel and conglomerates are replaced progressively by interbedded sand, silt and calcrete. The sand and silt are typically cross-laminated, calcareous, brown or white and, with scattered pebbles and cobbles. They tend to be more firmly cemented than the conglomerates. The calcrete is typically white, lacks obvious bedding, contains scattered grains of silica and altered igneous rocks and contains irregular fracture surfaces and vugs coated with iron and manganese oxides.

Towards the west where the alluvium becomes sufficiently fine-grained (Fig. 2.7). It is subjected to wind action and the area is partly covered by low sand dunes.

(ii) Desert plain deposits (Qes)

Most of the remaining flat or gently undulating parts of the area are underlain by desert plain deposits. They occur between the dune ridges mainly in the west and north of Al Ain area.

Typical exposures consist of low scarps at the margins of the ablation hollows and flats. They are of inter-layered pale gray laminated silt that is loosely cemented with carbonate, and red or brown sand locally showing dune bedding. These rocks types represent dune sands which have been cemented by salts at times of higher water table and that have been subsequently re exposed by ablation. Adjacent parts of the plains are covered with nodules of sandstone formed by surface cementation of these rocks types and by scattered

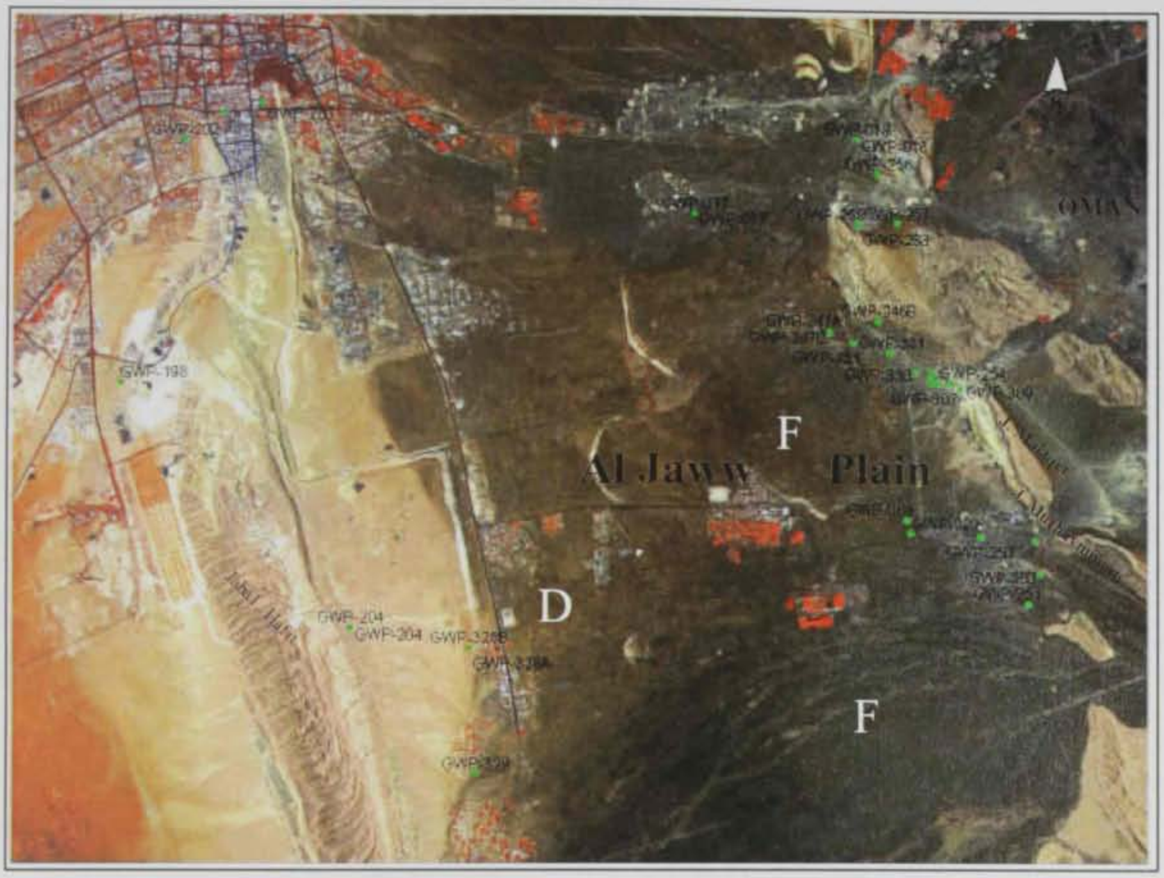

Fig. (2.7) The main geological units of Al Jaww Plain, D= Desert plain deposits, mainly gravels, F= Fluviatile deposits.

pebbles of serpentinite, gabbro, limestone and chert. Sections exposed in borrow pits near Jabal Muhayjir and elsewhere show that inter-layered gravel, pebbly calcrete, nodular limestone and calcareous silt also make up a part of the desert plain deposits. These deposits are present between the dune ridges, mainly in the western and northern parts of the study area. They are distinguished from fluvial deposits by being unrelated to the present drainage pattern. Desert plain deposits are interlayered, laminated and loosely cemented by carbonate silt and sand. They represent dune sands which were cemented by salts at times of higher water tables and then re-exposed by ablation (El- Saiy, 2002).

(iii) Mixed deposits (QTm)

These deposits, which are present in the northern part of the study area, include calcrete, serpentinite granules and calcareous sandstones. They are very similar to the Miocene rocks. The lack of diagnostic fossils, however, makes their indeterminate (Hunting Geology and Geophysics, 1979).

(iv) Sabkha deposits (Qsb)

Sabkha deposits occur where the main wadi channels enter the sand dunes and at other locations within the dunes liable to flooding by rising groundwater. Sabkhas are also developed on the lower parts of gravel and sand plains at and west of Ain Bu Sukhanah. The main rock type is loosely cemented calcareous siltstone. Visible gypsum, which is common in the Sabkhas near the coast, is rare in the Al Ain area except around Ain Bu Sukhanah.

(v) Aeolian sand (Qd)

The greatest part of the area is covered by sand dunes. They vary in color from red and pink to white. Hunting Geology and Geophysics (1979) emphasized that grains of these sand dunes are well-rounded carbonates and quartz with minor proportions of basic and ultrabasic igneous rockfragments.

2.5 Structural Setting

Al Ain area is located on a structural pattern ranging between the uplifted, highly-deformed rocks of the Oman Mountains at the east and the buried, flat-lying to gently-folded strata of western Abu Dhabi Emirate (Hunting Geology and Geophysics, 1979; Schlumberger, 1981; Robertson et al., 1990). The history of these structural elements is summarized with reference to (a) compressive deformation exposed in the mountains and (b) similarly developed structures to the west of the range (primarily those structures in the shallow subsurface beneath the piedmont and the northern dune area). The main remarkable structural elements of Al Ain area are elaborated in the following section.

2.5.1 Structures in the Oman Mountains

The rocks exposed in the northern Oman Mountains have suffered from a complex compressive deformation primarily due to Late Cretaceous obduction of the Semail ophiolites and associated sedimentary and volcanic rocks formed as a result of this obduction (Glennie *et al*., 1974; Coleman, 1981 & 1981; Lippard *et al*., 1986, Patton and OConner, 1988; Boote *et al*., 1990 and Warburton *et al*., 1990).

Major structures formed in response to ophiolite emplacement include: i) several sets of east to-northeast dipping thrust faults and nappes; ii) uplift and collapse of regional culminations above stacked thrust sheets; iii) intense folding associate with thrust folding; and iv) pervasive internal deformation (shearing tectonic dismemberment and mélange development) in the Hawasina and rocks (Searle et al., 1990 and Warrak, 1987).

Regional mapping has identified complex folding and faulting in the Bedrock Mountains of the western Oman Mountains adjoining the eastern margin of the study area (Fig. 2.4).

2.5.2 Structures west of the Oman Mountains

Based on structural interpretations of seismic reflection profiles, several studies have documented the presence of a large buried system of folds and thrust faults bordering the western flank of the Oman Mountains (Boote et al., 1990; Dunne et al., 1990; and Warburton et al., 1990).

Woodward (1994) used 94 reprocessed seismic sections covering Al Ain area (Fig. 2.8) for outlining the major structural elements that affect the Quaternary aquifer. Most of the thrust faults were identified by offset and/or by aligned truncation of shallow reflectors. (Fig. 2.9) shows a comprehensive map of subsurface structures for the western flank of the Oman Mountains in Al Ain area.

Most of the deformation in the zone is under a surficial cover of alluvium and eolian sand, although some structures produce mountains ranging in size from Jabal Hafit in the south to small bedrock outcrops protruding through the sand cover in the northern dune area, such as Bida Bint Saud, Jabal Mohayer and Qarn Saba. The orientation, style, and geometry

Fig. (2.8) Amoco seismic lines and uphole-survey locations (afterWoodward, 1994).

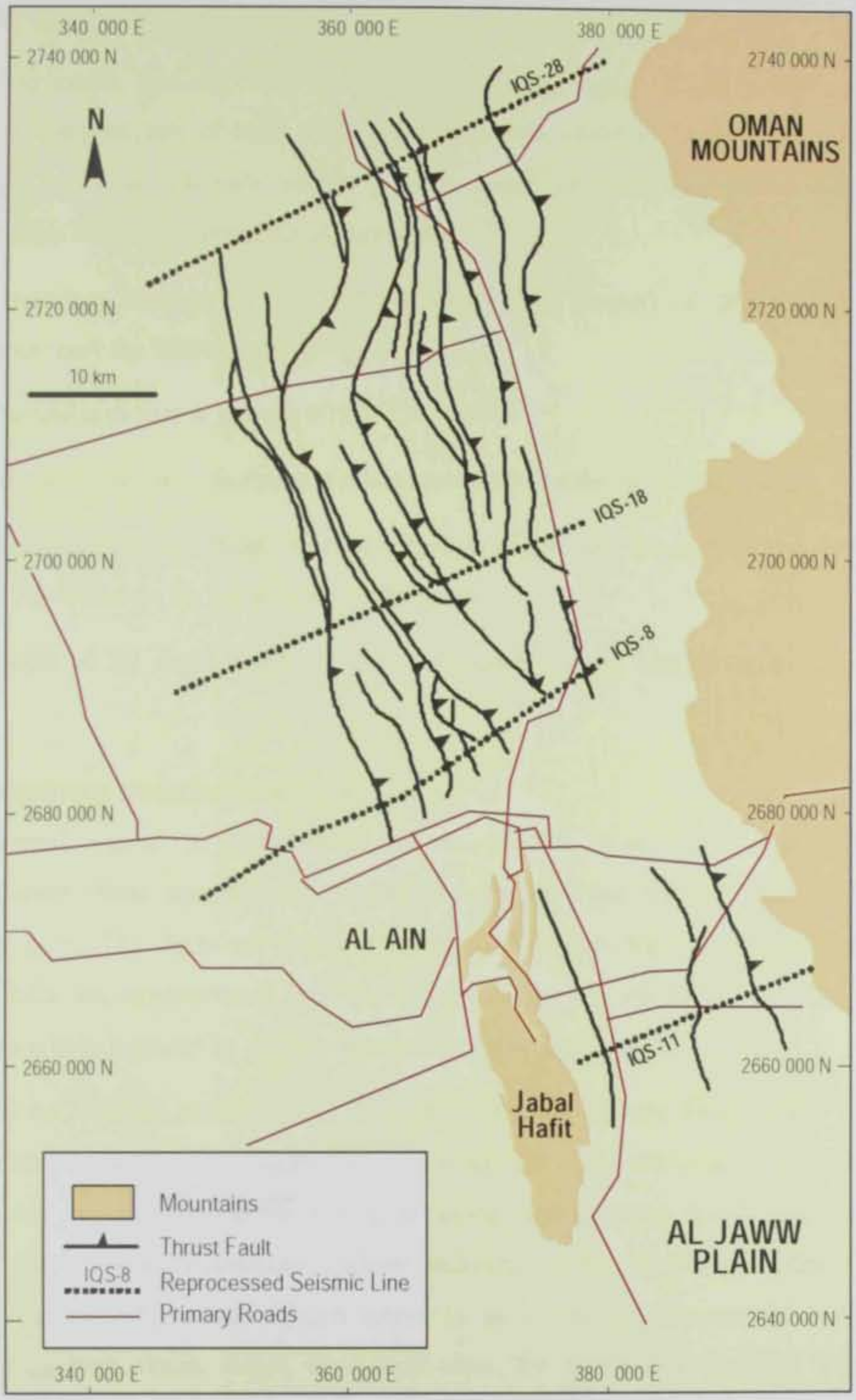

Fig. (2.9) Generalized subsurface structural features in Al Ain area (after Woodward, 1994).

of subsurface structures are similar in many aspects to the faults and folds exposed in the bedrock of the Oman Mountains.

Two structural domains have been defined on the basis of deformational style and complexity. A complex belt of tight folds and thrust faults underlie the northern dune area. A less deformed zone of relatively simple compressional structures, as shown in (Fig. 2.9) extends from Jabal Hafit eastward under Al Jaww Plain.

The boundary between the two regimes trends ENE beneath the Wadi Al Ain system. The two regimes share the followings:

(i) The fold axes have a general NNW-SSE trend.

(ii) All the major thrust faults are dipping eastward at moderate to steep angles.

(iii) The distal (western-most) structural elements of each domain are anticlines (Jabal Hafit south of Al-Ain, and a buried anticline to the north).

(iv) West of the distal anticlines, the undisrupted layered bedrock is dipping gently to the west.

2.5.3 The northern structural regime

This structural regime is characterized by an episodic, compressive tectonism. Starting from the western distal anticline, the folding consists of three sets of alternating anticline-syncline fold pairs. The folds are doubly-plunging; the eastern ones are symmetrical whereas the western folds are asymmetrical; with the axial surfaces dipping slightly to the west. Most of the folds have been ruptured by a series of imbricate thrust faults.

There are six sub parallel zones of major, eastward-dipping thrust faults. The F1 and F6 thrust zones consist of single faults; the F3, F4 and F5 zones are made up of two branching thrusts, whereas the F2 zone comprises three inline discontinuous thrusts. The deformation sequence of the post-Late Cretaceous shallow sediments is one of an initial phase of folding followed by thrusting. The thrust system seems to be a leading imbricate fan with westward propagating piggyback thrust. Based on seismic data, the northern anticline is thought to be either unfaulted or less faulted with little displacement along the thrust plain. In the central part of the anticline, the fold becomes more compressed, where the limbs begin to dip quite steeply, and a thrust fault develops near the central part of the fold and ruptures the fold west of its crest. As compressional deformation increases, the throw of the thrust increases and the anticline begins to be decapitated. At the southern end of the anticline, seismic sections show that the fold is broad and unfaulted, and the limbs are dipping at low angles. Warrak (1996) studied the origin of the Hafit anticline and analyzed its structural pattern. He concluded that the structure was formed as a result of one-sided compression acting from ENE and grew as a detachment fold. Also, the reversed verence and the fold superposed on the limbs of Hafit folds were formed due to simple shear as it moved up a listric, east-dipping thrust plane. Warrak (1986) emphasized that the Hafit anticline grew synchronously with the sedimentation from just before the Middle Eocene until the end of the Miocene.

2.5.4 The southern structural regime

The southern structural regime is dominated by Jabal Hafit, the distal fold, and Al Jaww Plain. The mountain is a composite anticline with a sinuous doubly-plunging fold axis. This large amplitude fold is asymmetric with a vertical to steeply-overturned eastern limb.

The Al-Jaww Plain (500 km^2) is a westward-sloping, low-relief alluvial piedmont bounded on the east by the Oman Mountains and on the west by Jabal Hafit. Structurally, the plain is underlain by a series of southerly-plunging folds that comprise a central anticline flanked by synclines, and easterly-dipping thrust fault located near the eastern boundary of the plain (Fig. 2.10). The major fold is a syncline whose axis is about 6 km long east of Jabal Hafit. All folds and faults have axial traces that are subparallel to Jabal Hafit, which has an axial trace striking about N20° W.

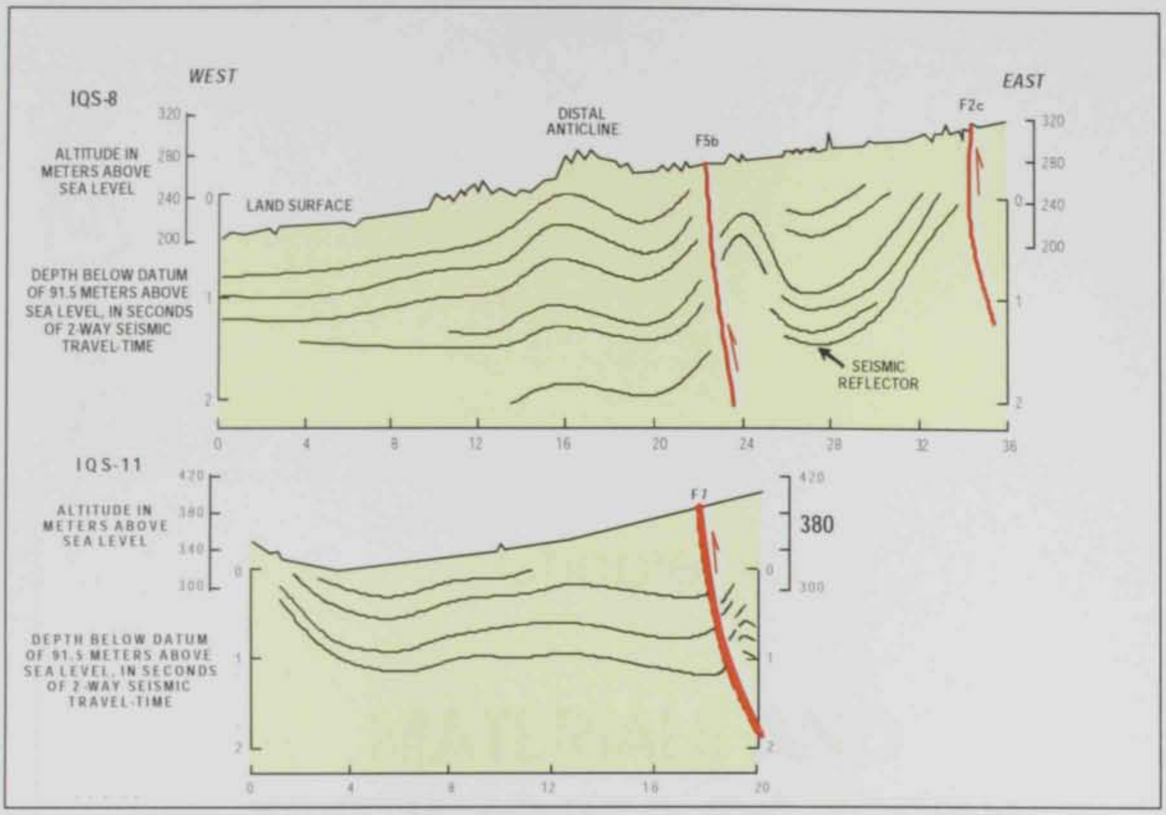

Fig. (2.10) Interpreted seismic lines at Al Jaww Plain and north of Al Jaww Plain, see Fig.2.9 for location (modified after Woodward, 1994).

Chapter III

MATERIALS AND TECHNIQUES OF STUDY

MATERIALS AND TECHNIQUES OF STUDY

The theoretical background of the implemented geophysical techniques is discussed in this chapter.

3.1 Materials

This study is based on various data collected from different sources including field trips to the area under investigation. These data include.

1. Meteorological data collected from the Departement of Civil Aviation (Abu Dhabi International Airport). These data are recorded at Al Ain Intrnational Airport, which represents the nearest metrological station to the study area.
2. Records of the water wells drilled in the study area, provided by National Drilling Company (NDC) and Water and Electricity Departement (WED) of Al Ain Distribution Company, Al Ain.
3. The lithologic logs of many wells, which were drilled at Al Jaww Plain.
4. Periodical recording for the measurements of groundwater depth in available wells by NDC and WED.
5. Chemical analyses of previous periodical records of groundwater samples provided by NDC and WED.
6. Topographic maps of scale 1:50,000 and land sate image for Al Ain area.
7. Surface geophysics including Direct Current (DC) resistivity and Transient Electromagnetic (TEM). Data from borehole geophysics logged by Schlumberger Middle East at Al Jaww Plain are also used.

3.2 Direct Current (DC) Resistivity Method

3.2.1 General

Applied geophysics is known as a large group of various methods and techniques developed to investigate the subsurface. By the geophysical methods, a lot of information is acquired, which can be used for various aspects. Geophysical techniques are considered as one of the most accurate and cost saving methods used in hydrogeology, engineering and geoenvironmental investigations. This achievement is related to the expanding interpretative skills of the geophysicists and the increasing acquaintance of the engineers and geologists with its basic geophysical principles.

The electrical methods in general include different techniques and instruments depending on the nature of the method used in prospecting. Some of these methods make use of the natural currents and others depend on injection of artificial currents into the earth. For more details about these different techniques reference is made to Reynolds (1997), Parasins (1997), Telford et al., (1990), Robinson and Coruh (1988) and Dobrin (1976).

The DC-resistively methods of geophysical exploration are popular and proved to be successful and have many implications in the fields of geoenvironment and hydrogeology. Electrical resistively methods were developed in the early 1900 but have become widely used since the 1970_s, primarily due to the availability in the search for suitable groundwater sources. These methods have also been used to monitor types of groundwater pollution; in engineering surveys to locate sub-surface cavities, faults and fissures permafrost, mineshafts and in archaeology for mapping out a real extent of remnants of buried foundations of ancient buildings, amongst many other applications. Electrical resistively methods are also employed extensively in downhole logging as will be elborated in the section of borehole geophysics.

3.2.2 Basic concepts of the resistivity method

Resistively is one of fundamental electrical properties of soils and rocks. The term (Resistivity) is used because earth materials behave like electrical resistors, impeding currents flow through the ground. The materials, ability to conduct currents is controlled by a number of factors, including the moisture content, clay content, porosity or compaction and the presence of free ions. For example, resistance to current flow decreases with increasing ionized water or salt content.

Resistivity (ρ) is a bulk property of material describing how well that material inhibits current flow. This is slightly different from resistance, which is not a physical property. If we consider current flowing through a unit cube of material, (Fig. 3.1) resistivity is defined as the voltage measured across the unit cube's length (V/m)

Divided by the current flowing through the unit cube's cross sectional area (I/m^2). This results in units of Ohm m^2 /m or Ohm-m.

It is expressed by the following formula:

$$\rho = \frac{r.A}{L} \qquad (3.1)$$

Where **r** is the resistance of a conductive material having a length **L** and across sectional area **A**

Consider an electric circuit in which the earth is the resistor. Two metal stake electrodes are connected at two different locations to the battery terminals, as shown in (Fig. 3.2). The electrodes connected to the positive terminal is called the source, the other connected to named the negative terminal is the sink. Due to the difference in potential between these electrodes current is obliged to flow along paths leading from the source to the sink. The source electrode is positively charged therefore it pushes positive electric charges outward into the ground. The result is that electric current flows outward from the source, into the ground. Assuming that resistivity is constant through the model of the earth, the current moves away from the source, radiating outward and uniformly in all directions as shown by the paths in (Fig. 3.2).

Now consider the resistance encountered by current that has traveled a distance from the source. Because it spreads outward in all directions, it has moved through a hemispherical zone. The current flows out of this zone when it moves across the area of $2\pi d^2$, which is the surface of the hemisphere. According to Equation (3.1), the resistance **r** can be expressed by the product of resistivity ρ and the distance d that the current has traveled divided by the area $2\pi d^2$ then

$$r = \frac{\rho d}{2\pi d^2} = \frac{\rho}{2\pi}\left(\frac{1}{d}\right) \qquad (3.2)$$

The charge in potential resulting from the flow of current through this hemispherical zone can be found from Ohm's law, which relates the current, potential difference, and resistance such that

$$V = ir \qquad (3.3a)$$

then

$$V = ir = \frac{i\rho}{2\pi}\left(\frac{1}{d}\right) = V_0 - V_d \qquad (3.3b)$$

Where, $V_0 - V_d$ is the difference between the electric potential V_0 at the source and the potential V_d at any point in the ground at a distance d from the source.

Considering the sink electrode, if the potential at the source is V_0, the potential at the sink will be $-V_0$, for it is connected to the negative terminal of the battery. Similarly, we can use ohm's law to find the difference between the electric potential $-V_0$ of the sink and the potential V_d at all points which far by a distance d from it. Thus

$$V = ir = \frac{i\rho}{2\pi} = V_d - V_0 \qquad (3.4)$$

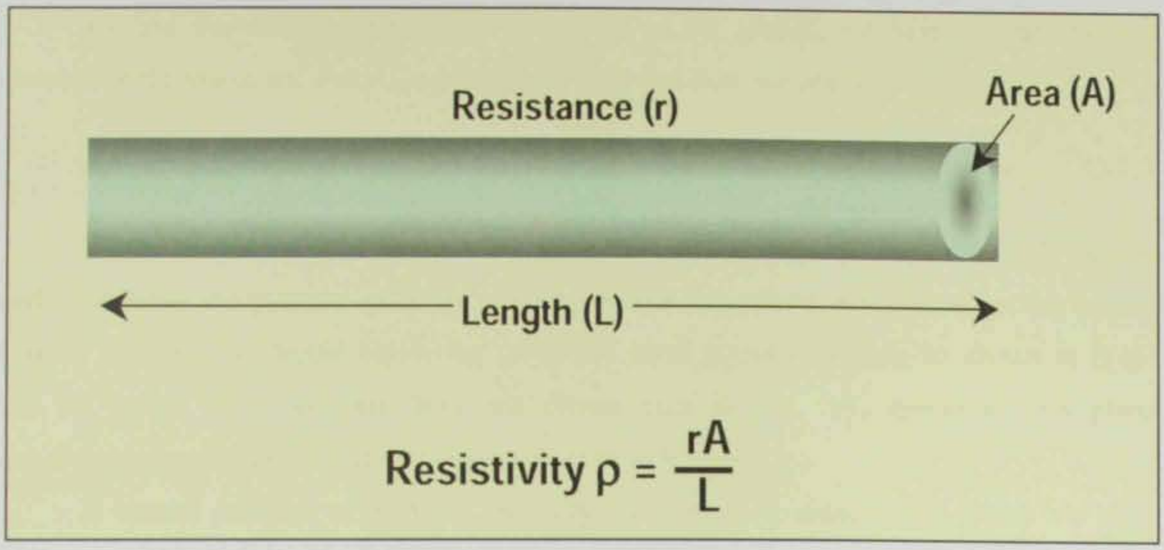

Fig. (3.1) Basic definition of resistivity across a homogeneous medium.

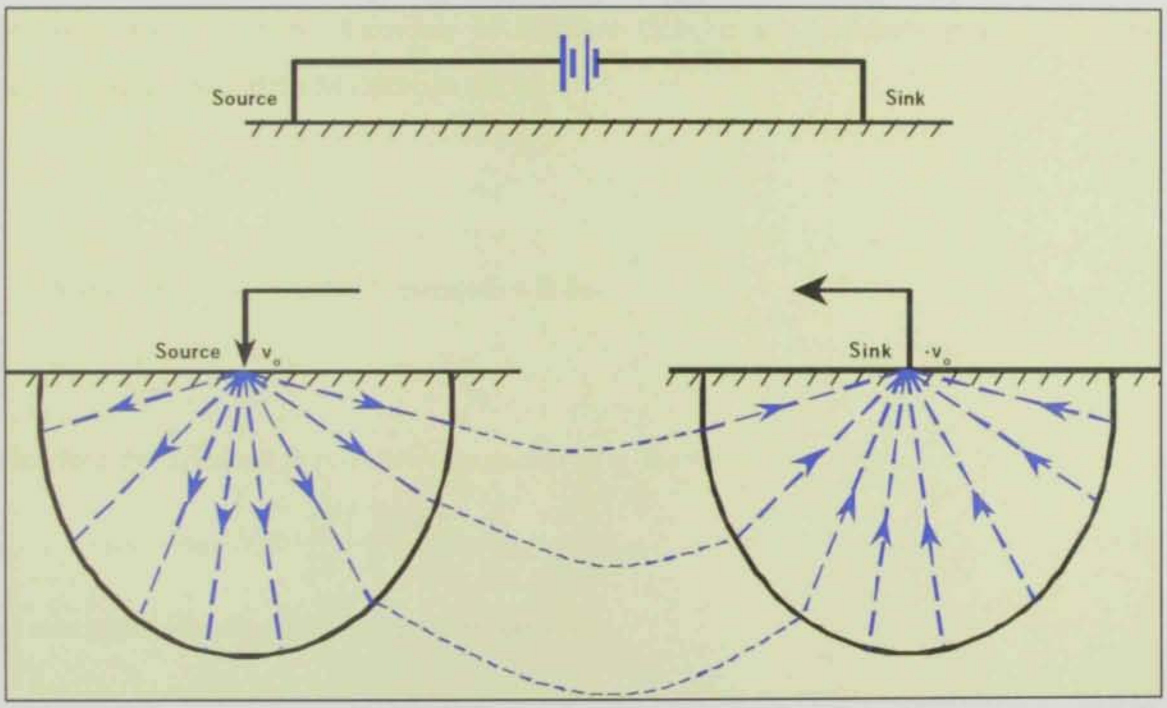

Fig. (3.2) Current lines radiating out from a source electrode and converging on a sink electrode.

To find the electric potential V at a point in the ground, we have to combine the potentials of the source and sink. Using Equations (3.3) and (3.4), we obtain

$$V = \frac{i\rho}{2\pi}\left(\frac{1}{d_1}-\frac{1}{d_2}\right) \tag{3.5}$$

Where d_1 and d_2 are the distances to the source and the sink. Equations (3.5) can be used to calculate the potential point by point throughout the ground then, by connecting points of equal potential, we would obtain the pattern of equal potential surfaces as shown in (Fig. 3.3). the pattern of equipotential lines and current lines in (Fig. 3.3) applies for any plane surface containing the source and sink, regardless of its inclination.

In normal practices of electrical resistivity surveying it is usual to use source and sink electrodes connected to a battery, or some other source of electric power, to compel current to flow in the ground. An ammeter is included to measure current. Two other electrodes connected to a voltmeter are placed in other positions to measure differences in potential.

In (Fig. 3.4), the source and sink electrodes are A and B, and the so called potential electrodes are M and N. According to Equation (3.5), if the resistively ρ is uniform, the electric potential V_M at the M electrode will be.

$$V_M = \frac{i\rho}{2\pi}\left(\frac{1}{d_1}-\frac{1}{d_2}\right) \tag{3.6}$$

And the potential V_N at the N electrode will be

$$V_N = \frac{i\rho}{2\pi}\left(\frac{1}{d_1}-\frac{1}{d_2}\right) \tag{3.7}$$

Therefore, the difference in potential V_{MN} measured by the voltmeter will be

$$V_{MN} = V_M - V_N = \frac{i\rho}{2\pi}\left(\frac{1}{d_1}-\frac{1}{d_2}-\frac{1}{d_3}+\frac{1}{d_4}\right) \tag{3.8}$$

by rearranging Equation (3.8) to express resistively

$$\rho = 2\pi\frac{V_{MN}}{i}\left(\frac{1}{d_1}-\frac{1}{d_2}\frac{1}{d_3}+\frac{1}{d_4}\right)^{-1} \tag{3.9}$$

most of the work with resistivity instruments is based upon apparent resistivity (ρ_a) instead of true resistivity (ρ), because the ideally uniform subsurface is rare.

Thus the value obtained from Equation (3.9) is called the apparent resistivity ρ_a. Equation (3.9) can be expressed as:

$$\rho_a = \frac{V_{MN}}{i} G \tag{3.10}$$

Where

$$G = \frac{2\pi}{1/d_1 - 1/d_2 - 1/d_3 + 1/d_4} \tag{3.11}$$

is the geometrical factor that depends on the electrode arrangement.

For more detail about the theory, different types of electrode configurations, data acquisition and methods of interpretations, are given in Koefoed (1968), Dobrin (1976), Robinson and Coruh (1988), Lowrie (1997), Parasnis (1997), Reynolds (1997) and Sharma (1997).

3.2.2.1 Electrode arrays

Most electrical resistivity surveying is done with one or more of the various electrode configurations. (Fig. 3.5) shows the most common electrode arrays used in resistivity survey. The electrode configuration which has been used during this study is the Schlumberger electrode array, illustrated in (Fig. 3.5b). In this configuration, the current electrodes A and B are at equal distance **S,** in opposite directions from the center of the array. The potential electrodes M and N are between A and B at equal distance from the center of the array, S/2

From Equation (3.11), the geometrical factor for this array becomes

$$G_s = \frac{2\pi}{\frac{1}{S-(a/2)} - \frac{1}{S+(a/2)} - \frac{1}{S+(a/2)} + \frac{1}{S-(a/2)}} = \frac{\pi(S^2-(a/2)^2}{a} \tag{3.12}$$

Therefore, the formula used in the Schlumberger configuration can be written as follows:

$$\rho_a = \pi\,(\frac{S^2\ a^2/4}{a})\,\frac{VMN}{i} \tag{3.13}$$

To measure apparent resistivity, the subsurface of the earth is energized through two current electrodes, and the resulting potential is measured by two nonpolarizing electrodes, and values of I and V_{MN} are read from the ammeter in the current circuit and the voltmeter in the potential circuit. These values are used with the appropriate geometrical factor in Equation (3.10).

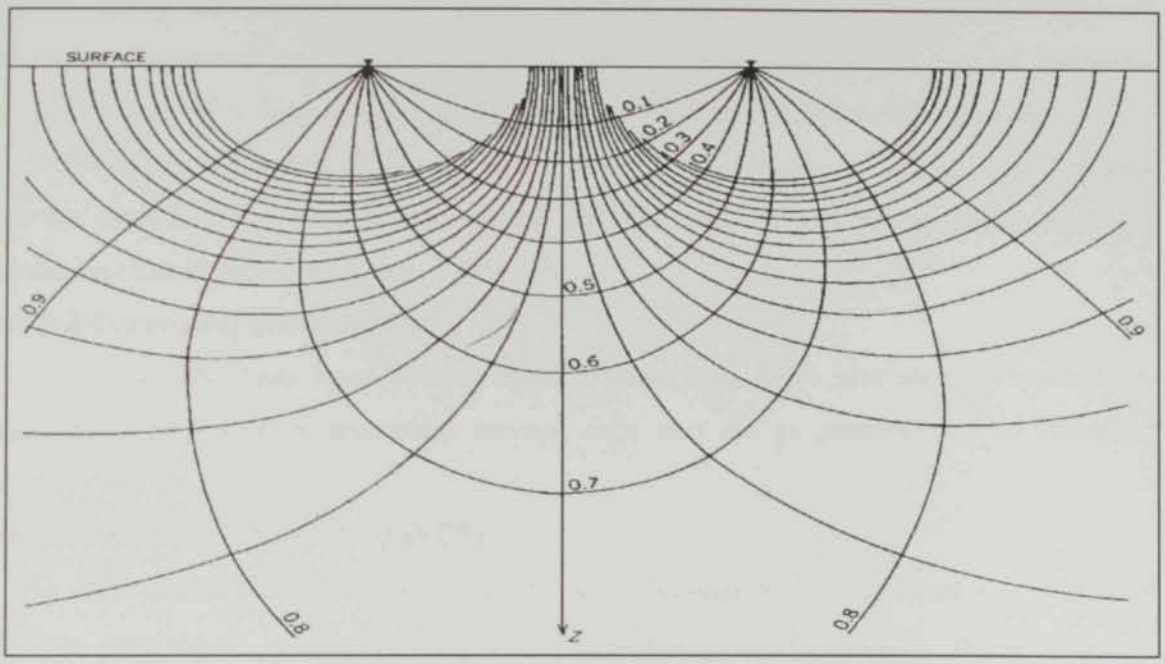

Fig. (3.3) Current lines and equipotential surfaces produced by a source and sink in a medium of uniform resistivity. (After Van Nostrand and Cook, 1966).

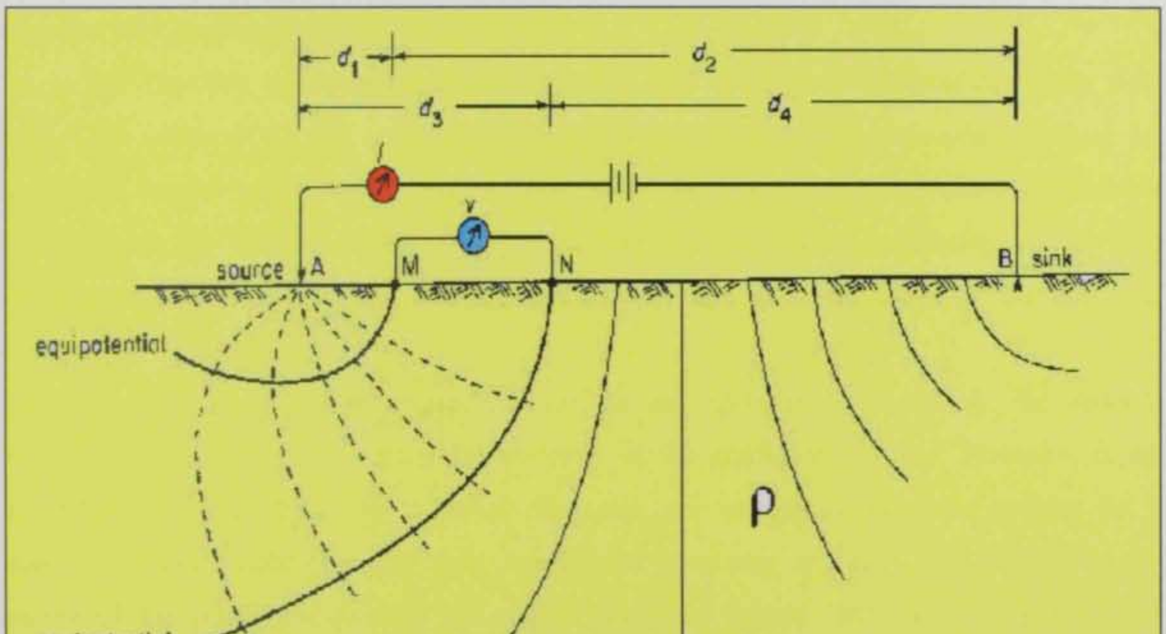

Fig. (3.4) Current electrodes A and B and potential electrodes M and N are used to measure potential difference V, which depends on the zone resistivity.

The depth of investigation is generally controlled by the current electrode spacing. Greater depths are achieved as the current electrode separation is increased. Each type of electrode arrangement has its own depth of current penetration, in the case of horizontal layers. The depth of probing is also controlled by the resistivities of the subsurface materials.

A very general rule of thumb with certain reservations can be applied which implies that the depth of penetration ranges between one third and one fifth of the current electrode separation (Van Nostrand and Cock, 1966).

3.2.2.2 Surveying procedures

Many procedures have been designed (Habberjam, 1979) and although several are occasionally employed in specialized surveys, only two are in common use as elaborated below.

Vertical Electrical Sounding (VES)

The resistivity sounding is one of the most economical methods used in the field of shallow geophysical investigations such as engineering, hydrogeological, geoenvironmental and archaeological investigations. The man power and time required for performing Schlumberger sounding are less than those required for Wenner array. Also, the effect of near surface lateral inhomogeneities is less under the Schlumberger array (Zohdy, 1974), as the separation MN is generally smaller than AB.

The objective of sounding is to determine the variation of electrical resistivity with depth. This method is also called (electric drilling). An electrical sounding is done by measuring several values of apparent resistivity with successively increasing electrode spacing, with the center of the configuration and its orientation remaining fixed. With increasing electrode spacing, current penetration increases and consequently the depth of investigation.

Therefore, in the Wenner configuration, as the electrode array expands, the distance (a) is increased equally by keeping the midpoint of the configuration fixed. However, in the Schlumberger configuration, the potential electrodes can remain in the same position for a series of readings with changing only the current electrodes spacing. Then, increasing the spacing of the potential electrodes for another series of current electrode spacing to obtain readable measurements for both V and I. In all cases MN spacing must be kept to about 1/5 of the AB spacing.

Electrical Profiling

The objective of electrical profiling is to determine the lateral variations in resistivity of the ground along profiles with stations used for measurements of ρ_a. The coverage of the

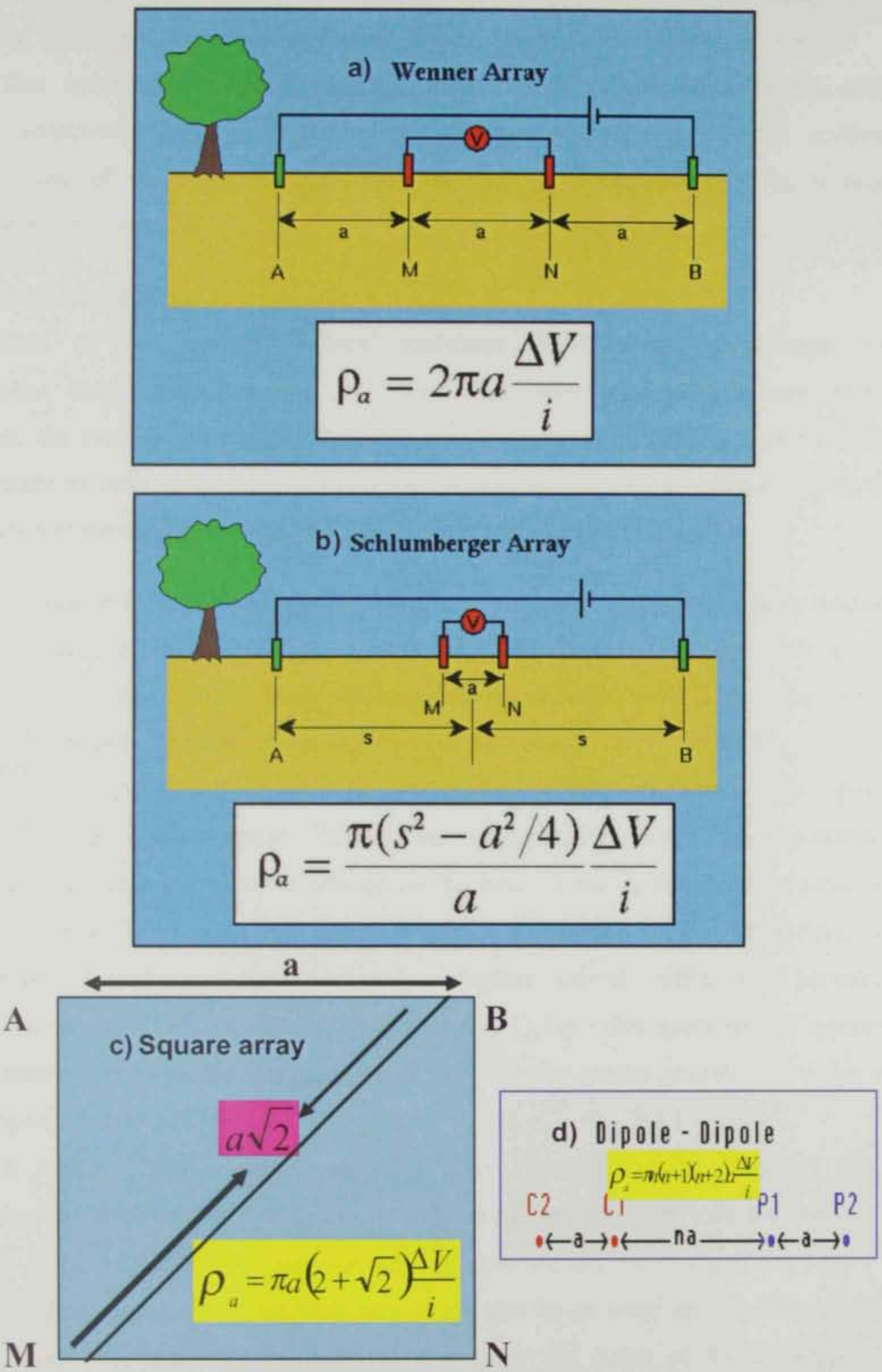

Fig. (3.5) Common electrode arrays (configurations) used in DC resistivity and their corresponding geometrical factor.

area of investigation with a number of such profiles can be used for construction of resistivity maps representing resistivity at different electrode separations, i.e., at the depth of current penetration related to this electrode separation (e.g. in case of Wenner array) (Fig. 3.5a).

This technique is useful in detecting local shallow inhomogeneities in the subsurface and is employed typically in delineating geologic boundaries, fractures, cavities, etc. Generally any of the electrode arrays may be used, however, the selection is depending mainly on the field situation.

3.2.2.3 Data acquisition

Data of nine vertical electrical soundings (VES) using Schlumberger electrode configuration along profile crossing Al Jaww Plain (after MAF, 1985) have been used. Moreover, the available instrument "Sting R1 IP^{TM}" Resistivity meter (Fig. 3.6) has been used in this study to carry individual VES near to borehole for purpose of calibration and training. Presentation of the data, processing and interpretation are discussed in chapter six.

3.3 Principles of Time Domain Electromagnetic Techniques for Resistivity Sounding

Conventional DC resistivity techniques have been applied for many years to a variety of geotechnical applications. More recently electromagnetic techniques, have been used effectively to measure the resistivity (or its reciprocal, the conductivity) of the earth.

Electromagnetic techniques can be broadly divided into two main groups. In frequency-domain instrumentation (FDEM) the transmitter current varies sinusoidally with time at a fixed frequency which is selected on the basis of the desired depth of exploration of the measurement (high frequencies result in shallower depths). On the other hand, in most time-domain (TDEM) instrumentation, the transmitter current, while still periodic, is a modified symmetrical square wave, as shown in Fig. (3.7a). After every second quarter-period the transmitter current is abruptly reduced to zero for one quarter period, whereupon it flows in the opposite direction.

A typical TDEM resistivity sounding survey configuration is shown in Fig. (3.7b). The transmitter is connected to a square (usually single turn) loop of wire laid on the ground. The side length of the loop is approximately equal to the desired depth of exploration except that, for shallow depths (less than 40 m) the length can be as small as 5 to 10 m in relatively resistive ground. A multi-turn receiver coil, located at the centre of the transmitter loop, is connected to the receiver through a short length cable.

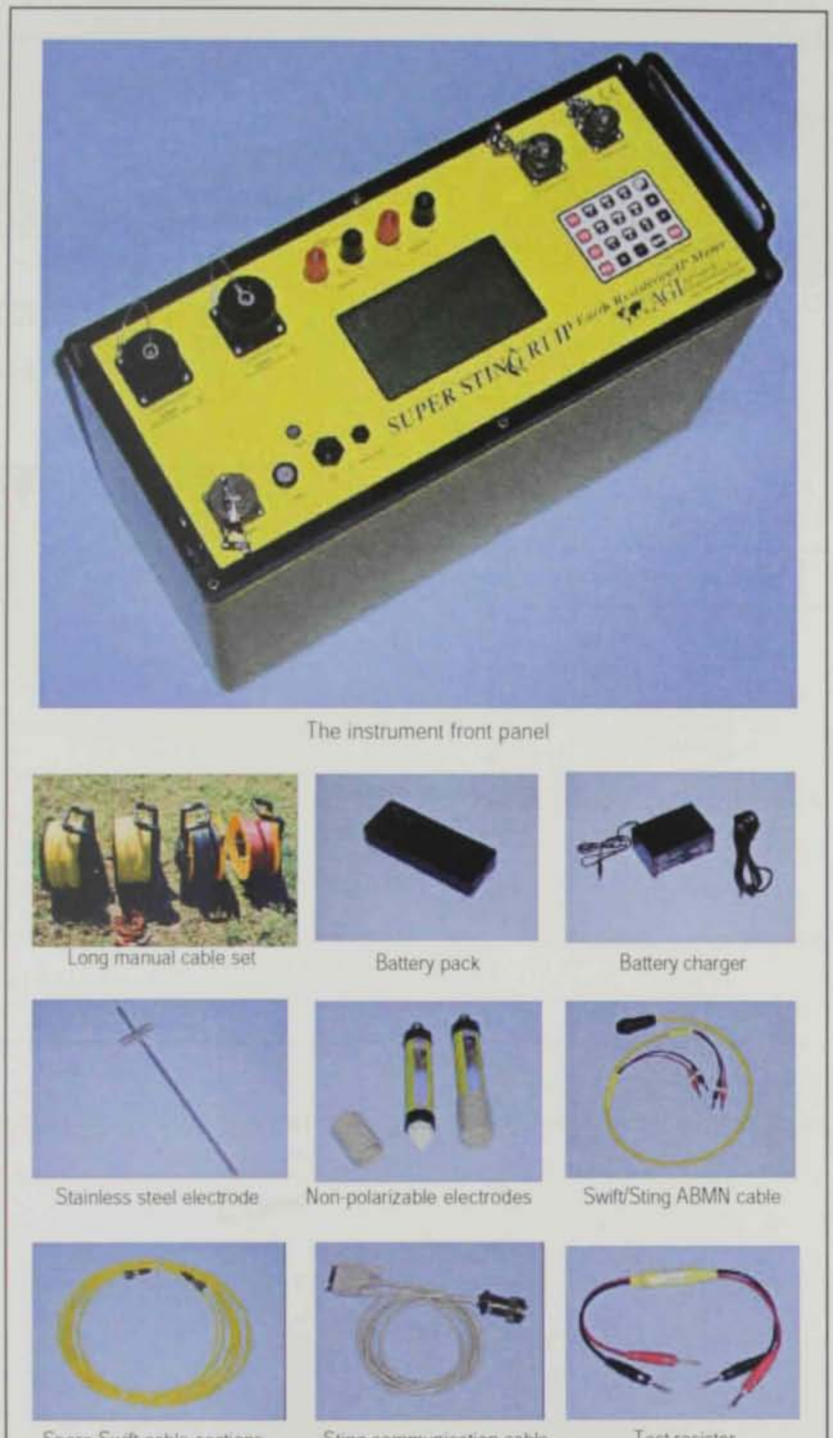

Fig. (3.6) Super Sting R1 IP earth resistivity and IP meter and its accessories.

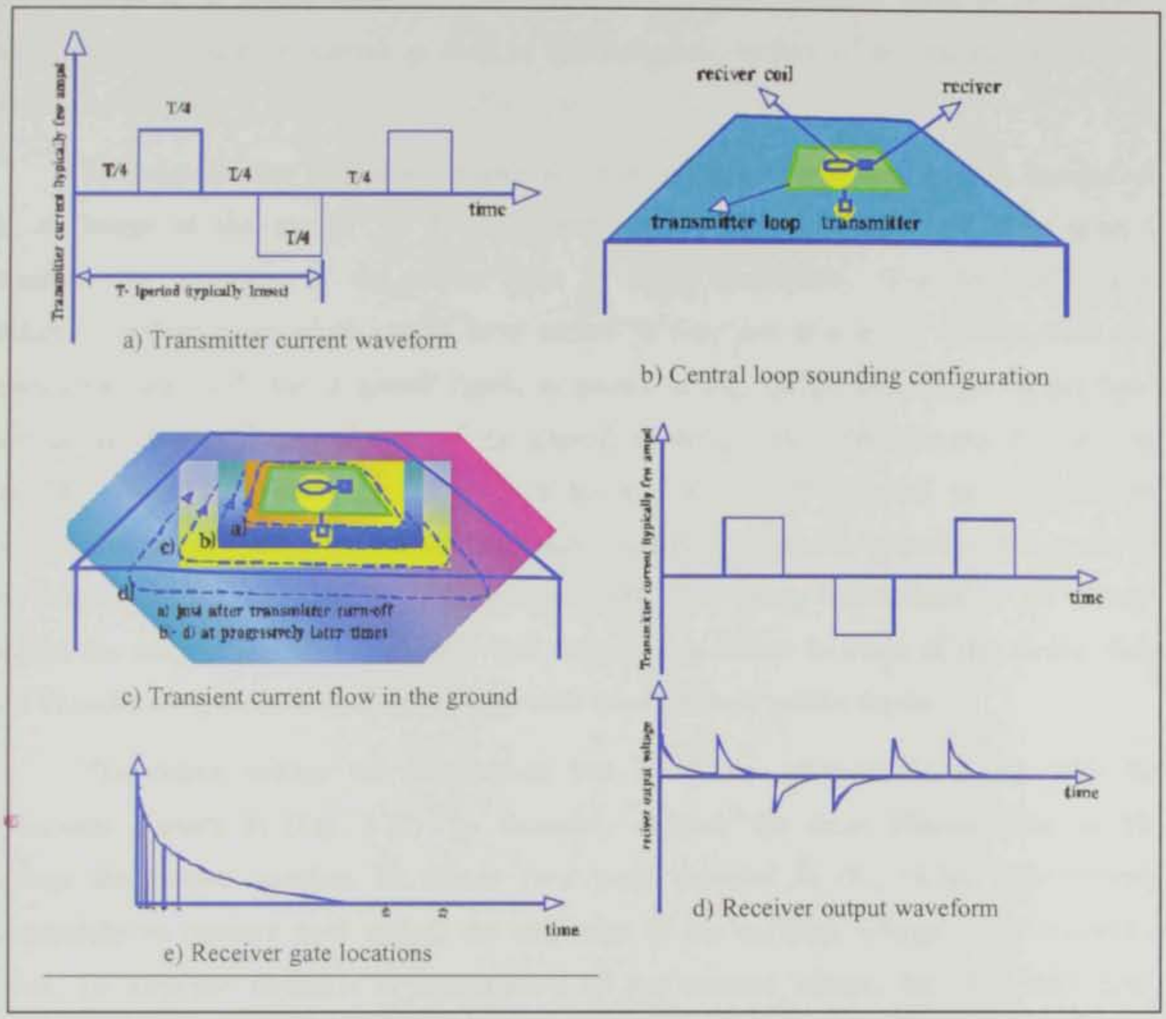

Fig. (3.7) Principles of time domain electromagnetic techniques for resistivity sounding.

In TDEM resistivity sounding, the process of abruptly reducing the transmitter current to zero induces, in accord with Faraday's law, a short duration voltage pulse in the ground, which causes a loop of current to flow in the immediate vicinity of the transmitter wire, as shown in Fig. (3.7c).

Immediately after transmitter current is turned off, the current loop can be thought of as an image in the ground of the transmitter loop. However, because of finite ground resistivity the amplitude of the current starts to decay immediately. This decaying current induces a voltage pulse which causes more current to flow, but at a larger distance from the transmitter loop, and also at greater depth, as shown in Fig. (3.7c). This deeper current flow also decays due to finite resistivity of the ground, inducing even deeper current flow and so on. The amplitude of the current flow as a function of time is evaluated by measuring its decaying magnetic field using a small multi-turn receiver coil usually located at the center of the transmitter loop. From the above it is evident that, by making measurement of the voltage out of the receiver coil at successively later times, measurement is made of the current flow and thus also of the electrical resistivity of the earth at successively greater depths.

The output voltage of the receiver coil is shown schematically (along with the transmitter current) in (Fig. 3.7d). To accurately measure the decay characteristics of this voltage the receiver contains 20 narrow rime gates indicated in (Fig. 3.7e), each opening sequentially to measure (and record) the amplitude of the decaying voltage at 20 successive times. To minimize distortion in measurement of the transient voltage, the early time gates, which are located where the transient voltage is changing rapidly with time, are very narrow. The later gates, situated where the transient is varying more slowly, are much broader. This technique is desirable since wider gates enhance the signal-to-noise ratio, which becomes smaller as the amplitude of the transient decays at later times. It is noted from (Fig. 3.7d) that there are four receiver voltage transients generated during each complete period (one positive pulse plus one negative pulse) of transmitter current flow. However, measurements are made only of those two transients that occur when the transmitter current has just been shut off. In this case accuracy of the measurement is not affected by small errors in location of the receiver coil. This feature offers a very significant advantage over FDEM measurements, which are generally very sensitive to variations in the transmitter coil/receiver coil spacing since the FDEM receiver measures while the transmitter current is flowing. For more details about TDEM resistivity sounding refernce is made to McNeill (1994).

Three types of equipment systems manufactured by Geonics limited, Ontario, Canada, were used for electromagnetic surveys done by US Geological Survey, (1993) at Al Ain area. The EM-34, is a frequency domain terrain conductivity meter (TCM) that uses a portable loop-loop receiver and transmitter configuration to collect conductivity data at three preset separation frequencies and two different loop orientations (McNeill, 1980, Fitterman and others, 1991). Six measurements are recorded at a series of stations spaced at intervals of 10, 20, and 30 m along a profile line. Results are used to produce geoelectric resistivity cross-sections with fair to good resolution to depths below land surface of about 40 m.

Two types of transient electromagnetic (TEM) systems were used to obtain vertical sounding with higher resolution and greater depths, relative to TCM surveys. The TEM systems use battery or generator driven transmitters to supply square wave direct current at two base frequencies into large wire loops lay on the ground. The on-off source current in the loop induces eddy currents in the subjacent ground; these currents decay as they diffuse downward and outward. The ground response, in turn, induces transient voltages in a receiver coil. These transient voltages, which are recorded digitally in 40 channels with prescribed time delays, are converted to apparent resistivities.

The EM-47 system uses a small loop (40 meters on a side), low transmitting current (3 amperes), and high frequencies to give high resolution soundings over a depth range of 0 to 100 m. Deeper soundings (extending to 300 m), but with lower-resolution, are provided by the large loop (100 to 200 m on a side), high transmitting current (30 amperes), and low frequencies of the EM-37 system.

Transient electromagnetic (TEM) data provided by NDC along some wadis crossing al Jaww Plain are used to determine the paleochannel geometry along these profiles and to map the depth of the conductive clay layer of Tertiary age that forms the base of the aquifer. Data presentation and discussions of results are given in chapter six.

3.4 Borehole Geophysics

3.4.1 General

Well logging methods are essential tools in groundwater exploration and development. In borehole geophysics, a suitable sensor is lowered to the bottom of the borehole and the logs are continuously recorded in terms of depth when the sensor (called 'Sonde) is drowning upwards gradually with a uniform speed.

Normally, logging is carried out in water wells as test boreholes recommended after through geological and surface geophysical surveys. Geophysical logs help understand the hydrogeology of the area clearly as the strata chart prepared from the mixed up samples recovered at the time of drilling is not reliable. While the logs are used for stratigraphic correlation from well to well, these may be used for detection of bed boundaries, porous and permeable zones, saline water bearing zones, fractured zones and groundwater flow pattern, having a strong bearing in groundwater development and management of large scale water supply schemes.

Electric resistivity and electromagnetic methods presented in the earlier sections help in the selection of drilling points recommended for test borehole in both hard and soft rock areas. The drilling points are recommended after the geoelectric section and the subsequence lithological sections are obtained on necessary correlation of data. As soon as the drilling of the borehole starts, well logging is carried out for in situ evaluation of the aquifer's characteristics through measured physical properties.

3.4.2 Logging in groundwater development

The subsurface geophysical methods (logging techniques) available for oil, water and mineral exploration are numerous (Nath et al., 2000). Of these, the following logs play an important role in detailing water wells and related groundwater development.

- Self potential (S.P) logging,
- Conventional resistivity logging (normal and lateral),
- Natural gamma and radioactive traces,
- Caliper logging (as a substitute for Caliper log, drilling time log is used for fractured zones) and
- Temperature logging (typical geothermal gradient of 1-1.3 °F per 100 feet is taken as a suitable for temperature log).

Other logs like neutron, sonic and gamma-gamma ray (density) logs known as porosity tools may be used. Table (3.1) lists the utility of geophysical logs used for groundwater exploration.

Surface electrical resistivity can be carried out to locate the drilling site for groundwater pumping. Once the borehole is drilled and geophysically logged, the formation water resistivity value can be used for noting the chemical quality of groundwater. The thickness of porous and permeable zones and their lateral extent obtained from geophysical surveys help in fixing the spacing and yield of wells, phasing the annual recharge and discharge of the aquifer causing no overdraft and minimizing mutual interferences among the

Table (3.1). Utility of geophysical logs for exploration of groundwater

TYPE OF LOG	UTILITY							
	WATER QUALITY	PERMEABILITY	POROSITY	WATER TABLE	LITHOLOGY	FORMATION CONTACTS	CORRELATION	BEDDING
CALIPER		?					?	
GAMMA-RAY					?	?	?	
SPONTANEOUS POTENTIAL	?	?						
DUAL INDUCTION	?	?		?		?	?	?
MICRO-RESISTIVITY	?	?						?
NEUTRON	?		?	?	?	?		
DENSITY	?	?	?		?	?		
SONIC		?	?	?	?	?		
PHOTO-ELECTRIC					?	?		
COMPUTER-PROCESSED	?		?	?	?	?	?	?

pumped wells. The well logging methods together with pump test play a dominant role in the development, planning and management of groundwater resources.

3.4.3 Logging in water wells

The methods listed in section (3.4.2) and implemented for water wells are elaborated in the following section.

3.4.3.1 S.P logging

S.P. is the self potential or spontaneous potential of electrochemical origin controlled by the concentration difference of the electrolytes in boreholes (drilling mud) and formations (formation water) within borehole drilled with fresh water mud. The S.P. (mV) across a porous and permeable bed is given by the expression:

$$S.P.\ (mV) = -K \log R_{mf}/R_w \qquad (3.14)$$

K is a constant, dependent on absolute temperature (value equal to 80 at 24 °C, for example), R_w is the resistivity of formation water and R_{mf} is the resistivity of the mud filtrate ($R_{mf} = 0.8\ R_m$) calculated from the resistivity of mud (R_m) at the corresponding temperature.

S.P. (always negative) log plotted to the record (Fig. 3.8) has three major applications: (i) definition of bed boundaries, (ii) correct location of porous and zones and (iii) determination of formation water resistivity (R_w). The total dissolved salt (TDS) may be calculated for the formation water in parts per million (ppm) from the empirical relation.

$$TDS = 0.64 * EC \text{ in micromhos/cm} \qquad (3.15)$$

Where EC = electrical conductivity of formation water given by,

$$EC = 10000/R_w \qquad (R_w \text{ in } \Omega\text{-m}) \qquad (3.16)$$

Once TDS is known, chlorinity of the water may be evaluated using the empirical relation.

$$\text{Chlorinity (in ppm)} = 0.6\ (TDS - 400\ ) \qquad (3.17)$$

When salinity of formation water is less than that of mud, positive S.P. anomaly is recorded. This is termed as S.P reversal (Fig. 3.8) and is an important diagnosis for fresh water aquifers, normally encountered in the coastal areas. When S.P. is used in combination with resistivity logs the following situation may occur.

i. No S.P and a high resistivity means: (a) NaCl concentration in the formation water and the borehole mud are the same, and (b) a hard non-porous bed which shows increase in resistivity but no S.P. to be resolved through sonic log.
ii. A strong negative S.P. but no distinct resistivity anomaly means a saline water aquifer.

3.4.3.2 Point resistance logging

This is the simplest and cheapest approach where a constant and regulated amount of current is fed through two spherical lead electrodes, one at the surface mud pit and the other in the borehole. Normally this is recorded simultaneously with S.P. log and plotted to the right side of the record. The measured resistance becomes proportional to the resistivity of the material close to the electrode. This is used for detection of resistive porous and permeable fresh water saturated zones against low resistivity adjacent shale and clay bed estimation of their thicknesses. The saturated zones interpreted from S.P. log are confirmed through point resistance log.

3.4.3.3 Resistivity logging (normal and lateral)

Beside point resistance, normal and lateral logs are used both for qualitative and quantitative interpretation in water wells. The apparent resistivities obtained from these logs give the true resistivity (R_t) of the formation. The $R_t = R_0$ (read from the log) is the resistivity of the bed completely saturated with formation water. Knowing R_0 from resistivity log and the value of R_w from S.P. log, resistivity formation factor (F) and porosity (φ) can be calculated from the relations:

$$F = R_0/R_w \tag{3.18}$$

$$F = (1/\varphi^2) \tag{3.19}$$

Where F is a measure of the tortuosity of the path for groundwater flow. Using Archie's relation $F = (a/\varphi^m)$ where $a = 1$ and cementation factor $m = 2$ the porosity (φ) of the formation is calculated using equation (3.19).

3.4.3.4 Natural gamma ray logging

This is the record of natural gamma ray intensity originating mainly from radioisotope Potassium-40 (K^{40}) present only in clay or shale. The shale or clay bed shows higher gamma ray counts compared to sand.

Gamma ray log is suitable for S.P. log, which becomes practically non-existent in case of holes drilled with saline mud. Thus, when S.P. log fails to demarcate bed boundaries of clay or shale from adjacent sand, gamma ray log is the only alternative. In hydrogeology, the volume proportion of shale in shaly sand is generally obtained from gamma ray intensity amplitude.

In tracer technique, weak radioactive sources like Bromine-82 (half life = 36 hours) and Iodine-131 (half life = 8 days) are used as the tracers for determination of the direction of the movement of the groundwater within borehole, through single hole and multiple hole measurements. Other logging tools like neutron, sonic and density, if available, may be used for determination of porosity of the aquifer.

3.4.3.5 Neutron log

Neutron log records the response due to neutron-capture gamma rays which depend on the hydrogen content of the formation. Hydrogen content is a measure of the porosity for non-shale sand. This method of logging is used to calculate the porosity.

3.4.3.6 Sonic log

Sonic log records the time required for a sound wave to travel through unit length of formation. The following expression is used for calculation of porosity for uniform intergranular porosity

$$\varphi = \frac{\Delta t_{log} - \Delta t_{matrix}}{\Delta t_{liquid} - \Delta t_{matrix}} = \qquad (3.20)$$

Where Δt's are the travel times (in microsecond) for unit length of formation (recorded from the log) matrix and the liquid filling the pores.

3.4.3.7 Gamma-gamma ray or density log

Gamma-gamma ray or density log measures the intensity of scattered gamma-rays which is dependent on the density of the formation. Both neutron and sonic logs are affected by shale content of the formation and the porosity values are altered considerably Density log, which is independent of chemical behavior and is not affected by shale contamination and is given by the following equation

$$\varphi = \frac{d_g - d_b}{d_g - d_f} x100(precent) \qquad (3.21)$$

Where, d_g is the grain density (gm/c^3) is known from the constituents of the formation (2.65 for sandstone, 2.70 for limestone and 2.85 for dolomite, for example); d_b is the bulk density is obtained from density log and d_f indicates the average fluid density.

As soon as the experimental borehole is drilled, logging of the borehole is carried out. This helps to define the total thickness of the aquifers and to determine strainers positions in wells.

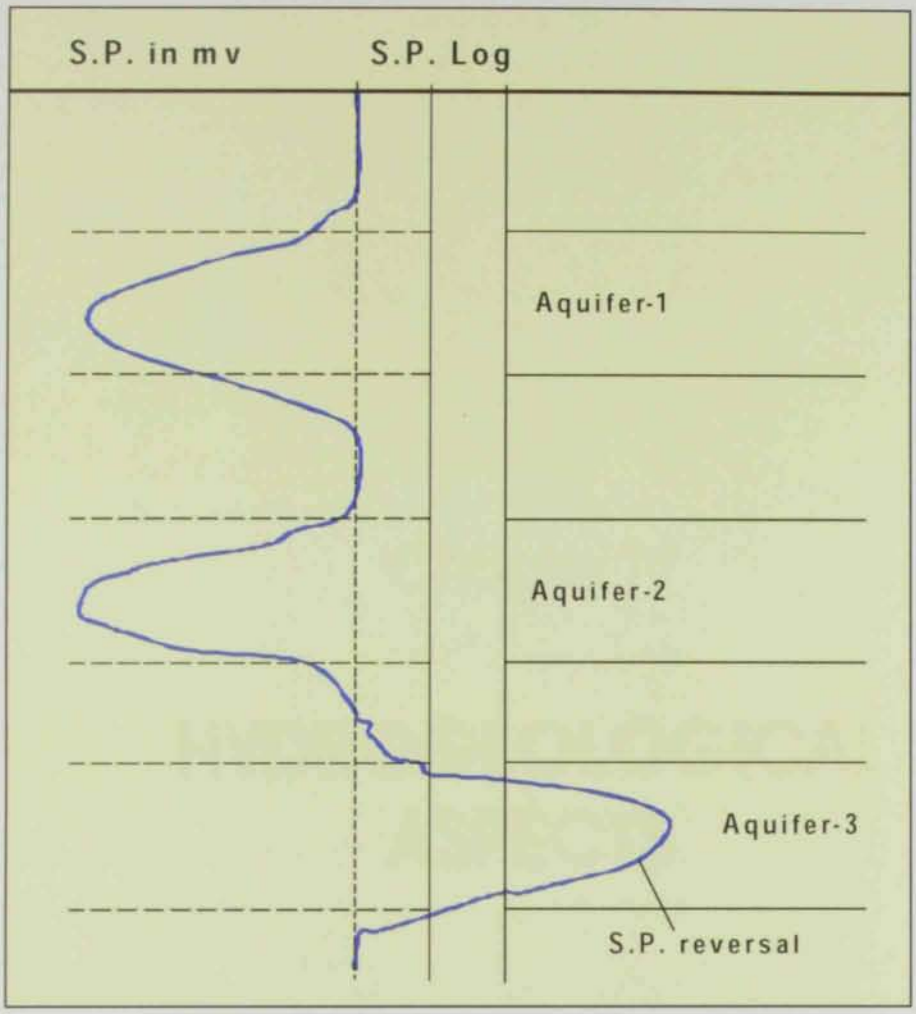

Fig. (3.8) A typical S.P. record (modified after Nath et al., 2000).

Chapter IV

HYDROGEOLOGICAL ASPECTS

HYDROGEOLOGICAL ASPECTS

4.1 General Outline

The study area is located in the southeast of Al Ain city and comprises Al Jaww Plain which is bounded by Oman Mountains range from the east and Jabel Hafit from the west (Fig. 1.6).

All of the major wadis crossing Al Jaww Plain originate from the Oman Mountains range (Fig. 4.1a&b) which forms the catchment and feeding area of the water resources in the investigated area. These catchments areas are made up of barren high mountains and hills rising up to elevations of 1500 m and is relatively impervious except for fault zones. The narrow valley is filled with alluvium and the intra mountain flat areas are covered with extensive gravel deposits.

Al Jaww Plain is a large spread of an area made up of gravel and sand outwashes from the Oman Mountains and deposited in the main wadies including Al Ain, Shik and Hamad which traverse the plain (Fig. 2.4).

The gravel progressively diminishes in size away from the hills and is replaced by thicker deposits of fine sands and silts. The vegetation is sparse comprising low trees (Fig. 4.1c).

All the rocks of Al Jaww Plain in Al Ain area are sedimentary including massive, fossiliferous Tertiary limestone of Lower Eocene, limestone with intercalations of Pelagic blue grey marls, gypsum and gypsiferous marls of Miocene age overlain by marls and clays with conglomerates of the Fars Formation. The latter forms the base of the Quaternary to recent deposits which include the aquiferous zones of the study area.

The main structural elements of the region is the two anticlines formed by Jabal Hafit and Jabal Huwayiah outcrops (Fig. 2.4). The younger rocks in Al Jaww Plain and in other basins complementary to the anticlines are deposited in sequence around these two main structures.

Jabal Hafit structure plunges northward from the Al Ain area while the Jabal Huwayiah plunges southward beneath the Al Jaww Plain. These structures have influenced the subsurface geology of the plain, especially through the synclinal area which has been formed between them. The Fars Formation which forms the base of the Quaternary aquifers

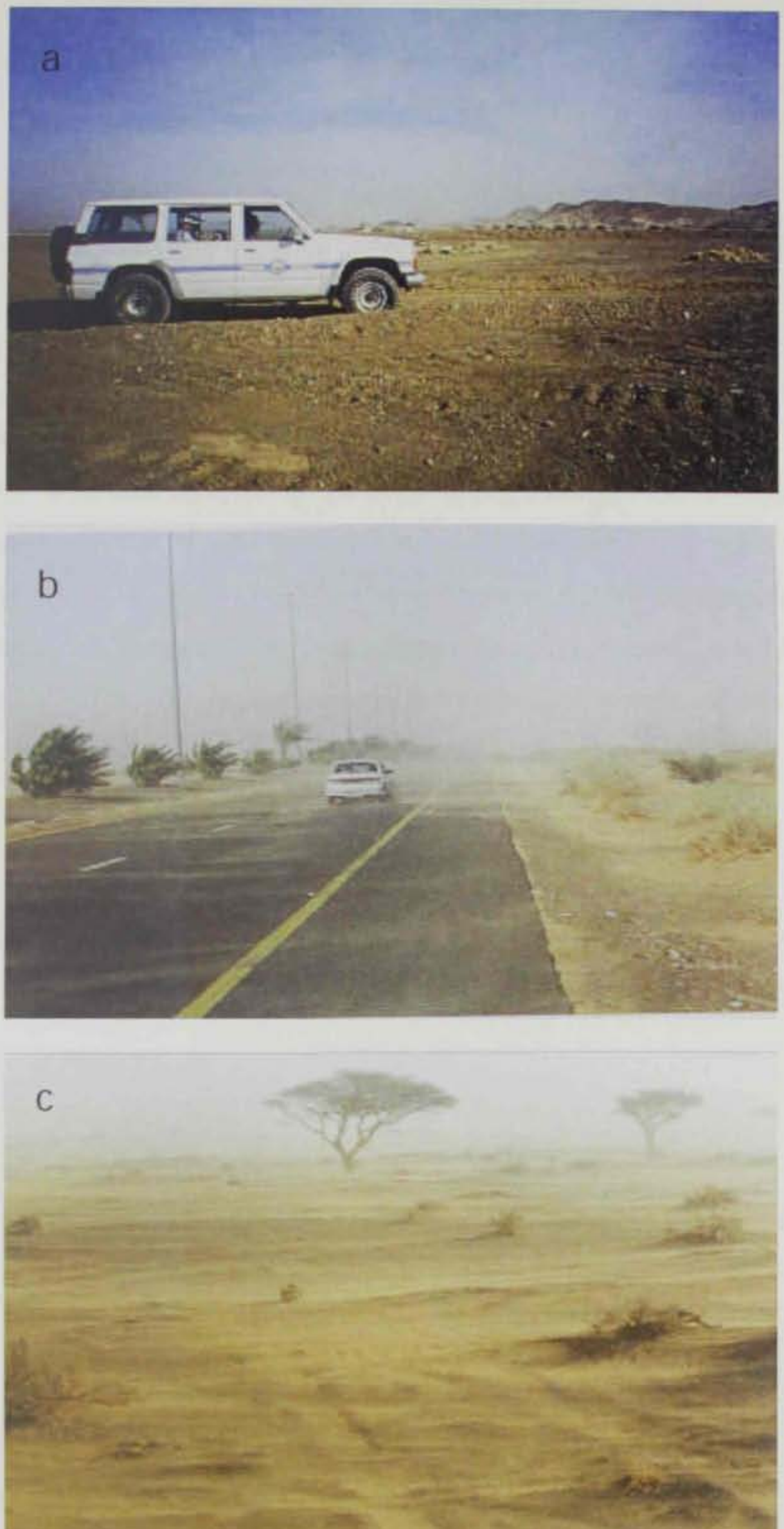

Fig .(4.1) Photos of Al Jaww Plain.

deposits is thickest in the axial region of the syncline while the subsurface folding of the Tertiary rocks has controlled the thickness of this formation.

4.2 Climate

The meteorological data, given in Table (4.1) are compiled from the data obtained from the Department of Civil Aviation (Abu Dhabi International Airport) for Al Ain International Airport meteorological station. Generally, the study area is characterized by dry arid conditions. The analysis of the climate data of Al Ain area is given below.

4.2.1 Temperature

The mean maximum temperature is 46.7 °C and was in June 1998, while the mean minimum temperature is 10.8 °C and was recorded in January 2001 (Fig. 4.2 a through c) and Table (4.1). Fig. (4.2b) indicates that the monthly mean maximum temperature is 38.1°C which was recorded in August 1998. The monthly mean minimum is 17.2 °C and was recorded in January 2001. The highest maximum temperature is recorded between June and September. The temperature variation from one year to another is relatively small.

4.2.2 Rainfall

Al Ain lies in an arid desert belt which is characterized by low rainfall (less than 150 mm/y). The main rain falls between November and March but the maximum is during January and February. Fig. (4.3a) shows the histogram of rainfall for the period from 1994 to 2002.

The wettest year was 1996, where the total annual rainfall reached 162.5 mm. While the driest year was 2001 as no rainfall was traced. Years 1995 and 1997 are regarded rainy years as the rainfall reached to 119.8 and 134.9 mm, respectively. Fig. (4.3b) shows group of total monthly rainfall at Al Ain for the period from 1994 to 2002. It could be concluded that the main rain falls between January and March. In summer months the rain is rare and if exists it would be in the order of a few millimeters. However, in July of 1995 the rainfall reached about 48.8 mm (Fig. 4.3b).

4.2.3 Humidity

Although, Al Ain area is located in a non coastal area, the humidity is relatively high. The mean maximum humidity value recorded in Al Ain International Airport in the period 1994-2002 is 92% and was recorded in January 1998. The minimum humidity value is 9% and was recorded in June 2000 (Fig. 4.4 a through c). However, there are seasonal differences

Table (4.1) Summary of meteorological data at Al Ain International Airport from 1994 to 2002.

A) MONTHLY TOTAL RAINFALL (mms) AT AL AIN (1994-2002).

YEAR	JAN	FEB	MAR	APR	MAY	JUN	JUL	AUG	SEP	OCT	NOV	DEC	Total
1994				0	0	0	6	0	7.8	0	0	0	13.80
1995	0	14.8	40.8	1	0.5	0	48.8	1.1	0	0	0	12.8	119.80
1996	77.3	0.6	63.3	Trace	0	10.6	4.2	4.7	0	0	0.6	1.2	162.50
1997	53.5	0	55.9	9	0	0	Trace	Trace	0	3.4	4.4	8.7	134.90
1998	28.2	30.5	7.6	5.3	0	0.4	Trace	7	Trace	0	0	0	79.00
1999	Trace	Trace	16.8	0	3.6	0	0	1.8	Trace	0	0	0	22.20
2000	Trace	0	Trace	0	0	0	17.3	Trace	0	3.4	Trace	10.6	31.30
2001	Trace	0	Trace	0	0	0	Trace	0	Trace	Trace	0	0	Trace
2002	0	0	24.9	10.8	1.8	0	0	0.8	Trace	0	1.3	0.2	39.80

B) MAXIMUM RAINFALL IN 24 HOURS (ONE DAY) (mms) AT AL AIN (1994-2002).

YEAR	JAN	FEB	MAR	APR	MAY	JUN	JUL	AUG	SEP	OCT	NOV	DEC	Maximum
1994													
1995													
1996	17.7	0.6	24.1	Trace	0	9.6	2.4	4.5	0	0	0.6	1.2	24.10
1997	46.2	0	30.4	5.8	0	0	Trace	Trace	0	3.4	3.2	8.7	46.20
1998	5.2	16.3	7	5.2	•	0.4	Trace	6.8	Trace	0	0	0	16.30
1999	Trace	Trace	16.8	0	3.4	0	0	1.2	Trace	0	0	0	16.80
2000	Trace	0	Trace	0	0	0	17.3	Trace	0	3.4	Trace	10.6	17.30
2001	Trace	0	Trace	0	0	0	Trace	0	Trace	Trace	0	0	Trace
2002	0	Trace	19.7	6.8	1	0	0	0.4	Trace	0	1.3	0.2	19.70

C) MEAN DAILY DRY BULB TEMPERATURE (DEG. C) AT AL AIN (1994-2002).

YEAR	JAN	FEB	MAR	APR	MAY	JUN	JUL	AUG	SEP	OCT	NOV	DEC	Average
1994				28.7	32.7	35.2	34.9	36.3	33.1	29.2	25.3	19.7	30.51
1995	18.5	19.8	21	26.9	32.1	34.7	33.1	36.5	33.4	30.2	24.2	20.2	27.55
1996	18.5	20.7	23.4	28.5	34.1	35.3	38.1	36.3	33.4	28.7	23.4	19.3	28.31
1997	17.5	19.9	21.5	25.7	32	35.7	35.6	35.9	34.7	30.3	24	19.7	27.71
1998	17.8	20.4	24.7	29.2	34.1	37.9	37.8	37.4	35.2	31	25.3	22.8	29.45
1999	19.1	22.6	23.1	29.9	33.2	37.2	37.1	38.1	34.3	30.3	25.4	20.5	29.23
2000	19.3	19.6	22.6	31.3	32.9	35.2	37.6	37.2	33.4	30.1	24.6	20.1	28.68
2001	17.2	19.7	24	28.6	34.4	35.7	36.9	37.1	34	30.5	24.3	23.1	28.79
2002	19	19.9	24.8	28.3	34.6	35.8	37.1	36.7	34.2	30.7	24.3	20.7	28.80

D) MEAN DAILY MAXIMUM DRY BULB TEMERATURE (DEG. C) AT AL AIN (1994-2002).

YEAR	JAN	FEB	MAR	APR	MAY	JUN	JUL	AUG	SEP	OCT	NOV	DEC	Average
1994				37	41.4	44.3	43.6	43.9	41.3	36.8	32.4	26.3	38.56
1995	25.7	26.7	28	35	41.4	44.7	41.9	44.3	41.7	38	31.7	25.9	35.42
1996	24	27.7	29.8	37.1	42.2	43.7	46.3	44.2	41.5	36.7	30.6	26.4	35.85
1997	23.9	27.1	27.7	33.3	40.8	44.2	44.1	44.6	43.2	37.7	30.2	25.9	35.23
1998	23.5	26.8	32.3	37.7	42.6	46.7	45.9	45	42.7	38.5	33.1	30.3	37.11
1999	26	29.7	30.7	38.9	43.1	46.4	45.2	46	42.2	38.5	32.9	28.1	37.31
2000	26.3	27.4	31.3	40.2	43.1	44.6	46	45	41.1	37.6	31	26.9	36.71
2001	24.3	27.3	31.8	37.5	43.4	44.4	44.5	44.8	42	38.1	31.6	30	36.64
2002	25.5	27.1	32.1	36.3	43.2	44.7	45.5	45.1	42.2	38.5	31.2	27.1	36.54

E) MEAN DAILY MINIMUM DRY BULB TEMERATURE (DEG. C) AT AL AIN (1994-2002).

YEAR	JAN	FEB	MAR	APR	MAY	JUN	JUL	AUG	SEP	OCT	NOV	DEC	Average
1994				21.2	24.8	26.9	28.5	30.1	26.1	23	19.6	13.4	23.73
1995	12.7	13.8	15.7	19.8	23.8	25.7	26.5	30.2	26.2	23.3	17.8	16	20.96
1996	13.9	14.9	18.2	20.5	26	28	30.9	29.6	26.4	21.7	17.2	13.1	21.70
1997	11.8	13.9	16.1	19.1	23.5	27.8	28.7	28.5	27	24	18.8	14.5	21.14
1998	12.9	14.7	18.1	21.2	25.9	29.9	30.9	30.7	28.3	24.7	18.5	16.1	22.66
1999	12.9	16.5	16	21.4	24.3	28.4	29.7	31.4	27.5	23.1	19.3	14.1	22.05
2000	13.3	13.1	15.2	23	23.8	26.3	30.5	30.6	27	23.3	19.1	14	21.60
2001	10.8	12.7	16.3	20.1	25.6	27.3	30.3	30	26.9	23.4	18.1	17.4	21.58
2002	13.2	13.2	18.1	20.6	26	27.8	28.8	29.2	27.1	23.5	18.2	14.8	21.71

F) MEAN MAXIMUM RELATIVE HUMIDITY % AT AL AIN (1994-2002).

YEAR	JAN	FEB	MAR	APR	MAY	JUN	JUL	AUG	SEP	OCT	NOV	DEC	Average
1994				49	50	56	70	60	65	63	74	79	
1995	56	81	87	57	49	63	81	57	66	67	78	88	
1996	88	84	83	62	44	68	49	56	76	71	77	82	70.17
1997	90	83	85	75	52	61	73	78	70	74	84	88	76.08
1998	92	86	77	66	50	50	57	54	63	67	85	88	69.58
1999	87	84	79	58	59	48	63	48	65	77	81	83	69.33
2000	89	85	79	53	62	60	40	43	64	70	73	85	66.92
2001	86	82	74	54	46	57	53	44	63	71	76	78	65.33
2002	76	75	67	65	47	56	52	61	66	68	73	75	65.08

G) MEAN DAILY TOTAL EVAPORATION AT AL AIN (1994-2002).

YEAR	JAN	FEB	MAR	APR	MAY	JUN	JUL	AUG	SEP	OCT	NOV	DEC	Average
1994				14.9	18	19.7	15.5	16.9	15.4	12.6	8.7	6.5	14.24
1995	5.7	7.5	8.5	14.5	19.9	19.8	15.4	18.5	16.2	13.7	8.5	5.3	12.79
1996	5.1	7.6	10.3	15.7	20.1	18.9	21.5	18.3	16.3	13.1	8.9	6.3	13.51
1997	5.5	8.8	8.5	12.9	20.4	21.3	18	18.1	17.2	13.6	7.6	5.9	13.15
1998	5.2	7.8	12.8	17	20.4	21	21.9	20.4	17.7	14	8.7	7.1	14.51
1999	6.4	8.8	11.8	17.1	19.4	22	19.7	21.1	16.9	13	8.9	6.9	14.33
2000	6.7	8.1	12	17	19.1	19.6	20.4	19.3	15	12.9	9	6.5	13.80
2001	6.3	8	11.4	15.6	19.3	19.1	19.4	20.1	16.5	13	9.1	7	13.75
2002	7.1	9	11.7	15.8	18.9	20.4	20.3	18.1	17.1	13.6	8.7	7.1	14.07

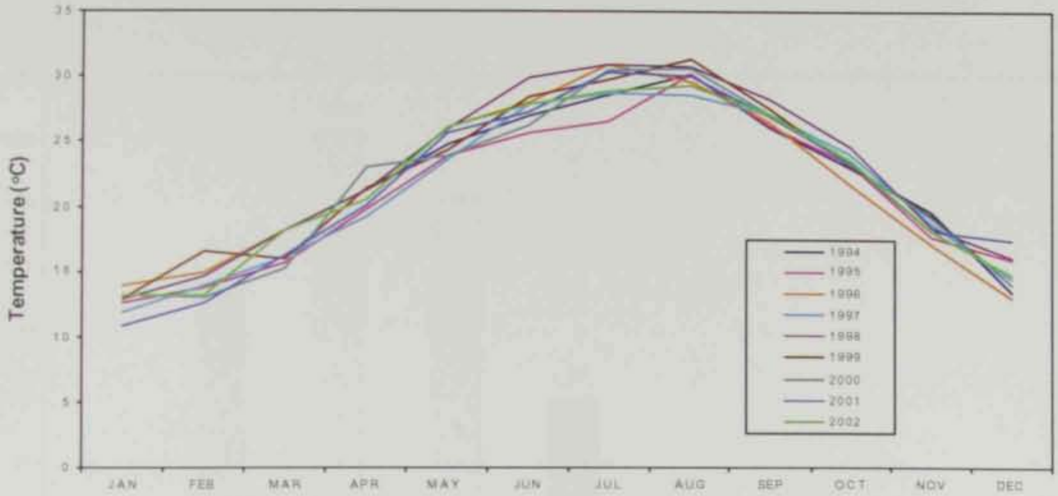

Fig. (4.2a) Mean minimum temperatures at Al Ain (1994-2002).

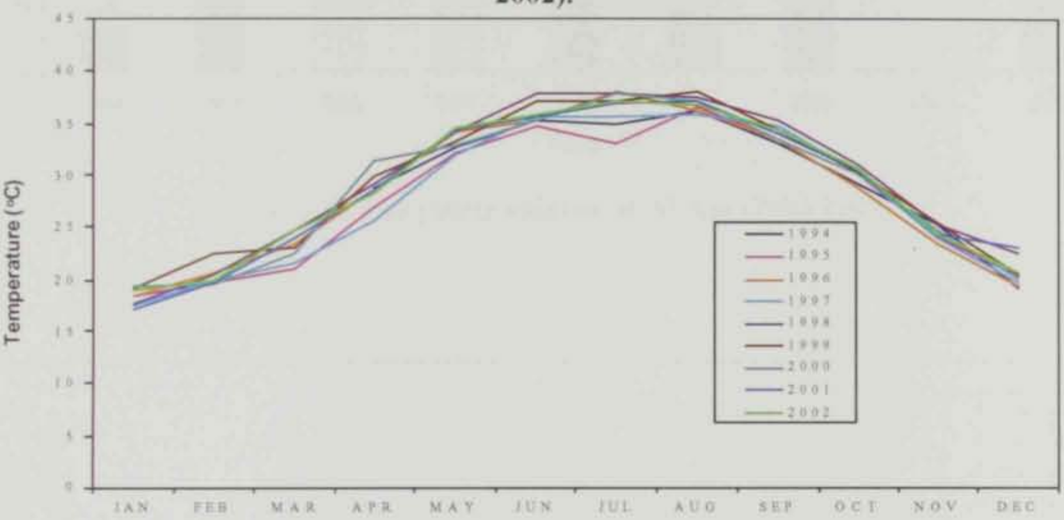

Fig. (4.2b) Mean temperatures at Al Ain (1994-2002).

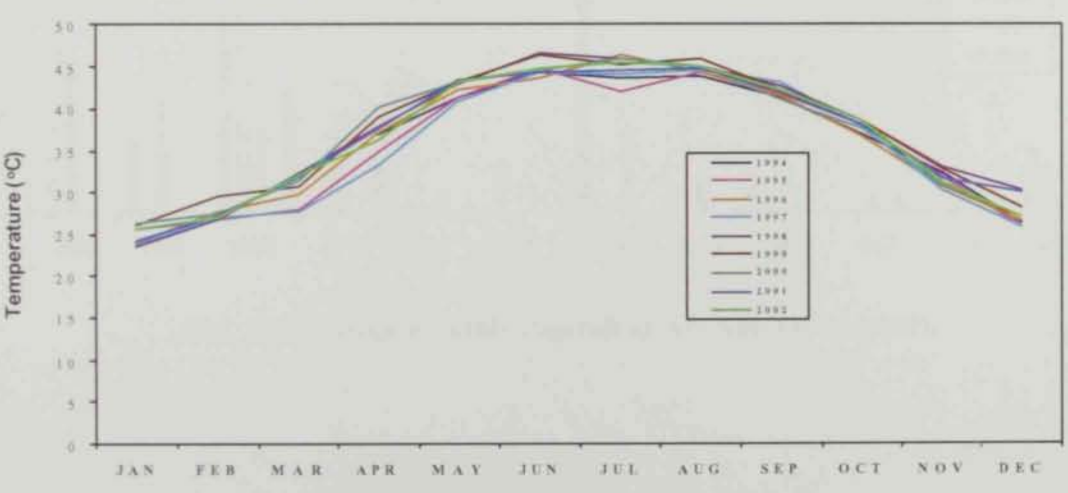

Fig. (4.2c) Mean maximum temperatures at Al Ain (1994-2002).

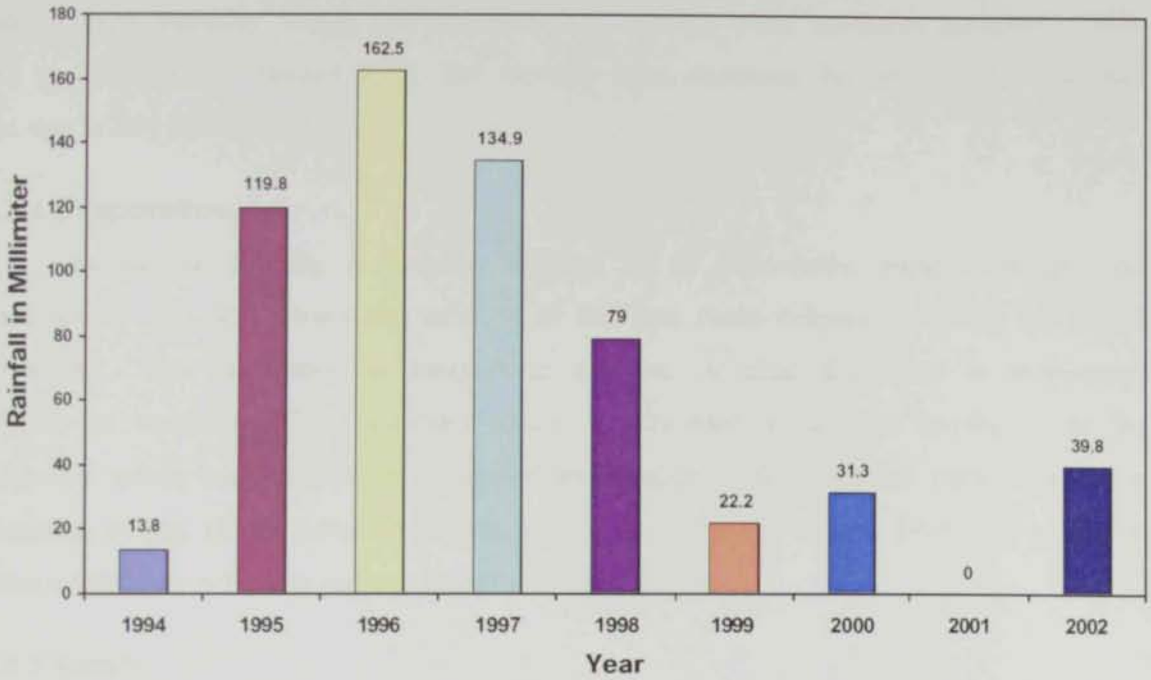

Fig. (4.3a) Total yearly rainfall at Al Ain (1994-2002).

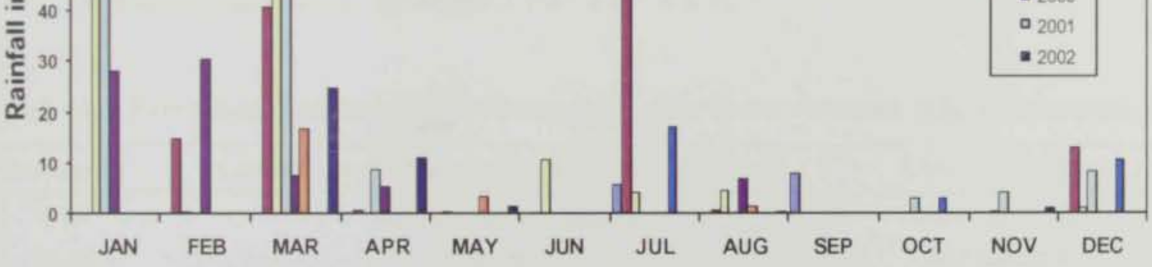

Fig. (4.3b) Total monthly rainfall at AL Ain (1994-2002).

in the winter months which are associated with higher humidity's value while in the summer months small humidity values are noticeable. The monthly mean maximum humidity is 74% and was recorded in January 1998. The monthly mean minimum humidity is 25% recorded and was in July 2000 (Fig. 4.4b).

4.2.4 Evaporation

Evaporation intensity is generally affected by air temperature, relative humidity and wind speed. Fig. (4.5) shows the variation of the total mean evaporation during the period 1994-2002. The evaporation is irregular in duration. A clear fluctuation in evaporation intensity is recognized. The maximum values are recorded in summer months, while the minimum values are recorded in December and January. The maximum mean evaporation according to Fig. (4.5) reached to 22 mm and it was recorded in June 1994. The minimum mean evaporation is 5.1 mm and was recorded in January 1996.

4.2.5 Aridity

Using the data obtained from meteorological station of Al Ain International Airport and applying the Emberger formula (1955), the mean degree of aridity (Q) is determined as follow:

$$Q = [100 \times R / (M+m)(M-m)] \quad (4.1)$$

Where: R is mean total annual rainfall (mm/year).

M is mean maximum temperature of the hottest month

m is mean minimum temperature of the coldest month.

The aridity scale used by Emberger is shown in Table (4.2).

Table (4.2) Prevailing climatic conditions corresponding to the different values of dryness.

Value of Q	Corresponding annual rainfall intensities (mm/year)	Climatic conditions
0-20	0-200	Desert conditions
20-45	200-400	Arid conditions
45-65	400-800	Semi-arid conditions

Applying the above formula, it is concluded that the study area belongs to the desert conditions domain.

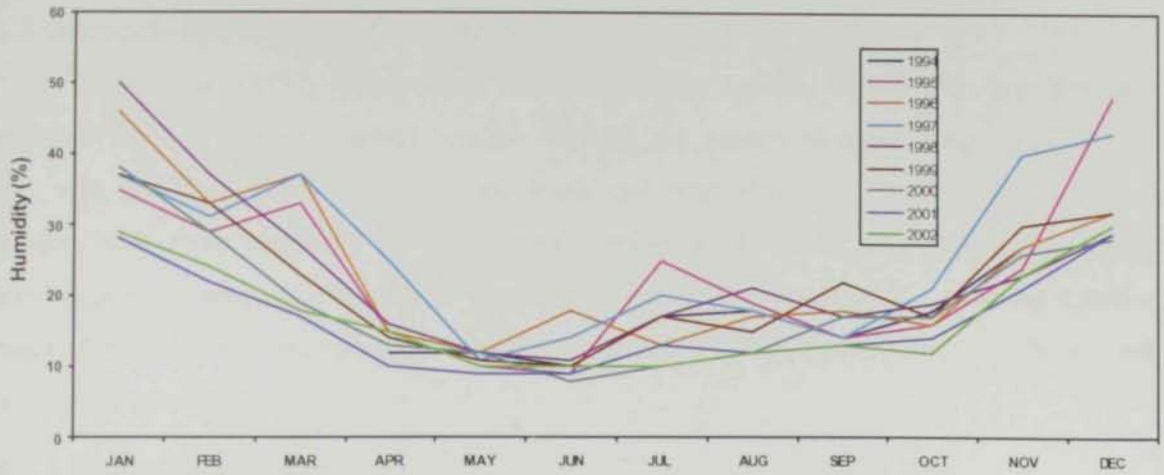

Fig. (4.4a) Mean minimum relative humidity at Al Ain (1994-2002).

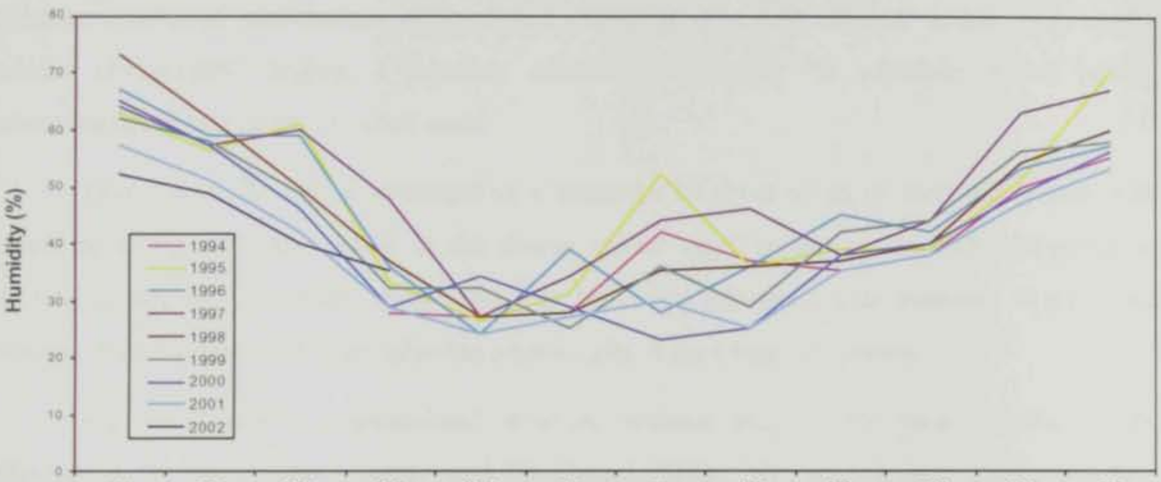

Fig. (4.4b) Mean humidity at Al Ain (1994-2002).

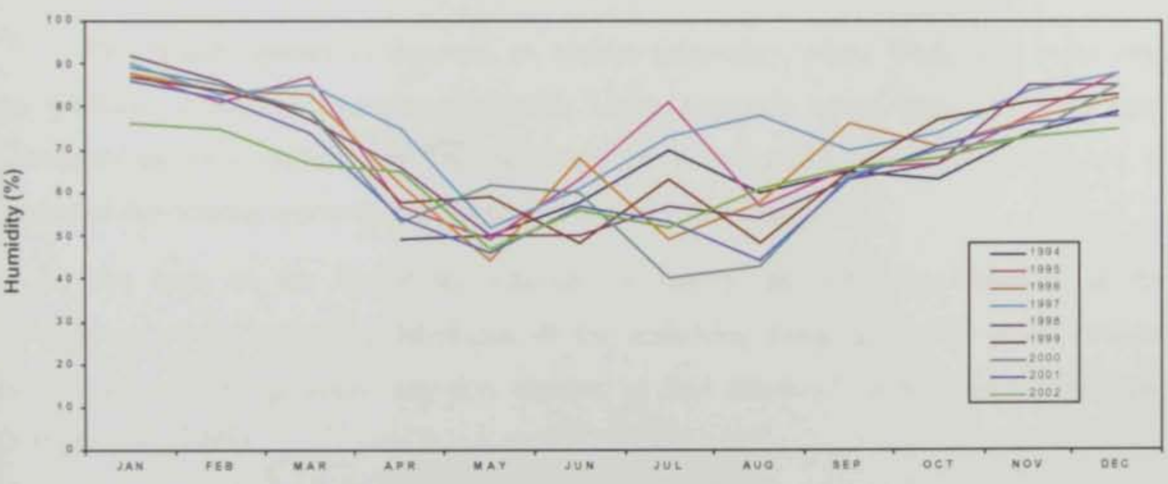

Fig. (4.4c) Mean maximum humidity at Al Ain (1994-2002).

4.3 Groundwater Bearing Formation

Rizk et al., (1997) reported that the main existing aquifers in the UAE are, fractured ophiolite rocks in the east, gravel aquifers flanking the eastern mountain ranges on the east and west and sand dune aquifers in the south and west (Fig. 4.6). A discussion on these aquifers with more emphasis on the aquifers existing on the study area (Quaternary aquifer and Jabal Hafit limestone aquifer) is provided hereafter. For more details about the different types of aquifers in UAE, reference is made to Garamoon, 1996, Bakhit, 1998, and Rizk 1999 and Alsharhan et al., 2001.

4.3.1 Quaternary aquifer

The most important aquifer in the study area is the Quaternary aquifer. Quaternary-age deposits consist of near-surface and surficial sediments of mixed alluvial, aeolian and locally, sabkha (Evaporates) origins. Quaternary alluvium represents the principle water bearing lithostratigraphic unit relative to other units.

Quaternary alluvium is composed of a sequence of about 60 m of sand and gravel with interbeds of silt and clay. Most of the coarse clastic units contain a clay-rich matrix that is usually calcareous. The bulk of the alluvium has been deposited after transport within wadi systems draining westward from ophiolitic source rocks in the Oman Mountains.

Fig. (4.7) shows a generalized structure contour map of the basal contact of the alluvium in Al jaww Plain (Menges and Woodword, 1993). This map depicts a generally low-relief surface that contains a significant westerly directed trough on the eastern margin of the plain near Jabal Zarub.

This trough appears to represent an incised paleovalley where Wadi Shik exists onto the piedmont through a bedrock gap in the Oman Mountain range front. Thus, the sub-Quaternary erosional surface may have developed by lateral stream planation between loci of marked of downcutting approximately coincident with modern drainages.

The base of the Quaternary alluvium is usually an abrupt unconformity at the juxtaposition of the contrasting lithologies of the underlying Neogene section which contains clastic sections with generally clay-rich textures at thin dispersed sand or gravel interbeds (Menges et al., 1993).

Quaternary alluvium deposited across an erosional unconformity cut across a variety of Tertiary to Cretaceous rocks underlying the piedmont along the western front of the Oman

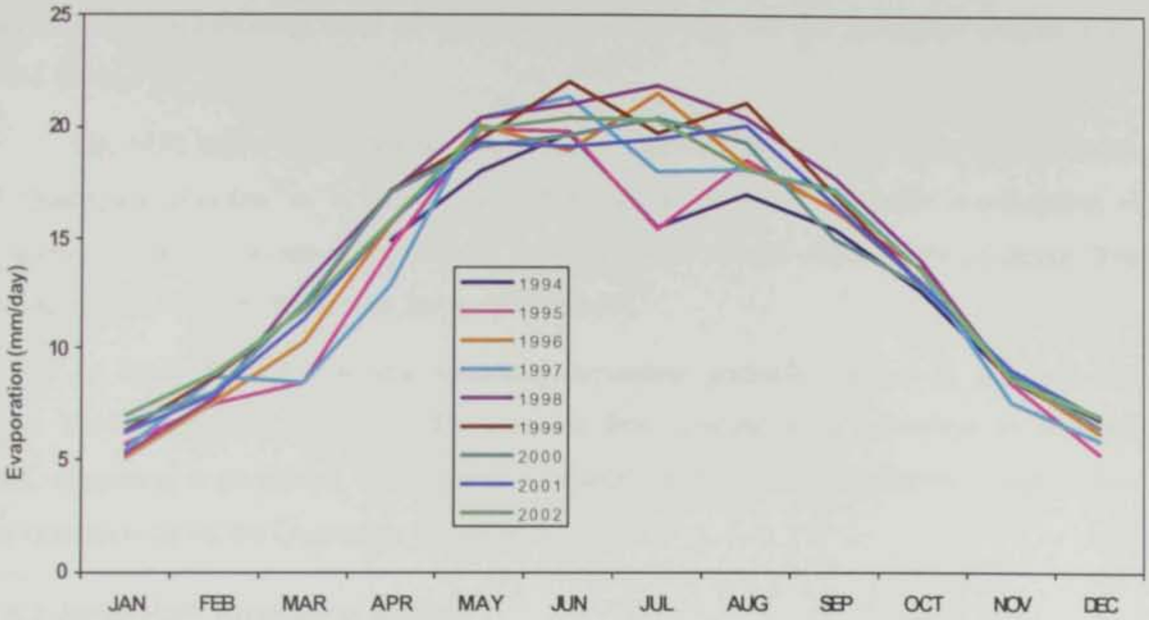

Fig. (4.5) Mean total evaporation at Al Ain (1994-2002).

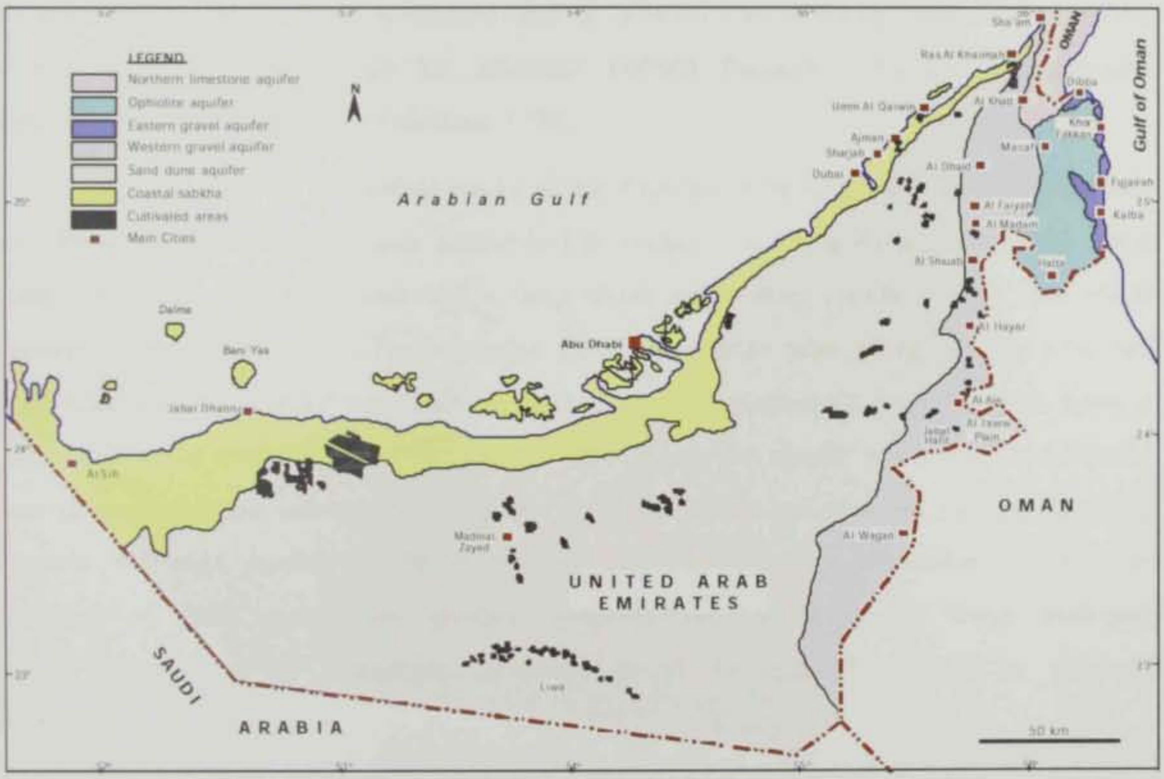

Fig. (4.6) The main water bearing units (aquifers) in the United Arab Emirates (after Rizk et al., 1997).

Mountains. This erosional surface discordantly truncates older rocks including folded and locally faulted sedimentary rocks of Eocene to Miocene age; see the geological sections (Fig. 4.11a through d).

Fig. (4.8) shows the thickness of Quaternary alluvium in Al Jaww Plain. The thickness of Quaternary alluvium in Al Jaww varies from 12 to 50 m. The thicker accumulation of Quaternary alluvium occurs at the bedrock gabs along the eastern edges of the piedmont. The alluvium irregularly thins to the west across the piedmont.

Al Jaww Plain has several westward decreasing gradually wedges of sediment with radial fan-like geometry pieces of the sediment fans coincide with palevalleys at the wadi gaps, suggesting a persistence in the general location of drainage and sediment dispersal from the mountains during the Quaternary (Bown et al., 1991).

4.3.2 Jabal Hafit limestone aquifer

Jabal Hafit is composed of 1500 m thick limestone and marl interbeds with gypsum and dolomite and evaporate formations of Lower Eocene to Miocene age. Limestone of the Middle Eocene of Dammam Formation constitutes an aquifer in Jabal Hafit. The aquifer is characterized by extensive dolomitization and is affected by numerous faults and fractures. Porosity is virtually nill except for infrequent unfilled fractures, vugs and heterogeneous secondary porosity (Whittle and Alsharhan, 1994).

Fig. (4.9) shows a conceptual model of the three water bearing zones in the Jabal Hafit area. These are: a fresh water zone replenished by meteoric water, a mixing zone where fresh water mixes with brackish water, and a deep saline water zone (White, 1977). The model supports a mixture of two different sources fresh water from rain falling on the Jabal and saline water moving upward from 2000 m deep by gas or temperature drive. Brackish water is formed due to the mixing of the two types of water. Then, the aquifer water cools and become more dilute. For more information about the geometry and distribution of geologic units that comprise the main aquifer of the study area and the structural deformation affecting the hydrology of these units, some geologic cross-sections are developed. These geological sections guided with the stratigraphic sequence in Al Ain area (Table 4.3) are discussed below.

The subsurface of Al Jaww Plain based on seismic interpretation has been discussed in chapter two. The Pre-Quaternary bedrock underlying Al Jaww Plain is deformed by a series

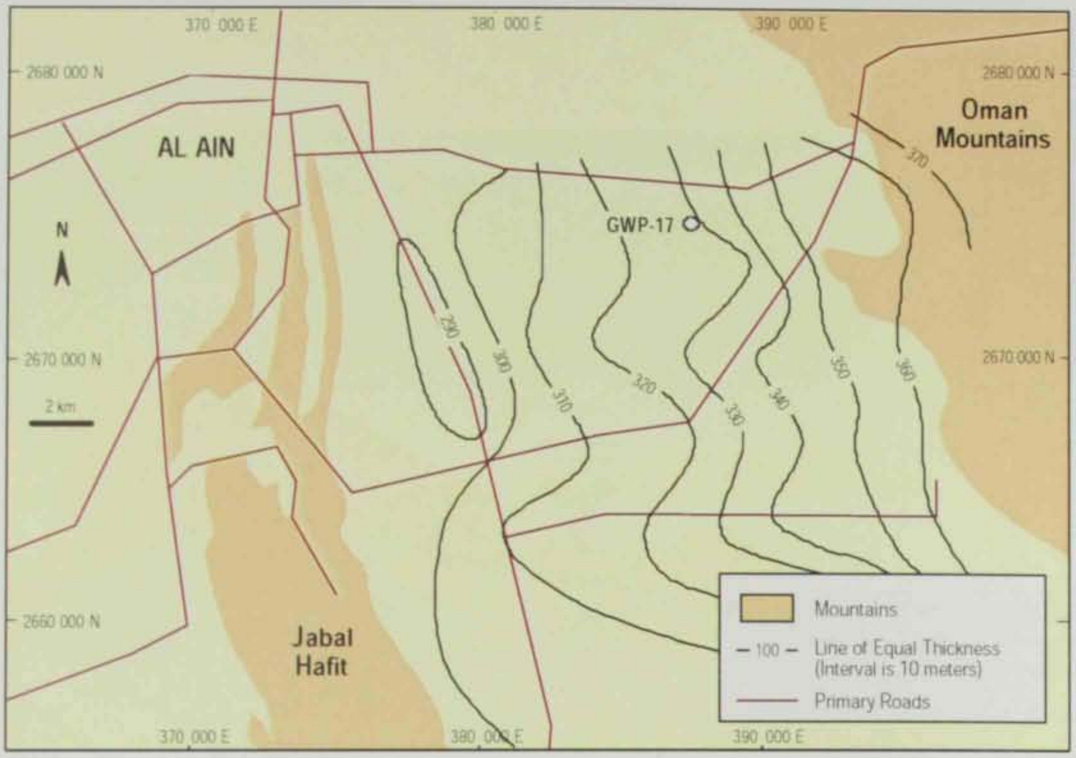

Fig. (4.7) Base of Quaternary alluvium in Al Jaww Plain (modified after USGS, 1993).

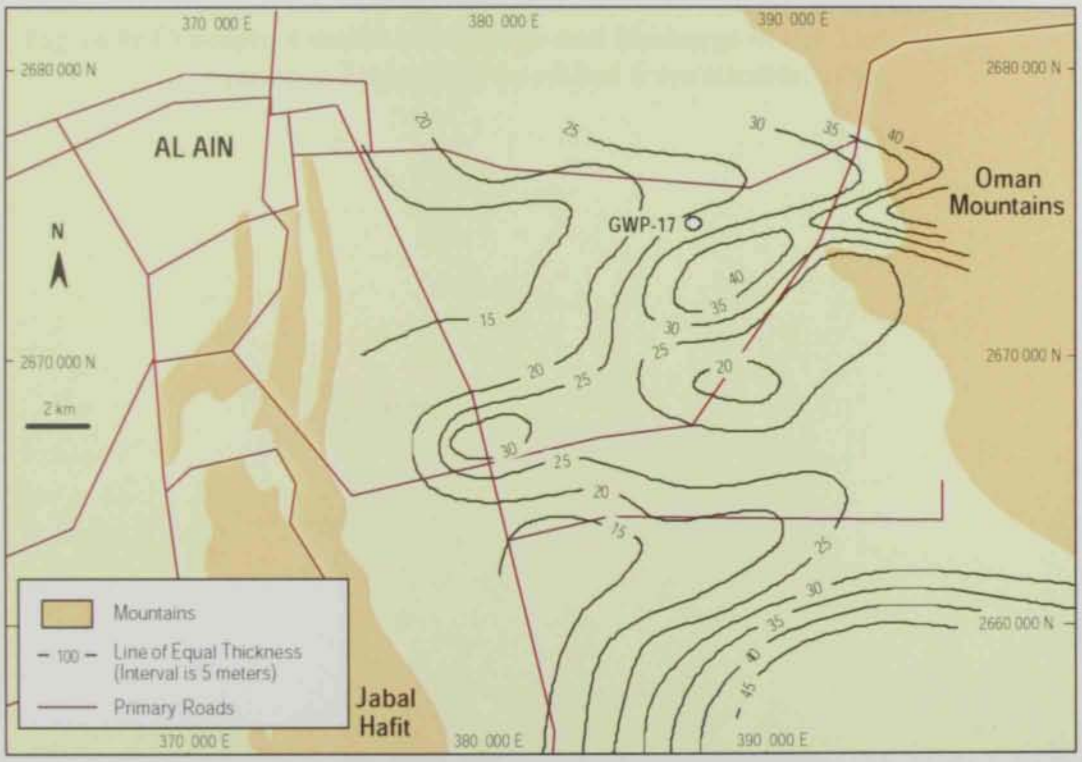

Fig. (4.8)Thickness of Quaternary alluvium in Al Jaww Plain (modified after USGS, 1993).

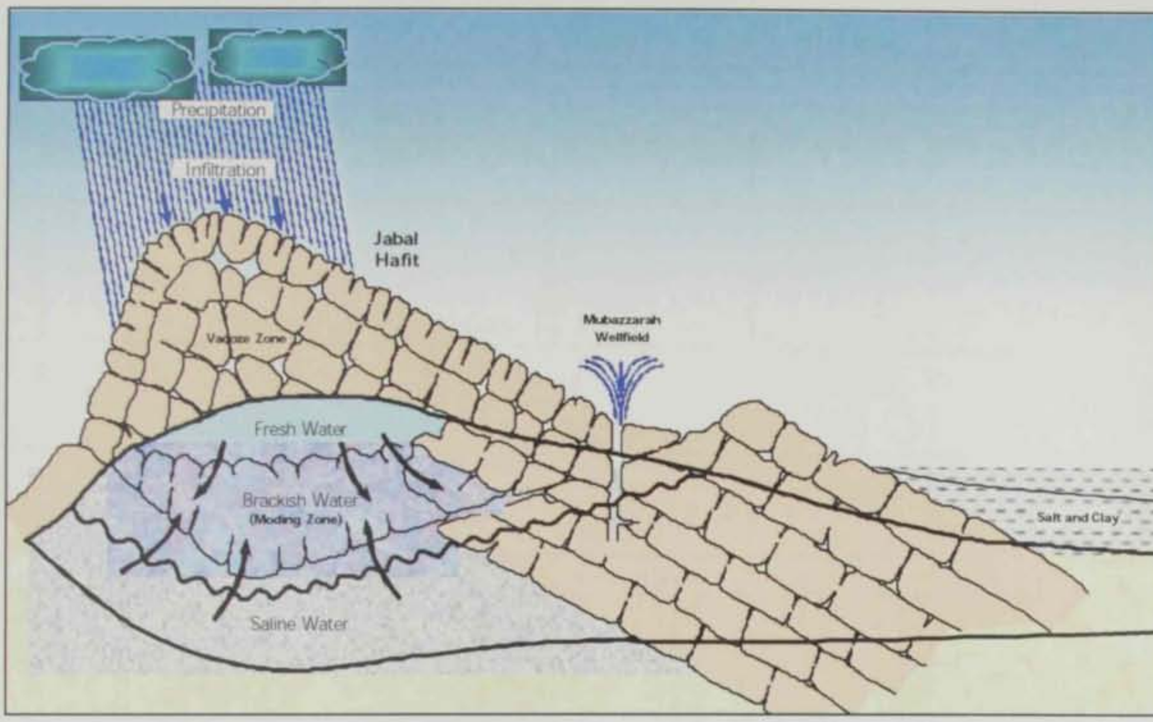

Fig. (4.9) Conceptual model of recharge and discharge of the Tertiary limestone aquifer at Jabal Hafit (modified from Khalifa, 1997).

Table (4.3) Geological formations and their water bearing properties in Al Ain area, (after Gibb et al., 1970).

AGE			FORMATION	UNIT SYMBOL INTERIM REPORT	UNIT SYMBOL THIS REPORT	LITHOLOGY	SURFACE EXTENT, THICKNESS	GROUNDWATER POTENTIAL
QUATERNARY-RECENT				Q	Q	Calcium carbonate cemented pebble gravel and conglomerates, with clasts of ultrab-basic rocks, limestone and cherts includes Sabkhas& aeolian sand. Increasing content of calcium carbonates, silt and clay to the south and west of Al Ain. Degree of alteration of clasts increasing towards Bu Samarah	Extensive at surface. Gravels of mountain front derived from Hawasina and Semail rock weathering. Gravels up to 43m (TW1A) in Al Jaw plain. Lateral equivalents of gravel to west of Al Ain are highly cemented, argillacous, calcareous and up to 600m thick	Main exploted aquifar in Al Ain district, unconfined, permeability decreasing away from mountain front and recharge channels water fresh to slightly brackish but saline west of Jabal Hafit. yields are high in north Al Jaww Plain recharge channel
TERTIARY	PALEOGENE	MIOCENE	Lower Fars	Td	Tc2	Upper part or post-gypsum Fars pink brown mottled marls and clays with conglomerates	Widespread in Al Jaww Plain poorly expossed on the surface may exceed 150m thickness	Acts as aquiclude to Unit **Q** aquifer
				Tc	Tc1	Evaporites sequence. Gypsum anhydrite-halite with blue-grey marls overlying hard massive limestone	Base marked by oolitic limestone (possibly the base of the Miocene marker at 377m in BH2 Encoun tered in deep Fars basins in Al Jaww Plain	Gypsum layers contain brackish to saline water, confined except near zones of leakage from unit Q. aquifers and outcrop, permeability very low
	NEOGEN	OLIGOCENE	?		Tb2	Calcareous clays and thin limestone	Exposed on flanks of Jabal Hafit with northwards continuation	None
					Tb1	Intercalated fossiliferous limestone and blue-grey marls overlying hard massive limestone. Often rich in Nummulites	in structure at depth. Encountered in shallow sub surface in north Al Jaww Plain. Underlies oolite marker in BH2. Probably underlies Fars Formation in south Al Jaww Plain	Fossliferous limestone layers are hydraulically connected with unit Q aquifers in north Al Jaww Plain but permeability is very low. Cavernous limestone connected with unit Q aquifer in Mutarah Muweyql area
MESOZOIC		Lower Eocene? Middle Eocene? Upper Eocene	u/ c? Dammam	Tb	Ta2	Intercalated limestone and pelagic blue-grey marls, part gypsiferous with underlying brown fossiliferous crystalline limestone, with shale Cherty at base	Extensive in subsurface. At least 210m thick in BH 15. Occurs below 600m in south Al Jaww Plain	Fractured and very permeable limestone part of unit Q aquifer at BH14 but between Mutarad and Al Ain limestones provide poorly permeable restricted aquitards; water fresh to brackish in leakage zones but slightly saline between ridges Jabal Hafit
				Ta	Ta1	Massive, fossiliferous limestone and thick gypsiferous marls intervals, marly limestone with chert nodules towards bases	Probably occurs below 210m in BH15. in core of Jabal Hafit structure. Base at 125m in BH 19	Not known, but productive fresh water aquifers unlikely
		Campenian/ Upper Cretaceous		Kc	Kc	Marls with thin grey argillaceous dolomitic limestones. Scarce pelagic fossils. May contain blue-grey aroon clays and siltsone with pyrite and mica. Limestone firm, calcitised,part entobreochlated Some nodular or vein gypsum	Cut at 125m in BH19. Near surface in BH30. Possible fracture porosity. Probably more than 500m thick	limestone provides poorly permeable fresh water aquifers north of Jabal Auha
			Semail ultra basic complex	Kb	Kb	Igneous, ultrabasic rocks, gabbros spillites and serpentinites	Very thick, weathering products contribute to main aquifer mat-arial to the west of outcrop not investigated	Probebly none
			Hawasina Group	Ka	Ka1	Contoured Imestone, chert and radiolarite sequence	Not penetrated by drilling	No likely potential

of southerly dipping plunging folds comprising a central anticline flanked by syncline (Fig. 2.10).

An easterly dipping reverse forms the eastern structural boundary between the plain and the outer mountains of the Oman Mountains. The most pronounced fold is a western syncline with an axis located about 6 km east of Jabal Hafit. The axial traces of folds are orientated approximately sub parallel to the trend of Jabal Hafit.

4.3.3 Recharge of the Quaternary aquifer

The main source for the recharge to Quaternary aquifer at Al Jaww Plain is the rainfall on the Oman Mountains. The system is recharged through three sources: groundwater underflow through gaps (drainage basin exit points) infiltration of flood flows carried onto the piedmont plains overlying the aquifer and groundwater flow through fractured bedrock along the entire mountain front. The fractured bedrock east of the piedmont plain may also recharge the shallow aquifers (US Geological Survey, 1993).

The Quaternary aquifer may also be recharged by the infiltration of precipitation in the interdune areas and gravel plain and from Jabal Hafit where the precipitation percolates rapidly through the permeable limestone rocks of Jabal Hafit.

There are other sources that recharge Al Ain aquifer such as irrigation return flow, upward vertical recharge from deeper rocks (fault zone) and infiltration of water lost from heavy water transmission lines.

4.4 Geological Cross Sections

For the Quaternary aquifer in the study area, some geological cross sections are considered (Figs. 4.11 a through f). The locations of the boreholes are given in Fig. (4.10). Investigations of these cross sections guided with the two maps presented in Figs. (4.7) and (4.8), revealed the following with consideration of the stratigraphic sequence from younger to older.

1) Near NW-SE strip of the middle part of Al Jaww Plain, the Quaternary aquifer unit attains its maximum thickness (boreholes 11 and 12, cross section C-C' Fig. 4.11c). The location of these sites of high Quaternary thickness near to Jabal Zaroub appear to represent the incised palleovalley where Wadi Shik exits onto the piedmont through bedrock gab in the Oman Mountains range front. Towards the limestone ridges, the aquifer thickness diminishes gradually to about 10 m or less

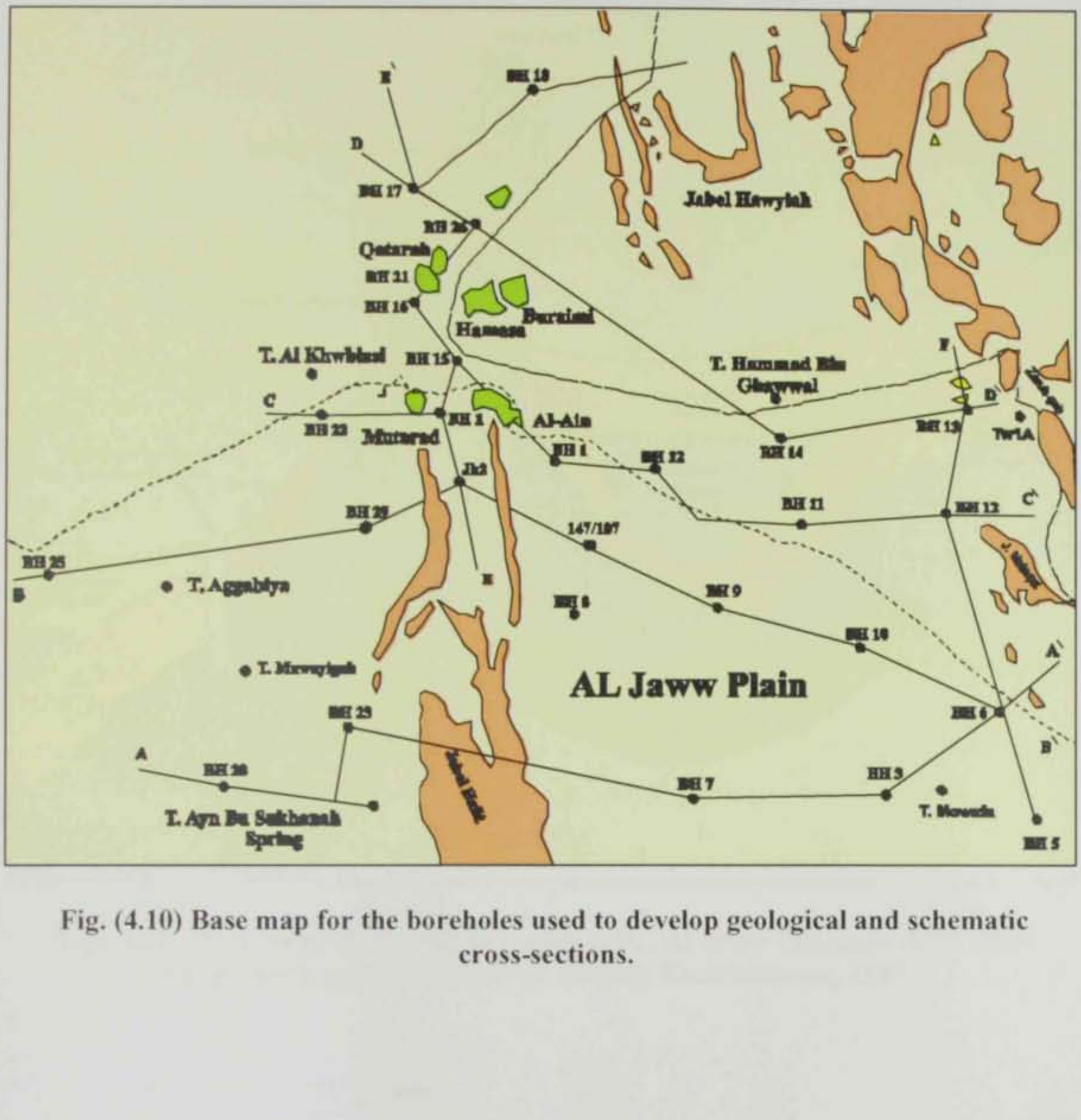

Fig. (4.10) Base map for the boreholes used to develop geological and schematic cross-sections.

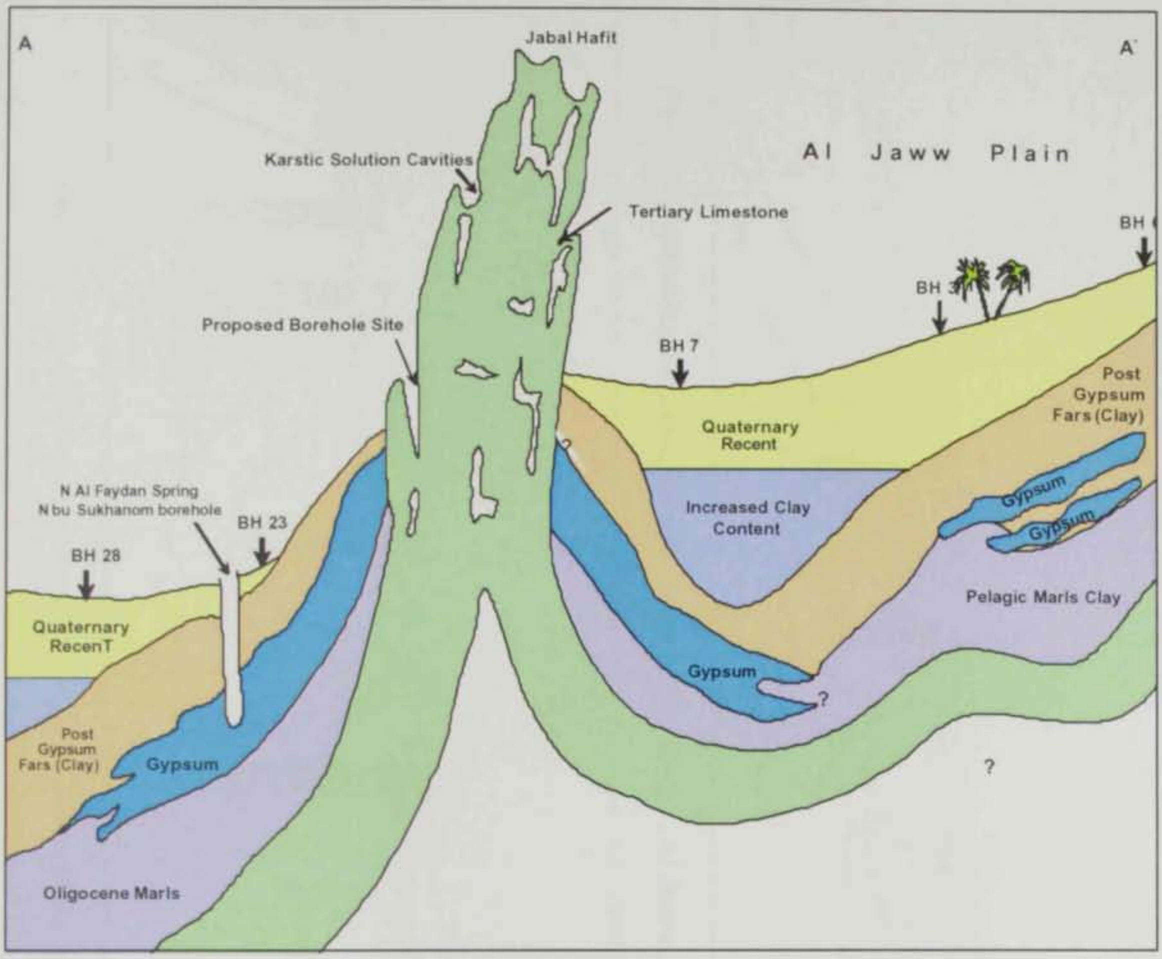

Fig. (4.11a) Schematic section along profile A-A`, Al Jaww Plain (modified after GeoConsult and Bin Ham Well Drilling Establishment, 1985).

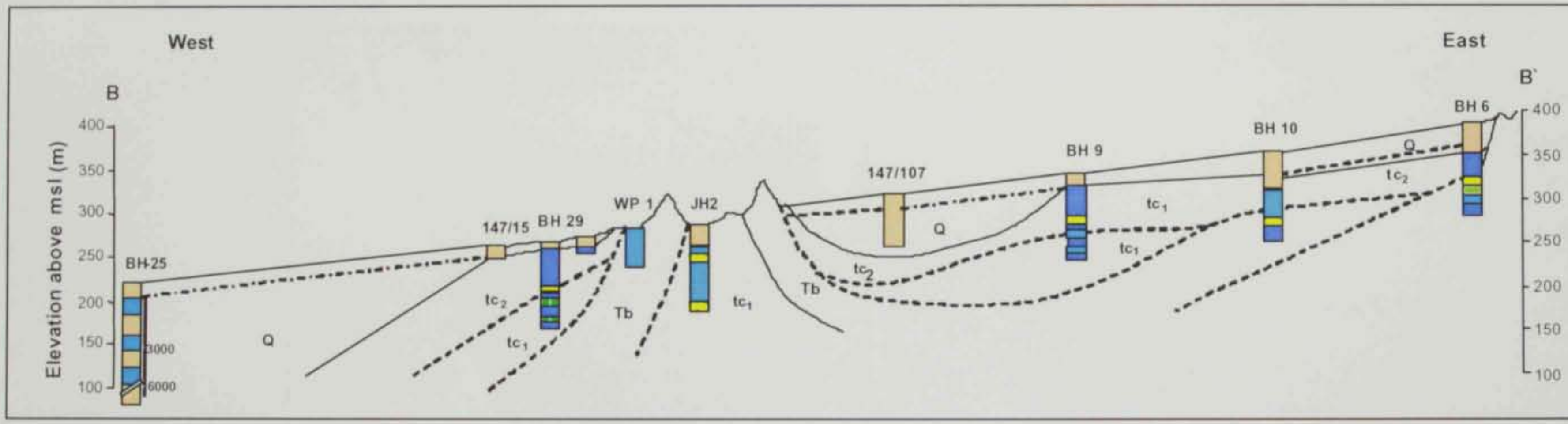

Fig. (4.11 b) Geological cross section along profile B- B` , Al Jaww Plain (modified after Saqr, 1980).

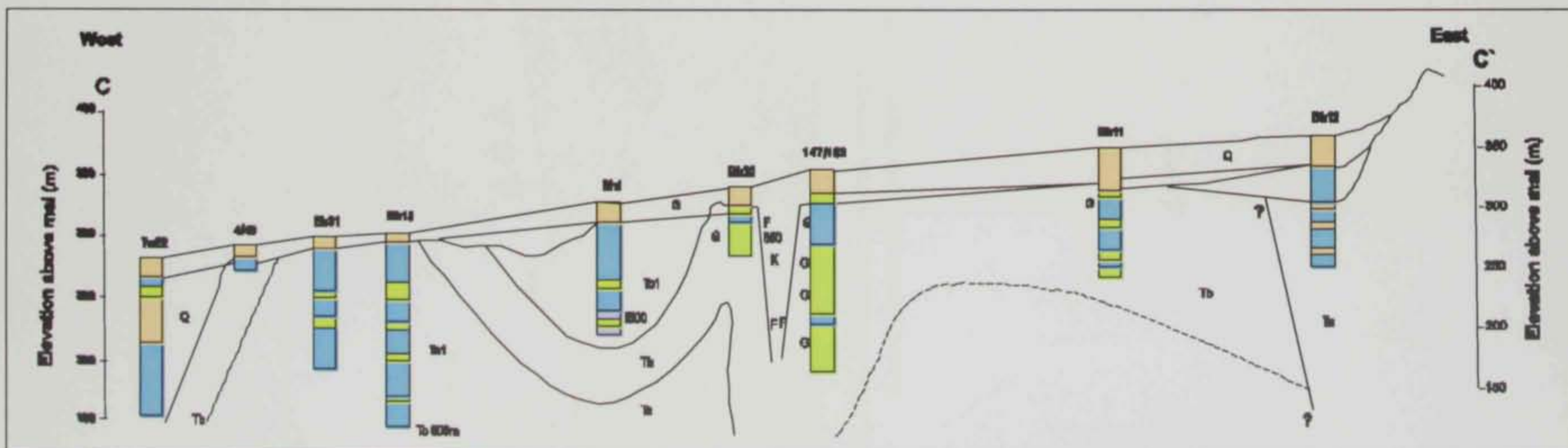

Fig. (4.11c) Geological cross-section C-C`, Al Jaww Plain (modified after Saqr, 1980).

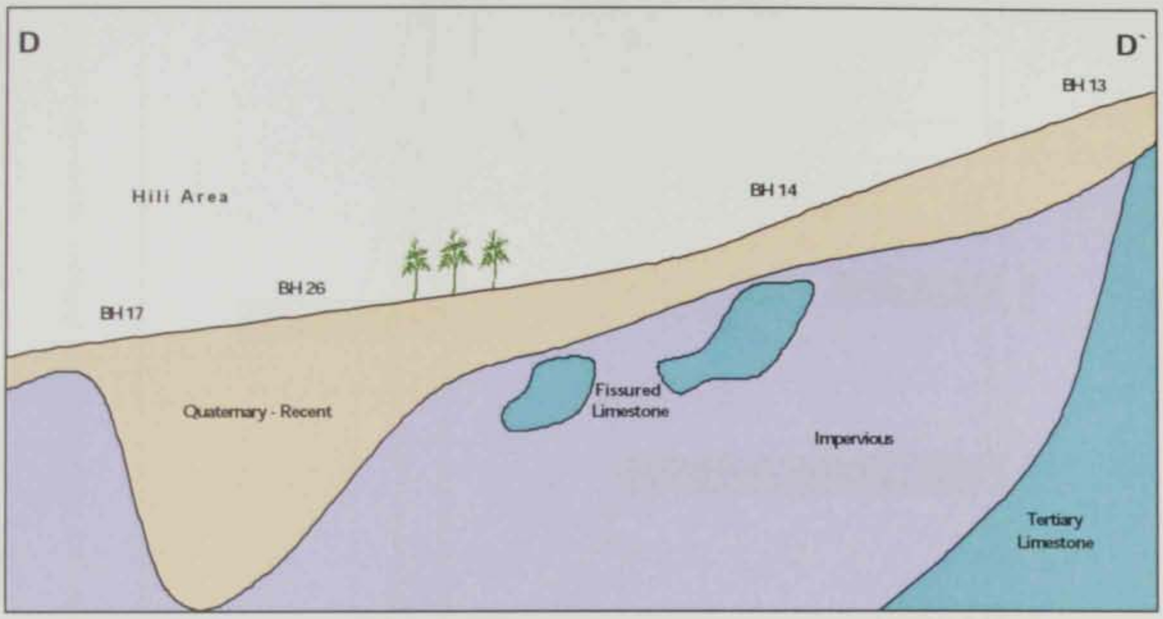

Fig.(4.11d) Schematic section along profile D-D`Al Jaww Plain (modified after GeoConsult and Bin Ham Well Drilling Establishment (1985).

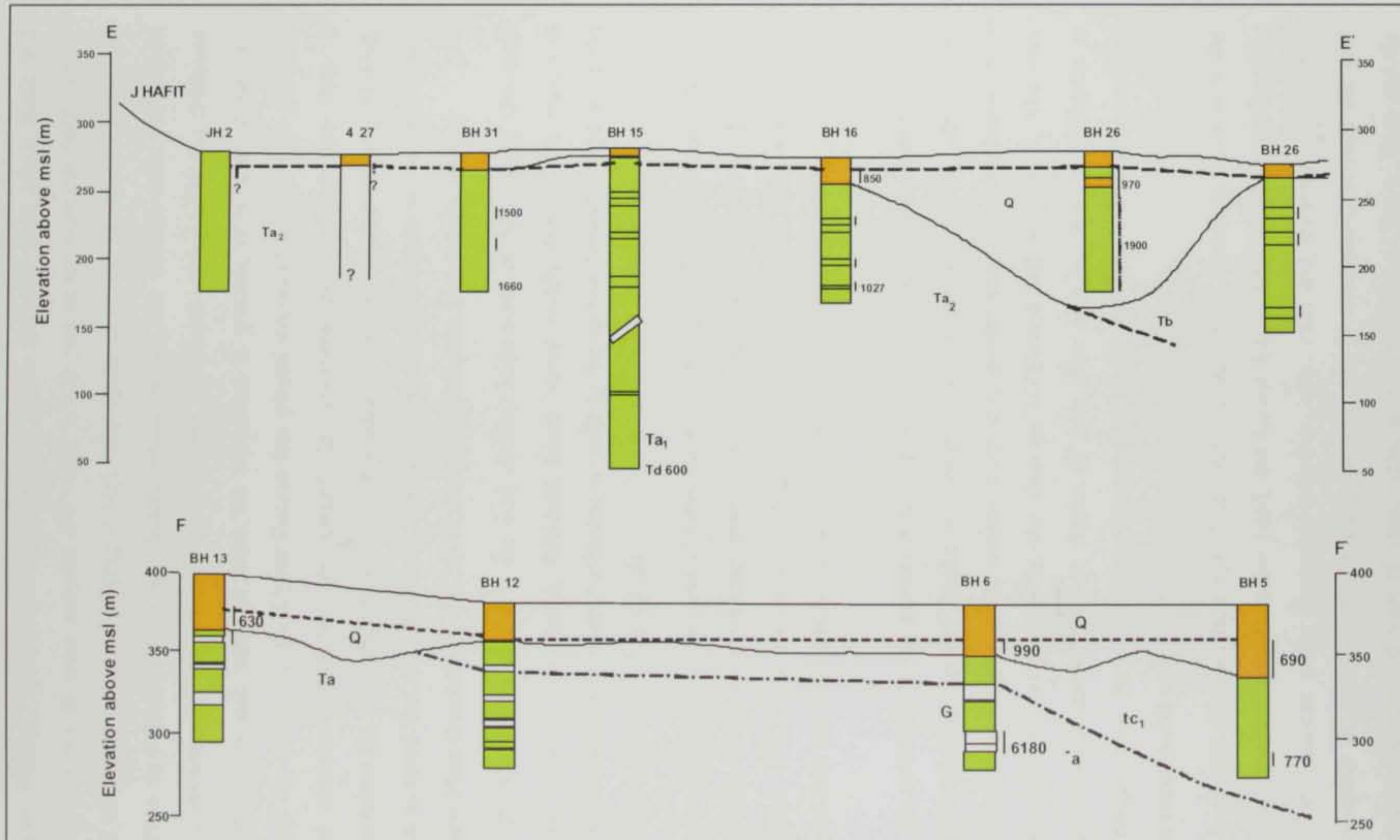

Fig.(4.11e&f) Schematic section along profiles E-E`& F-F`, Al Jaww Plain (modified after Saqr, 1980).

near Jabal Malaqet, Jabal Hafit and disappears at the foots of both Jabals Hafit and Malaqat, as shown in cross sections B-B` (Fig. 4.11b) east to the borehole BH6 and to the east of BH12, section C-C`(Fig. 4.11c). The thickness of the Quaternary unit at Al Jaww Plain is controlled by many factors which include the distance from the alluvial fans as it decreases by the effect of wind and the ephemeral wadies while the thickness of the Quaternary unit increases when the subsurface is syncline or a basin shape like. Moreover, the erosion of the Upper Eocene has played important rule in such effective structural elements which in turn control the thickness of the Quaternary unit. It increases when the subsurface is syncline or a basis shape like. Along section B-B` (Fig. 4.11b) it is noted that the Quaternary unit has its minimum thickness in the middle part of Al Jaww Plain (boreholes 9 and 10). Eocene-Oligo-Miocene are relatively high.

2) The Quaternary aquifer to the west of Jabal Hafit north of Al Ain city (the oasis area) attains a considerable thickness which varies widely from a few meters to 100 meters or even more. Reference is made to the section beneath BH26 along the cross section D-D` (Fig. 4.11d).

3) In the Plain lying to the west of Jabal Hafit, the thickness of the Quaternary deposits has wide range, it gets thicker towards the west; see for example B-B` (Fig. 4.11b) beneath BH25 and section C-C` (Fig. 4.11c) beneath Tw22. In these areas the old rocks have low relief which results from either erosion or structural effects.

From the schematic cross section A-A` (Fig. 4.11a) it is clear that from Jabal Hafit to westward, the Tertiary rocks are dipping to the west and are covered by Quaternary sediments in the western plain area. In this area, the Fars Formation is represented by evaporates as the data of BH23 and BH28 indicate. The Fars Formation is encountered at depths of less than 100 m. Ain Bu Sukhana is emerged from Fars Formation (Evaporates) where the Fars Formation overlying the impermeable marl sediments which belong to Oligocene.

4) Along these sections, the Upper Fars Unit (Td) acts as an aquiclude for most of the Quaternary unit. On the other hand, the Lower Fars Oligo-Miocene (Tc) consists of the evaporate series (gypsum), anhydrite, clay, marl and limestone which act as an aquifer of poor potential. Such an aquifer unit is encountered beneath the area lying to the east and west of Jabal Hafit, as a part of the Al Jaww Plain and the western plain, respectively. The average thickness of this unit is 50 m, although

an exceptional thickness of about 200 m has been recorded at the southern border of the Al Jaww Plain. In some locations this unit does not exist due to the outcropping of the older rocks at these sites. Geoconsult and Bin Ham Well Drilling Est., (1985) reported that the Lower Fars exists with a considerable thickness at the southern part of Al Jaww Plain. At that site the Lower Fars is overlain by a gravel layer of abnormal thickness (200 m), which is attributed to the accumulated deposits carried by Wadi Muraykhat. Such condition has led to the occurrence of a relatively good aquifer (the gravel layer) above a poor aquifer (the Lower Fars). In Al Jaww Plain, the altitude of the top of a thick sequence of less permeable rocks (that comprise the basal confining system) declines from about 360 m at Zaroub gab to about 150 m near Jabal Hafit. The altitude of the top declines to about 60 m where Quaternary aquifer contains a thicker zone of fresh water west of the northern end of Jabal Hafit. The basal confining system is dominated by slightly permeable mudstone, claystone, evaporate, and limestone units of the Fars Formations in the Al Jaww Plain. Geoconsult and Bin Ham Well Drilling Est., (1985) reported that the Caliper Log revealed that the Lower Fars unit was confirmed by drilling data.

5) The Eocene Limestone Unit (Ta, Tb) consists of fossiliferous limestone with gypsiferous marl in its lower part and intercalations of limestone and marl with a cherty base into upper part.

The limestone has a fractured nature and sometimes very permeable (to the North of Al Jaww Plain) and sometimes of extremely low permeability (at the Northern limit of Jabal Hafit). In borehole No.15 along section E-E` (Fig. 4.11e), the limestone has a thickness of more than 600 m while in borehole No. 25 along section B-B` (Fig. 4.11b) in the western plain, the drilling down to 600 m does not reach the top of this formation.

Figs. (4.12 a through c) show three geological cross sections crossing Al Jaww Plain. The locations of these cross-sections are presented in the inset map of Fig. (4.12a).

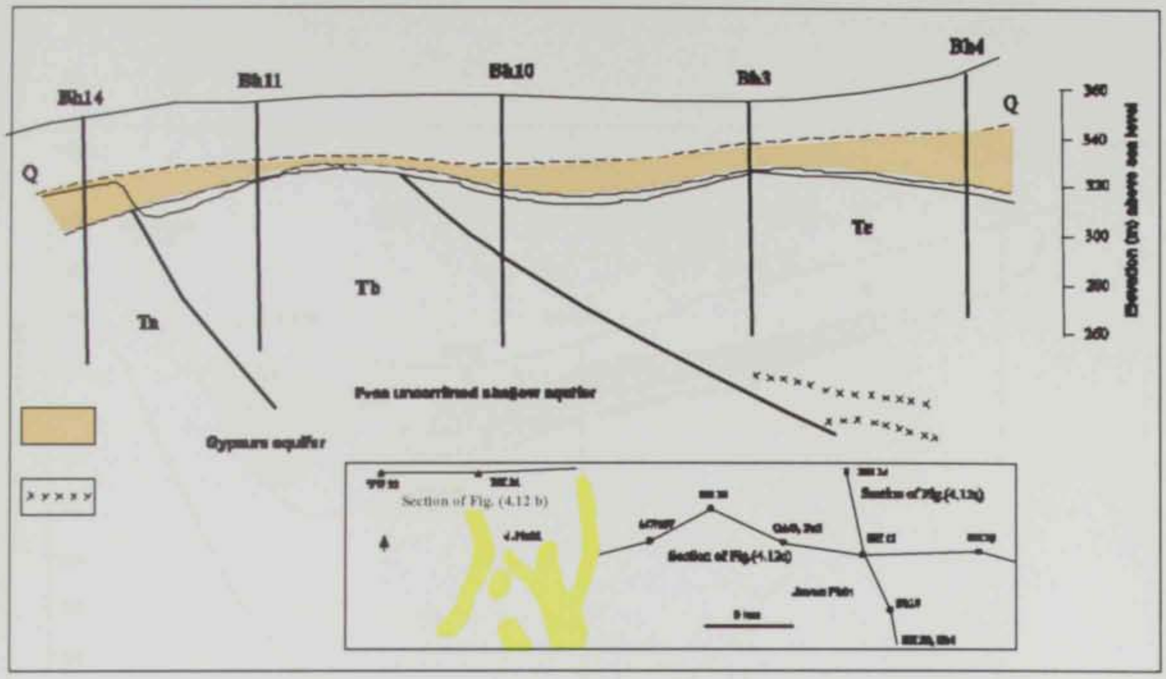

Fig. (4.12a) Geological cross-section showing the changes in the thickness of shallow aquifer at Al Jaww plain (modified after Saqr, 1980).

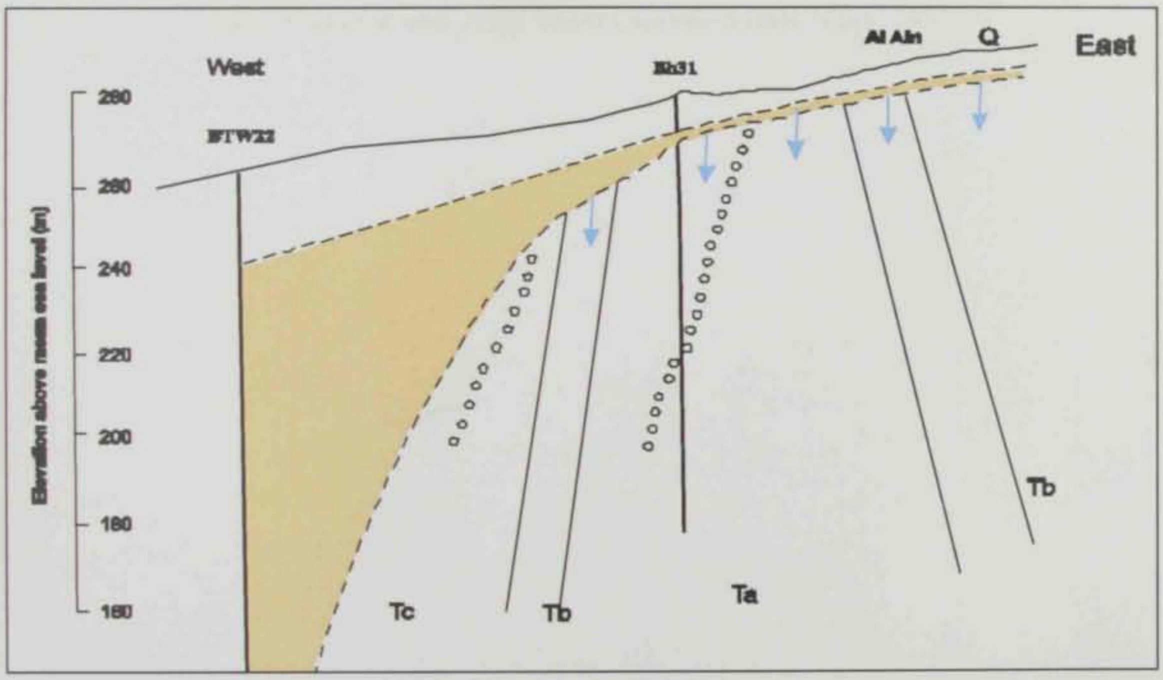

Fig. (4.12 b) Geological cross-section along north of Al Jaww Plain showing the shallow aquifers (modfied after Saqr, 1980).

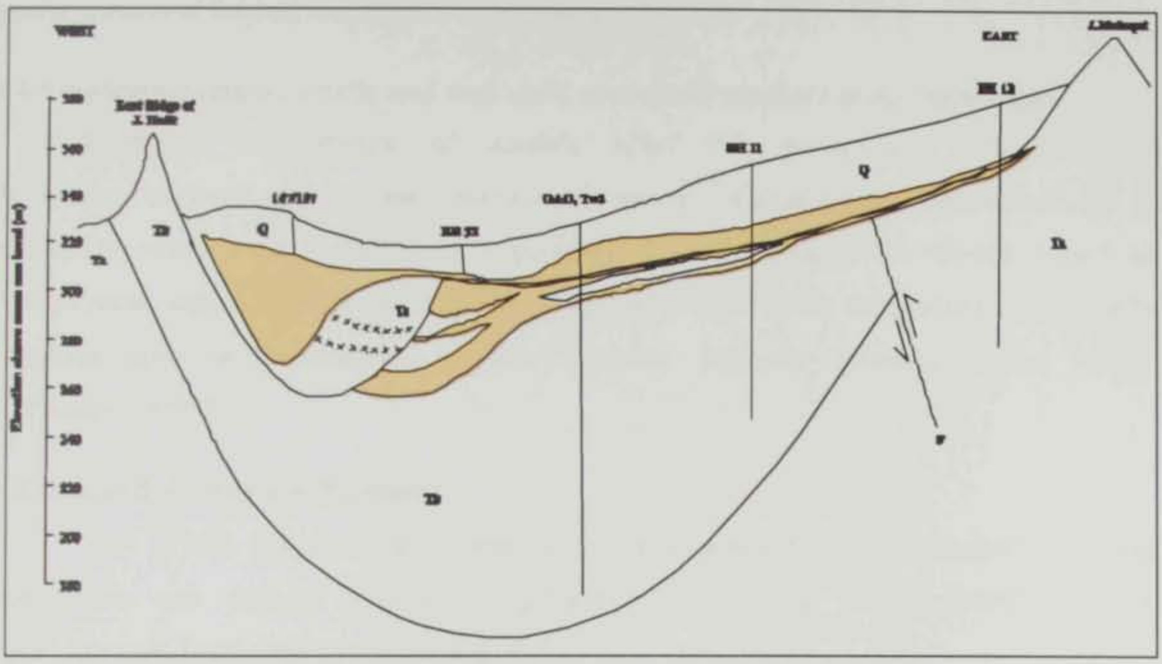

Fig. (4.12c) Shallow aquifers and gypsum aquifers along Al Jaww Plain between Jabal Malaqat and Jabal Hafit (modfied after Saqr, 1980).

These sections indicate the condition of the shallow aquifer at Al Jaww Plain. In areas where the thickness of the aquifer is small, it will not be productive. These shallow aquifers generally consist of conglomerates cemented with calcareous. Except at BH4, the shallow aquifer consists of fissured limestone of Upper Eocene (Ta Unit).

4.4.1 Hydraulic characteristic and well yield of shallow aquifers at Al Jaww Plain

Hydraulic characteristics of aquifers affect the groundwater movement and distribution to local and regional groundwater systems. Groundwater gradients change in relation to where water is added to or removed from the groundwater system. Based on Petrophysical logs, Jorgensen and Petricola (1993) estimated values for geohydrologic aquifer properties such as transmissivity, aquifer thickness, hydraulic conductivity and storage coefficient (Table 4.4).

4.5 Groundwater Flow Systems

Toth (1963) suggested that most of the flow nets can be distinguished into local, intermediate and regional systems of groundwater flow and are controlled by local topography and basin shape geometry (Fig. 4.13).

The local groundwater is considered of good water quality type, such as those of Masafi and the Al Jaww Plain area. Also Khatt springs (Ras Al Khaimah) and Maddab spring (Al Fujairah) are local groundwater flow systems (Rizk et al., 1997).

Local groundwater flow system characterizes the eastern mountain where the hydraulic cycle is fast and the groundwater has a short residence time. The water of these systems has a low salinity (500-1500 mg/l) with HCO_3^- water type and magnesium ion (Mg^{2+}) as dominant cation.

In the intermediate groundwater flow system, the groundwater is mainly brackish (1500-10000 mg/l) and has a moderate residence time. It belongs to SO_4^{2-} water type and the calcium ion (Ca^{2+}) is the dominant cation. Al Ain Al Faydah (Al Ain) to the west of Al Jaww Plain seems to belong to this system.

Table (4.4) Thickness of near-surface permeable material, aquifer thickness, thickness of saturated eolian dune sand, and fresh water thickness (after US Geological Survey, 1993).

[m, meters; nd, no data; est, estimated]

Groundwater Project Well Number	UTM COORDINATES		THICKNESS OF NEAR SURFACE PERMEABLF2 MATERIAL (m)	WATER-LEVEL1 ALTITUDE (m)	LAND-SURFACE ALTITUDE (m)	THICKNESS OF SATURATED EOLIAN DUNE SAND (m)	AOUIFER THICKNESS (m)	FRESH-WATER THICKNESS (m)
1	2677489.5	393675.8	nd	381.5	408.20	0.0	nd	nd
2	2677553.0	393665.5	nd	381.5	408.41	0.0	nd	nd
3	2677490.7	393634.2	nd	381.5	407.90	0.0	nd	nd
4	2677498.4	393649.1	nd	381.5	408.05	0.0	nd	nd
5	2675789.0	389344.6	nd	351.7	377.34	0.0	nd	nd
6	2667305.7	386313.8	72	322.2	342.52	0.0	51.3	51.0
7	2664080.4	380942.0	102	300.5	322.30	0.0	80.3	0.0
8	2665971.9	393220.5	110	358.2	397.92	0.0	88.0	29.0
9	2669147.5	390728.0	102	347.9	369.65	0.0	80.3	39.0
10	2658958.7	381480.3	117	302.2	317.41	0.0	102.1	40.0
11	2662909.3	385939.8	81	319.1	337.83	0.0	62.0	62.0
11A	2662911.2	385903.1	81	319.1	337.75	0.0	62.1	62.0
14	2668360.8	380303.5	130	298.0	320.60	0.0	106.9	40.0
15	2671155.0	386144.1	40	325.1	348.52	0.0	16.2	18.0
16	2677390.0	384530.3	46	321.5	343.36	0.0	23.9	24.0
17	2674345.8	388463.8	43	341.9	367.30	0.0	17.2	20.0
18	2676791.5	393546.3	44	378.6	403.39	0.0	19.4	22.0
19	2676523.7	380702.6	50	301.7	320.10	0.0	31.9	nd
20	2664216.2	395299.9	107	371.0	389.59	0.0	88.1	nd
21	2684295.2	375639.1	55	279.0	288.63	0.0	45.2	45.0
22	2660340.9	367988.3	76	228.7	233.98	28.2	104.4	0.0
66	2684691.5	369033.2	nd	258.3	269.06	0.0	nd	est32
67	2685922.0	365786.1	0	246.2	268.16	78.0	68.1	nd
68	2664639.0	395194.4	nd	369.5	388.43	nd	nd	nd
80	2670276.1	380371.1	nd	298.8	323.50	nd	nd	nd

In the third type (regional groundwater flow system), the groundwater is characterized by the high salinity content of greater than 10000 mg/l. The coastal sabkhas represent the main discharge of this groundwater system. It has a long residence time and it is of Cl^- water type. The sodium ion (Na^+) is the dominant cation in this system (Rizk et al., 1997).

To assess water level changes in Al Jaww Plain, the available data about water levels from both NDC and WED were used in this analysis. Historical data for water level measurements of four wells at Umm Ghafa area (south east of the study area (Fig. 4.14) were considered. The water levels fluctuated in the period from 1982 to 2001. Water levels rise during rainy years and drop during the years of less precipitation. Guided with Fig. (4.3a), it could be noted that there is a rise in the water level for the period from 1995 to 1998, while there is a drop in the 1998 as the total rainfall was low (about of 17 mm). Also from this hydrograph, there is another drop in the water levels in the year 1986. The rates of pumping and evapotranspiration were assumed fixed during the period of water levels measurements.

Figs. (4.16a through d) show water levels fluctuation along four cross sections in Al Jaww Plain. The locations of this cross section are shown in Fig. (4.15). There is a slightly decrease in water levels in the period from 1995 to 2002 for all the wells included along these cross sections. This analysis indicates that the water resources in Al Jaww Plain is in balance.

Water level maps for Al Jaww Plain during the period from 1995 to 2002 are shown in Figs. (4.17a through k). The following can be deduced:

1) Fluctuations in water level have been observed along with displacement in the positions of the equipotential line. This displacement is attributed to the variation of discharge rate. Fig. (4.18) shows the change in the position of equi potential line 300 for the years 1995, 1999 and 2001.

2) The groundwater level decreases gradually from east (about 400 m above sea level near Oman Mountain) to about 200 m (towards Jabal Hafit). The contours of equal water level are quite uniform and parallel to each other. They follow a north-south trend with slight deflections in the main recharge zones (around Jabal Hafit and the Zarub gab).

3) In the Al Ain area and west of Jabal Hafit the distance between the contours is somewhat increasing, perhaps due to higher permeability but most possibly due to the pumping in this area (see the water level map of 1995 Fig. 4.17a).

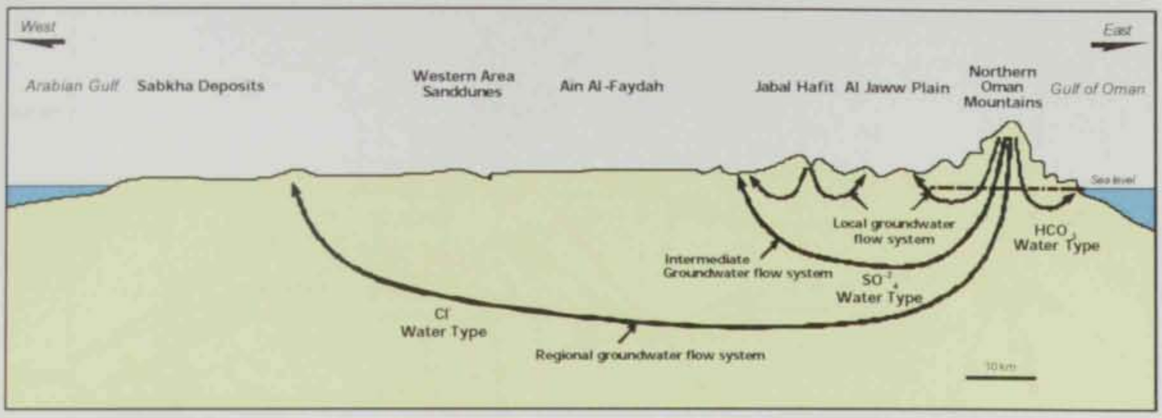

Fig. (4.13) Different groundwater flow system in UAE (after Rizk et al., 1997)

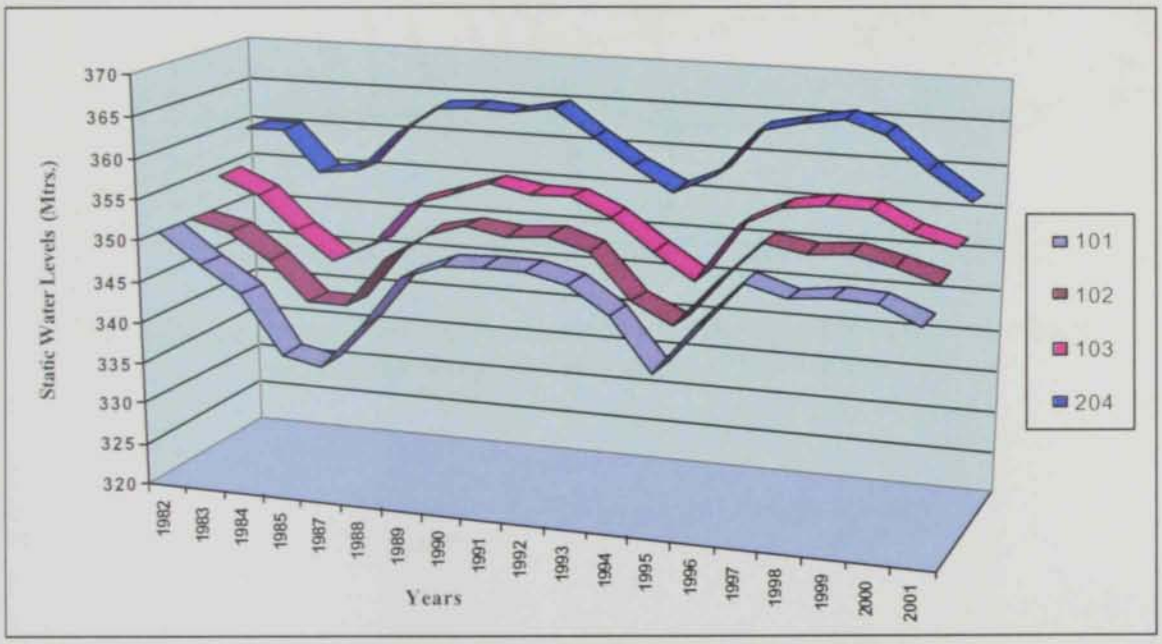

Fig. (4.14) A graph showing the water level fluctuations for some wells in Umm Ghafa area, Al Jaww Plain.

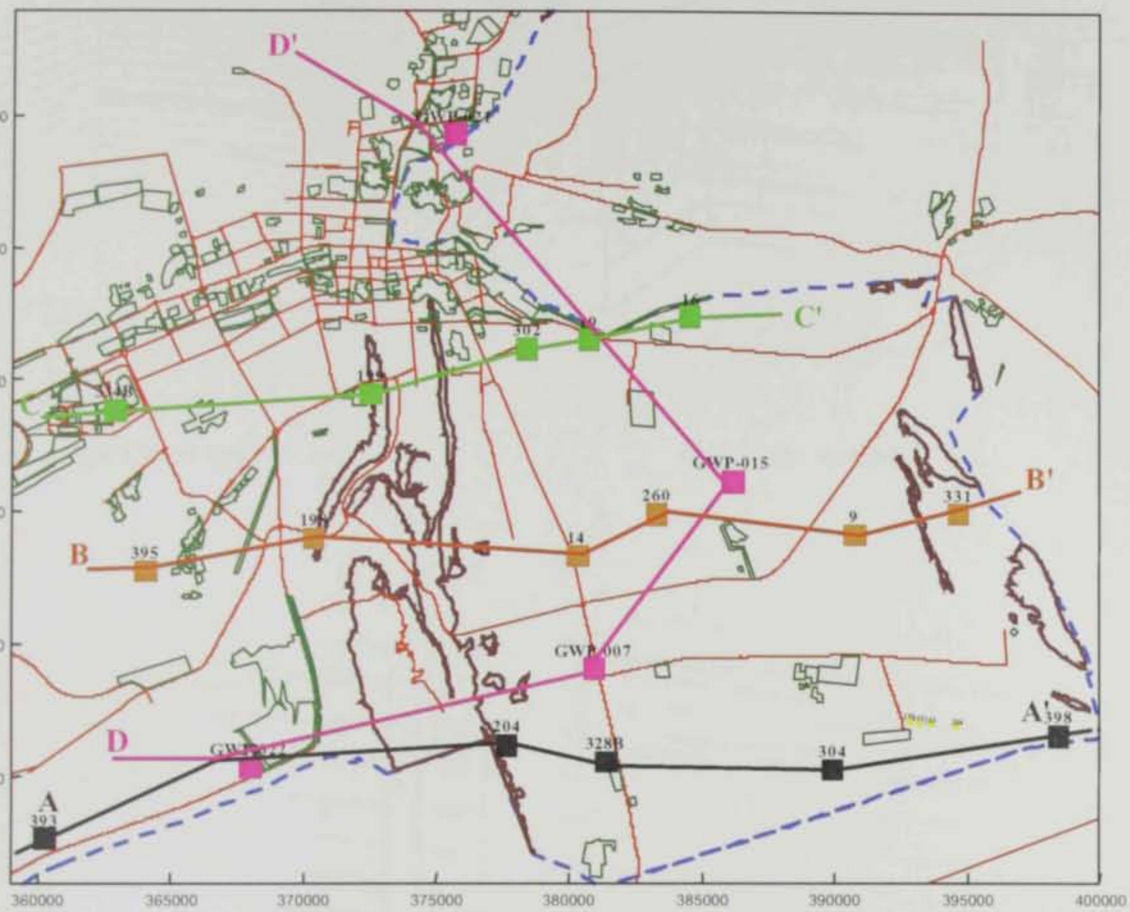

Fig. (4.15) Base map showing the locations of wells used for static water level oscillations along the study area, Al Jaww Plain.

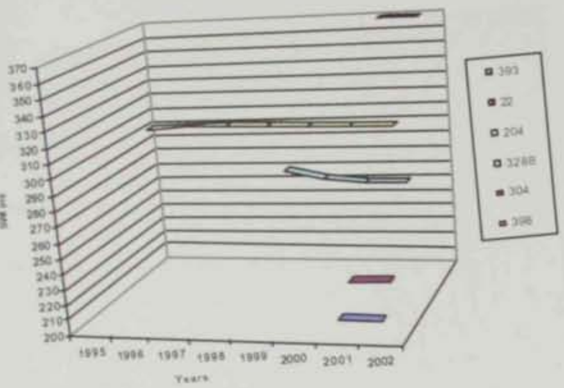

(a) Cross section A-A`

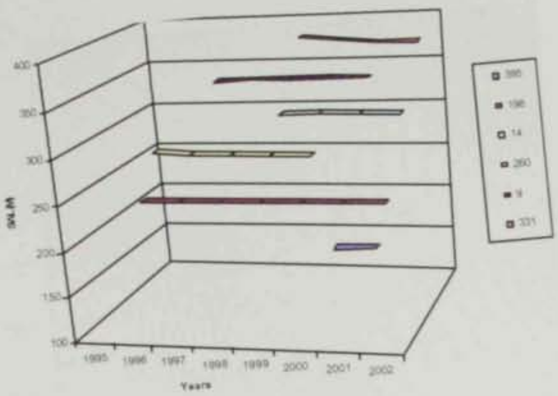

(b) Cross section B-B`

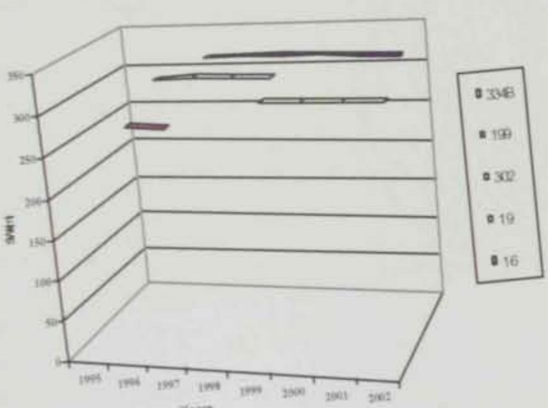

(c) Cross section C-C`

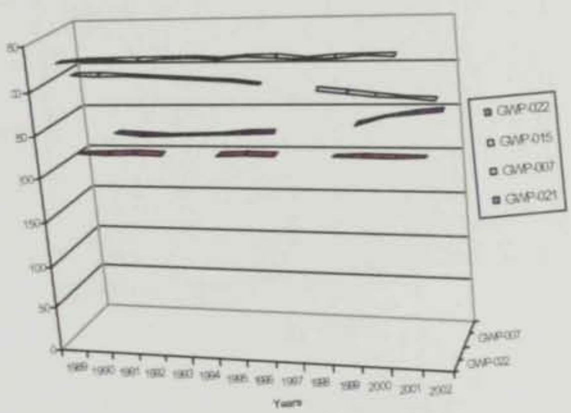

(d) Cross section D-D`

Fig. (4.16) SWL oscillations from 1995 to 2002 along wells of different cross sections, see (Fig. 4.15) for location of the cross-section.

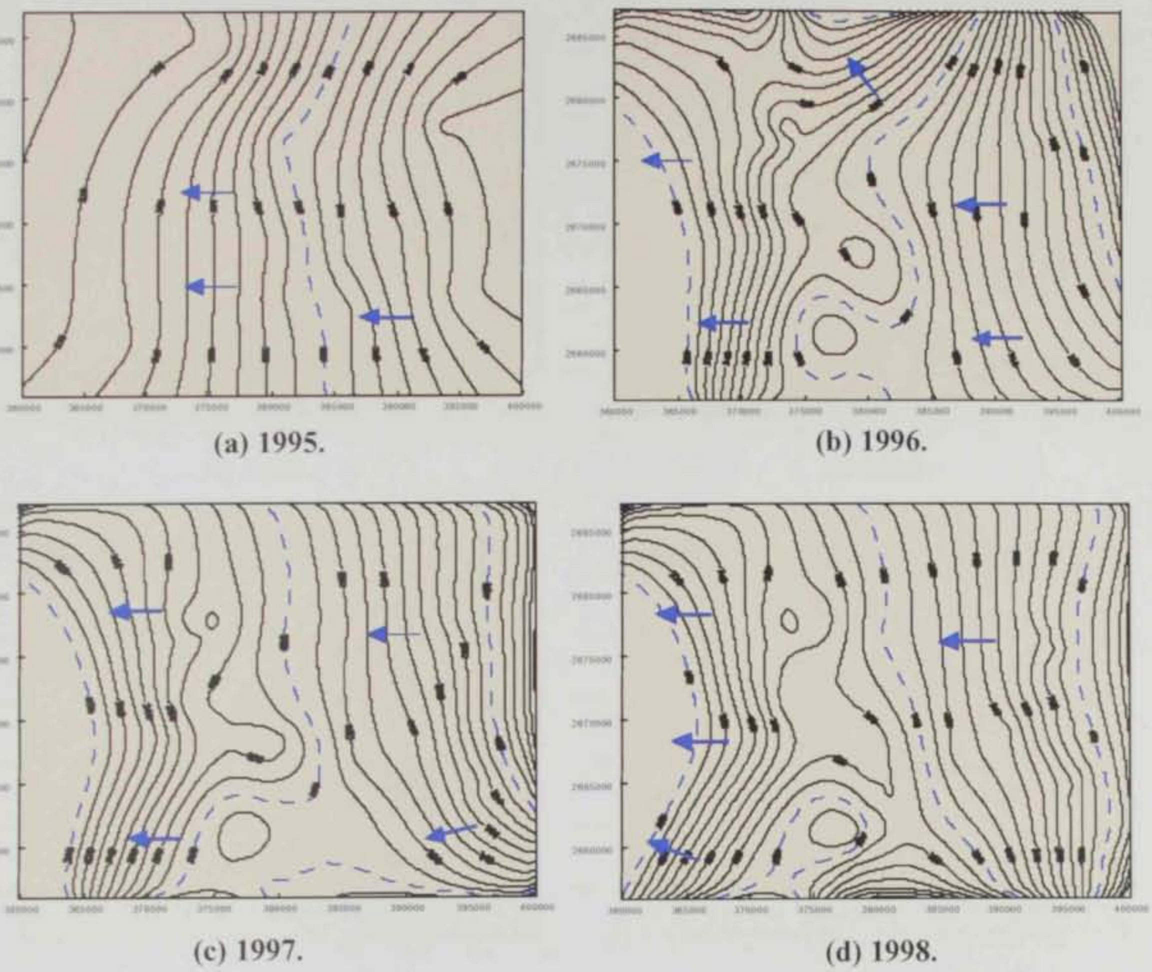

Fig. (4.17) Static water level at AL Jaww Plain in 1995 through 2002.

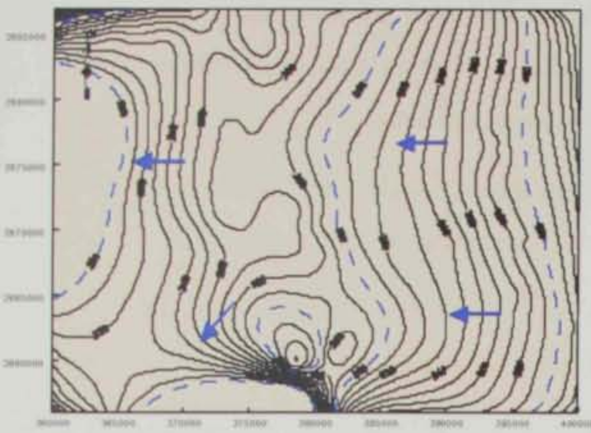

(e) 1999.

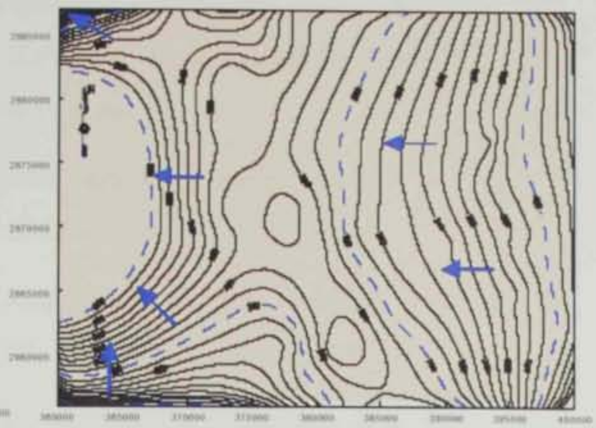

(f) 2000.

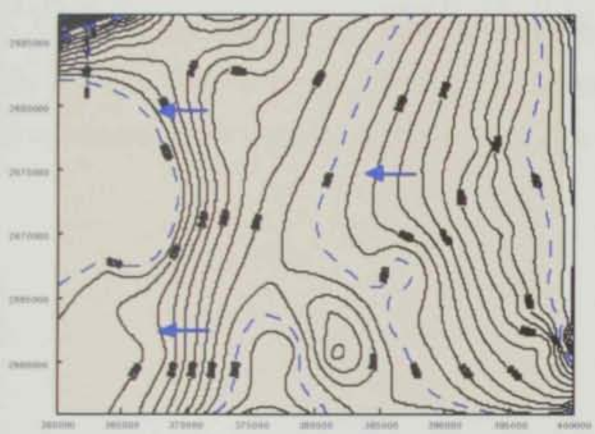

(g) 2001.

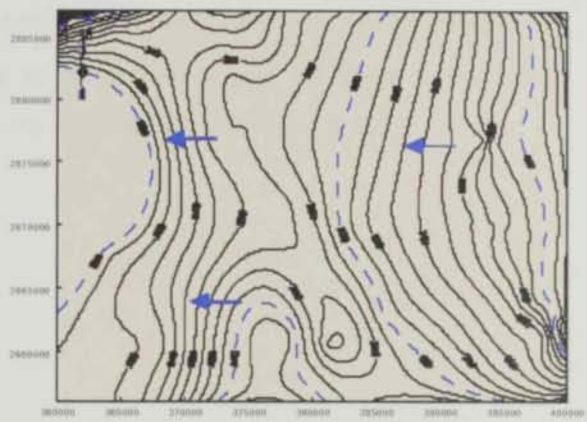

(h) 2002.

Fig. (4.17) Cont. Static water level at AL Jaww Plain in 1995 through 2002.

4) A groundwater mound near Jabal Hafit was found parallel to the eastern edges of the mountain and channeled groundwater around the northern and southern ends of Jabal Hafit (Fig. 4.17a through h). Two possible explanations for the mound may be given:

   a) Increased groundwater recharge from rainfall infiltering through the more permeable limestone units of Jabal Hafit.

   b) The upward movements of groundwater through fractures associated with the Jabal Hafit anticline.

The constructed water level maps are in a good match with the map (Fig. 4.19), which was constructed, based on seismic uphole survey data (Woodward and Menges, 1991).

Generally, the depth to water level decreases with distance from the Oman Mountains. The depth to water from the alluvial plain surface in the eastern part of the study area is about 30 m, whereas in the western part of the study area, the depth to water is about 3 m.

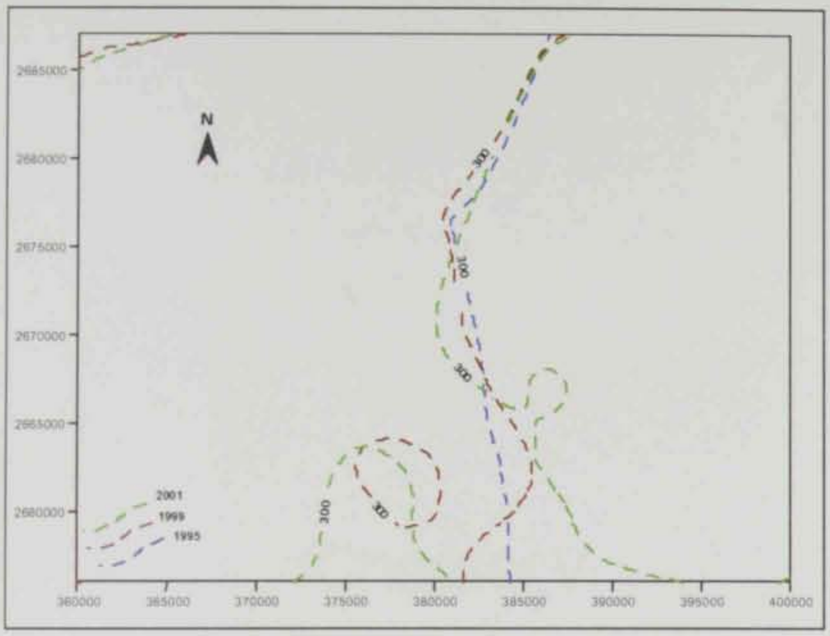

Fig. (4.18) Location of equipotential line 300 in 1995, 1999 and 2001, at Al Jaww Plain.

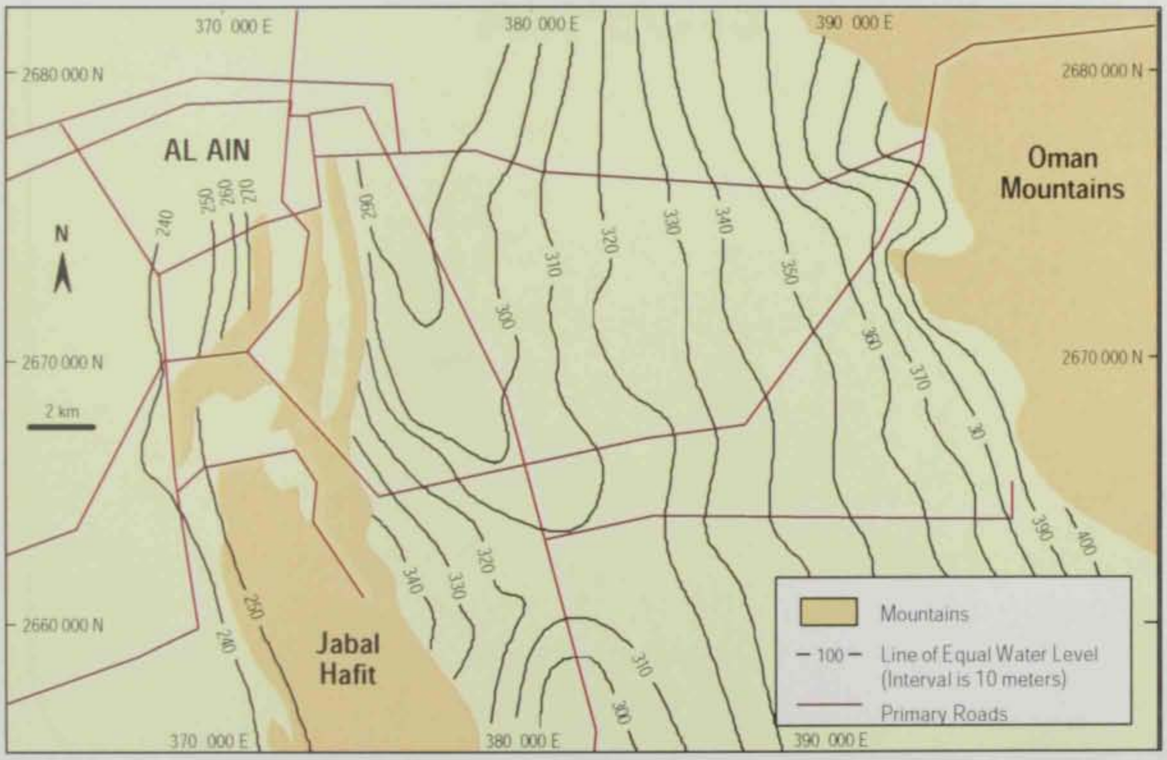

Fig. (4.19) Water table map based on uphole seismic, 1981 (after Woodward &Menges, 1991).

Chapter V

HYDROGEOCHEMICAL ASPECTS

CHAPTER FIVE

HYDROGEOCHEMICAL ASPECTS

5.1 Background

The geochemical characteristics of groundwater give important information regarding the geologic history of the enclosing rocks, sources of groundwater recharge, and the velocity and direction of flow. The chemical composition of groundwater may significantly change due to the admixture of other water, natural biological processes in aquatic plants and animals, and as a result of direct or indirect human activities.

The hydrochemistry of groundwater in the UAE has been discussed by many investigators including, among others , US Geological Survey, (1993), Garamon (1996), Rizk et al, (1998), Rizk (1999) and Alsherhan et al., (2001).

The water resources in the study area can be grouped under two major sources; groundwater and surface water. The groundwater is mainly encountered in Quatenary aquifers. The surface water is encountered in the flajes and as an outflow from Al Ain Faydah. The determination of the water quality of these resources is based on the hydrochemical data provided by NDC and WED.

In this study, data of 202 observation and production wells (Fig. 5.1a) are used. The locations of wells and their numbers are provided in Figs. (5.1b and 5.1c). The chemical results are given in Appendix (A). The following discussions and interpretations are made based on the results included in Appendix (A).

5.2 Hydrogeochemical Characteristics

The main characteristics of the groundwater in the Quaternary aquifer including, hydrogen ion concentration (pH), electrical conductivity (E.C.), total dissolved salts (T.D.S.), and hydrochemical properties; distribution of major constituents (K^+, Na^+, Mg^{++}, Ca^{++}, Cl^-, SO_4^{--}, No^-_3 and HCO_3^-) are presented hereafter.

5.2.1 Physical properties

The quality of water must suit the purpose of its intended useage. It must has suitable physical quality. Three criteria are generally used in the preliminary assessement of groundwater quality. These criteria include pH (acidity/alkalinity), total dissolved salts (T.D.S.) and specific electrical conductance (EC).

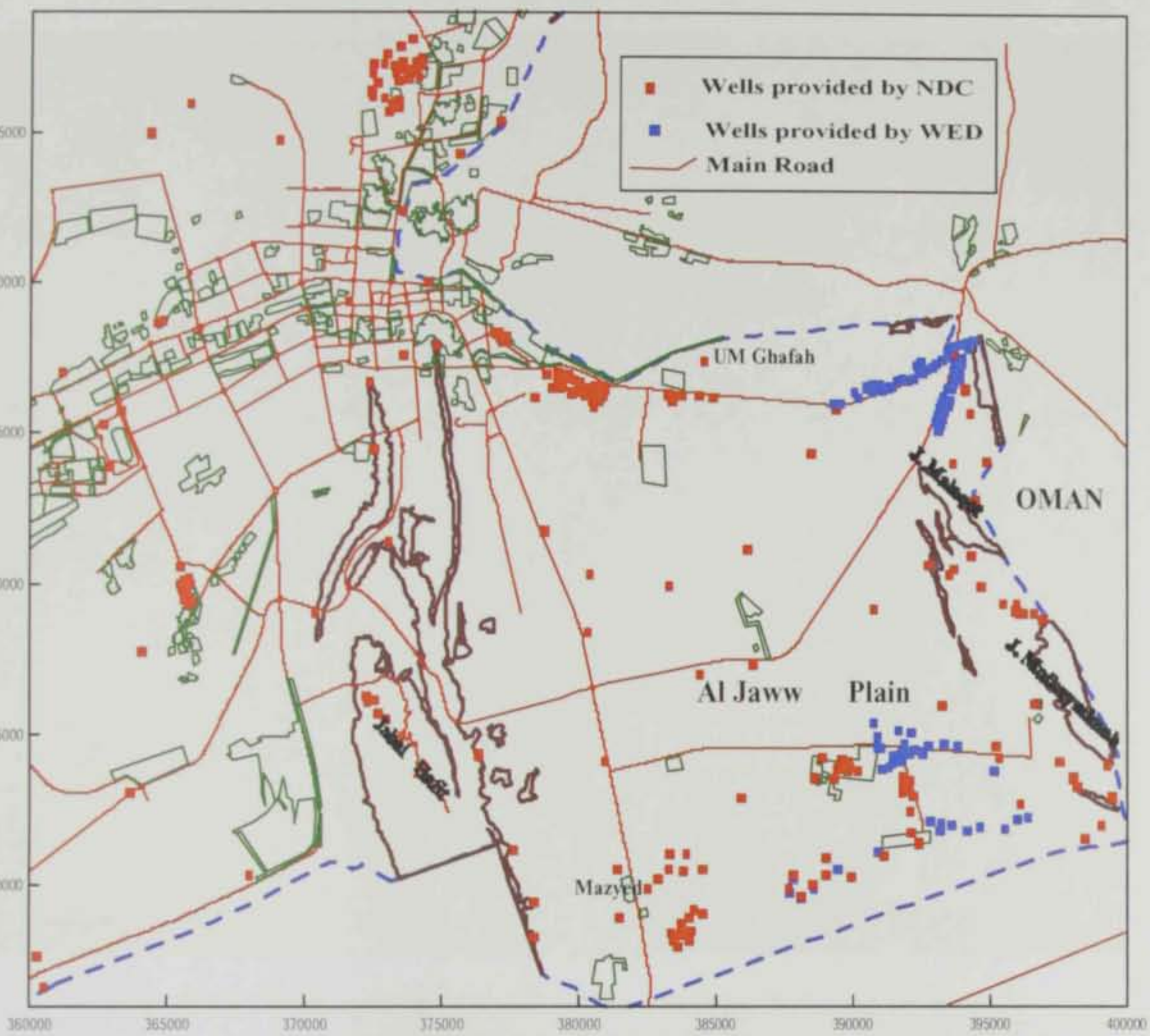

Fig. (5.1a) A base map including the locations of wells at Al Jaww Plain.

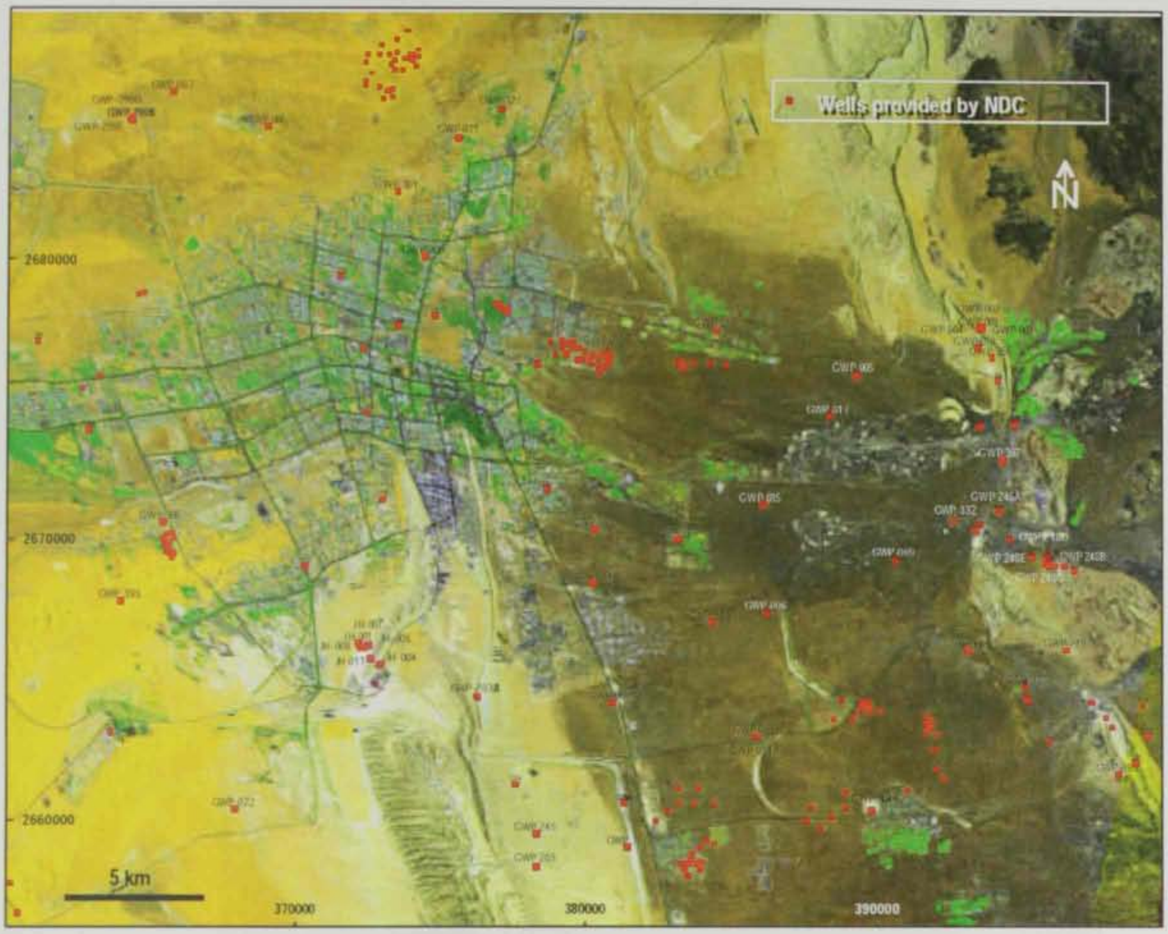

Fig. (5.1b) Wells and their numbers provided by National Drilling Company (NDC), Al Jaww Plain.

Fig. (5.1c) Location map of the wells provided by Water and Electricity Department (WED), Al Jaww Plain.

5.2.1.1 Hydrogen ion concentration (pH value)

pH is a measure of the acidity and alkalinity of the groundwater, or hydrogen ion concentration on a logarithmically calculated scale, Gymer (1973). pH has a major influence on the water geochemistry, because it affects ionic strength, organic carbon content, mobility of metallic ions and the oxidation/reduction potential. The pH affects to a great extent the growth of both plant and soil micro-organisms, degree of ionization, extent of hydrolysis and buffering action. Worsley (1929) further stated that the addition of salts to water may cause a reduction in the pH value depending on the quality and quantity of the added salts, whereas leaching of salts may cause a rapid rise in its pH value. Exchangeable cations like K^+, Na^+, Mg^{++}, Ca^{++}, and hydrogen, affect the water reaction properties. Sodium and potassium cations make water slightly more alkaline than calcium and magnesium. Moreover, the presence of $CaCO_3$ with considerable quantity rises the pH value of water and makes it alkaline as shown in the following equations:

$$H_2O + CaCO_3 \rightarrow CO_3^{--} + H_2O$$

$$CO_3^{--} + H_2O \rightarrow HCO_3^{-} + OH^{-}$$

$$CO_3^{--} + 2H_2O \rightarrow H_2CO_3 + 2OH^{-}$$

In the present work, water samples can be calssified according to the pH value as:

pH value	Type of water
<6	Acidic
6-7	Slightly acidic
7-8	Slightly alkaline
8-9	Alkaline

The groundwater samples of the Quaternary aquifer have pH values ranging between 7 to 11.6 (alkaline type) with an average value of 9.3. The distribution patterns of pH of the groundwater in the Quaternary aquifer is shown in Fig. (5.2). There is no specific trend for the pH patterns. These patterns have irregular distribution but do not completely match with the water salinity, (Fig. 54). A great part of the aquifers is alkaline, particularly in eastern and western parts of the study area. The high value of pH concentration in the west and east side has resulted from the increase of $CaCO_3$ from Jabel Hafit and from carbonate units of Oman Mountains. The pH values are inversely propotional to the salinity content. However, relatively low pH values are observed along the rest of the area.

5.2.1.2 Electrical conductivity (E.C.)

Electric conductivity (E.C.) refers to the ability of substance to conduct electrical current. It depends on the concentration of charged ionic and species in the water. Hence, the measure of conductance is used to approximate the total concentration of ionic species present. The measurement of electrical conductance is usually in micromohs per centimetres (μmhos/cm). The measurements are standardized to 25°C. For a very rough estimate of the total dissolved salt in parts per million in fresh water, the specific conductance of the water in micromhos should be multiplied by 0.6-0.7 according to the cation and anion types.

The distribution of electrical conductivity of the groundwater is shown in Fig. (5.3). The western and eastern parts have E.C. less than 4000 (μ mhos/cm). In the transition zone the E.C. ranges between 4000-8000 (μ mhos/cm). The area located near the centre is characterized by high values of E.C. ranging between 12000-16000 (μ mhos/cm). The electrical conductance of water depends on the salinity content. The similarity between salinity and electrical conductance is demonstrated in the salinity map (Fig. 5.4).

5.2.1.3 Total salinity distribution

The total salinity of natural water is a measure of the ion concentration which may be affected by dissolution and evaporation processes. In natural water which contains a variety of conic and non conic species, the values of E.C. are not simply related to T.D.S. However, some water sources may display well defined relationships. The variation in the salinity is relatively influenced by evaporation, lithologic characteristics of the aquifers, transportation process, solubility of salts by falajes, and the rate of discharge of the groundwater from the aquifer.

In the Quaternary aquifer, the total salinity ranges between 240 and 51000 ppm, with a mean value of 2550 ppm. The distribution of salinity content is shown in Fig. (5.4). The salinity increases from east to west in the direction of groundwater flow. The higher salinity content recorded for the central and western areas can be attributed to the influence of the marine sedimentary facies which are encountered at shallow depths in these areas as shown in the geological cross-sections (Fig. 4.11a through f).

According to Chebotarev classification (1955), the salinity content of the different water samples are classified into several catergories. These categories are presented in Table (5.1) and (Fig. 5.5).

Table (5.1) Classification of the water samples in the area of study, based on Chebotarev's classification (1955).

Water Class	Water Subclass	TDS	Well No
FRESH	GOOD POTABLE	< 500	**WED**(6,8,9,11,12,13,14,15,16,17,18,19,21,23,24,28,32,35,37,38,39,40,41,44,46,48,49,50,51,52,53,101,102,103,105,204,206,207,404,406,409,411,501,502,503,504,505,506,507,601,602,603,604,605,606,607,608,609,610,611,612,613,614,615) **NDC**(19,002GHAF,002MARK,002SAA,002 SHIR,003SAA,003SAA,003SHIR,004SHIR,005SAA,008SHIR,009SHIR,011SHIR,017BSAA,019SHIR,019BSAA,021BSAA,037SOH,040SHIR,064GHAF,037SOH,040SHIR,064GHAF,066SAA,075GHAF,106GHAF,107GHAF,108GHAF,109GHAF,149SAA,18,248A)**48.02%**
	FRESH	500 - 700	**WED**(201,508,412) NDC(246B,001SOHHIR,053BSAA,037GHAF30SHIR,033S,247B,201,412,508,002ZAK,003GHAF,010MEZ,011MEZ,012SOH,028MEZ,029GHAF,029SHIR)**9.41%**
	FAIRLY FRESH	700 - 1500	**WED**(201,508,412) NDC(246B,001SOHHIR,053BSAA,037GHAF30SHIR,033S,247B,201,412,508,002ZAK,003GHAF,010MEZ,011MEZ,012SOH,028MEZ,029GHAF,029SHIR)**14.36%**
BRACKISH	SLIGHTLY BRACKISH	1500 - 2500	**WED**(201,508,412) NDC(246B,001SOHHIR,053BSAA,037GHAF30SHIR,033S,247B,201,412,508,002ZAK,003GHAF,010MEZ,011MEZ,012SOH,028MEZ,029GHAF,029SHIR)**5.94%**
	BRACKISH	2500- 3200	**WED**(201,508,412) NDC(246B,001SOHHIR,053BSAA,037GHAF30SHIR,033S,247B,201,412,508,002ZAK,003GHAF,010MEZ,011MEZ,012SOH,028MEZ,029GHAF,029SHIR)**3.96%**
	DEFINITELY BRACKISH	3200 - 4000	**WED**(201,508,412) **NDC**(246B,001SOHHIR,053BSAA,037GHAF30SHIR,033S,247B,201,412,508,002ZAK,003GHAF,010MEZ,011MEZ,012SOH,028MEZ,029GHAF,029SHIR)**3.96%**
SALINE	SLIGHTLY SALINE	4000 - 6500	**WED**(201,508,412) NDC(246B,001SOHHIR,053BSAA,037GHAF30SHIR,033S,247B,201,412,508,002ZAK,003GHAF,010MEZ,011MEZ,012SOH,028MEZ,029GHAF,029SHIR)**7.43%**
	SALINE	6500 - 7000	**WED**(201,508,412) NDC(246B,001SOHHIR,053BSAA,037GHAF30SHIR,033S,247B,201,412,508,002ZAK,003GHAF,010MEZ,011MEZ,012SOH,028MEZ,029GHAF,029SHIR)**1.49%**
	VERY SALINE	7000 - 10000	
	EXTREMELY SALINE	>10000	**NDC**(198,199,200,002NIAD,002ZAK,003NIAD,006NIAD,007NIAD,008NIAD,011NIAD,013NIAD)**5.45%**

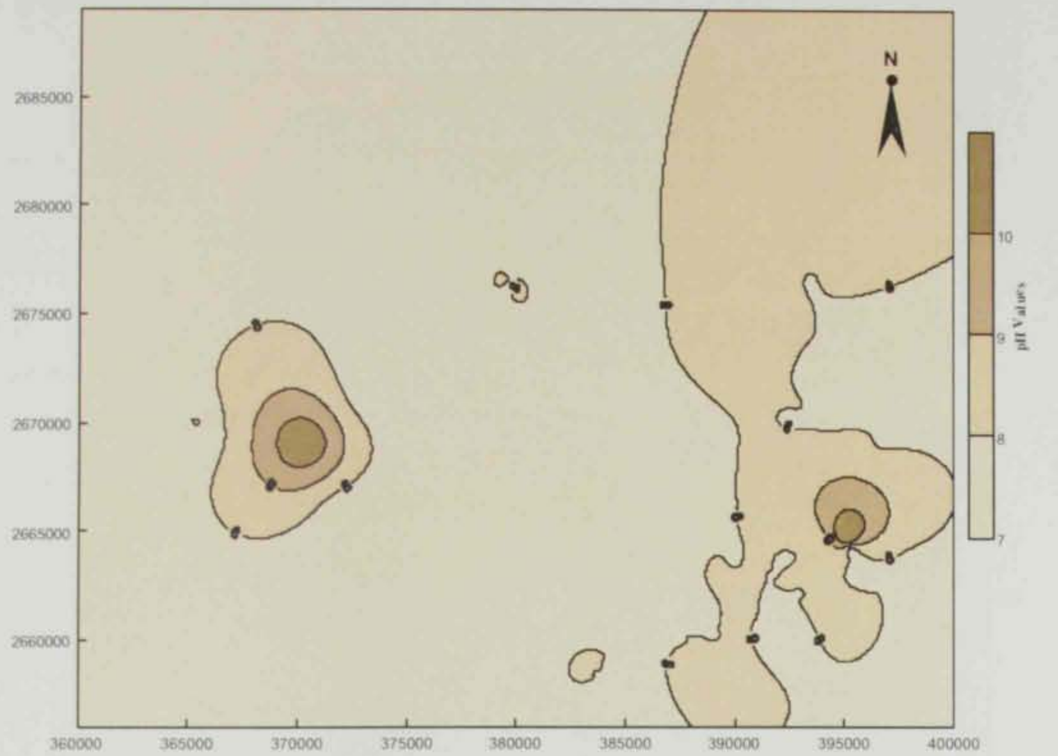

Fig. (5.2) Distribution map of the pH for the Quaternary aquifer in Al Jaww Plain.

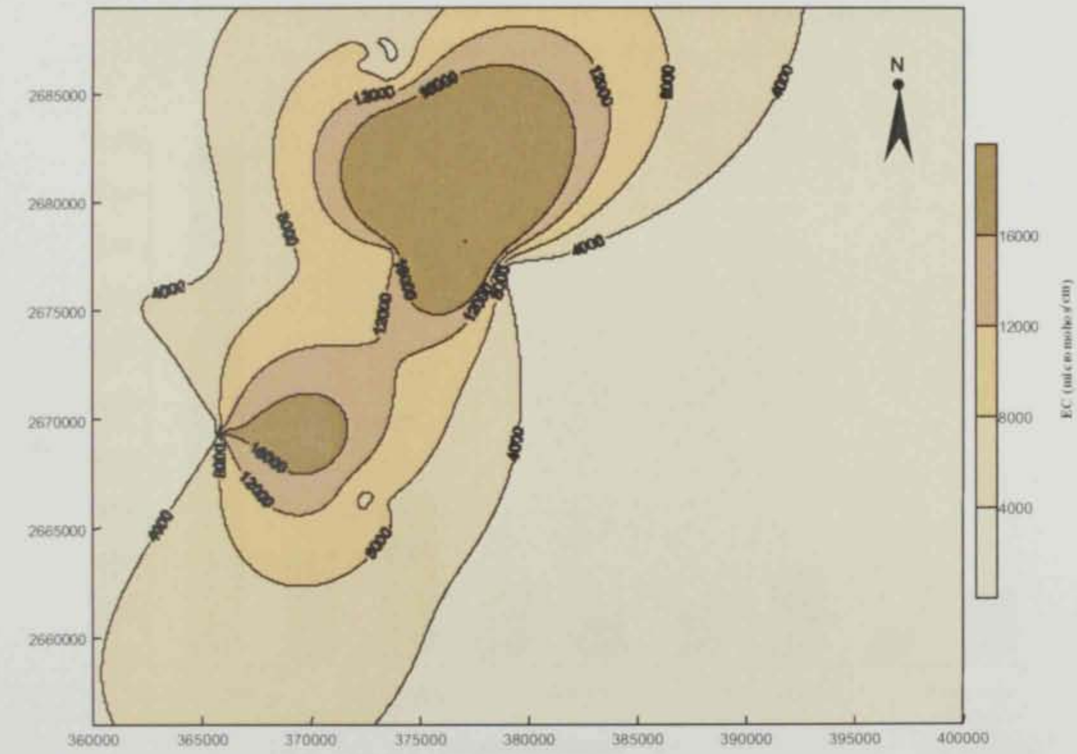

Fig. (5.3) Distribution map of the Electrical Conductivity (EC) for the Quaternary aquifer in Al Jaww Plain.

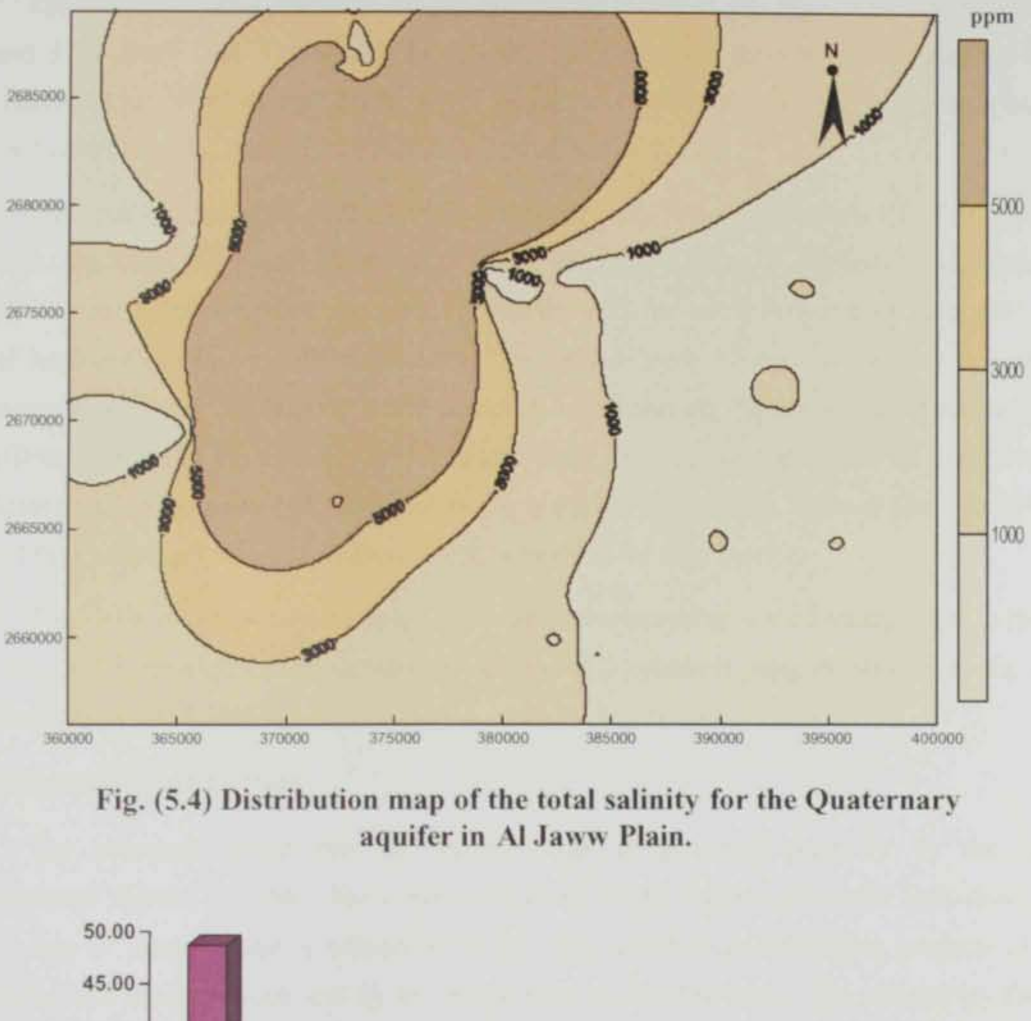

Fig. (5.4) Distribution map of the total salinity for the Quaternary aquifer in Al Jaww Plain.

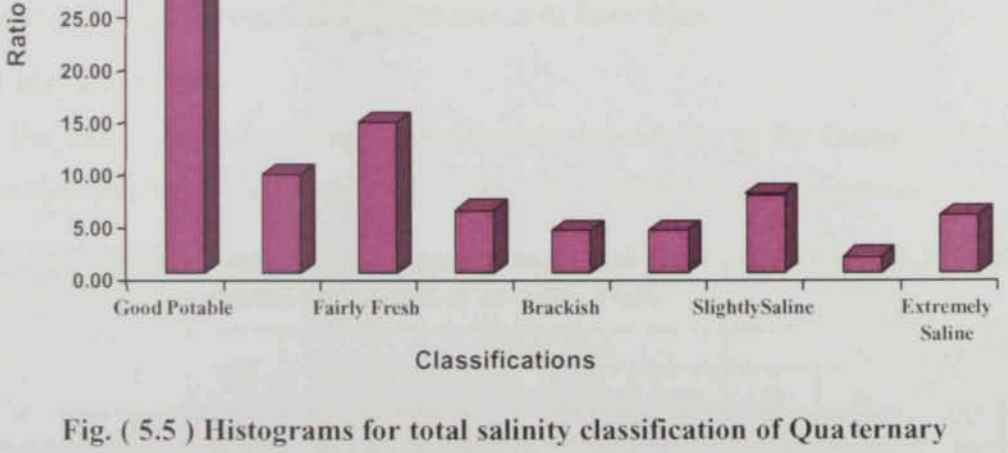

Fig. (5.5) Histograms for total salinity classification of Quaternary aquifer in Al Jaww plain.

5.2.1.4 Total hardness

The calculated total hardness for the Quaternary water at the study area varies between 150 and 3270 ppm. (Fig. 5.6) shows the distribution of the total hardness (TH) along the study area. There are two areas of high (TH); one is located at the northwestern part of the area and the other one area is located to south at the middle part of the study area.

The total hardness of water could be divided into two main types. The first includes carbonate hardness (temporary hardness), which is expressed as a portion of calcium and magnesium that would combine with the bicarbonate and the small amounts of carbonate. This type of hardness can be virtually removed by boiling the water, where calcium and magnesium carbonates precipitate. The second is the non-carbonate hardness (permanent hardness), which is the difference between the total hardness and carbonate hardness, and is caused by those amounts of calcium and magnesium that would normally combine with sulfate, chloride and nitrate ions. Most of the Quaternary water at Al Jaww Plain belongs to the first type.

The wells of temporary hardness water are corresponding to the recharge area, while the wells of some permanent hardness salts are located at a relatively long distance from the fresh water recharge (Fetter, 1988).

5.2.2 Chemical properties

The chemical composition of natural water is governed primarily by the natural environmental factors, to which the water is exposed in the hydrologic cycle. Specifically, the composition of natural water is influenced by the type and amount of soluble products of rock weathering and decomposition and by the terrain traversal by that water. The parameters that best relate to the major constituents of a water are potassium (K), sodium (Na), magnesium (Mg), calcium (Ca), chloride (Cl), sulphate (SO^{--}), carbonate (CO^{--}) and bicarbonate (HCO^{-}). Each of these parameters and their relationship to each other are discussed. Table (5.2) illustrates statistics about the distribution of these constituents at Al Jaww Plain.

5.2.2.1 Major cations

The major sequence of cations dominance in groundwater of the Quaternary aquifer at Al Jaww Plain area has the order Na > Ca > Mg >K , Table (5.2) and the appendix .

Table (5.2). Statistical analysis for the parameters of physical properties (pH, Ec, TDS, TH) and for the major cations and anions of Al Jaww Plain.

Analysis / Values	pH	Ec	TDS	TH	Major Cations				Major Anions			
					Na^+	Ca^+	K^+	Mg^{++}	Cl^-	So^-	Hco_3	No_3
Minimum	7	375	240	150	8	14	0	2	38	22	12	0.14
Maximum	11.6	75000	51000	3270	8650	2400	350	1200	25347	2840	2489	26
Mean	7.9	3834.5	2550.5	365.4	648.6	236.8	32	154.2	1325	337.3	223.4	7.221

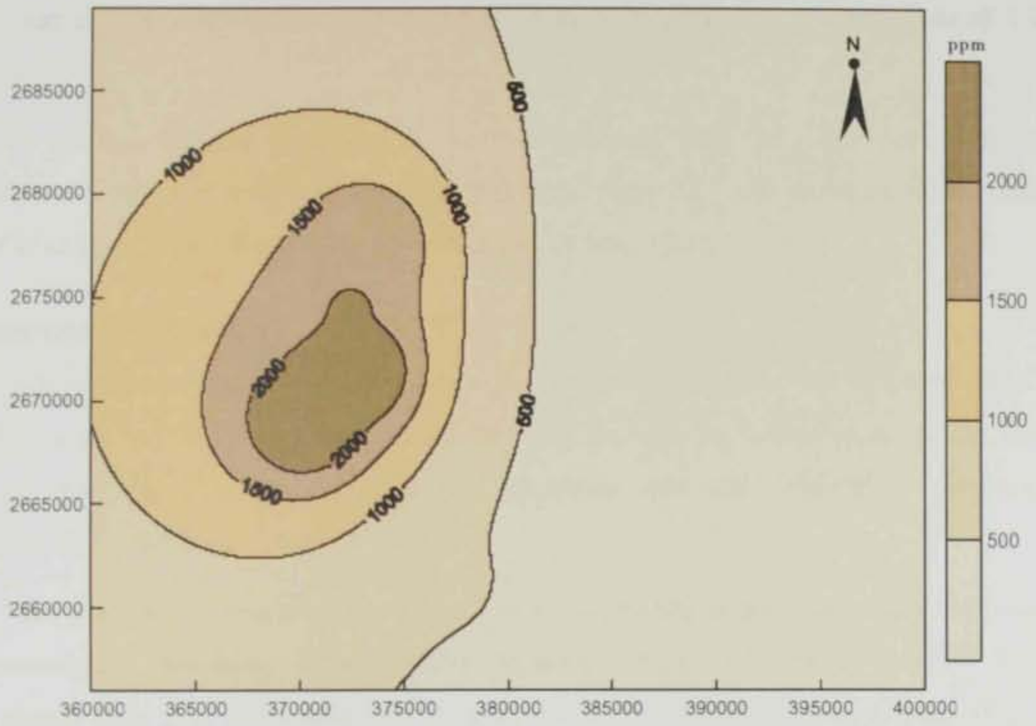

Fig. (5.6) Distribution map of the total hardness for the Quaternary aquifer in Al Jaww Plain.

Calcium distribution

The common form of calcium in the sedimentary rocks is carbonate specially the limestone and dolomite which are distributed in the study area specifiely at Jabal Hafit. The calcuim ion Ca^{+} concentration ranges between 14 to 2400 ppm with a mean value of 236.8 ppm.

A gradual increase from east to west is observed (Fig. 5.7). The concentration of calcium in the east and middle is less than 500 ppm. High Ca concentration is encountered west of Jabal Hafit, mainly due to the carbonate rocks of Jabal Hafit.

Magnesium distribution

The common source for magnesium in the groundwater is the dolomite ($MgCO_3$, $CaCO_3$) magnesite ($MgCO_3$) and limestone ($CaCO_3$) in the sedimentary rocks, biotite, hornblend and augite in igneous rocks and serpentine, talc and tremolite in metamorphic rocks (Davis and De Weist, 1966).

The presence of magnesium ion Mg^{2+} in the freshwater is less than calcium due to the low geochemical abundance of magnesium (Mathess, 1982). The concentration of Mg^{2+} in water ranges from 2 to 1200 ppm with a mean value of 145.2 ppm. Contour map (Fig. 5.8) shows a general increase in Mg^{2+} concentration from east to west. The maximum Mg^{2+} concentration exists on the western side of Jabel Hafit and is related to the solution of dolomite which is abundant at Jabal Hafit. High Mg^{2+} is located in the western part of the study area and is related to the released magnesium from chemical fertilizers (Terao et al., 1993). This area is intensively cultivated (Fig. 5.1a).

Sodium distribution

Sodium ion is considered as one of the most important ions in natural water. The source of sodium in water depends on the rock type through which the water moves. The main source for the presence of most sodium ions (Na^{+}) in the natural water s the release of soluble products during the weathering of plagioclase feldspars, which are typical constituents of many igneous rocks. It is also common in evaporates and argillaceous sediments. The value of (Na^{+}) ranges between 8 and 8650 ppm with a mean value of 648.6 ppm. The sodium distribution is presented in (Fig. 5.9). The concentration of Na^{+} increases from east to west. Most of Al Jaww area has (Na^{+}) concentration of less than 500 ppm, while the area west of Jabal Hafit has the highest concentration.

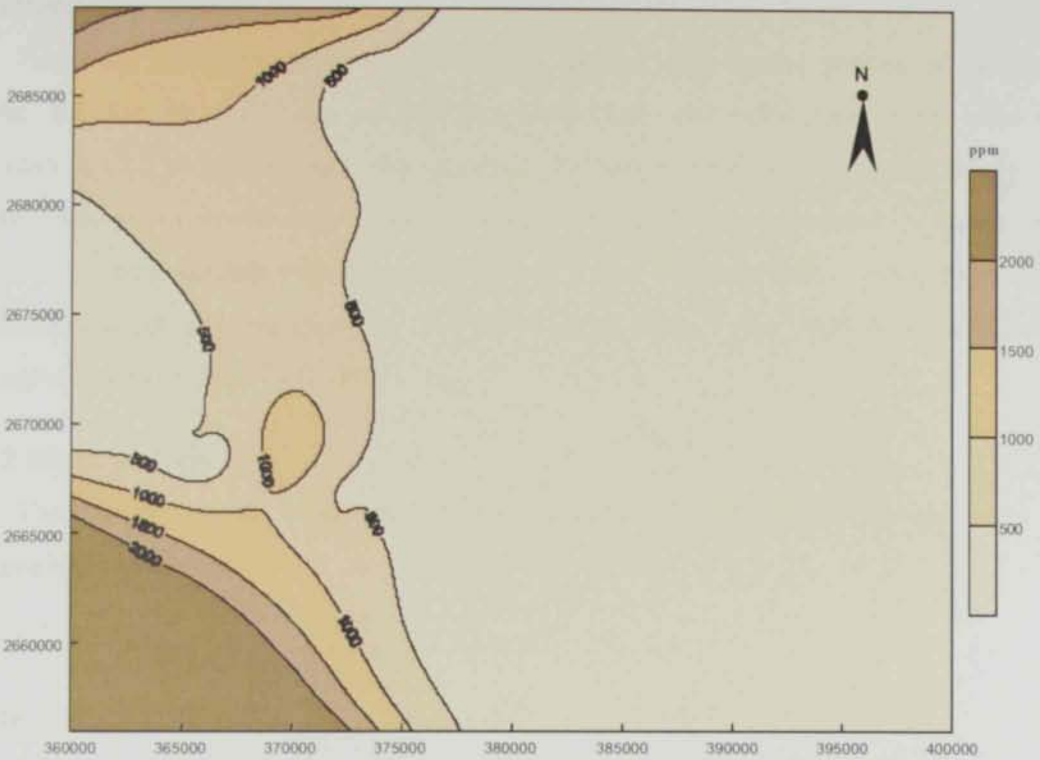

Fig. (5.7) Distribution map of the calcium cation for the Quaternary aquifer in Al Jaww Plain.

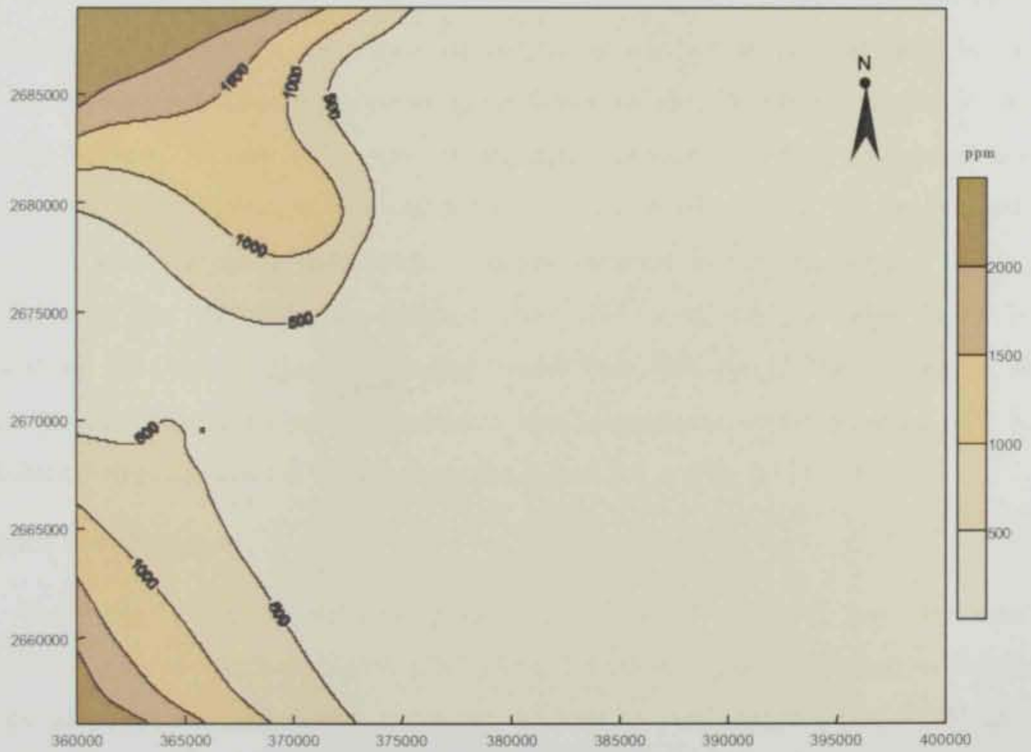

Fig. (5.8) Distribution map of the magnesium cation for the Quaternary aquifer in Al Jaww Plain.

Potassium distribution

Potassium content is generally lower than sodium. The natural sources of potassium in water are the igneous rocks as feldspars (orthoclase and microcline) some mica and sedimentary rocks as silicate and clay minerals. Potassium concentration is commonly less than one-tenth the concentration of sodium in natural water because potassium is hardly taken into solution. The potassium content ranges between 2 and 350 ppm with a mean value of 32 ppm. Potassium ion concentrations are low at Al Jaww Plain, while high K^+ concentrations are recognized west of Jabal Hafit (Fig. 5.10).

5.2.2.2 Major anions

The sequence of the major anion in the groundwater of the Quaternary aquifer at the study area has the order of:

$Cl^- > SO^{2-} > HCO^- > NO^{2-}$

Bicarbonate distribution

The presence of bicarbonate ions HCO^- in the groundwater is derived from carbon dioxide in the atmosphere, in soils and by dissolution of carbonate rocks (Davis and De Weist, 1966). In the absence of calcareous sediments and carbonate rocks most of HCO^- in groundwater results from the dissolution of carbon dioxide within the soil zone by organic decay. Bicarbonate ion concentrations in groundwater of the Quaternary aquifer in Al Ain area range between 12 and 2489 ppm. Bicarbonate represents the third dominance anion in the study area. The distribution of bicarbonate is shown in (Fig. 5.11). The iso-concentration contour map shows irregular distribution. The concentration in the area located at the most eastern part of the study domain reaches about 200 ppm. On the other hand, HCO^- concentrations are high at the western part (more than 400 ppm). The decline in HCO^- between the two concentrations of bicarbonate area is attributed to the presence of a buried alluvial channel that runs in a SW direction, see the dashed line in (Fig. 5.11).

Sulphate distribution

The most extensive and important occurrences of sulphate ions in water are sedimentary rocks as gypsum ($CaSO_42HO_2$) and anhydrite ($CaSO_4$). During weathering, the sulphides which are in contact with water are oxidized to yield sulphate that is carried off in water. In arid region, the leaching of sulphate from the upper soil sediments causes the sulphate to be the principle anion in the underlying groundwater. Further addition of sulphate

Fig. (5.9) Distribution map of the sodium cation for the Quaternary aquifer in Al Jaww Plain.

Fig. (5.10) Distribution map of the potassium cation for the Quaternary aquifer in Al Jaww Plain.

to the groundwater arises from the breakdown of organic matters in the soil and from addition of leachate sulphates in fertilizers. The value of the sulphate in the study area ranges between 22 and 2840 ppm (Fig. 5.12). There is a steady increase in So_4^{--} from the east to west.

Chloride distribution

The chloride ion (Cl^-) is widely distributed in natural water. Most (Cl^-) in the groundwater is from three sources including ancient seawater entrapped in sediment, solution of halite and related minerals in evaporate deposits and solution of dry fallout from the atmosphere especially in the arid region (Davis and DeWeist, 1966).

The value of the chloride in the study area ranges between 38 and 25347 ppm. Low values of the chloride concentration are encountered in the eastern side, while high values are observed in the north and south of the study area. There is a steady increase in Cl^- from east to west in the direction of water flow, (Fig. 5.13).

Nitrate distribution

The dissolved nitrogen in form of nitrates (NO_3^-) is the most common contaminant identified in groundwater. Nitrate in groundwater generally originates from several natural and man induced sources on land surface. Nitrate or nitrogen has proved to be a health hazard when it occurs in drinking water at concentrations in excess of 10 mg/l. The Nitrate distribution is given in (Fig. 5.14).

The main source of nitrate in groundwater is related to the intensive use of chemical nitrogen fertilizers in agriculture. This is clearly demonstrated in the western part of the study area, where most of the farms are located (Fig. 5.14).

5.3 The Ion Dominance

The ion dominance detection is quite helpful in the water quality assessment and classification. Three Semi logarithmic profiles, Schoellers diagram after (Schoellers, 1962), were constructed within the study area (Fig. 5.15). The three profiles are oriented SE-NW (Figs. 5.16, 5.17 and 5.18). Generally, these diagrams indicate the predominance of sodium, followed by magnesium, followed by calcium and then by potassium. On the other hand, the chloride ions predominate followed by sulphate and then bicarbonates.

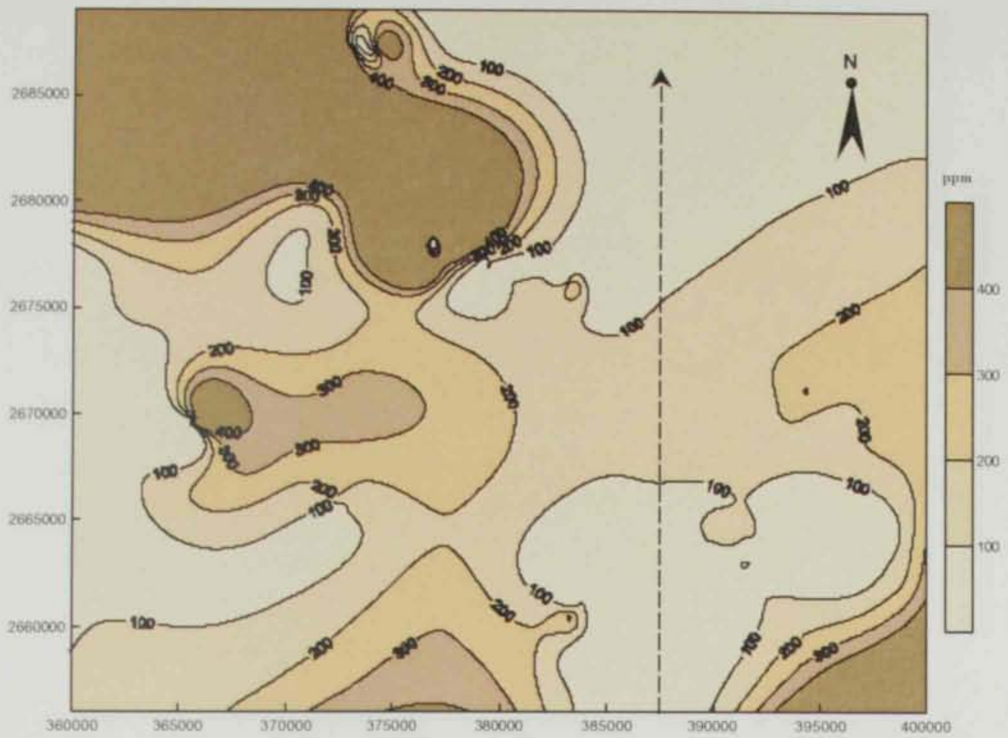

Fig. (5.11) Distribution map of the bicarbonate anion for the Quaternary aquifer in Al Jaww Plain.

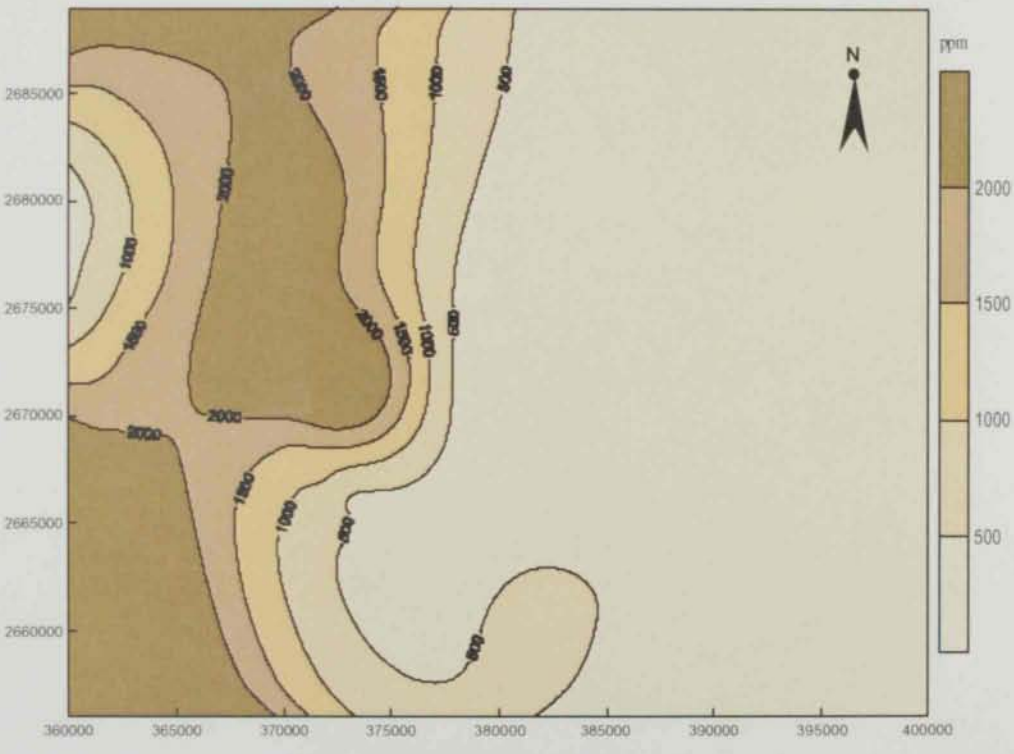

Fig. (5.12) Distribution map of the sulphate anion for the Quaternary aquifer in Al Jaww Plain.

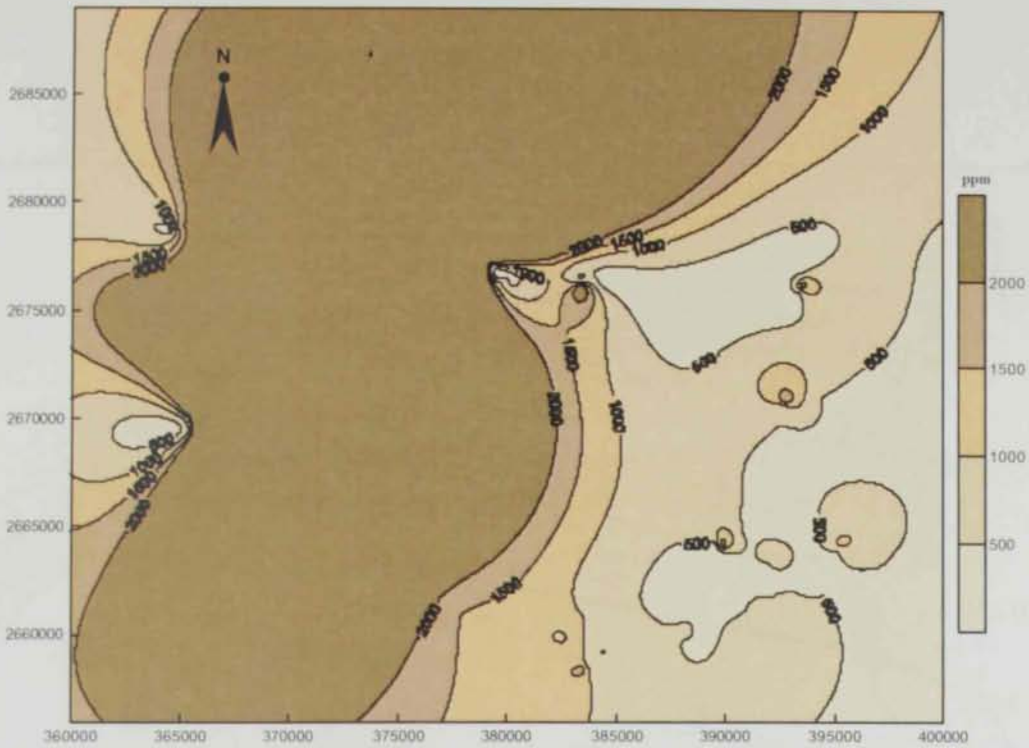

Fig. (5.13) Distribution map of the chloride anion for the Quaternary aquifer in Al Jaww plain.

Fig. (5.14) Distribution map of the nitrate anion for the Quatemary aquifer in Al Jaww plain.

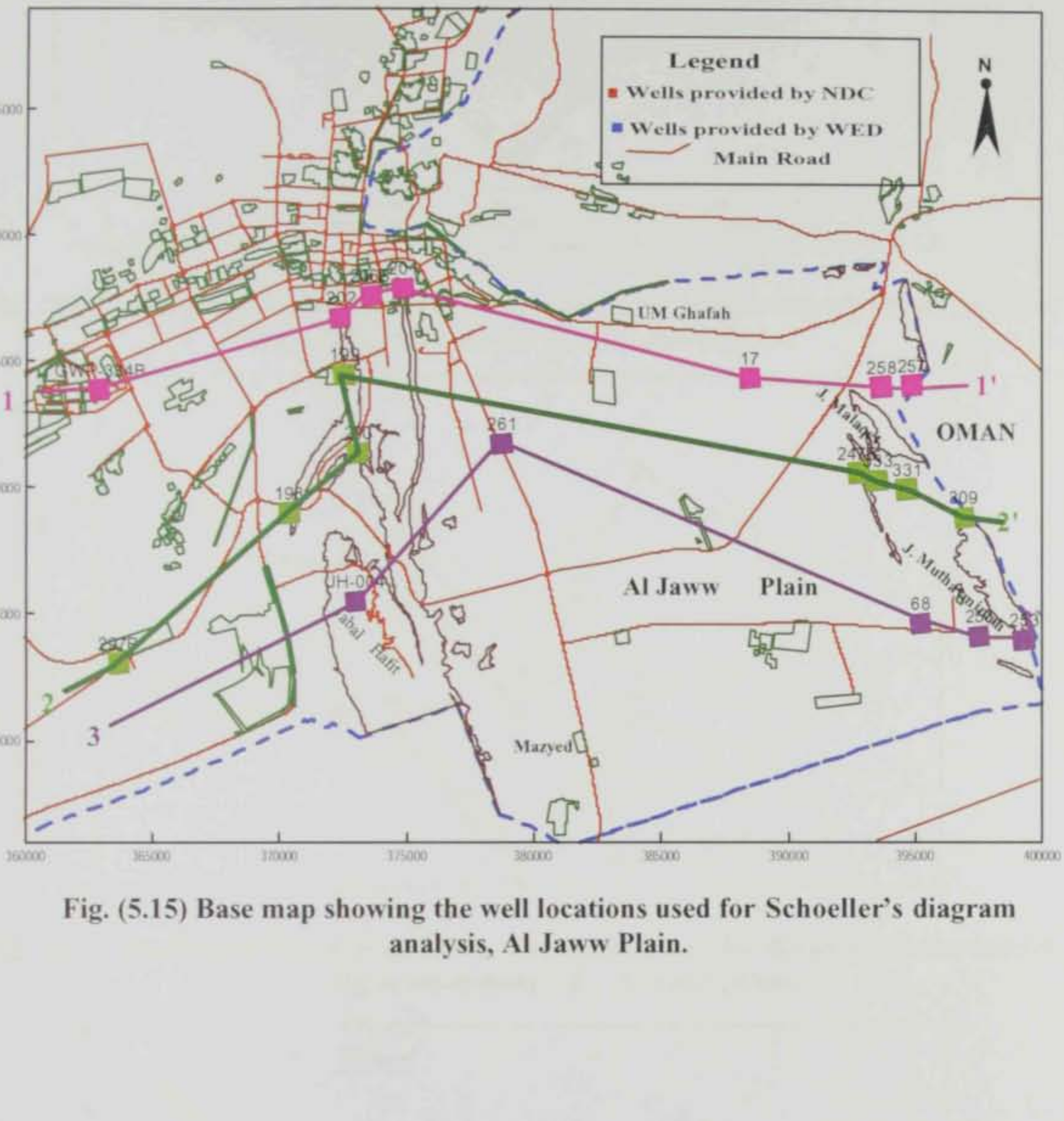

Fig. (5.15) Base map showing the well locations used for Schoeller's diagram analysis, Al Jaww Plain.

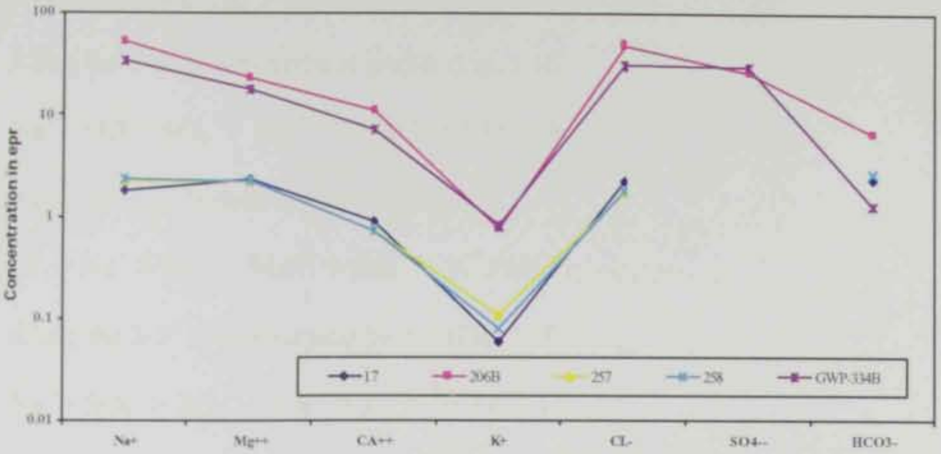

Fig. (5.16) Semi-logarithmic diagram for Quaternary aquifer showing the dominance ions along cross-section 1-1', Al Jaww Plain.

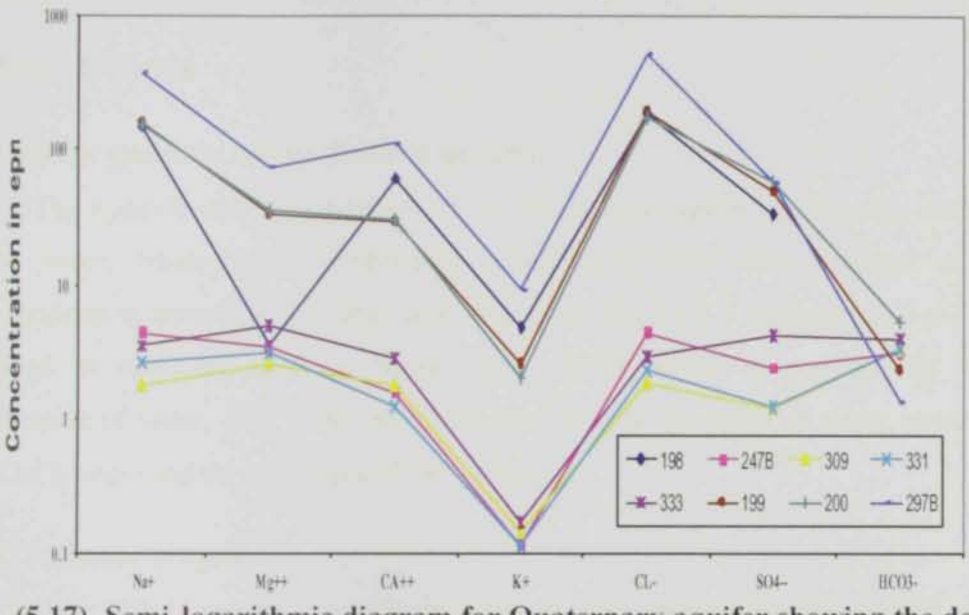

Fig. (5.17) Semi-logarithmic diagram for Quaternary aquifer showing the dominance ions along cross-section 2-2', Al Jaww Plain.

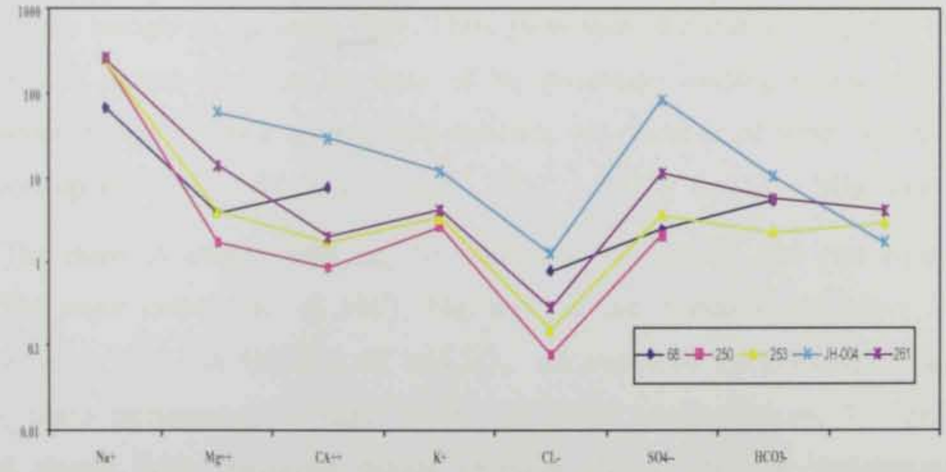

Fig. (5.18) Semi-logarithmic diagram for Quaternary aquifer showing the dominance ions along cross-section 3-3', Al Jaww Plain.

From the hydrochemical cross sections, it can be concluded that:

Along the 1-1` hydrochemical profile (Fig. 5.16)

$Na^{+} > Cl^{-} > SO_4^{--} > Mg^{++} > Ca^{++} > HCO_3^{-} > K^{+}$

Along the 2-2` hydrochemical profile (Fig. 5.17)

$Cl^{-} > Na^{+} > Ca^{++} > Mg^{++} > So_4^{--} > K^{+} > HCO_3^{-}$

Along the 3-3` hydrochemical profile (Fig. 5.18)

$Na^{+} > SO_4^{--} > Mg^{++} > Ca^{++} > K^{+} > HCO_3^{-} > Cl^{-}$

Along these sections diversity in water genesis within Quaternary aquifer is demonstrated.

5.4 Water Genesis

5.4.1.Water genesis using (Sulin's graph)

The hydrochemical composition of the Quaternary aquifer reflects the meteoric origin of the water, where the hydrochemical parameter $rk^{+}+rNa^{+}/rCl^{-}$ expressed in equivalent concentrations is always greater than unit. Where the letter (r) expresses that the relation is calculated in epm, by applying Sulins graph (1948) which is prepared for the genetic classification of water, (Fig. 5.19), the Quaternary reveals two types of water genesis, the first is of $CaCl_2$ origin and the second is of $MgCl_2$ origin.

5.4.2. Trilinear diagram

Piper (1944) suggested a form of linear diagram representing the analysis of water by three plotted points. The cations are plotted on the triangle to the lower left and the anions are plotted on the triangle to the lower right. These plots show the relative properties of the main constituents of natural water on the basis of the percentage reacting values (r%). The third point, plotted in the diamond shaped field indicates the character of water as represented by the relationship among $Na^{+} + K^{+}$, $Ca^{++} + Mg^{++}$, $CO_3^{--} + HCO3^{-}$ and $Cl^{-} + SO_4^{--}$ ions.

The diamond shaped field can be subdivided horizontally into two equal triangular fields. The major cations (K^{+} & Na^{+}), $Mg^{++}$and $Ca^{++}$are plotted in the lower left triangle, while the anions (CO_3^{--} & $HCO3^{-}$), Cl^{-} and SO_4^{--} are plotted on the in the lower right triangle. The two points representing the major cations and anions composition are then plotted in the diamond shaped field. Numerous natural chemical changes can be demonstrated by the trilinear diagram. If the analysis represents regional water and a mixture, it will plot on a straight line. Thus this diagram can be used for the detection of water quality changes by the mixing of water.

In this study the data of the chemical analysis of the groundwater samples are plotted on Piper diagram (Fig. 5.20). The investigated Quaternary type can be discriminated in sub areas of the diamond shaped filled. The appearance of most of the samples in the upper triangle of the diamond shaped field, points to the dominance of Ca-Mg and CO_3 -HCO_3 water types.

It should be noticed that water at Al Jaww Plain is enriched in Mg^{++} that is dissolved from Mg-rich Ophiolite rocks. This plot is in good match with the data plotted on Sulin's diagram (Fig. 5.19).

5.5 Water Quality Evaluation and its Availability for Use

The most important factors to determine the suitability of water quality for irrigation purposes are the total concentration of soluble salts and the sodium adsorption ratio. Sodium and salinity hazards represente severe problems in arid areas where salt accumulation in the soil is seldom flushed by rainwater.

a) Evaluation of water for irrigation using the relation between (SAR and EC)

The suitability of the water for irrigation purpose depends on the classification proposed by salinity laboratory staff (1954). This classification is based on the electrical conductivity in micromohos per centimetre and sodium adsorption ratio (SAR). According to this classification, the characteristics of irrigation water which is most important in determining its suitability are:

1) Sodium Hazard: expressed as, sodium absorption ratio, which is defined by the equation:

$$S.A.R. = \frac{Na^{+}}{\sqrt{\frac{Ca^{++} + Mg^{++}}{2}}}$$

Where, Na^{+}, Ca^{++} and Mg^{++} are in meq/l. SAR has long been used as a measure of sodium hazard. It predicts reasonably well the degree to which irrigation water tends to enter into cation exchange reactions in soil. High values of SAR imply a hazard of sodium replacing absorbed Ca^{++} and Mg^{++} and this replacement is damaging to soil structure.

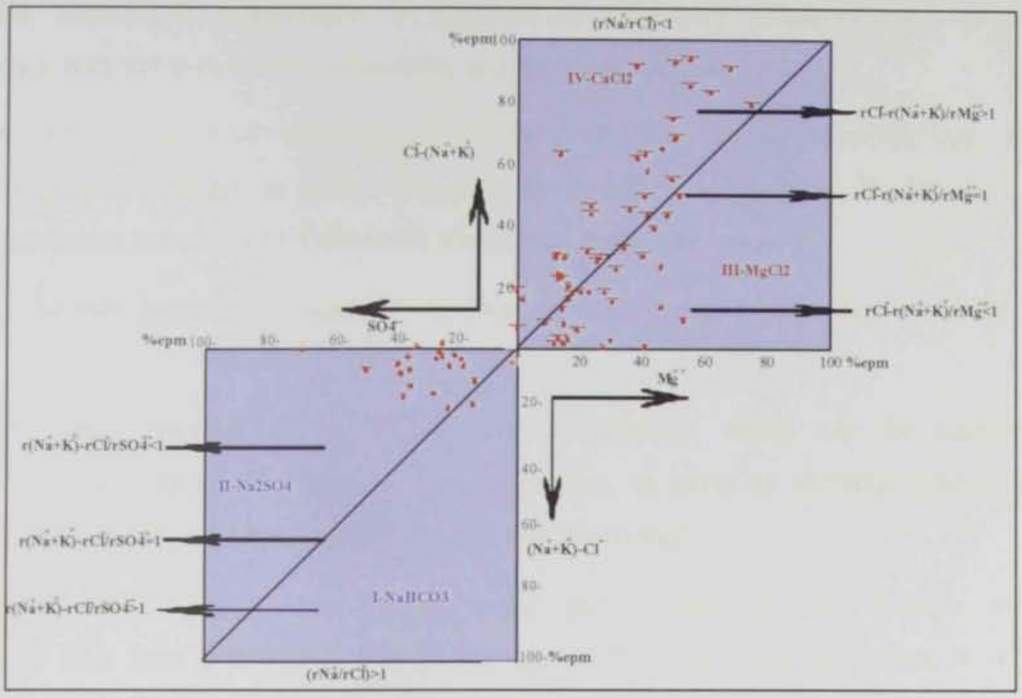

Fig. (5.19) Sulin's graph for genetic classification for the Quaternary aquifer in Al Jaww Plain.

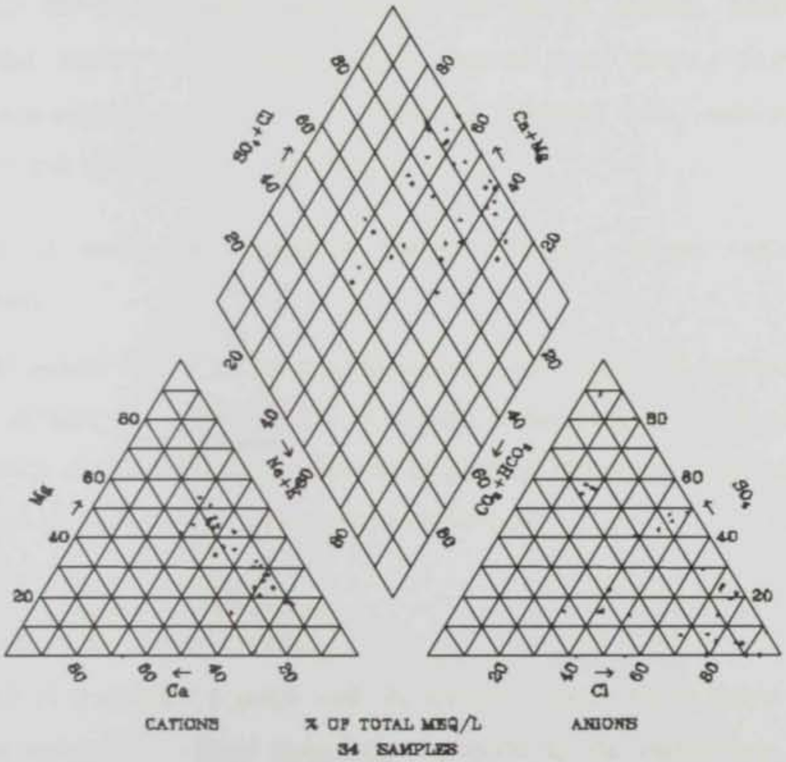

Fig. (5.20) Piper's trilinear diagram for classification of Quaternary aquifer, Al Jaww Plain.

The sodium-ion concentration is important in classifying irrigation water because sodium reacts with soil to reduce its permeability and cause hardening of the soil.

According to the SAR values (Fig. 5.21), the groundwater in the east of the study area has a limited harmful effect on plants when used for irrigation. To the west, the groundwater can cause moderate to high harmful effects for plants when applied for irrigation.

2) Salinity Hazard, expressed as electrical conductivity in micromohos/cm at 23 °C.

The total concentration of soluble salts in irrigation waters can be adequately expressed for the purpose of diagnosis and classification in terms of electrical conductivity. The conductivity is useful since it is readily and precisely determined.

Nearly all irrigation water which could used without adverse impacts for a considerable time have conductivity values less than 2.250 micromhos/cm. Water of higher conductivity can be used occasionally, but for the crop production it might not be suitable.

This classification diagram is divided into 16 classes according to salinity and sodium hazards. Fig. (5.22) shows the sodium and the salinities hazard diagram. Inspection of this figure indicates that sodium and salinity hazards increase with distance from the Oman Mountains. This westward increase in salinity hazard is consistent with westward increase of electric conductivity and TDS (Figs. 5.3 and 5.4).

b) Evaluation of water for irrigation purposes using sodium content (Wilcox, classification).

The soluble sodium content of water is an important indicator of its quality and suitability for irrigation. The increase of sodium ion content in groundwater leads to a high content of these ions in the soil, which in turn has a great effect on its physical properties. Wilcox (1955) defined sodium percentage in terms of common cations (epm) as follows:

$$Na^{+}\% = \frac{(Na^{+} + K^{+})x100}{Na^{+} + K^{+} + Mg^{++} + Ca^{++}}$$

Wilcox (1955) designated a graph with the total cations or anions (epm) expressed by the horizontal axis against the sodium percentage expressed by the vertical axis. This graph is subdivided into five zones (excellent, good to permissible, permissible to doubtful, doubtful to unsuitable and unsuitable) to delineate water concerning its suitability for irrigation. Based

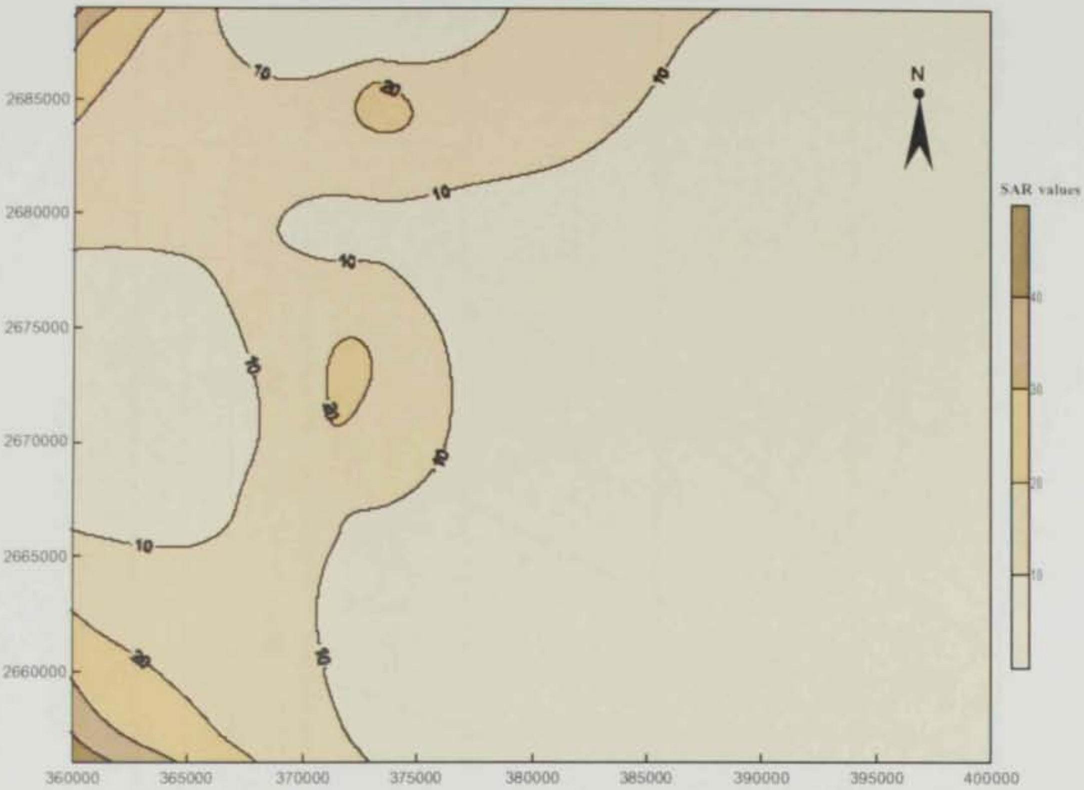

Fig. (5.21) Distribution map of the sodium adsorption ratio (SAR) for the Quaternary aquifer in Al Jaww Plain.

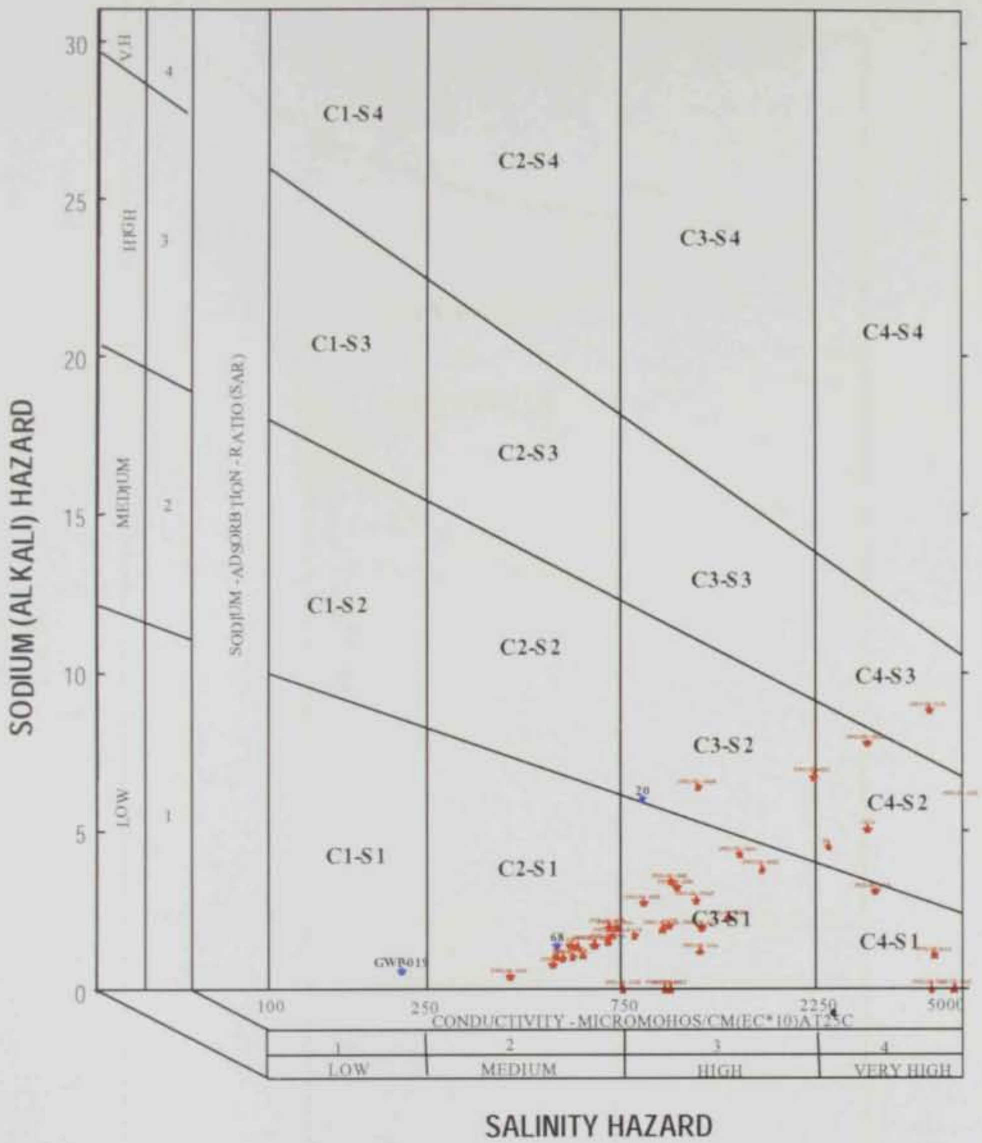

Fig. (5.22) Diagram for the classification of irrigation water (U.S. Salinity Laboratory Staff, 1954) for the Quaternary aquifer in Al Jaww Plain.

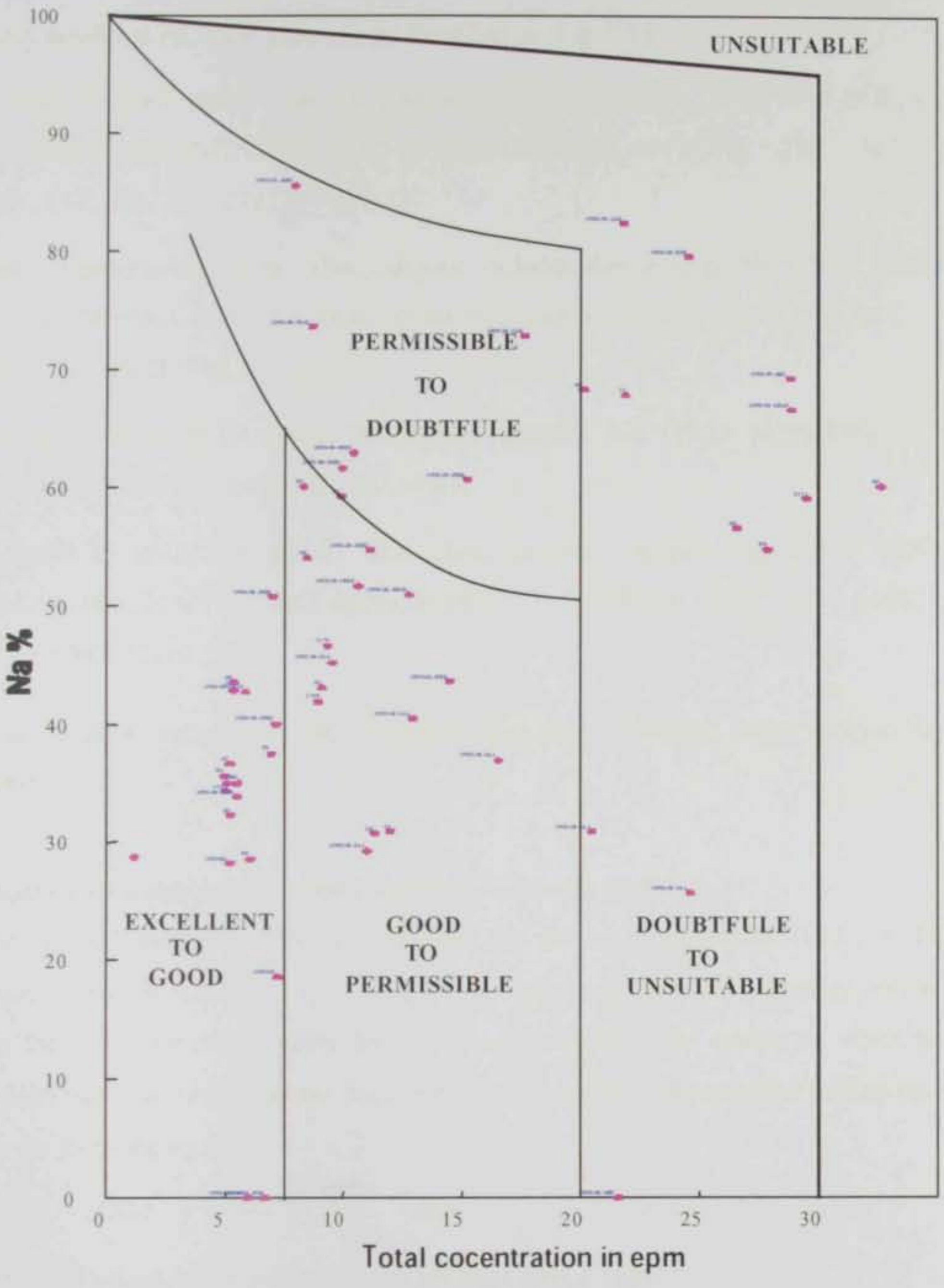

Fig. (5.23) Wilcox`s classification of groundwater of the Quaternary aquifer in Al Jaww Plain.

on the classification established by Wilcox (1955) for irrigation purposes, the groundwater of the Quaternary aquifer at Al Jaww plain can be classified as (Fig. 5.23).

1. Excellent to good water: This category includes samples No GWP (019-018), GWD (040SHIR-034SHIR-028-002GHAF-001SOH-028MEZ-001SOH), 250, 307, 309, 248A, 258, 308, 250, 254, 257 and 331.

2. Good to permissible water: This category includes the samples No GWD (065SAA-002SAA-068SAA-042SHIR-149SAA-041SHIR-003GHAF-033SHIR), 333, 68, 246B, 253, 247B, 330, 252 and 251.

3. Permissible to doubtful water: it includes samples No GWD (029SHIR-030SHIR-007SHIR-001ZAK-010NIAD-005AMM).

4. Doubtful to unsuitable water. This class includes samples No GWD (005SAA-003SAA-004GHAF-007MEZ-003SOH-002ZAK-011MEZ), 333, 68, 246B, 253, 247B, 330, 251and 252.

5- Unsuitable class: the sample No.329 falls in this class. However, some samples fall out of scale.

c) Evaluation of water using residual sodium carbonate (R.S.C.)

The residual sodium carbonate represents the excess of carbonate (CO_3^{--} + HCO_3^-) over the lime elements (Ca^{++} + Mg^{++}). It gives an indication for water alkalinity and is used to estimate the suitability of the water for agricultural purposes. The quality of water samples has been determined according to the scale after Eaton (1950). The residual sodium carbonate is shown in the following equation:

$$R.S.C. = (CO_3^{--} + HCO_3^-) - (Ca^{++} + Mg^{++}).$$

Where all values of cations and anions are expressed in epm.

The residual sodium carbonate is used to distinguish between the different water classes for irrigation purposes because high concentration of HCO_3^- leads to an increase in pH values causing the dissolution of organic matter. Moreover, high concentration of HCO_3^- in irrigation water leads to the increase of its toxicity and affects the mineral nutrition of plants. The residual sodium carbonate of Quaternary aquifer varies from -197 to 40 epm with a mean value of -6.1 epm. Generally, the distribution of residual sodium carbonate in the Quaternary aquifer ranges from good to unsuitable quality (Fig. 5.24). The eastern part of the

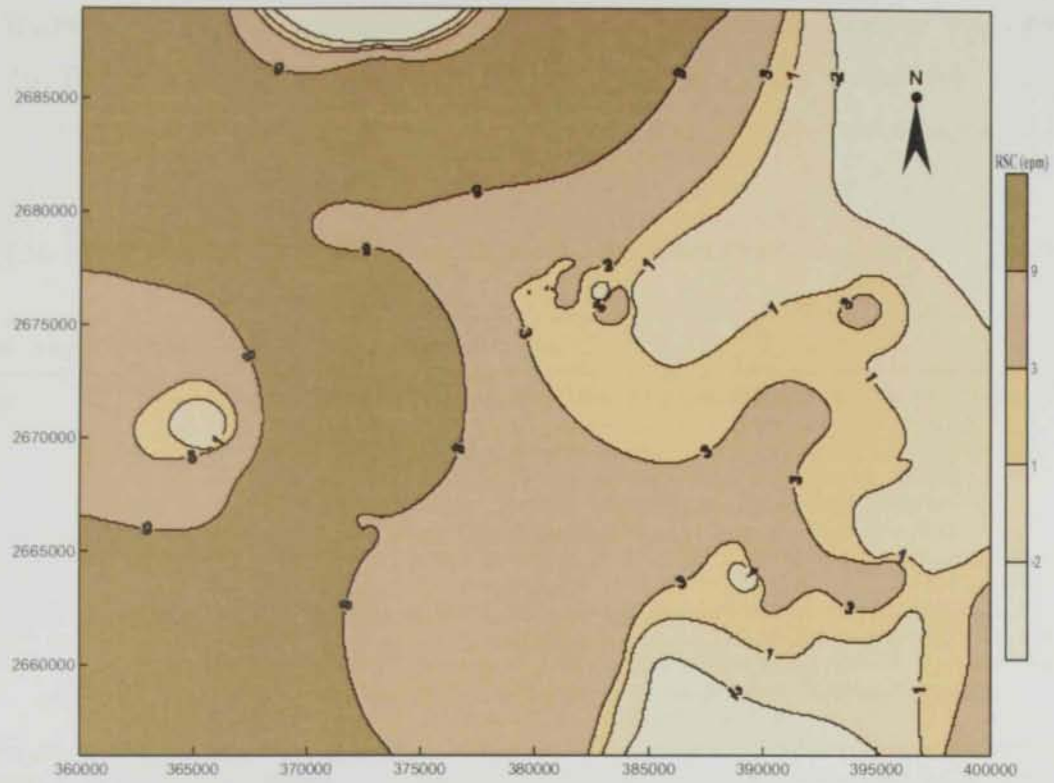

Fig. (5.24) Distribution map of the residual sodium carbonate (RSC) for the Quaternary aquifer in Al Jaww Plain.

study area has R.S.C. ranging between less that -2 to 3 epm while the western part of the Quaternary aquifer at Al Jaww plain has concentrations greater than 9 epm.

According to Eaton classification (1950), the water samples are classified into three classes. The first class has (R.S.C) less than 1.25 epm (good quality). The second class ranges 1.25 to 2.5 epm (medium quality). The third class has more than 2.5 epm (unsuitable quality). Table (5.3) lists the samples numbers and their relevant classes.

Table (5.3). Suitability of water according to R.S.C. for Quaternary aquifer at Al Jaww Plain.

Residual Na_2CO_3	Quality	Samples No.
< 1.25 epm	Water of good quality, used for the irrigation of all soils	17-18-20-68-198-204-206A-206B-246B-247A-247B-248A-250-251-252-253-254-256-257-258-259-307-308-309-328A-328B-329-330-331-333-GWP(334A-334B-335-336-19)-JH(001-002-004-005-007-008-009-010)-199-200-261-297A-297B-GWD(001SOH-001ZAK-002GHAF-002SAA-002SHIR-003GHAF-003SAA-003SHIR-003SOH-004GHAF-004GHAF-004ZAK-005AMM-005NIAD-005SAA-005ZAK-007MEZ-007SHIR-007ZAK-008SHIR-008ZAK-009MEZ-009SHIR-009ZAK-010NIAD-011MEZ-014SHIR-015MEZ-016MEZ-017MEZ-018MEZ-019MEZ-019SHIR-020MEZ-020SHIR-021MEZ-022MEZ-028MEZ-029MAS-029SHIR-030SHIR-031MAS-033SHIR-034MAS-034SHIR-035SHIR-035SOH-037SOH-040SHIR-042SHUR-042SHIR-065SAA-068SAA-106GHAF-108GHAF-109GHAF-112GHAF-149SAA-149SAA)
1.25-2.5 epm	Water of medium quality used in case of good drainage especially rich with calcium	GWD(001MAQ-EQ-002ZAK-003MAQ-EQ-014ZAK-022MAS-032SHIR-075GHAF-107GHAF)
> 2.5 epm	Unsuitable water, especially in poor drainage or when soluble calcium	GWD(002NIAD-002ZAK-003NAD-005MEZ-006NIAD-007NIAD-008MAS-008NIAD-010MEZ-010ZAK-011MAS-011NIAD-012NIAD-013NIAD-020DAI-021MAS)

Chapter VI

GEOPHYSICAL INVESTIGATIONS

GEOPHYSICAL INVESTIGATIONS

6.1. General

Surface and borehole geophysical methods constitute a part of preliminary site evaluation for groundwater investigations. Geoelectrical surveying and well logs would be useful for those areas in which the unconsolidated deposits are important like for the case of the Al Jaww Plain. The data from the geophysical surveying can guide the selection of the sites to conduct test borings and provide information to correlate between them. These borings or wells are needed to determine the subsurface geologic units. The term borings referred to uncased holes drilled in unconsolidated overburden (Fetter, 1994). Logging of these borings, with wireline geophysical tools, is important for evaluating the aquifer's characteristics and management of groundwater resources.

In this study, the D.C resistivity method (Vertical Electrical Sounding, VES), Time Domain Electromagnetic (TEM) and wireline geophysical logging data are implemented. The description of these methods are disussed in chapter three. The results and interpretation of these data are given below.

6.2 Vertical Electrical Sounding Results

Table (6.1) lists the qualitative and quantative interpretation of nine vertical electrical soundings along a profile trending SW-NE direction (Fig. 6.1).

6.2.1 Qualitative interpretation

The first step in the interpretation of an apparent resistivity-sounding curve is to define the curve shape. This can be classified simply for the three layer case into one of four basic curve types, which are H ($\rho 1>\rho 2<\rho 3$), A ($\rho 1<\rho 2<\rho 3$), K ($\rho 1< \rho 2>\rho 3$) and Q ($\rho 1>\rho 2>\rho 3$). These can also be combined to describe more complex field curves, that may have several layers such as HK, KH or more complex types. The curve shape is dependent upon the relative thickness of the in-between layers (i.e. layer two in a 3-layer model).

The relative magnitude of the true resistivities obtained from the levels of the flat portions or shoulders of the graph represents a useful starting point before conducting more detailed interpretations. The number of layers identified is equal to the number of turning points in the curve plus one (Reynolds, 1997). The presence of turning points indicate sub-

Table (6.1) Qualitative and quantitative interpretation of the Vertical Electrical Sounding (VES) resistivity data, Al Jaww Plain.

VES No	Curve Type	No of Layers	True resistivity (Ohm-m)									Thickness of Layers (m)								
			ρ_1	ρ_2	ρ_3	ρ_4	ρ_5	ρ_6	ρ_7	ρ_8	ρ_9	T1	T2	T3	T4	T5	T6	T7	T8	T9
1	QQH	5	180	42	4	2.4	9					1.3	7.8	163.8	8.2					
2	KQH	5	300	450	75	10	36					0.4	5.6	34	310					
3	QQH	5	200	75	37	3	290					0.7	8.3	226	165					
4	KQQH	7	450	1250	190	105	6	24	12			0.5	1.3	3.2	25.2	249				
5	QH	4	1300	85	7	67						2	25	220						
6	QQH	5	590	58	26	6	59					1.5	4.5	30	160					
7	QHKH	6	270	27	8	40	4	20				1	7.5	44	42	155				
8	HKHKHKH	9	269	7	23	5	16	11	23	10	22	0.7	1.5	4.2	4.5	19.2	21	70	860	
9	KQHKH	7	460	670	22	7	25	7.5	48			0.6	1.5	5.8	35.4	21.8	488			

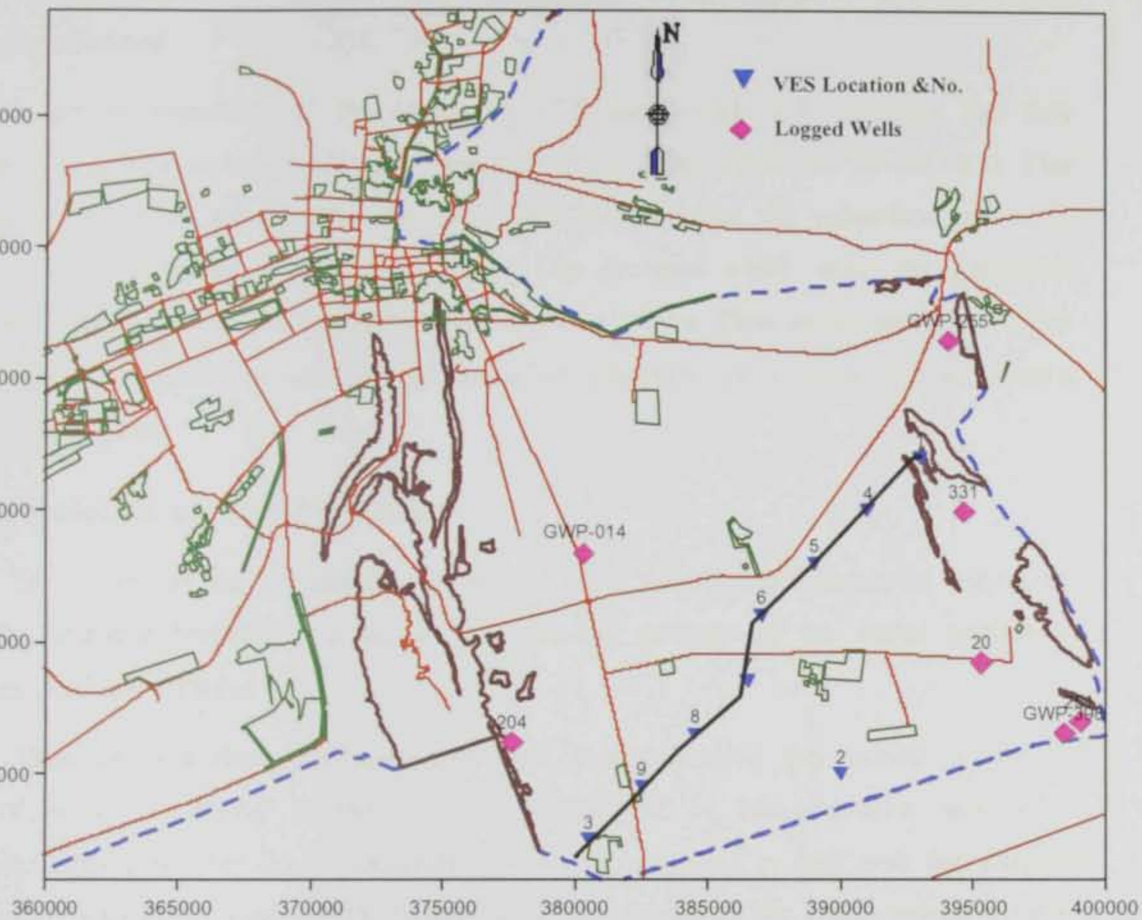

Fig. (6.1) Base map showing the locations of VES data and the available logged wells at Al Jaww Plain.

surface interfaces, so the number of actual layers must be one more than the number of boundaries between them. However, the coordinates of the turning points indicate the depth to a boundary to provide specific information about the true resistivities. The minimum number of horizontal layers and the relative magnitudes of the respective layer resistivities can also be estimated.

A general inspection of the interpreted VES data (Table 6.1) indicates that they represent four to nine layers of different types such as the QQH, KQH and HKHKHKH. This variation in the curve types within the study area revealed that the subsurface geoelectric model in the investigated area is complicated. The elements which make the geoelectric model not simple include, the subsurface structure of Al Jaww Plain as discussed in chapter two, variation of lithological units of the subsurface sequence and changes of total dissolve solids of groundwater.

6.2.2 Geoelectric section discussion

The review of the geoelectric section (Fig. 6.2) guided with lithological information from the available borehole data reveals a systematic variation in the lateral sedimentary sequence at Al Jaww Plain.

There are four main litho-geoelectric units illustrated along this section: a- top soil zone of resistivity ranging between 180 to 1300 O-m, b- litho-geoelectric unit with a resistivity ranging between 23 to 190 ohm-m which is interpreted as marl with finer materials (this zone contains the water table), c- third geoelectric unit with the lowest resistivity values ranging between 3 to 100 O-m, and is attributed to clay and marl and d- the fourth geoelectric layer with a resistivity ranging between 20 to 290 ohm-m and is interpreted as limestone and or gypsum.

Along this geoelectric section a remarkable ridge of relatively high resistivity at a depth of 200-500m and extends beneath VES 7 to VES 4 in the north east direction is encountered. The low resistivity values show the trend of thick shale-filled faults which reach a depth of 900 m or more at the extremity of the profile. These inferred faults are in good match with traced faults based on seismic reflection data, (Fig. 2.9).

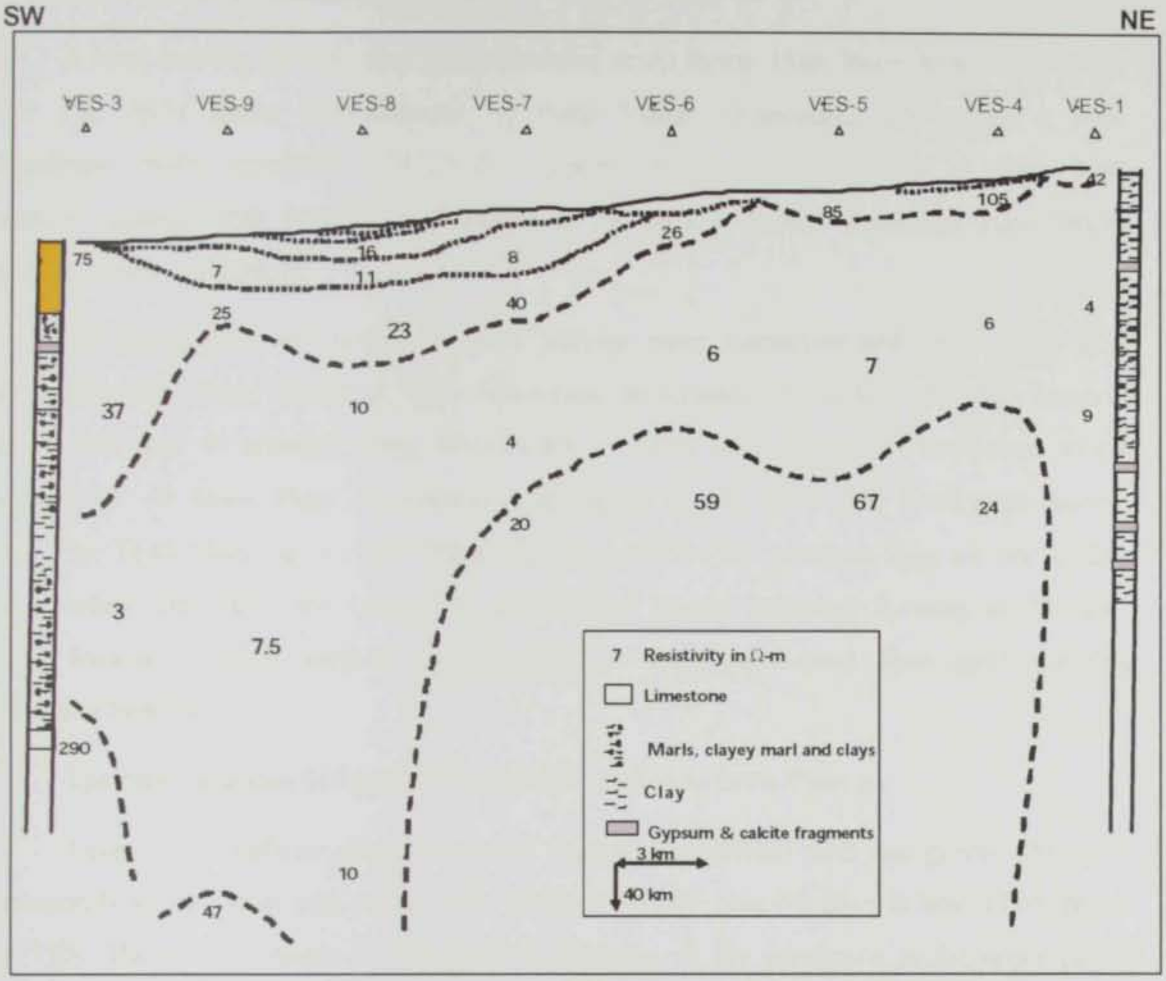

Fig. (6.2) Geoelectric cross section along profile trending southeast-northwest, Al Jaww Plain.

6.3 Time Domain Electromagnetic (TEM) Results

6.3.1 TEM data and resistivity model

A total number of 212 loop data measured at Al Jaww Plain have been provided by NDC. Fig. (6.3) shows the locations of these loops. Interpretated data using a one-dimensional model (program TEMIXGL, Interpex Ltd.) indicated three to four layer resistivity models (Table 6.2) for each station on the profile. Typical soundings from Zaroub line-2 are shown in Fig.(6.4).

The three resistivity models of TEM become more conductive with depth. This is in good agreement when correlated with lithological information from the available borehole data located near to relevant loops. The model of TEM data in the interdune area to the northwest of Al Jaww Plain is reviewed and shown in Fig. (6.5) (US Geological Survey, 1993). The TEM Model at Al Jaww Plain and the model in the interdune area are not similar. The interdune area does not contain an alluvial-type layered sequence (existing at Al Jaww Plain). Instead, a thick resistive accumulations of variably-cemented dune sand overlying conductive bedrock.

The main three identfied geoelectric-litologic units at Al Jaww Plain are:

Layer-1 is a surficial zone of loose to weakly consolidated sand and gravel. This zone corresponds to the upper part of the very resistive (> 200 ohm-m) layer in both TEM models and VES. The resistive nature of this layer is indicative of dry conditions in the upper part of the alluvium.

Layer-2 is a thick zone of gravel and sand comprising the bulk of the alluvium. This zone has moderate and generally downward increase in the amounts of interstitial cement. The moderate to relatively small resistivity in this middle interval suggests partial satuaration and/or the presence of a clay-rich matrix (Fig. 6.6). However, at certain locations along the measured loops, there is a zone of coarse cemented gravel of a varying thickness at the bottom of the alluvial section. This zone appears to represent a basal deposit of the satuarated channel gravels.

The third layer has a resistivity range from 5 to 11 Ohm-m. This low resistivity layer is composed of bedrock consististing of marl, caly, mudstone, or shale. In some places in the deeper depth this zone would have resistivities of less than 5 Ohm-m probably due to the increase of salinity with depth (see Fig. 6.8a below loop No.10). The depth to the boundary

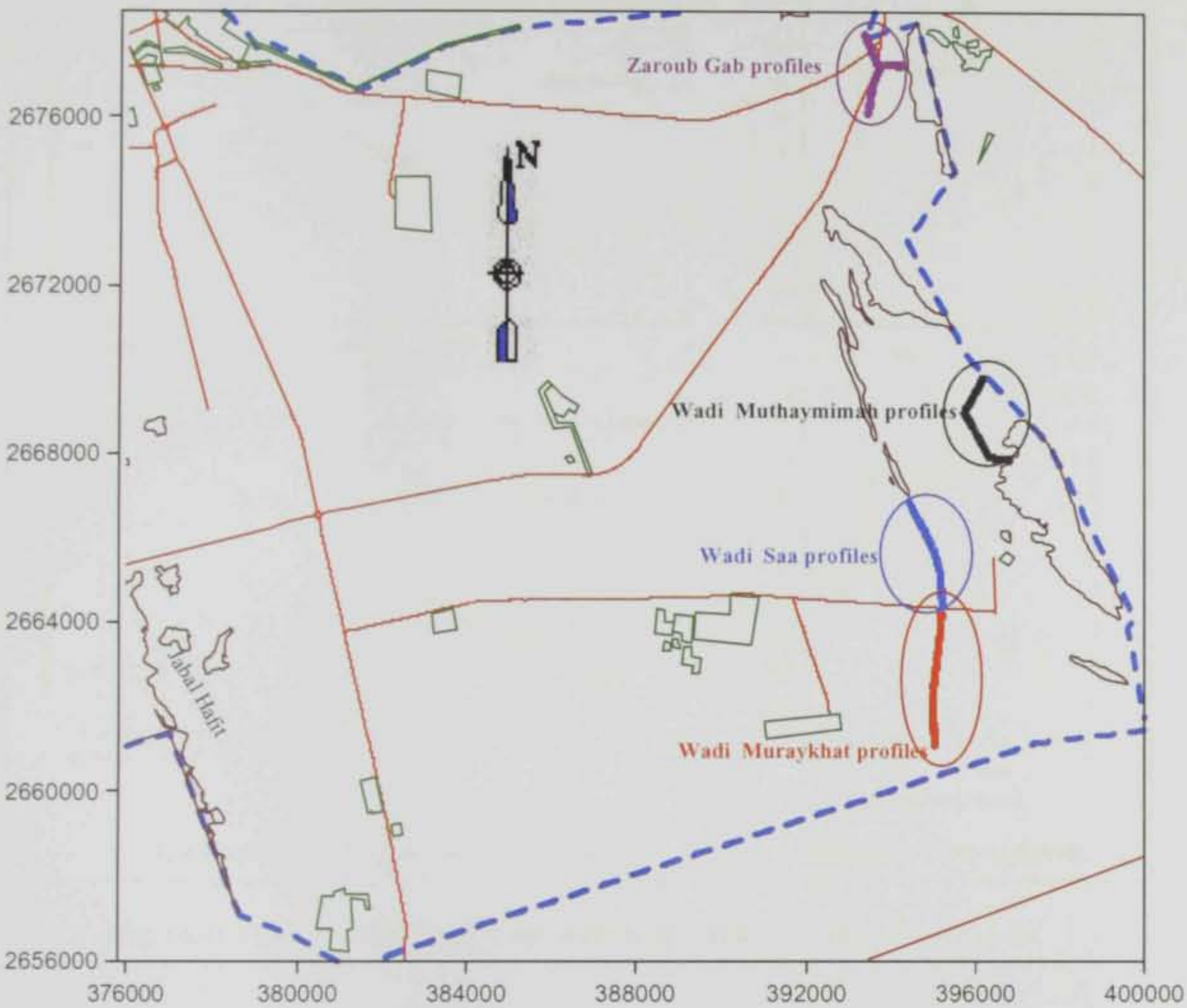

Fig. (6.3) Base map showing the locations of TEM profiles at Al Jaww Plain.

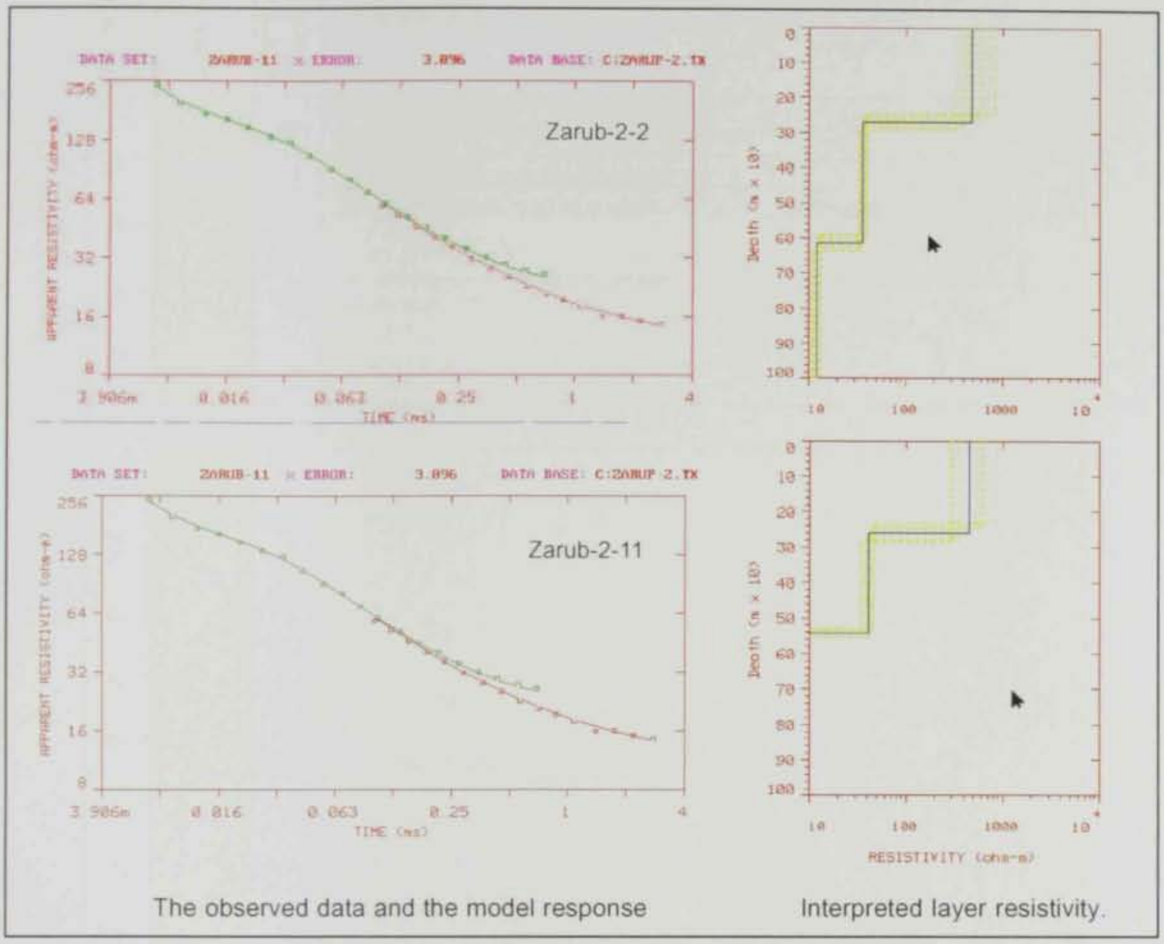

Fig. (6.4) Typical TEM data from sounding Zarub-2-2 and Zarub-2-11.

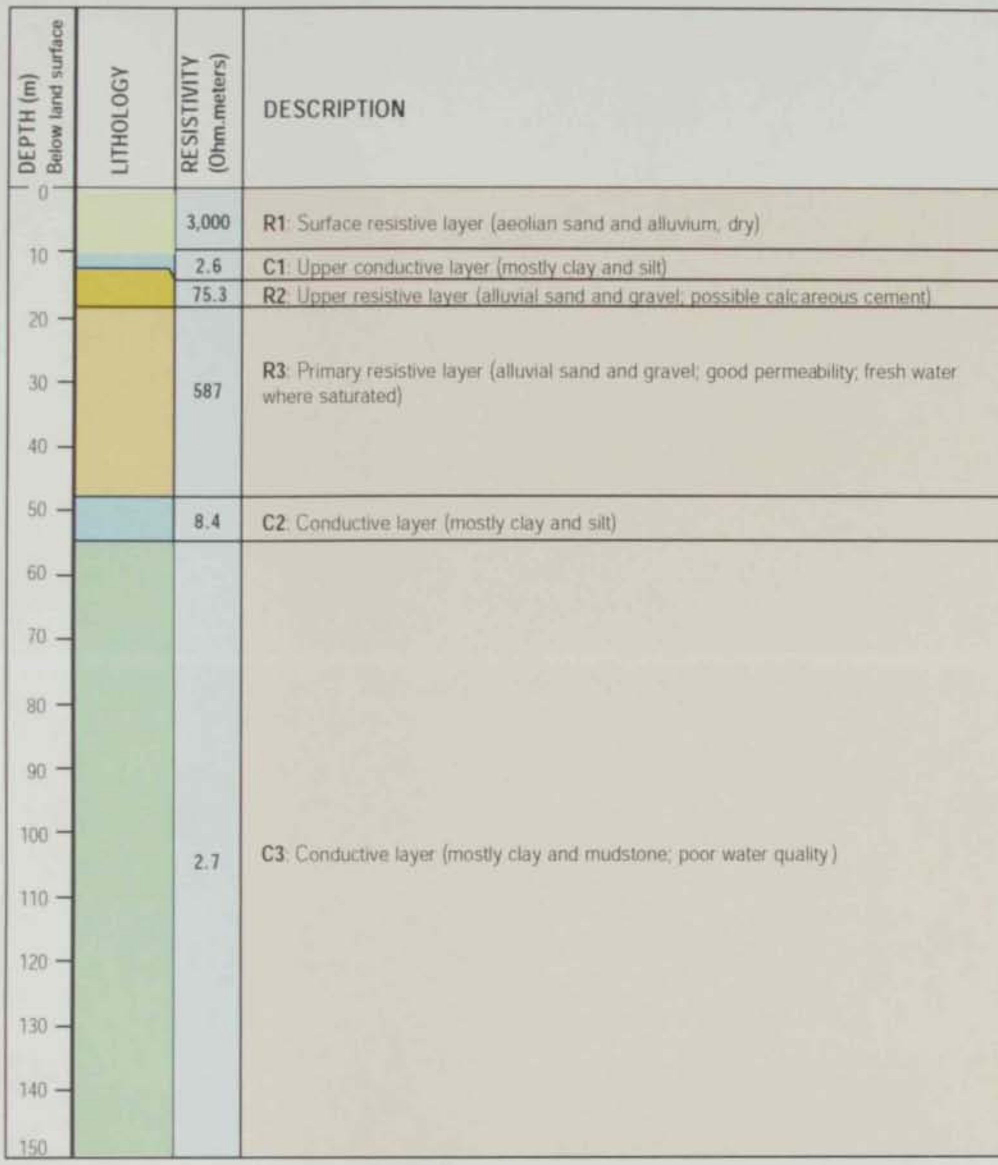

Fig. (6.5) Transient electromagnetic model of typical resistivities for interdune soundings at Al Qura'a, north of Al Jaww Plain (after US Geological Survey, 1993).

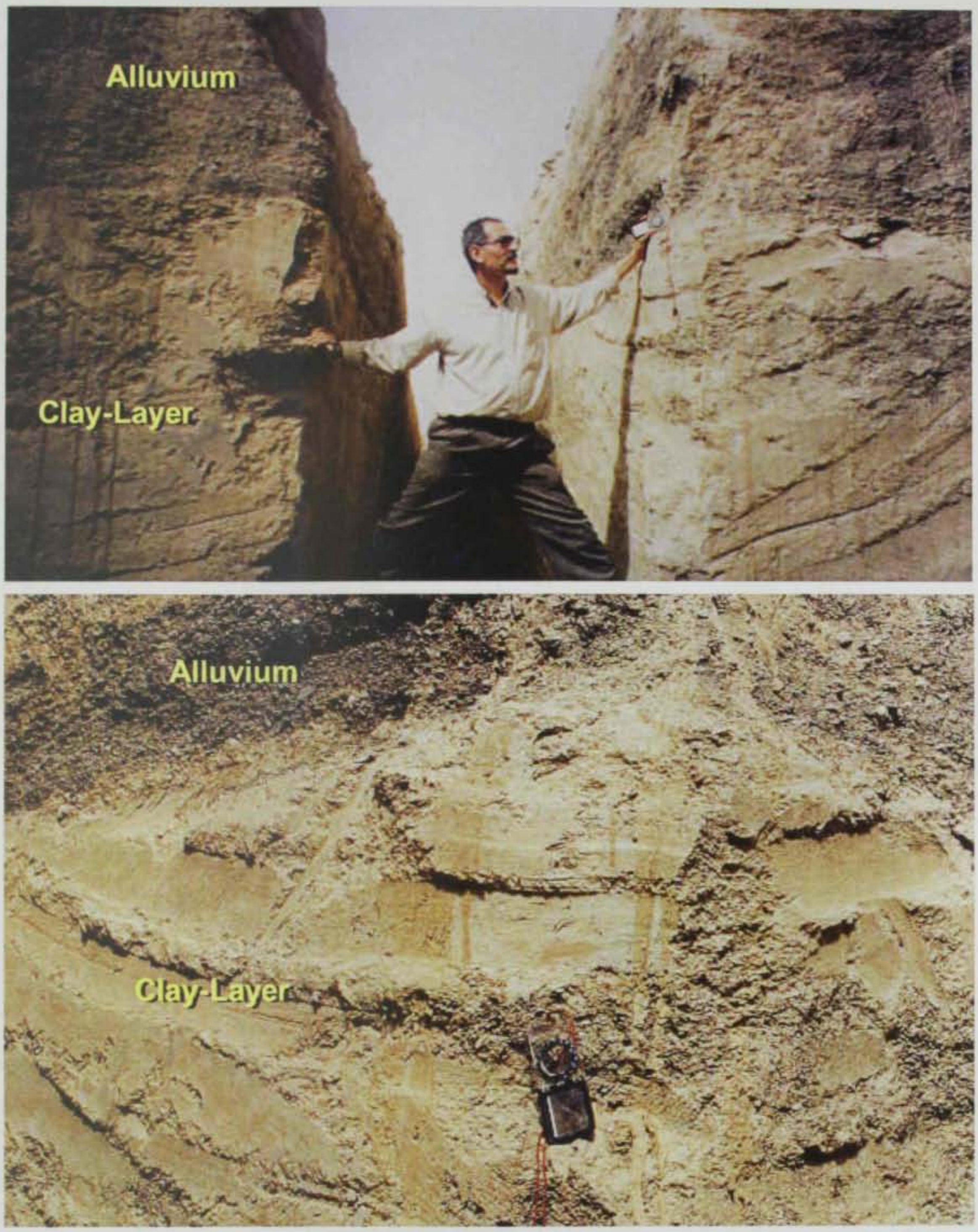

Fig. (6.6) Photos showing the presence of clay layer at shallow depths of drilled trenches at Al Jaww Plain.

Table (6.2) Qualitative and Quantative interpretation of the Time Domain Electromagnetic (TEM) data along some wadis of Al Jaww Plain.

Line No	VES No	Curve Type	No of Layers	True resistivity (Ohm-m)				Thickness of Layers (m)		
				ρ_1	ρ_2	ρ_3	ρ_4	T1	T2	T3
Wadi Muraykhat-	1	H	3	694.3	10.76	13.36		23.58	60.8	
	2	H	3	304.1	9.19	41.51		25.52	62.43	
	3	H	3	192.9	9.3	20.73		27.87	81.65	
	4	Q	3	243.6	12.28	8.55		26.94	34.19	
	5	Q	3	261.5	18.45	8.33		26.52	38.51	
	6	H	3	245.3	10.86	20.95		28.98	42.64	
	7	H	3	190.9	9.83	21.02		30.2	37.75	
	8	Q	3	352.4	15.68	10.14		25.79	18.92	
	9	H	3	336.6	11.53	17.56		26.53	47.96	
	10	Q	3	232.7	17.79	11.18	15	25.83	22.86	
	11	Q	3	361.8	18.98	12.69	3.83	25.49	33.8	
	12	Q	3	618.3	17.64	5.98		27.68	77.2	
	13	Q	3	517	17.01	15.74		26.9	102.8	
	14	H	3	203.4	13.37	69.35		29.58	76.13	
	15	Q	3	465.4	15.16	3.71		24.86	22.1	
	16	Q	3	428.9	28.76	10.59		24.68	17.16	
	17	Q	3	474.5	30.66	10.96		24.06	9.7	
	18	Q	3	477.7	32.79	10.64		21.73	8.59	
	19	Q	3	463.8	18.86	11.58		25.77	21.69	
	20	Q	3	618.2	20.2	12.52		24.36	34.3	
Wadi Muraykhat-	1	Q	3	593.1	32.56	12.47		23.04	18.41	
	2	Q	3	607.2	29.19	12.13		22.49	20.07	
	3	Q	3	641.5	29.59	12.66		26.24	11.5	
	4	H	3	706.5	15.41	27.57		25.18	80.07	
	5	H	3	341.8	14.85	795		27.35	25.38	
	6	Q	3	355.9	18.06	13.53		25.81	22.54	
	7	Q	3	442.2	15.51	13.2		26.8	20.8	
	8	H	3	598.9	12.84	20.93		28.12	43.39	
	9	H	3	566	12.72	14.21		28.03	24.46	
Wadi Sa'a-1	1	H	3	402.4	13.17	50.32		25.77	34.81	
	2	H	3	564.8	21.94	31.13		22.57	16.3	
	3	Q	3	705.9	38.3	23.74		18.56	50.69	
	4	Q	4	691	43.72	23.2		16.89	37.05	
	5	Q	3	674.8	23.78	9.61		21.47	68.63	
	6	Q	3	965.4	22.47	12.12		20.82	52.33	
	7	Q	3	989.8	22.91	10.68		18.09	32.65	
	8	H	2	237.3	9.55	20.52		29.24	50.78	
	9	H	2	473.7	8.23	21.01		21.71	26.47	
	10	QH	4	499.5	7.51	0.6	15	23.51	17.43	52.93
	11	HK	4	504.7	10.03	13.37	3.83	23.86	16.27	47.19
	12	Q	3	319.4	12.89	6.59		24.88	58.97	
	13	Q	3	257.6	15.94	4.53		24.52	38.18	
	14	Q	3	291.3	19.47	5.6		23.09	30.64	

Line No	VES No	Curve Type	No of Layers	True resistivity (Ohm-m)				Thickness of Layers (m)		
				ρ_1	ρ_2	ρ_3	ρ_4	T1	T2	T3
Wadi Sa'a-2	1	Q	3	248.7	18.6	4.36		26.49	35.73	
	2	Q	3	283.2	21.1	4.27		25.8	35.13	
	3	Q	3	460.9	23.14	6.14		26.04	34.31	
	4	Q	3	545.5	19.71	5.28		25.75	28.88	
	5	Q	3	618.1	19.43	5.1		25.15	29.24	
	6	Q	3	618.3	20.27	5.23		25.5	26.67	
	7	Q	3	615.7	20.1	4.34		25.44	26.89	
	8	Q	3	607.8	22.92	4.54		23.94	33.28	
	9	Q	3	623.8	20.59	5.95		24.18	28.09	
	10	Q	3	633.6	13.68	5.06	15	26.59	27.27	52.93
	11	Q	3	823.5	11.49	3.3	3.83	22.85	69.76	47.19
	12	Q	3	762.1	14.37	5.02		23.12	27.85	
Wadi Muthaymimah-	1	Q	3	1132.2	9.39	2.52		22.24	46.59	
	2	Descending	2	842.6	2.67			25.67		
	3	H	3	1161.2	1.59	14.03		28.12	22.59	
	4	HK	4	1791.1	2.7	9.66	3.07	29.14	4.96	47.32
	5	Q	3	1725.2	21.29	9.46		22.89	35.21	
	6	H	3	2273.9	12.29	106.5		25.88	72.02	
	7	Q	3	311.6	24.91	3.07		25.69	16.24	
	8	Q	3	445.5	16.25	10.34		25.16	18.3	
	9	H	3	485.3	12.18	62.84		25.69	74.66	
	10	Q	3	200.4	15.25	8.93		27.4	36.25	
	11	Q	3	222.1	12.29	5.74		28.7	29.42	
Wadi Muthaymimah-	1	Q	3	218.6	14.57	7.32		28.62	34.24	
	2	Q	3	251.2	26.62	12.46		26.05	15.8	
	3	Q	3	396.3	23.21	12.65		28.77	9.87	
	4	Q	4	423.9	13.92	9.54		27.89	23.32	47.32
	5	Q	3	344.8	15.23	8.09		27.23	24.02	
	6	Q	3	323.8	11.36	8.96		30.41	22.37	
	7	Q	3	459.4	10.22	9.51		28.81	28.98	
	8	Descending	2	413.2	9.46			29.57		
	9	Descending	2	219.7	9.44			31.1		
	10	Descending	2	219.7	9.56			31.04		
	11	Q	3	228.9	11.37	6.65		28.93	36.56	
	12	Q	3	245.5	13.28	8.87		31.15	40	
	13	Q	3	314.4	14.17	9.03		29.76	46.66	
Wadi Muthaymimah-3	1	Q	3	251.4	12.78	7.33		30.51	50.59	
	2	Q	3	200.7	11	8.87		31.99	38.96	
	3	Q	3	214.7	18.15	5.73		28.15	12.1	
	4	Q	3	255.1	23.41	5.06		23.18	13.44	
	5	Q	3	420.8	12.66	4.41		20.7	10.53	
	6	Q	3	424.2	13.57	9.7		29.06	12.03	

Line No	VES No	Curve Type	No of Layers	True resistivity (Ohm-m)				Thickness of Layers (m)		
				ρ_1	ρ_2	ρ_3	ρ_4	T1	T2	T3
Zarub Gap-'	1	H	3	589.3	2.32	5.36		19.92	8.58	
	2	Descending	2	756.4	5.62			19.33		
	3	Q	3	417.8	8.16	4.95		21.31	36.33	
	4	Q	3	477.3	16.64	5.65		18.94	21.19	
	5	Q	3	468.7	30.72	5.57		19.75	30.97	
	6	Q	3	458.2	46.23	5.64		18.02	39.12	
	7	Q	3	466.8	56.05	6.38		17.11	44.04	
	8	Q	3	519.9	52.49	6.98		19.14	49.02	
	9	Q	3	528.5	61.17	7.96		18.74	47.12	
	10	Q	3	590.8	41.04	10.28	15	25.22	33.84	52.93
	11	Q	3	672.3	33.07	8.54	3.83	26.19	29.34	47.19
	12	Q	3	693.5	29.24	7.48		27.03	29.47	
	13	Q	3	722	27.54	8.13		26.12	29.19	
	14	Q	3	732.2	24.77	7.74		25.96	26.75	
	15	Q	3	729.2	29	8.23		25.19	23.86	
	16	Q	3	726	29.55	7.55		24.12	24.96	
	17	Q	3	723.4	38.31	8.73		19.74	33.74	
	18	Q	3	374.7	13.03	41.8		25.92	33.15	
	19	Q	3	406.2	43.79	8.12		18.94	35.14	
	20	Q	3	408.6	46.25	7.97		19.12	32.65	
	21	Q	3	871.9	10.84	6.15		42.13	13.35	
	22	Q	3	1224.8	8.43	5.59		39.68	13.57	
	23	Descending	2	1349.1	7.04			37.07		
	24	Q	3	718.7	11.08	7.2		23.16	30.68	
	25	Q	3	672	11.34	7.51		21.95	32.9	
	26	Q	3	714.6	17.02	8.58		20.4	28.48	
Zarub Gap-2	1	Q	3	650.3	31.91	8.02		27.64	39.83	
	2	Q	3	661.9	35.48	10.53		26.34	36.36	
	3	Q	3	685.5	31.82	7.35		25.94	37.75	
	4	Q	3	728.4	35.3	8.08		25.96	36.65	
	5	Q	3	785.5	35.63	8.62		26.2	35.03	
	6	Q	3	795.3	40.72	8.28		25.87	36.79	
	7	Q	3	813	45.73	7.03		24.23	37.97	
	8	Q	3	835.1	49.56	8.09		23.57	39.37	
	9	Descending	3	859.2	7.06			23.59	38.17	
	10	Q	3	875	42.94	7.44		23.48	35.31	
	11	Q	3	879	43.53	8.39		23.68	30.14	
Zarub Gap-3	1	Q	3	892.8	42.06	7.7		25.32	30.2	
	2	Q	3	902.5	38.88	7.31		24.8	27.8	
	3	Q	3	899.7	38.26	7.08		24.66	25.45	
	4	Q	3	849.1	39.63	5.43		23.5	26.35	
	5	Q	3	901	28.51	5.57		26.63	21.22	
	6	Q	3	923.1	22.93	4.81		28.33	18.67	
	7	Q	3	916.7	26.91	5.3		27.1	17.31	
	8	Q	3	924.7	25.63	5.14		26.84	17.19	
	9	Q	3	973.9	18.16	4.85		28.07	15.84	
	10	Q	3	996.8	15.85	4.73		28.58	14.61	
	11	Q	3	1000.3	15.33	4.4		28.72	14.57	
	12	Q	3	992	15.81	3.77		28.41	15.65	
	13	Q	3	995.5	14.79	3.59		28.45	15.38	
	14	Q	3	918.1	20.68	5.66		918.1	20.68	5.66

between the second and third layer, commonly in the range of 35-60 m, varies from one sounding to another along the profile. This variation is less than that encountered in the first layer. This layer corresponds to what is called "basal confining system" which is dominated by slightly permeable mudstone, claystone, evaporite, and limestone units of the Fars formations in the Al Jaww Plain (as discussed in chapter four).

6.3.2 TEM cross sections

The model results are used to produce geoelectric resistivity cross-sections to depths below land surface of about 40 m. These geoelectric resistivity cross-sections represent the wadi profile and are composed of a series of EM-47 soundings located at intervals of 40 to 120 m to the side of the profile. Table (6.3) and the inset maps of Figs. (6.7b,6.8b,6.9b and 610 b) describe these TEM-profiles.

Table (6.3) Electromagnetic (TEM-47) Profiles data at Al Jaww Plain.

Site	Line	Total Profile Length (m)	Number TEM loops
Zaroub Gap	1	1350	26
	2	530	11
	3	700	14
Wadi Muraykhat	1	2250	19
	2	900	9
Wadi Muthaymimah	1	900	11
	2	1230	13
	3	520	6
Wadi Saa	1	1400	14
	2	500	12

Loops model results are interpretated to form resistivity cross-sections termed wadi profiles. These wadi profiles provide valuable high-resolution subsurface information on the buried paleochannels in wadi gaps. This information would help understand the process of groundwater recharge in the shallow alluvial aquifer.

Four geoelectric cross-sections (Figs 6.7 to 6.10) are constructed along Wadi Muraykhat line-1, Saa line-1, and Wadi Muthaymimah line-2 and Zarub line-2, respectively. These geoelectric cross-sections provide additional information on the subsurface geometry of Quaternary alluvium along the eastern margin of Al Jaww Plain. The gaps at the wadis

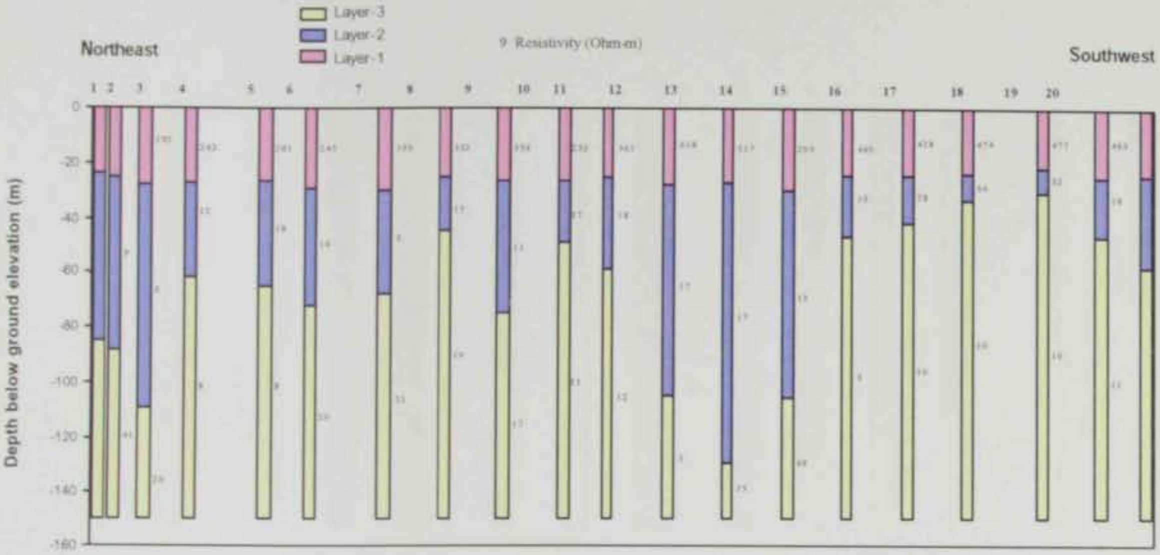

Fig. (6.7a) Wadi Muraykhat line 1 geoelectric models showing the variation of resistivity with depth.

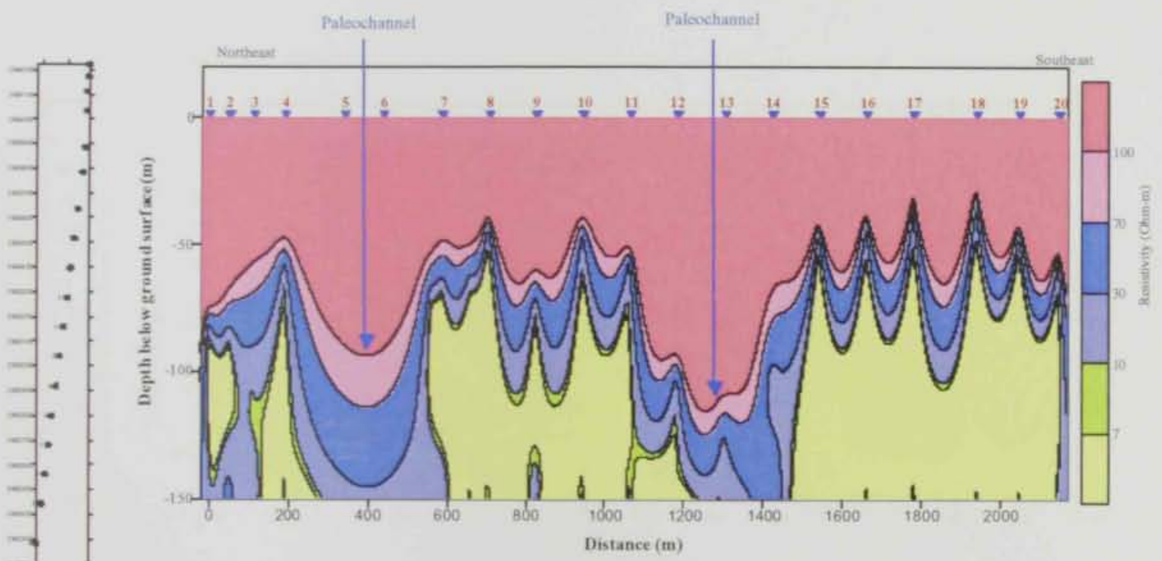

Fig.(6.7b) Interpreted resistivity cross section of Wadi Muraykhat line-1, Al Jaww Plain.

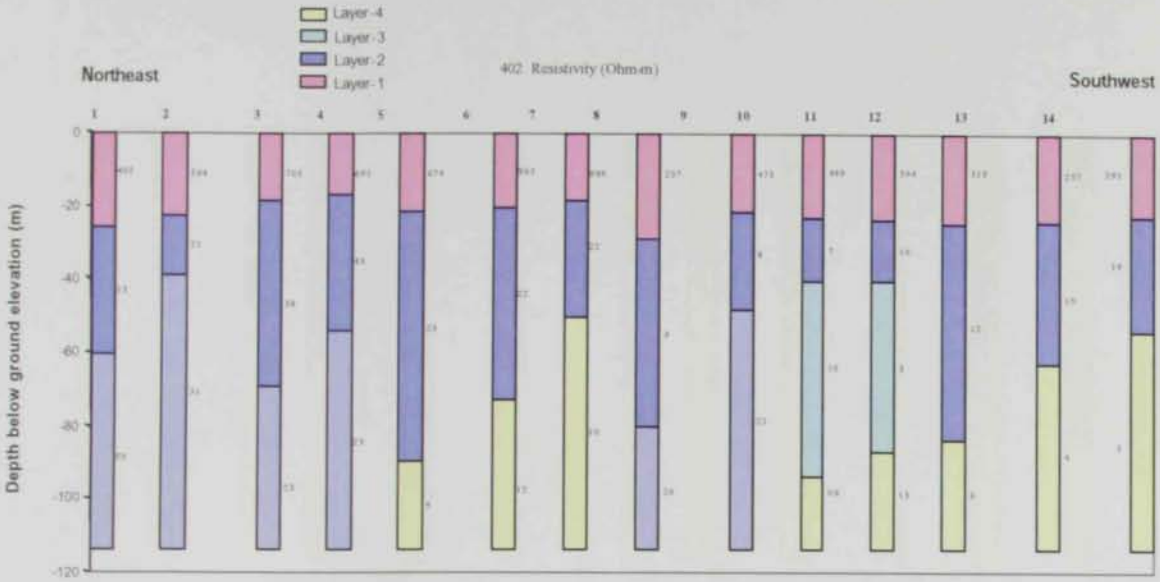

Fig.(6.8a) Wadi Saa line 1 geoelectric models showing the variation of resistivity with depth.

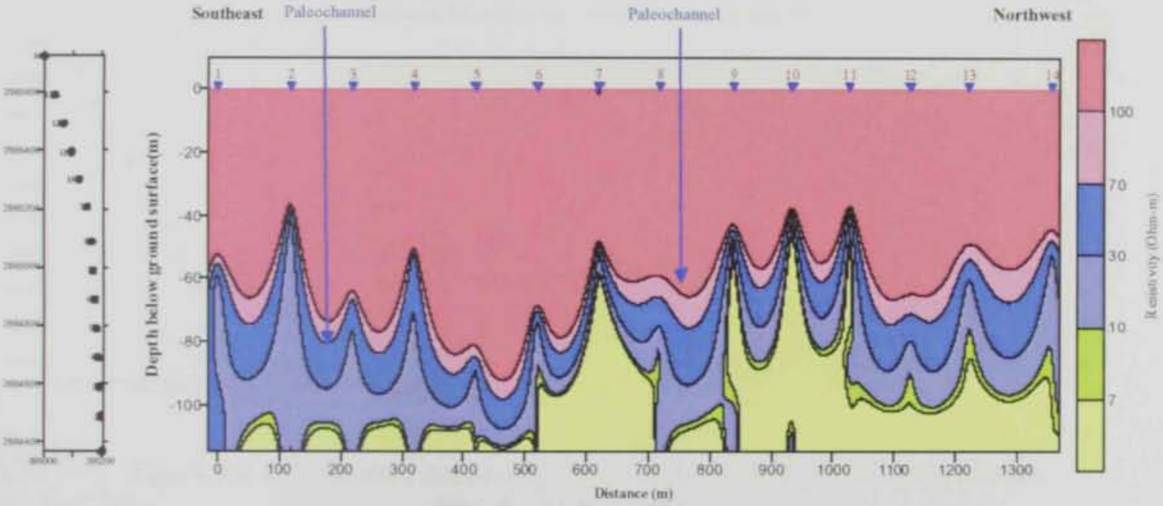

Fig.(6.8b) Interpreted resistivity cross section of Wadi Saa line-1, Al Jaww Plain.

Fig.(6.9 a) Wadi Muthaymimah line 2 geoelectric models showing the variation of resistivity with depth.

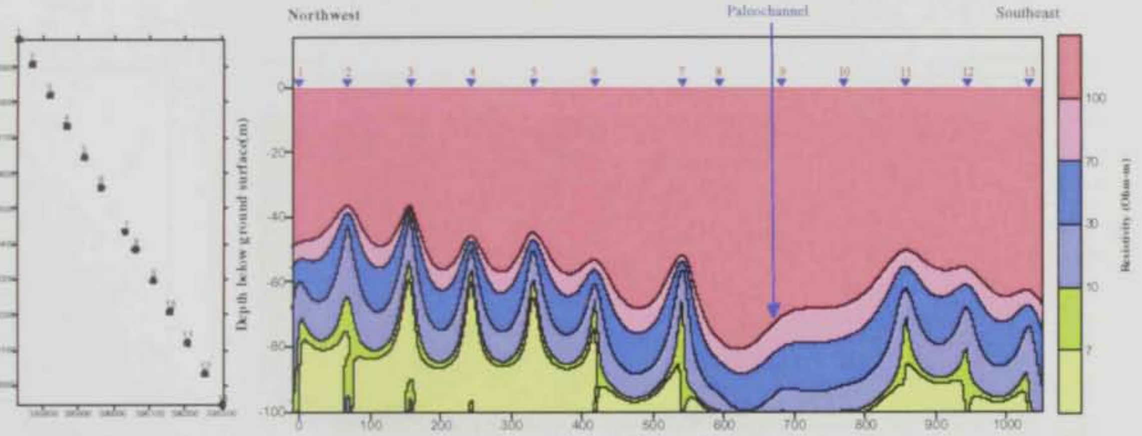

Fig.(6.9b) Interpreted resistivity cross section of Wadi Muthaymimah line-2, Al Jaww Plain.

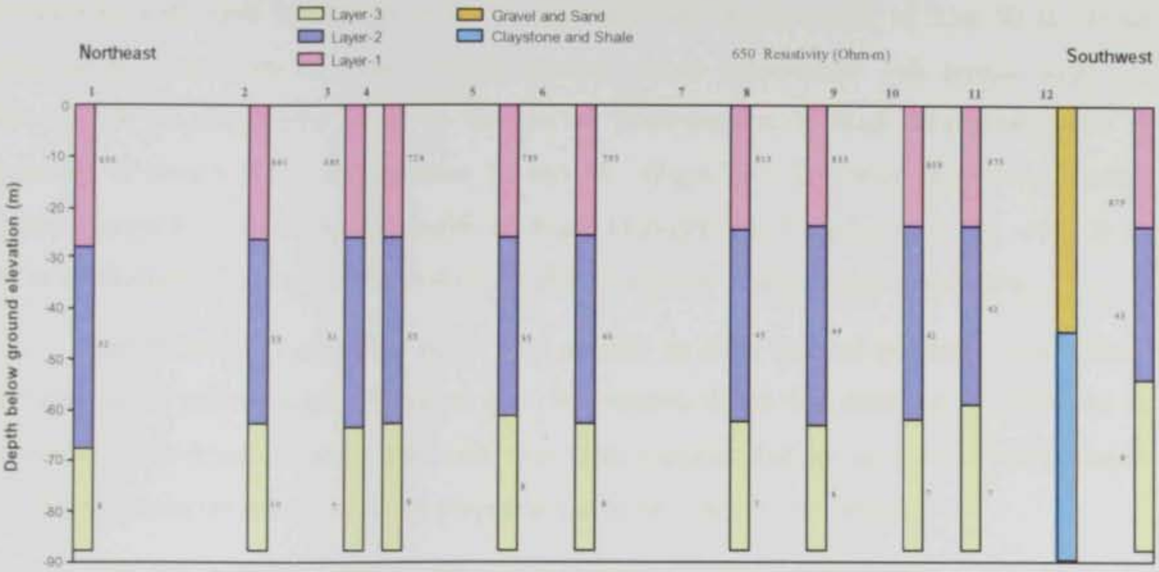

Fig. (6.10a) Zarub line-2 geoelectric models showing the variation of resistivity with depth.

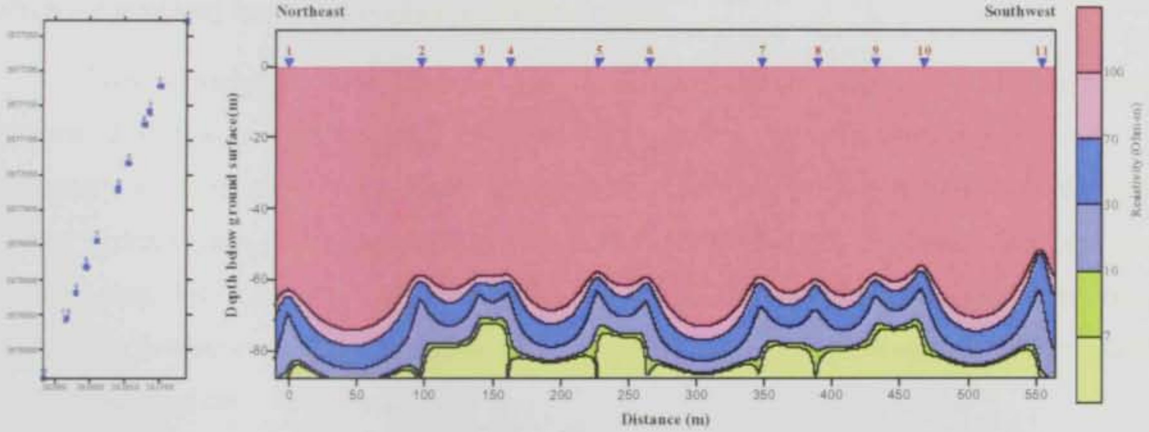

Fig.(6.10b) Interpreted resistivity cross section of Zarub gap line-2, Al Jaww Plain.

have wide, complex channel systems that are typically filled with 24 to 40 m of alluvium. The erosional contact at the base of the alluvium is generally irregular and broadly undulating, with relief locally up to 40 m, but commonly in the range of 5 to 10 m. These irregularities define one or more, variably distinct, deeper subchannels with typical widths of 200 to 500 m and depths of 45 to 60 m (see cross-sections of Wadi Muraykhat line-1 at locations of loop 5 and 6 and between 11 and 14 , (Fig.6.7b). The same feature is identfied beneath loops 8 to 10 along the profile of Wadi Muthaymimah line-2 (Fig. 6.9b), with 24 to 40 m of alluvium of coarse materials which are characterized by relatively high resistivities.

Zaroub line-2 (Fig. 6.10b) is not well situated to show channel geometry as it crosses the wadi at an oblique angle. However, this cross section shows that there can be variations in depositional envirnoment along the wadi axis. This suggests that for a more detailed analysis of channel geometry several traverses prependicular to the wadi axis are needed.

The constructed electromagnetic profiles can be used to infer lateral variations in the thickness and resistivity of the model layers. In EM models, the uppermost resistive layer tends to thin and the basal resistive layer tends to thick in the deep portions of buried paleochannels beneth active wadis (Figs. 6.7b & 6.9b). These paleochannels are promising sites of drilling water wells as they contain appreciable thickness of water bearing formation which are recharged from the surrounding mountain region.

These geoelectric cross sections are in a good match with the geological cross sections discussed in chapter four. Morever, they confirm the depositional framework of Quaternary alluvium at Al Jaww Plain, where wadis exist from the Oman Mountains througth narrow bedrock gaps and extend to the west across narrow flanking piedmont fans (see the geologic map, Fig. 2.4). However, wadi systems disappear beneath the eolian sand cover and there is no defined expression of surface channels along the westward projection of the wadis in the interdune areas.

6.4. Borehole Geophysics (Wireline Logging)

Borehole geophysics offers a great deal in the way of practical application to hydrogeology. Borehole geophysical methods were developed primary in the petroleum industry and virtually in all oil and gas wells. In the water well industry the use of geophysical logging is generally restricted to either research projects or high capacity municipal and industrial wells.

Borehole geophysics is considered as the most reliable and accessible geological-geophysical method for determining rock petrophysics and areas of high porosity and permeability, that would produce high quantities of groundwater. However, zones of an aquifer with high salinity water and the regional groundwater flow pattern can also be identified if a number of wells are used. In addition, it can be used for locating the saline /fresh water interface in the coastal regions. It is considered as one of the best branches of geophysical science treatable by computer for the ability of transferring the usable set of logs into a continuous sequence of numbers and digits.

On the other hand, the existing lithological columns of the drilled wells do not replace using the wireline logs. This is because the reliability of lithologic well log depends on the method of drilling and sample recovery as well as the knowledge and skills of the person who is making the log. There are also many existing wells for which records of the subsurface geology are available.

Generally, a suite of geophysical logs is made rather than only a single type. The method tends to be a complementary, one may confirm another, and certain interpretations are made on the bases of two or more logs.

Wireline logs have been utilized in this study comprising conventional Resistivity, Gamma Ray, Self-Potential and Temperature logs of 7 logged boreholes. Locations of these wells are combined with VES location (Fig. 6.1).

Petrophysical logs are analyzed to determine the depth to water table, depths and thickness of permeable rock strata, resistivity of formation water in the permeable strata and hydraulic properties of penetrated formations. Permeable zones were identified by inspection of the resistivity. Permeability in clastic material is often a function of clay content. Most permeable aquifer material, such as sand and gravel are resistive and can be identified on the resistivity log. However, water resistivity and clay conductivity also affect the resistivity log.

Figs. (6.11 to 6.13) present plots of the different type of geophysical logs recorded for boreholes GWP-398, GWP-255 and GWP-251 respectively.

Inspection of these plots indicate remarkable log responses due to lithological changes. The hydrogeological conditions are clearly demonstrated. Table (6.4) summarizes the description of lithology versus depth for these three wells.

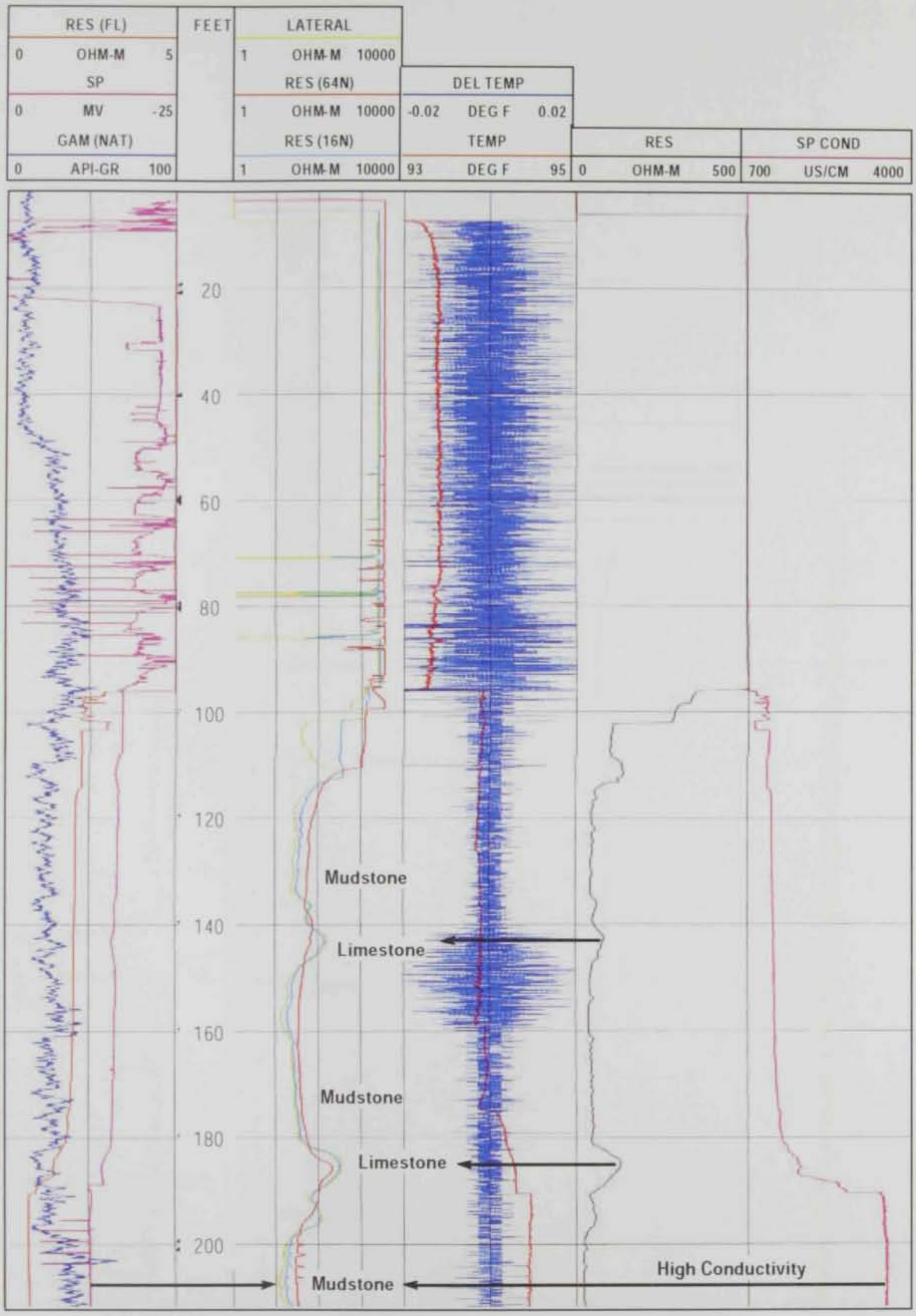

Fig. (6.11) Petrophysical logs for well GWP-398.

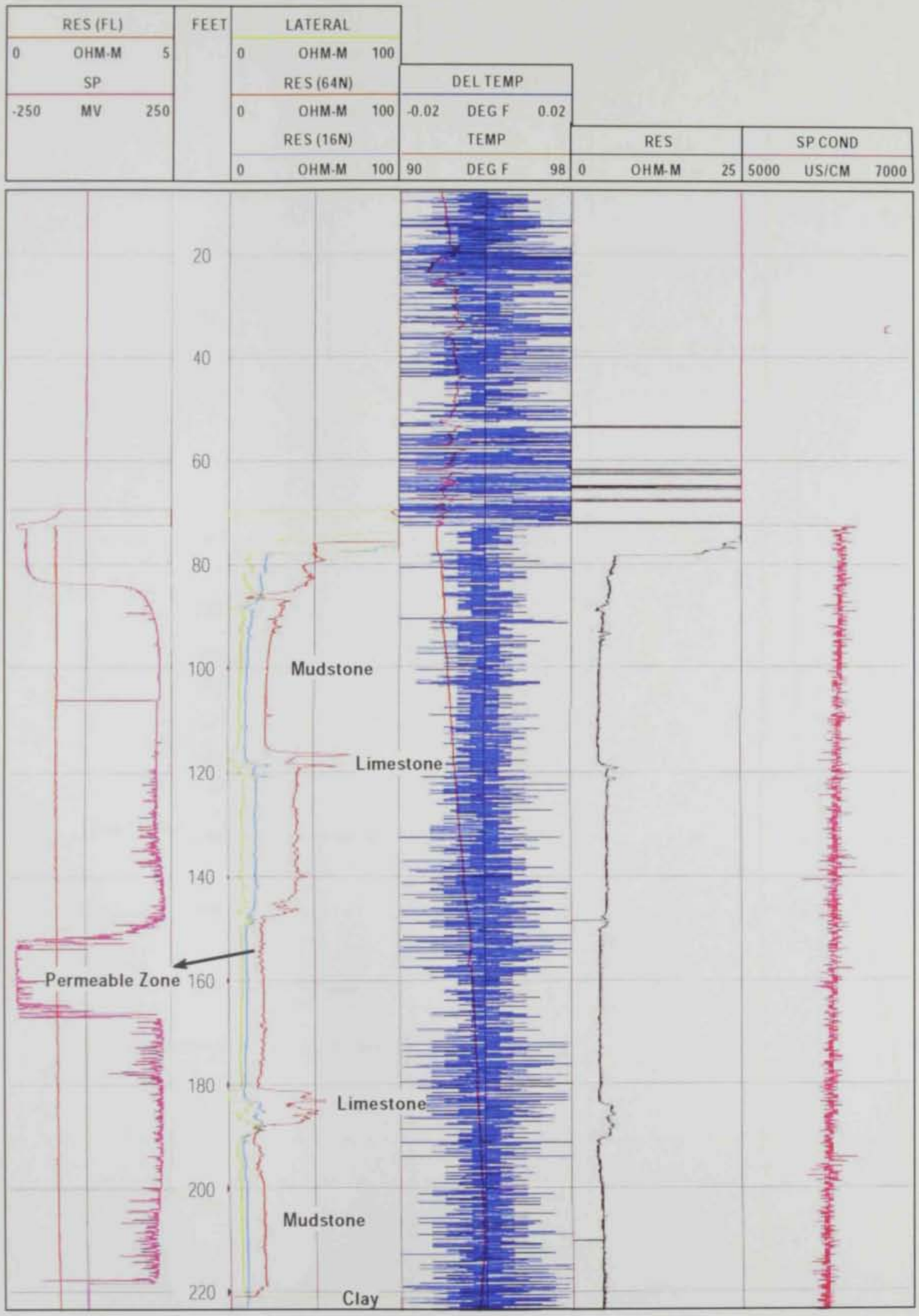

Fig. (6.12) Petrophysical logs for well GWP-255.

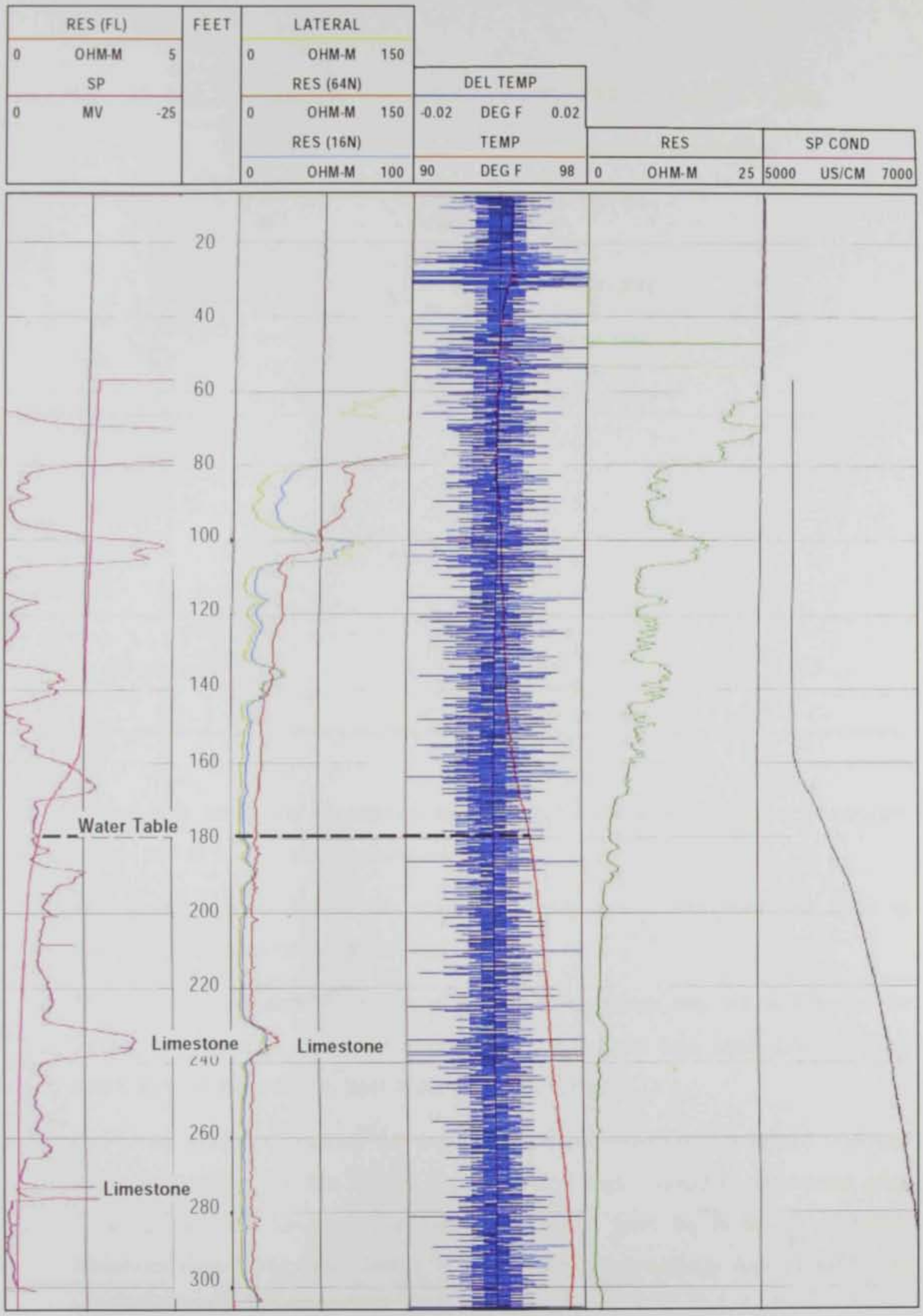

Fig. (6.13) Petrophysical logs for well GWP-251.

Table (6.4) Lithology description for the wells GWP-398, GWP-251 and GWP-2551.

Well No.	Depth (ft)	Description of Lithology
GWP-398	50	Gravel, weakly cemented
	60	Clay, sandy
	140	Mudstone
	150	Siltstone, calcareous, gray
	180	Mudstone
	190	Limestone, yellowish brown
	210	Mudstone
	220	Siltstone, calcareous, gray
GWP-251	50	Gravel, sandy
	70	Marl
	80	Gravel
	95	Claystone
	110	Limestone
	310	Mudstone
	330	Limestone
GWP-255	40	Gravel
	80	Gravel, clayey
	195	Clay, yellow, sticky
	253	Clay, gray, silty, calcareous

Guided with lithological records of these boreholes (Table 6.4) and the geophysical log plots (Figs. 6.11 to 6.13), it could be concluded that:

1- The aquifer consists mainly of gravel and sandy gravel interbeded with mud as indicated from resistivity and gamma logs.

2- The aquifer is underlain by mudstone and claystone, which may act as a barrier for vertical percolation of groundwater. Resistivity and gamma logs along GWP-398 are clearly defining this mudstone layer at depth of 200 ft (Fig. 6.11).

3- Due to the mud intercalations, the groundwater is not restricted to a limited thickness within the aquifer. For this reason, the geophysical logs should be considered when finalizing the well for production where the screen must be faced by permeable formations (less shaly). This feature is remarkable from resistivity logs of GWP-398 at intervals 120 to 140 ft and from 150 to 185 ft (Fig. 6.11).

Chapter VII

SUMMARY AND CONCLUSIONS

SUMMARY, CONCLUSIONS AND RECOMMENDATIONS

7.1 Summary

Water resources constitute the most important element for the sustainable development. Water has always been regarded as the sources of life, without which no life could exist on the earth. Availability of water with sufficient quantities and proper qualities is vital for agriculture and industrial development.

In arid and semi arid regions water is very scarce and is thus valuable. Rainfall events are scattered and infrequent. Surface water runoff is very limited. Surface water bodies are almost absent. Due to the harsh climatic conditions, evaporation rates are very high. Therefore surface water resources do not contribute significantly to the water budget. Groundwater resources are thus critical for the nation's development. In the absence of desalination plants and other non-conventional water such as treated wastewater, groundwater would be the only freshwater resource.

The UAE is located in an arid region. The groundwater constitutes the only natural water resource in the country. Groundwater has been overexploited to meet the increasing water demands. Despite the wide expansion in the construction of desalination plants in the different Emirates, the groundwater resources still contribute by the largest share in the water budget of the country. The importance of the subject matter of this thesis can not, therefore, be overemphasized.

This study is devoted to the quantitative and qualitative assessment of the groundwater resources in Al Jaww Plain which is located in the eastern part of Al Ain City. It represents one of the main plains at Al Ain with an area of about 500 km^2. The study includes a comprehensive review and assessment for various aspects related to groundwater resources in Al Jaww Plain including climatology, hydrology, hydrogeology, and geochemistry of the system.

The thesis is composed of seven chapters. Chapter One presents an introducting for the subject. The physical location of the UAE and the prevailing climatic conditions including evaporation and evapotranspiration rates, mean annual temperature, relative humidity and wind speed and directions are presented. The conventional and non-conventional water resources in the UAE are quantified based on previous investigations. These sources include rainfall, seasonal floods, falajes, groundwater, springs, as well as desalination water and treated wastewater (reclaimed water). Emphasis is then devoted to the quantitative assessment of the water resources in Al Ain area. The aim of the current study and it is expected results are also included at the end of this chapter.

Chapter Two is devoted to the geological and geomorphological aspects of Al Ain area. A comprehensive review for the classification of the geomorphic units in Al Ain area including mountains, gravel plains, drainage basins, sand dunes, interdune areas, and inland sabkhas is presented in details. The stratigraphy of Al Ain area and the rock sequence from Cretaceous to Quaternary are described. The focus is then directed to the geology of Al Jaww Plain including fluvial deposits, desert plain deposits, mixed deposits, sabkha deposits and aeolian sand. The chapter is concluded with the structural setting of Al Ain area compressing the structures of Oman Mountains and the northern and southern structural regimes.

Chapter Three presents a comprehensive review for the different techniques employed in geophysical investigations and electrical soundings. The Direct Current Resistively method is discussed and its basic concepts and surveying procedures are presented. The principles of Time Domain Electromagnetic techniques for resistively sounding are discussed. The different methods for Borehole Geophysics including S.P. logging, point resistance logging, resistively logging, natural gamma ray logging, neutron log, sonic log and gamma-gamma ray or density log are presented.

The hydrogeological aspects of Al Ain constitute the subject matter of Chapter Four. The prevailing climatic conditions in Al Ain area including temperature, rainfall, humidity, evaporation, and aridity are outlined. The groundwater bearing formations encompassing the Quaternary aquifer and Jabal Hafit limestone aquifer are presented. Several cross sections were deduced for Al Jaww Plain. The groundwater flow system in the study area and the historical fluctuations of the groundwater levels are discussed at the end of this chapter.

Chapter Five is devoted to the hydrogeochemical aspects and groundwater in the study area. The physical properties including the hydrogen ion concentration (pH), electrical conductivity, total salinity distribution and total hardness and the chemical properties including the major cations and anions are discussed. The distribution of various physical and chemical elements and the ion dominance in the groundwater are elaborated. The water genesis including analyses by Sulin's graph and Trilinear diagram is discussed. The chapter is concluded with an assessment of the suitability of groundwater for irrigation purposes based on SAR, EC, sodium content and residual carbonate.

Chapter Six elaborates the field activities and the geophysical investigations that have been conducted within the course of this investigation. The results of vertical electrical sounding along with the quantitative interpretation for the apparent resistivity-sounding curve are presented. Geoelectrical sections are deduced and discussed. The time domain electromagnetic results are presented and analyzed. Available data for the borehole geophysics are discussed.

Chapter Seven presents a summary of all the activities conducted within the course of this study. The conclusions and main findings of the study are presented. Recommendations for future investigations are also made.

7.2 Conclusions

Based on the integration of borehole data, Vertical Electrical Sounding data, Electromagnetic (TEM), borehole geophysics, meteorological data along with the review of the geomorphological and geological information of study area, the following conclusions are made:

1- Al Jaww Plain is characterized by a relatively thin surficial aquifer of slight to moderate permeability overlying a thick basal confining unit of very low permeability. The thickness of the aquifer ranges from zero to more than 100 meters. The aquifer is composed of interbeded rock and sediment. Rainfall in the Oman Mountains and Jabal Hafit contributes to the recharge of the Quaternary system.

2- The hydrogeological situation at Al Jaww Plain is affected by main structural elements which are north to northwest trending folds associated with northeast-dipping thrust and reverse faults.

3- Groundwater flow is generally from East to West. However, this flow system is affecting by local features such as Jabal Hafit, where a groundwater mound is encountered on the east flank of Jabal Hafit. This mound is recognized on the developed water level maps. The comparison of 1995 through 2002 water level maps shows some decline in the water levels which is associated with the decrease of recharge rate (mainly rainfall) and the increase of groundwater pumping.

4- The total dissolved content of the water shows a general increasing trend from east to west. The fresh water is associated with Wadi courses locations. An area of high total dissolved solids content is encountered west from Jabal Hafit. This increase of TDS is attributed to the brine moving upward near Ain Al Faydah. This is also attributed to the existence of sabkhas in areas of low elevation west of Jabal Hafit, at locations where the water table is near or at the land surface.

5- Vertical Electrical Soundings (VES) results portrayed the lithostratigraphy beneath Al Jaww Plain. A ridge of relatively high resistivity at depths of 200-500 m, related to gypsum with clay intercalation, is traced. The constructed cross section reveals a trend of thick shale-filled faults which reach a depth of 900 m. Shall aquifer of quaternary has been delineated as channel-like structure. According to these results, no deep aquifer of importance is present.

6- Time Domain Electromagnetic data along wadi profiles at Al Jaww Plain has been successfully traced the erosional unconformity that crosses Tertiary to Cretaceous rocks. These unconformities represent the paleochannels in the bed rock that were formed in the geological past by the ancient wadis. These paleochannels are promising targets for fresh groundwater, as they contain appreciable thickness of water bearing formations that are recharged from the surrounding mountain region.

7- The borehole geophysics identified the mudstone and claystone, which act as barriers for vertical percolation of groundwater. Also the permeable zones and shaly zones within the aquifer are identified. The geophysical logs should be considered when finalizing the well for production in which the screen must be placed at the permeable formations (less shaly).

7.3 Recommendations

1- Recharge areas should be monitored to prevent developments that might reduce recharge or contaminate the recharge area.

2- A comprehensive water resources database for information regarding well locations, meteorological data, water quality, water levels and water use should be developed. This database should be accessible by researchers and scientists in the different fields of water resources.

3- A monitoring system for groundwater levels and quality should be established, maintained and updated.

4- The construction of new groundwater pumping wells should be fully controlled by local authorities. The pumping rates should also be monitored to avoid over pumping practices.

5- Detailed analysis of paleochannel geometry should be done. Several TEM traverses for perpendicular to the wadi axis are recommended.

6- The treated wastewater can be fully utilized in the irrigation and horticulture. This would help sustain the groundwater resources at Al Jaww Plain.

REFERENCES

References

Abdelghany, O., (in prep.). Contribution to the Late Cretaceous/Tertiary Stratigraphy, West of the Northern Oman Mountains.

Abou El-Enin, H.S., (1993). Structurally controlled features in Jabal Hafit. Bull. Geog. Soc., Kuwait, v.151, p1-63.

Abu-Zeid, M.M., Baghdady, A.R. and El-Etr, H.A. (2001). Textural attributes, mineralogy and provenance of sand dune fields in the greater Al Ain area, United Arab Emirates, Journal of Arid Environment, V 48, (4), p 475-499.

Al-Shamsei, M.H., (1993). Drainage basins and flash flood hazards in Al Ain area, United Arab Emirates. M.Sc. Thesis, United Arab Emirates University, 151p.

Alsharhan, A.S., Rizk, Z.A., Naim, A.E.M., Bakhit, D.W., and, AlHajari, S.A., (2001). Hydrogeology of An Arid Region: The Arabian Gulf And Adjoining Areas, Elsevier, Publishing Company, New York, 331p.

Baghdady, A.R., (1998). Petrography, Mineralogy, and Environmental Implications of the sand dune fields of the greater Al Ain area, United Arab Emirates, Ph.D. Thesis, Geol Dep., Fac. Sci., Ain Shams Univ., Egypt, 304 p.

Bakhit, D.W.M., (1998). Environmental and management problems in hydrology of the United Arab Emirates. Ph.D. Thesis, University of South Carolina, Columbia, 407p.

Boote, D.R.D., Mou, D. and Waite, R.I., (1990). Structural evolution of the Suneiyah foreland, Central Oman Mountains. In: Rovertson, A.H.F., Searle, M.P. and Ries, A. C. (edits.). The geology and tectonics of the Oman Region. Geol. Soc. London, Spec. Publ., V49, p397-418.

Bown, T.M., Hadley, D.G., Brouwers, E.M., and Imes, J.L., (1991). Neogene-Quaternary tectonosedimentary evolution of a part of eastern Abu Dhabi Emirate, UAE: Geol. Soc. Am., Abstracts with programs, 1991 Annual Meeting, V. 23, no.5, p 289.

Chebotarev, I.I., (1955). Metamorphism of natural water in the crust of weathering. Geochim et Cosmoch. Acta, V l.7, part I, p 22-48. Part II, p 137-170 and Part III p 148-212, London and New York.

Coleman, R.G., (1981). Tectonic setting for ophiolite obduction in Oman. Journal of Geophysical Research, V 86, no B4, p 2497-2508.

Davis, S.N. and De Weist, R.J. (1966). Hydrogeology. John Wiley and Sons, New York, 463p.

Dobrin, M.B., (1976). Introduction to geophysical prospecting. Third ed., Mc Graw-Hill Co., New York.

Dune, L.A., Manoogian, P.R., and Pierini, DF., (1990). Structural style and domains of the northern Oman Mountains (Oman and United Arab Emirates). In Robertson, A.H.F., Searle, M.P., and Ries, A.C., (eds), The Geology and Tectonics of Oman Region. Geological Society of London Special Publication (49), p375-386.

Eaton, F.M., (1950). Significance of carbonates in irrigation water. Soil. Sci., v 69, no. 2, p 123-133.

El-Saiy, A.K., (2002). Petrology, geochemistry and framework of sedimentation of the Quaternary aquifer rocks north of Al Ain. UAE. M. Sc. Thesis, Geol. Dep., Fac. Sci., Suez Canal University, 203p.

El-Shami, F., (1990). The hydrochemistry of the spring at Ain bu Sukhnah, UAE. Arab J. Scient. Res., V 8 no 1, p 33-49.

Embabi, N.S., (1991). Dune types and patterns in the United Arab Emirates using Landsat TM-data. 24th Intern. Symp. on Remote Sensing of Environment, Rio dejaneiro, Brazil, p 27-31.

Emberger, L. (1955). Afrique due Nord-Desert Ecologic Vegetate Compte de recherches. Plant Ecology Reviews of Research, Paris, UNESCO.

Fetter, C.W., (1988). Applied hydrogeology: Macmillan Publishing Company, New York, second edition, 592p.

Fetter, C.W., (1994). Applied hydrogeology, 3rd edition , Prentice-Hall, Inc. A Simon & Schuster Company, Englewood Cliffs, New Jersey ,07632, USA, 691 p.

Fitterman, D.V., Menges, C.M, Al Kamali, A.M., and Jama, F.E., 1991.Electromagnetic mapping of buried paleochannels in eastern Abu Dhabi Emirate, U.A.E: Geoexploration, V.27, p.111-133.

Garamoon, H.K., (1996). Hydrogeological and geomorphological studies on the Abu Dhabi-Dubai-Al Ain triangle, UAE. Unpublished Ph.D. thesis, Geol. Dep., Fac. Sci., Ain Shames University, Egypt, 277p.

GeoConsult, and Bin Ham Well Drilling Establishment, (1985a): Project 21/81, Drilling of deep water wells at various locations in the UAE, V I, general part: UAE, Ministry of Agriculture and Fisheries, Water and Soil Department, unpublished report on file at Ministry of Agriculture and Fisheries, Dubai, 131p.

GeoConsult, and Bin Ham Well Drilling Establishment, (1985b): Project 21/81, Drilling of deep water wells at various locations in the UAE, V III, 1-Masfut, 2-Al Ain, 3Al Wagan, 4Medeisis, 5Liwa: UAE, Ministry of Agriculture and Fisheries, Water and Soil Department, unpublished report on file at Ministry of Agriculture and Fisheries, Dubai, 87 p.

Gibb, S.A. and Partners, (1970). Water resources survey, supplement to interim report, subsurface investigations in Al Ain area: Department of Development and Public Works, Abu Dhabi, 608p.

Glennie, K.W., Boeuf, M.G.A., Huhger Clarke, M.W., Moody Stuart, M., Pillar, W.F.H. and Reinhardt, B.M. (1974). Geology of the Oman Mountains. Koninklijk Nederlands Geol-Minjb. Genootschap. (Transactions of the Royal Dutch Geological and Mining Soc.), p 31-423.

Gymer, R. G. (1973). Chemistry: An Ecological Approach, Harper and Row, New York.

Habberjam, G.M., (1979). Apparent Resistivity Observation and the Use of the Square array Techniques. Geoexploration Monograph, 9, Borntraeger, Berlin, 152 p.

Hamdan, A.A., and Anan, H.S. (1989). The Paleocene tecto-sedimentary events of Jabal Malaqet., East of Al Ain., West of the Northern Oman Mountains. M.E.R.C., Ain Shams Univ., Earth Sci. Ser., (3), p 209-214.

Hamdan, A.A., and Anan, H.S. (1993). Cretaceous/Tertiary boundary in the United Arab Emirates. M.E.R.C., Ain Shams Univ., Earth Sci. Ser., (7), p 223-231.

Hamdan, A.A., and Bahr, S.A. (1992). Lithostratigraphy of the Paleogene succession of northern Jabal Hafit., Al-Ain area., UAE. M.E.R.C., Ain Shams Univ., Earth Sci. Ser., (6), p 201-224.

Hamdan, A.A., and El-Deeb, W. Z., (1990). Stratigraphy of the Paleogene succession of Jabal Malaqet, West of the Northern Oman Mountains., Fac. Sci., UAE Univ., (2), p30-39.

Hunting Geology and Geophysics Ltd. (1979). Report on a mineral survey of UAE., Al Ain Area. Ministry of Petroleum and Mineral Resources., Abu Dhabi., (9), 1-22p.

Hyde, L.W., (1992). Interregional advisory mission of water resources management, Abu Dhabi Emirate: United Nations Department of Technical Cooperation for Development, 86p.

HydroConsult, (1978): Reconnaissance report and development proposals, Abu Dhabi, (UAE) Eastern Region water resources: Government of Abu Dhabi, Ministry of Petroleum and Mineral Resources Report, 126 p.

Jorgensen, D.G., and Petricola, Mario, (1993). Petrophysical analysis of geophysical logs, National Drilling Company- U.S. Geological Survey, Groundwater Resources Project for Abu Dhabi, United Arab Emirates: U.S. Geological Survey Open-File Report 93-085, 58p.

Khalifa, A.A., (1995). Surface water and groundwater resources in UAE. Culture and Science Society, Meeting on Water Balance in U.A.E., Dubai,12p.

Khalifa, M.A., (1997). Hydrogeology of the geothermal fractured-rock well field at Jabal Hafit, Abu Dhabi Emirate. Proceedings of the 3rd Gulf Water Confer., Muscat, Sultanate of Oman, V.1,p. 125-140.

Koefoed, O.O, (1968). Geosoinding principles, 1- Resistivity Sounding Measurements. El-Sevier, Amsterdam.

Lippard, S.J., Shelton, A.W., and Gass, I.G., (1986). The ophiolite of northern Oman. The Geological Society of London, Memoir no. 11, 178 p.

Lowrie, W., (1997). Fundamentals of Geophysics. Cambridge University press.

Mathess, G. (1982). The properties of groundwater. New York: John Wiley and Sons.

Mayboom, P., (1966). Groundwater studies in the Assiniboine River drainage basn part I. The Evolution of a Flow System in South central Saskatchewan: Geol. Surv. Can. Bull., V 139,65p.

McNeil, J.D. (1980). Electromagnetic terrain conductivity measurements at low induction number. Golden, Colorado, Geonics Technical Note TN-6, p15.

McNeill, J.D. (1994). Principles and application of time domain electromagnetic techniques for resistivity sounding. Technical Note TN-27, Geonics limited, Ontario, Canada.

Meinzer, O.E., (1923). The occurrence of groundwater in the United States with discussion of principles, U.S. Geological Survey, Water Supply Paper, 492p.

Meju, M.A. (1992). An effective ridge regression procedure for resistivity data inversion. Computers & Geosiences, 18, (2/3), 99-118.

Menges and Woodward, US Geological Survey and United Arab Emirates National Drilling Company, (1993). Ground Water Resources of Al Ain area, Abu Dhabi Emirate. Unpublished administrative report 93-001, National Drilling Company, Abu Dhabi, UAE, 315 p.

Ministry of Agriculture and Fisheries, United Arab Emirates, (1986a). Drilling of deep water wells at various locations in U.A.E, Main Report, V1, MAF, U.A.E. Dubai, 214p.

Ministry of Agriculture and Fisheries, United Arab Emirates, (1986b). Drilling of Deep Water Wells at Various Locations in U.A.E, Main Report, V8, MAF, U.A.E., Dubai, 107p.

Ministry of Agriculture and Fisheries, Water and Soil Department,(1985). Project 21/81, Drilling of deep water wells at various locations in the UAE, VI, general part. unpublished report on file at Ministry of Agriculture and Fisheries, Dubai, 131p.

Ministry of Communications United Arab Emirates, (1996). U.A.E. Climate. Cultural Foundation Publications, Abu Dhabi, 240 p.

Nath, S.K., Patra, H.P. and Shahid, Sh. (2000). Geophysical prospecting for groundwater. A.A. Balkema, Rotterdam, Netherlands, 256pp.

National Atlas of U.A.E. (1993). UAE Univ., Al Ain., UAE.

Nolan, S.C., Skeleton, P.W., Clissold, B.P. and Smewing, J.D. (1990). Maastrichtian to Early Tertiary stratigraphy and paleogeography of the central and northern Oman Mountain. In: Robertson., A.H.F., Searle, M.P., and Ries, A.C., (edits). The Geology and tectonics of the Oman Region. Geological Society of London, Special publication, (49), p 495-519.

Parasnis, D. (1997). Principles of Applied Geophysics. London: Chapman & Hall.

Patton, T.L. and O'Conner, S.J. (1998). Cretaceous flexural history of Northern Oman Mountains foredeep., United Arab Emirates., AAPG Bull., (72), p797-809.

Piper, A. M. (1944). A graphic representation in the geochemical interpretation of water analyses. Trans. Amer. Geophysical Union, V. 25, p. 914-928.

Reynolds, J.M., 1997. An introduction to Applied and Environmental Geophysics, John Wiley & Sons. pp. 796.

Rizk, Z.S., (1998). Falajes of United Arab Emirates: Geological Settings and hydrogeological characteristics. Arab of the Jour. Sci. Eng., King Fahd University for Petroleum and Minerals, Dhahran, Saudi Arabia, V.23(1c), p.3-25.

Rizk, Z.S., (1999). A review article on water resources in the United Arab Emirates. Unpublished Article, Department of Geology, Faculty of Science-Menoufia University, Shebin El Kom, Egypt, 44p.

Rizk, Z.S., Alsharhan, A.S. and Shino, S., (1997). Evaluation of groundwater Resources of United Arab Emirates: Proceedings of 3 rd Gulf Water Conference, Muscat, Sultanate of Oman, v. 1, p. 95-122.

Rizk, Z.S., and El Etr, H.A., (1997). Hydrogeology and hydrogeochemistry of some springs in the United Arab Emirates. Arab Jour. Sci. Eng., King Fahd University for Petroleum and Minerals, Dhahran, Saudi Arabia, v.22 (1c), p.95-111.

Rizk, Z.S., Garamoon, H.K. and El Etr, H., 1998. Contribution to hydrogeochemistry of the Quaternary aquifer in the Al Ain area, United Arab Emirates. In: A.S. Alsharhan, K.W. Glennie, G.L. Whittle and C.G.ST.C. Kendall (eds.), Quaternary Deserts and Climatic Change, Published by Balkema, Rotterdam, p.439-454.

Robertson, A.H.F., Searle, M.P., and Ries, A.C., eds., (1990). The geology and tectonics of the Oman Region: Geological Society of London Special publication no. 49, p845.

Robinson, E.S., and Courth, C. (1988). Basic Exploration Geophysics, Cambridge University Press.

Schlumberger (1981). United Arab Emirates and Qatar: Schlumberger well Evaluation Conference, p271.

Searle, M.P., Cooper, D.J.W., and Watts, K.F., (1990). Structure of the jebal Sumeini-Jebal Ghawil area, northern Oman in Robertson, A.H.F., Searle, M.P., and Ries, A.C., eds., The Geology and Tectonics of the Oman Region: Geological Society of London Special Publication no (49), p361-374.

Sharma, P.V., (1997). Environmental and Engineering Geophysics, Cambridge University Press.

Sulin, U. A. (1948) Basis of classification of natural water. Moscow, U.S.S.R. (In Russian).

Teleford, W.M., Geldart, L.P., Sheeriff, R.E and Keys, D.A. (1990). Applied Geophysics, 2nd edn. Cambrigde: Cambridge University Press.

Terao, H., Yoshioka, R. & Kato, K. (1993): Groundwater pollution by nitrate originating from fertilizer in kakamigahara heights, central Japan. 29th Inter. Geol. Congress, International Association of Hydrogeologists, Kyoto, japan 51-62.

Terrates Ltd., (1973). Abu Dhabi Mineral Survey. Final Report (unpublished). Thomas, A.N. (1950). The Asmari Limestone of southwest Iran. Rept. 18th International geological congress., London., (6), p35-55.

Todd, D.K., (1980). Groundwater hydrology: John Wiley and Sons, New York (second edition), 535 p.

U.S. Salinity Laboratory Staff (1954). Diagnosis and improvement of saline and alkaline soils. U. S. Dept. Agri., Handbook No. 60, Washington, D. C., 60 p.

US Geological Survey and United Arab Emirates National Drilling Company, (1993). Ground Water Resources of Al Ain area, Abu Dhabi Emirate. Unpublished administrative report 93-001, National Drilling Company, Abu Dhabi, UAE, 315 p.

Van Nostrand, R.G., and Cood, K.L., (1966). Interpretation of resistivity data. U.S.G.S. Prof. Paper No. 499.

Warburton, J., Burnhill, T. J., Graham, R.H. and Isaac, K.p. (1990). The evalotion of the Oman Mountains foreland basin. In: Robertson, A.H.F., Searle, M.P. and Ries, A.C. (edits). The geology and tectonics of the Oman Region. Geological Society of London Special publication no., Publ., (49), 419-427p.

Warrak, M. (1986). Structural evolution of the Northern Oman Mountain front, Al Ain Region. Symposium on the hydrocarbon potential of intense thrust zones. Ministry of Petroleum and Mineral Resources., Abu Dhabi., (2), p375-431.

Warrak, M. (1987). Synchronous deformation of neoautochthonous sediments of the Northern Oman Mountains. 5th Conf. S.P.E., Bahrain., p129-136.

White, W.B., (1977). Conceptual models for carbonate aquifers: Revisted in Dilamarter, R.R., and Csallany, S.C. (edits), Hydrologic problems in krast region, U.S., Bowing Green, Kentucky, Western Kentucky University, p. 176-187.

Whittle, G.L. and Alsharhan, A.S. (1994). Dolomitization and chertification of the Early Eocene Rus Formation in Abu Dhabi, UAE. Sedimentary Geology, (91), p. 273-285.

Wilcox, L. V. (1955). Classification and use of irrigation water U. S. A., Salinity Lab., Circulation No. 969.

Woodward, D.G., and Menges, C.M., (1991a). Application of uphole data from petroleum seismic surveys to groundwater investigation, Abu Dhabi (United Arab Emirates): Geoexploration, V.27, p. 193-212.

Woodward, G.L. and Alsharhan, A.S. (1994). Dolomitization and chertification of the Early Eocene Rus Formation in Abu Dhabi, UAE. Sedimentary Geology, (91), p. 273-285.

Worsley, R. R. (1929) The hydrogen ion of Egyptian soil. Min. Agri., Bull. No. 83, pp. 1-33, Egypt.

Zohdy, A.A.R. (1974). Use of dar Zarrouk curves in the interpretation of vertical electrical sounding data. U.S. Geol. Surv. Bull., 1373-D, 41.

APPENDIX

Appendix (A) Chemical analysis of major cations and anions for the Quaternary aquifer, Al Jaww Plain

Well Num	UTME	UTMN	TDS	EC at 25 C°	pH	Units	Cations				Total		Anions		Total
			mg/l	m.mhos/cm			Na	CA	Mg	K	Cations	CL	SO4	HCO3	Anions
17	388463	2674345			8.25	ppm	41	18.5	28.3	2.4		78.75		144	
						epm	1.78338408	0.923154	2.3287389	0.061381	5.096657789	2.2214386		2.360656	4.582094384
						epm%	34.9912463	18.11292	45.691491	1.20434		48.480857		51.51914	
GWP 018	393546	2676791	299.5	502.5	7.8	ppm	34	18.7	33.7	2.2		66.7	38	144	
						epm	1.47890387	0.933134	2.773092	0.056266	5.241395545	1.8815233	0.791667	2.360656	5.033845677
						epm%	28.2158417	17.80315	52.907512	1.073492		37.377452	15.72688	46.89567	
20	395300	2664216	1306		7.4	ppm	340	47	46	36		405	295		
						epm	14.7890387	2.345309	3.7852294	0.920716	21.84029358	11.424542	6.145833	0	17.57037494
						epm%	67.7144685	10.73845	17.331403	4.215676		65.021615	34.97838	0	
68	395194	2664639	804		11.6	ppm	85	150		31		85	260		
						epm	3.69725968	7.48503	0	0.792839	11.97512849	2.3977433	5.416667	0	7.814409967
						epm%	30.8744886	62.5048	0	6.620713		30.683613	69.31639	0	
198	370366	2668998	13000	20000	11.3	ppm	3427	1205	42	184		6449.6	1600		
						epm	149.064811	60.12974	3.456079	4.705882	217.3565127	181.93512	33.33333	0	215.2684532
						epm%	68.5807888	27.66411	1.5900508	2.165052		84.515458	15.48454	0	
201	374810	2677881				ppm									
						epm									
						epm%									
202	372345	2676700				ppm									
						epm									
						epm%									
204	377637	2661181	1560	2400	7.225	ppm	345	150.4	46.605	8		535.795	298.41	274.75	
						epm	15.0065246	7.50499	3.8350134	0.204604	26.55113155	15.114104	6.216875	4.504098	25.83507773
						epm%	56.519341	28.26618	14.443879	0.770602		58.50226	24.0637	17.43404	
206A	373559	2677572	6240	9600	7.53	ppm	1840	311.85	348.35	30		2455.81	2217	490.4	
						epm	80.0347977	15.56138	28.664884	0.767263	125.0283222	69.275317	46.1875	8.039344	123.5021616
						epm%	64.0133342	12.44628	22.926712	0.613672		56.092393	37.39813	6.509477	
206B	373562	2677573	4745	7300	7	ppm	1200	218	289.14	30		1761.2	1270	405	
						epm	52.1966072	10.87824	23.792635	0.767263	87.63474942	49.681241	26.45833	6.639344	82.77891878
						epm%	59.561541	12.41316	27.149773	0.875524		60.01678	31.96265	8.020574	
246B	394286	2670955	520	800	7.5	ppm	86	41.6	36.74	4		101.2	59.36	301.3	
						epm	3.74075685	2.075848	3.0232462	0.102302	8.94215319	2.854725	1.236667	4.939344	9.030735894
						epm%	41.8328424	23.21419	33.808929	1.14404		31.611211	13.69397	54.69481	
247A	392732	2670617	1950	3000	8.15	ppm	400	104.52	81.74	5		848.4	204	171.2	
						epm	17.3988691	5.215569	6.726188	0.127877	29.4685032	23.932299	4.25	2.806557	30.98885639
						epm%	59.0422559	17.69879	22.825007	0.433945		77.228726	13.71461	9.056667	
247B	392728	2670605	630.5	970	7.86	ppm	100	31.36	40.26	4.5		150.82	111.9	184.9	
						epm	4.34971727	1.56487	3.3128986	0.11509	9.342575622	4.2544429	2.33125	3.031148	9.616840418
						epm%	46.5580097	16.74988	35.460228	1.231882		44.239508	24.24133	31.51916	
248A	395943	2669109	344.5	533	8.22	ppm	40	19.345	27.92	2.6		57.25	65.4	136.9	
						epm	1.73988691	0.965319	2.2974697	0.066496	5.069172089	1.6149506	1.3625	2.244262	5.22171293
						epm%	34.3229008	19.04294	45.322384	1.311776		30.927603	26.09297	42.97943	
250	397507	2664126			8.1	ppm	39	17	32	3.1		73			
						epm	1.69638973	0.848303	2.633203	0.079284	5.25718006	2.0592384	0	0	2.059238364
						epm%	32.2680546	16.13609	50.087747	1.508107		100	0	0	
251	399035	2661977				ppm	115	19	27	6.4		120	55	211	
						epm	5.87211831	1.397206	2.4686279	0.181586	9.919537433	3.3850494	1.145833	3.459016	7.989899092
						epm%	59.1975014	14.08539	24.886522	1.830586		42.36661	14.34102	43.29237	
252	399413	2662926				ppm	135	28	30	7.1		140	105	224	
						epm	5.87211831	1.397206	2.4686279	0.181586	9.919537433	3.9492243	2.1875	3.672131	9.808855407
						epm%	60.0088644	11.37398	26.653526	1.96363		40.261826	22.30128	37.4369	
253	399254	2663992				ppm	90	35	40	6		130	105	175	
						epm	3.91474554	1.746507	3.2915038	0.153453	9.106209019	3.6671368	2.1875	2.868852	8.723489271
						epm%	59.1975014	14.08539	24.886522	1.830586		42.0375	25.07598	32.88652	
254	396576	2669013		512	7.9	ppm	41	17	28	2.9		55			
						epm	1.78338408	0.848303	2.3040527	0.074169	5.009908935	1.551481	0	0	1.551480959
						epm%	35.5971357	16.93251	45.989911	1.480442		100	0	0	
256	394265	2675661				ppm	350	80	100	15		550	425	160	
						epm	15.2240104	3.992016	8.2287595	0.383632	27.82841764	15.51481	8.854167	2.622951	26.99192708
						epm%	54.7067053	14.34511	29.569628	1.378561		57.479444	32.80302	9.717538	

257	394845	2674067		577	7.8	ppm	53	15	27	4.3		60			
						epm	2.30535015	0.748503	2.2217651	0.109974	5.38559264	1.6925247	0	0	1.692524683
						epm%	42.8058768	13.89825	41.253864	2.042012		100	0	0	
258	393624	2674009		555	8	ppm	54	15	27	3.15		64		160	
						epm	2.34884732	0.748503	2.2217651	0.080563	5.399678048	1.8053597	0	2.622951	4.428310481
						epm%	43.4997662	13.86199	41.146251	1.49199		40.768588	0	59.23141	
259	395949	2669335		595		ppm	45	20	31	3.4		65	55		
						epm	1.95737277	0.998004	2.5509154	0.086957	5.593248734	1.8335684	1.145833	0	2.97940174
						epm%	34.9952749	17.84301	45.607045	1.554669		61.541496	38.4585	0	
307	396224	2669013				ppm	44	20	27	3.7		60	45	170	
						epm	1.9138756	0.998004	2.2217651	0.094629	5.228273815	1.6925247	0.9375	2.786885	5.416909929
						epm%	36.6062618	19.08859	42.495193	1.80995		31.245206	17.30692	51.44788	
308	396057	2669034				ppm	44	22	29	3		60	60	172	
						epm	1.9138756	1.097804	2.3863403	0.076726	5.474746591	1.6925247	1.25	2.819672	5.762196814
						epm%	34.95825	20.05215	43.588141	1.401459		29.372907	21.69312	48.93398	
309	396904	2668831				ppm	40	35	30	5.5		65	55	199	
						epm	1.73988691	1.746507	2.4686279	0.140665	6.095686709	1.8335684	1.145833	3.262295	6.241696822
						epm%	28.5429188	28.65152	40.497945	2.307615		29.376121	18.35772	52.26616	
328A	381374	2660544				ppm	675	80	85	23		900	700	155	
						epm	29.3605916	3.992016	6.9944456	0.588235	40.93528841	25.38787	14.58333	2.540984	42.51218718
						epm%	71.7244038	9.752016	17.086592	1.436988		59.71904	34.30389	5.977071	
328B	381392	2660554				ppm	675	80	90	19		815	725	201	
						epm	29.3605916	3.992016	7.4058836	0.485934	41.2444246	22.990127	15.10417	3.295082	41.38937557
						epm%	71.1868134	9.678923	17.956084	1.17818		55.545962	36.49286	7.961178	
329	381580	2656602				ppm	450	90	100	12.2		600	525	233	
						epm	19.5737277	4.491018	8.2287595	0.31202	32.60552565	16.925247	10.9375	3.819672	31.68241896
						epm%	60.0319342	13.77379	25.237316	0.956956		53.421574	34.5223	12.05613	
330	395458	2669339				ppm	105	21	32	8.5		145	76	134	
						epm	4.56720313	1.047904	2.633203	0.217391	8.465701672	4.090268	1.583333	2.196721	7.870322628
						epm%	53.949493	12.37823	31.104369	2.567907		51.970779	20.11777	27.91145	
331	394651	2669940				ppm	60	24	37	4.5		80	57	194	
						epm	2.60983036	1.197605	3.044641	0.11509	6.967165686	2.2566996	1.1875	3.180328	6.624527446
						epm%	37.4589967	17.18927	43.699851	1.651884		34.06582	17.92581	48.00837	
333	393492	2670287				ppm	80	55	60	6.5		100	200	240	
						epm	3.47977381	2.744511	4.9372557	0.16624	11.32778091	2.8208745	4.166667	3.934426	10.92196737
						epm%	30.7189364	24.22814	43.585374	1.467546		25.827531	38.14942	36.02305	
GWP-334A	362862	2673851				ppm	780	145	220	32		1100	1450	77	
						epm	33.9277947	7.235529	18.103271	0.818414	60.08500889	31.029619	30.20833	1.262295	62.5002476
						epm%	56.4663222	12.04215	30.12943	1.362094		49.647194	48.33314	2.019664	
GWP-334B	362880	2673843				ppm	780	145	220	32		1450	650	155	
						epm	33.9277947	7.235529	18.103271	0.818414	60.08500889	40.90268	13.54167	2.540984	56.9853301
						epm%	56.4663222	12.04215	30.12943	1.362094		71.777561	23.76343	4.459014	
GWP-335	361139	2676999				ppm	1100	270	190	34		2100	650	86	
						epm	47.84689	13.47305	15.634643	0.869565	77.82415214	59.238364	13.54167	1.409836	74.18986663
						epm%	61.4807725	17.31218	20.089706	1.117346		79.846975	18.25272	1.900308	
GWP-336	371566	2679371				ppm	2000	800	1200	55		6000	2300	170	
						epm	86.9943454	39.92016	98.745114	1.40665	227.0662688	169.25247	47.91667	2.786885	219.9560202
						epm%	38.3123155	17.58084	43.487355	0.619489		76.948323	21.78466	1.267019	
6	394150	2678020	358												
8	393900	2677960	248												
9	393680	2677920	256												
11	389250	2676000	256												
12			246												
13	393970	2677480	275	485	8.45	ppm						49.61	27		

						epm						1.3994358	0.5625	0	1.961935825
						epm%						71.329337	28.67066	0	
14	393950	2677300	288	487	8.44	ppm						51.597	42		
						epm						1.4554866	0.875	0	2.330486601
						epm%						62.454193	37.54581	0	
15	393740	2677310	246			ppm									
						epm									
						epm%									
16	393450	2677750	371			ppm									
						epm									
						epm%									
17	393660	2677120	249			ppm									
						epm									
						epm%									
18	393400	2677560	269			ppm									
						epm									
						epm%									
19	393635	2676910	320	595	8.4	ppm						77.396	62		
						epm						2.183244	1.291667	0	3.474910672
						epm%						62.828781	37.17122	0	
21	393900	267700	309			ppm									
						epm									
						epm%									
23	393225	2677420	288	470	8.35	ppm						52.588	31.5		
						epm						1.4834415	0.65625	0	2.139691467
						epm%						69.32969	30.67031	0	
24	393040	2677330	294			ppm									
						epm									
						epm%									
28	392870	2677220	262	467.5	8.29	ppm						52.585	33		
						epm						1.4833568	0.6875	0	2.170856841
						epm%						68.330477	31.66952	0	
29	393280	2676260	794			ppm									
						epm									
						epm%									
32	392710	2677120	279	460	8.3	ppm						50.105	31		
						epm						1.4133992	0.645833	0	2.059232487
						epm%						68.637182	31.36282	0	
33	393500	2676100	2024			ppm									
						epm									
						epm%									
34	393440	2675890	755			ppm									
						epm									
						epm%									
35	392540	2677020	269	470	8.35	ppm						57.55	25		
						epm						1.6234133	0.520833	0	2.144246591
						epm%						75.710194	24.28981	0	
37	393300	2675700	346			ppm									
						epm									
						epm%									
38	393050	2675600	346			ppm									
						epm									
						epm%									
39	393250	2675500	314			ppm									
						epm									
						epm%									
40	392360	2677040	262	440	8.4	ppm						47.62	24		
						epm						1.3433004	0.5	0	1.843300423
						epm%						72.874742	27.12526	0	
41	393150	2675300	269			ppm									
						epm									
						epm%									
44	392180	2676830	256	450	8.37	ppm						45.64	26		
						epm						1.2874471	0.541667	0	1.829113775

						epm%						70.386387	29.61361	0	
46	392010	2676760	256	450	8.36	ppm						45.64	22		
						epm						1.2874471	0.458333	0	1.745780442
						epm%						73.746221	26.25378	0	
48	391610	2676740	253	410	8.41	ppm						43.65	33		
						epm						1.2313117	0.6875	0	1.918811707
						epm%						64.170533	35.82947	0	
49	391440	2676560	250	447.5	8.505	ppm						46.625	34.5		
						epm						1.3152327	0.71875	0	2.033982722
						epm%						64.662925	35.33707	0	
50	391250	2676520	256	422.5	8.43	ppm						47.625	29.5		
						epm						1.3434415	0.614583	0	1.9580248
						epm%						68.612076	31.38792	0	
51	391790	2676780	262	430	8.36	ppm						45.64	33		
						epm						1.2874471	0.6875	0	1.974947109
						epm%						65.188941	34.81106	0	
52	391050	2676450	256	437.5	8.4	ppm						49.605	29		
						epm						1.3992948	0.604167	0	2.003461448
						epm%						69.843859	30.15614	0	
53	390875	2676400	250	444	8.41	ppm						47.62	30.5		
						epm						1.3433004	0.635417	0	1.97871709
						epm%						67.887442	32.11256	0	
54	392300	2677260	-	512.5	8.33	ppm						64.496	34.5		
						epm						1.8193512	0.71875	0	2.538101199
						epm%						71.681586	28.31841	0	
59	390660	2676350				ppm									
						epm									
						epm%									
62	390160	2676190		525	8.45	ppm						66.48	48		
						epm						1.8753173	1	0	2.875317348
						epm%						65.22123	34.77877	0	
63	392450	2677370		1353.5	8.145	ppm						325.46	45.5		
						epm						9.1808181	0.947917	0	10.12873472
						epm%						90.641312	9.358688	0	
65	390900	2676600		460	8.25	ppm						53.58	32.5		
						epm						1.5114245	0.677083	0	2.188507875
						epm%						69.061874	30.93813	0	
66	390690	2676590		436.5	8.28	ppm						48.619	30.5		
						epm						1.371481	0.635417	0	2.006897626
						epm%						68.338362	31.66164	0	
67	390480	2676520		462.5	8.38	ppm						57.55	34.5		
						epm						1.6234133	0.71875	0	2.342163258
						epm%						69.312558	30.68744	0	
72				550	8.33	ppm						73.43	48		
						epm						2.0713681	1	0	3.071368124
						epm%						67.44122	32.55878	0	
7	394350	2678090				ppm									
						epm									
						epm%									
7(w)	390030	2676350				ppm									
						epm									
						epm%									
10	394180	2677860				ppm									
						epm									
						epm%									
10(w)	389500	2676000				ppm									
						epm									
						epm%									
22	393670	2676700				ppm									
						epm									
						epm%									
27	393620	2676490				ppm									
						epm									
						epm%									

25	393400 2676480				ppm									
					epm									
					epm%									
26	393850 2676810				ppm									
					epm									
					epm%									
31©	393240 2676020				ppm									
					epm									
					epm%									
30©	393200 2675970				ppm									
					epm									
					epm%									
42©	393170 2675870				ppm									
					epm									
					epm%									
43	393090 2675090				ppm									
					epm									
					epm%									
45	392980 2675390				ppm									
					epm									
					epm%									
101	392817 2662106	401.55	617.5	7.9	ppm						112.7	95		
					epm						3.1791255	1.979167	0	5.158292196
					epm%						61.631358	38.36864	0	
102	393194 2662034	416	640	8.005	ppm						109.18	81.5		
					epm						3.0798307	1.697917	0	4.777747414
					epm%						64.461983	35.53802	0	
103	393592 2661994	407.85	627.5	8.02	ppm						116.68	83		
					epm						3.2913963	1.729167	0	5.020563
					epm%						65.558312	34.44169	0	
104	394134 2661825			8.19	ppm									
					epm									
					epm%									
105	395969 2662179	404.65	622.5	8.05	ppm						129.16	76.5		
					epm						3.6434415	1.59375	0	5.237191467
					epm%						69.568613	30.43139	0	
201	393146 2661796	616.95	949	8.12	ppm						245.05	111		
					epm						6.9125529	2.3125	0	9.225052891
					epm%						74.932393	25.06761	0	
204	394604 2661911	499.95	769	8.17	ppm						165.135	99.5		
					epm						4.6582511	2.072917	0	6.731167724
					epm%						69.204204	30.7958	0	
206	395525 2661895	401.8	618	8.155	ppm						122.18	77.5		
					epm						3.4465444	1.614583	0	5.061127762
					epm%						68.098349	31.90165	0	
207	396375 2662226	380.9	586	8.025	ppm						128.15	81		
					epm						3.6149506	1.6875	0	5.302450635
					epm%						68.175093	31.82491	0	
404	390923 2661092	433.9	667.5	8.15	ppm						116.05	87		
					epm						3.2736248	1.8125	0	5.086124824
					epm%						64.363832	35.63617	0	
406	389434 2660528	469.65	722.5	8.2	ppm						114.62	111.5		
					epm						3.2332863	2.322917	0	5.556202985
					epm%						58.192372	41.80763	0	
409	388545 2659896			8.195	ppm									
					epm									
					epm%									
410	387824 2660235	881	1355.5	8.09	ppm						227.35	255		
					epm						6.4132581	5.3125	0	11.72575811
					epm%						54.693761	45.30624	0	
411	388088 2659589	457.5	704	8.495	ppm						106.695	104		
					epm						3.009732	2.166667	0	5.176398684
					epm%						58.143358	41.85664	0	
412	387659 2659767	659.65	1015	8.335	ppm						179.75	141		

						epm						5.0705219	2.9375	0	8.008021862
						epm%						63.318032	36.68197	0	
501	391044	2663861	470.45	723.5	8.365	ppm						82.135	82		
						epm						2.3169252	1.708333	0	4.02525858
						epm%						57.559662	42.44034	0	
502	391287	2663910	460.35	708.5	8.335	ppm						72.645	85.5		
						epm						2.0492243	1.78125	0	3.83047426
						epm%						53.497925	46.50207	0	
503	591438	2664025	446.1	686	8.39	ppm						71.215	81		
						epm						2.0088858	1.6875	0	3.696385755
						epm%						54.347297	45.6527	0	
504	391740	2664350	476.7	733	8.45	ppm						81.16	79.5		
						epm						2.2894217	1.65625	0	3.945671721
						epm%						58.023624	41.97638	0	
505	392041	2664373	464.7	715	8.06	ppm						79.665	76.5		
						epm						2.2472496	1.59375	0	3.840999647
						epm%						58.506895	41.4931	0	
506	392512	2664385	474.15	729.5	8.075	ppm						81.64	81.5		
						epm						2.3029619	1.697917	0	4.000878585
						epm%						57.561405	42.4386	0	
507	391442	2664313	427.05	657	8.06	ppm						75.445	85.5		
						epm						2.1282087	1.78125	0	3.909458745
						epm%						54.437427	45.56257	0	
508	391752	2664090	589.25	906.5	8.075	ppm						151.9	115.5		
						epm						4.2849083	2.40625	0	6.691158322
						epm%						64.038364	35.96164	0	
601	395112	2663781	412.1	634	8.175	ppm						87.335	83.5		
						epm						2.4636107	1.739583	0	4.203194053
						epm%						58.612824	41.38718	0	
602	-	-	425.55	668.5	8.185	ppm						89.325	87		
						epm						2.5197461	1.8125	0	4.332246121
						epm%						58.16258	41.83742	0	
603	-	-	399.75	615	8.22	ppm						79.4	81		
						epm						2.2397743	1.6875	0	3.92727433
						epm%						57.031268	42.96873	0	
604	-	-	424.45	653	8.185	ppm						83.365	79.5		
						epm						2.351622	1.65625	0	4.007872003
						epm%						58.675077	41.32492	0	
605	393804	2664611	375.7	578	8.105	ppm						68.965	70		
						epm						1.9454161	1.458333	0	3.403749412
						epm%						57.155091	42.84491	0	
606	393282	2664650	420.55	647	8.12	ppm						87.335	73.5		
						epm						2.4636107	1.53125	0	3.994860719
						epm%						61.669502	38.3305	0	
607	392750	2664591	396.5	610	8.18	ppm						80.365	66		
						epm						2.2669958	1.375	0	3.641995769
						epm%						62.245975	37.75403	0	
608	392120	2665064	422.2	649.5	8.21	ppm						90.3	76.5		
						epm						2.5472496	1.59375	0	4.140999647
						epm%						61.512916	38.48708	0	
609	392245	2664515	413.1	635.5	8.105	ppm						95.765	76.5		
						epm						2.7014104	1.59375	0	4.295160437
						epm%						62.894285	37.10572	0	
610	391852	2664673	382.2	588	8.145	ppm						77.41	68.5		
						epm						2.1836389	1.427083	0	3.610722261
						epm%						60.476513	39.52349	0	
611	391637	2665155	423.8	652	8.155	ppm						97.29	81		
						epm						2.7444288	1.6875	0	4.431928773
						epm%						61.924027	38.07597	0	
612	390870	2664924	461.1	709	8.205	ppm						89.31	82.5		
						epm						2.519323	1.71875	0	4.23807299
						epm%						59.445012	40.55499	0	
613	390730	2665392	487	749	8.195	ppm						103.17	85.5		
						epm						2.9102962	1.78125	0	4.691546192

						epm%						62.032773	37.96723	0	
614	391025	2664579	464.9	715	8.16	ppm						104.2	86		
						epm						2.9393512	1.791667	0	4.731017866
						epm%						62.129362	37.87064	0	
615	390870	2664582	443.1	681.5	8.125	ppm						92.3	81		
						epm						2.6036671	1.6875	0	4.291167137
						epm%						60.675034	39.32497	0	
GWP-019	380702	2676523	334		7.3	ppm	31	45	42	8.1		38	32		
						epm	1.34841235	2.245509	3.456079	0.207161	7.257161457	1.0719323	0.666667	0	1.738598966
						epm%	18.5804376	30.94197	47.623014	2.854575		61.654949	38.34505	0	
JH-001	372244	2666247	4790	7150	7.24	ppm	31	45	42	8.1		2000	775	226	
						epm	47.84689	18.71257	11.108825	0.895141	78.56343081	56.417489	16.14583	3.704918	76.26824079
						epm%	60.902241	23.81843	14.139944	1.139386		73.972454	21.1698	4.857747	
JH-002	373020	2665926	5534	8260	7.14	ppm	1100	375	135	35		3000	450	123	
						epm	57.6337538	28.69261	12.343139	1.278772	99.94828023	84.626234	9.375	2.016393	96.01762758
						epm%	57.6635773	28.70746	12.349526	1.279434		88.136144	9.763832	2.100024	
JH-004	372970	2665491		9240	7.17	ppm	1325	575	145	50		2950	500	107	
						epm	57.6337538	28.69261	11.931701	1.278772	99.53684225	83.215797	10.41667	1.754098	95.38656192
						epm%	57.9019311	28.82613	11.987221	1.284723		87.240587	10.92048	1.838937	
JH-005	372456	2666119	3926	5860	7.14	ppm	975	325	140	33		1900	500	182	
						epm	42.4097434	16.21756	11.520263	0.84399	70.99156133	53.596615	10.41667	2.983607	66.99688817
						epm%	59.7391332	22.84436	16.227652	1.188859		79.998663	15.54799	4.453351	
JH-007	372535	2666174	4241	6330	7.34	ppm	1075	325	150	35		2000	625	198	
						epm	46.7594606	16.21756	12.343139	0.895141	76.21530544	56.417489	13.02083	3.245902	72.68422439
						epm%	61.3517985	21.27862	16.195093	1.174489		77.619992	17.91425	4.465758	
JH-008	372277	2666089	4790	7150	7.06	ppm	1200	425	145	40		2500	550	151	
						epm	52.1966072	21.20758	11.931701	1.023018	86.35891125	70.521862	11.45833	2.47541	84.45560495
						epm%	60.4414836	24.55749	13.81641	1.184612		83.501695	13.56729	2.931019	
JH-009	372746	2665997	6867	10250	7.03	ppm	1450	600	200	60		3300	600	122	
						epm	63.0709004	29.94012	16.457519	1.534527	111.003066	93.088858	12.5	2	107.5888575
						epm%	56.8190615	26.97234	14.826184	1.382418		86.522768	11.6183	1.858929	
JH-010	372146	2666131	6398	9550	7.08	ppm	1400	550	175	55		2900	750	154	
						epm	60.8960418	27.44511	14.400329	1.40665	104.1481303	81.80536	15.625	2.52459	99.95494983
						epm%	58.4706049	26.35199	13.826776	1.350624		81.84223	15.63204	2.525728	
199	372504	2674450	13650		7.62	ppm	3637	589.87	396.9	98.34		6747.3	2300	136.6	
						epm	158.199217	29.43463	32.659947	2.51509	222.8088838	190.33286	47.91667	2.239344	240.4888741
						epm%	71.0022035	13.21071	14.658278	1.12881		79.144145	19.92469	0.931163	
200	373063	2671356	13325		7.07	ppm	3522	609.32	425.5	78.32		6052.74	2840	322	
						epm	153.197042	30.40519	35.013372	2.003069	220.6186726	170.7402	59.16667	5.278689	235.1855527
						epm%	69.4397443	13.78178	15.870539	0.907933		72.598081	25.15744	2.244478	
261	378702	2671734				ppm	315	40	50	11		400	270	250	
						epm	13.7016094	1.996008	4.1143798	0.28133	20.09332706	11.283498	5.625	4.098361	21.00685854
						epm%	68.1898491	9.933686	20.476349	1.400116		53.7134	26.77697	19.50963	
297A	363662	2663094				ppm		2400	950	350		21800	2800	55	
						epm	0	119.7605	78.173215	8.951407	206.8851011	614.95063	58.33333	0.901639	674.1856074
						epm%	0	57.88744	37.785812	4.326753		91.213848	8.652415	0.133738	
297B	363665	2663084				ppm	8650	2200	900	350		18400	2700	81	
						epm	376.250544	109.7804	74.058836	8.951407	569.0412251	519.0409	56.25	1.327869	576.6187715
						epm%	66.1200853	19.29218	13.01467	1.573068		90.014569	9.755145	0.230285	
GWD-001-MAQ-EQ	363289	2675713	2944	4330	7.6	ppm						1065		122	
						epm						30.042313	0	2	32.04231312
						epm%						93.758253	0	6.241747	
GWD-001-MARK	364803	2678753	1600	2500	7.4	ppm									
						epm									
						epm%									
GWD-001-SOH	383187	2676240	700	748.5	7.7	ppm		52	50			134.5		48	
						epm	0	2.59481	4.1143798	0	6.709190136	3.7940762	0	0.786885	4.58096141
						epm%	0	38.67546	61.324537	0		82.822705	0	17.17729	
GWD-001-ZAK	365776	2669295	3320	5145.3	7.53	ppm	295	32	37	6		710		128	
						epm	12.8316659	1.596806	3.044641	0.153453	17.62656603	20.028209	0	2.098361	22.1265694
						epm%	72.7973101	9.059089	17.273024	0.870576		90.516557	0	9.483443	
GWD-002-GHAF	389578	2664152	405	633	7.8	ppm	58	18	29	4		156		24	
						epm	2.52283602	0.898204	2.3863403	0.102302	5.909681658	4.4005642	0	0.393443	4.794006798
						epm%	42.6898801	15.19885	40.380183	1.731088					

GWD-002-MARK	364620	2678670	240	375	7.7	ppm									
						epm									
						epm%									
GWD-002-NIAD	376905	2678342	51000	75000	7.3	ppm						25347		2489	
						epm						715.00705	0	40.80328	755.8103309
						epm%						94.601386	0	5.398614	
GWD-002-SAA	398170	2663268	460	719	7.7	ppm	140	103	63	4		71		73	
						epm	6.08960418	5.139721	5.1841185	0.102302	16.51574502	2.0028209	0	1.196721	3.199542186
						epm%	36.8715076	31.12013	31.388947	0.61942		62.597108	0	37.40289	
GWD-002-SHIR	379631	2676782	332	521	8	ppm						89		24	
						epm						2.5105783	0	0.393443	2.904020902
						epm%						86.451798	0	13.5482	
GWD-002-ZAK	365897	2669419	12614	18550	7.4	ppm	412	37	23	4		4313		1318	
						epm	17.9208351	1.846307	1.8926147	0.102302	21.76205901	121.66432	0	21.60656	143.2708733
						epm%	82.348987	8.484066	8.6968549	0.470092		84.919086	0	15.08091	
GWD-002-ZAK	365897	2669419	6970	10250	7.7	ppm						1988		342	
						epm						56.078984	0	5.606557	61.68554186
						epm%						90.911067	0	9.088933	
GWD-003-GHAF	389687	2664042	560	875	7.8	ppm									
						epm									
						epm%									
GWD-003-GHAF	389687	2664042	726	1134	7.8	ppm	126	28	30	50		284		12	
						epm	5.48064376	1.397206	2.4686279	1.278772	10.62524958	8.0112835	0	0.196721	8.208004809
						epm%	51.5813179	13.14986	23.233599	12.03522		97.603299	0	2.396701	
GWD-003-MAQ-EQ	362664	2675296	3005	4420	7.5	ppm						1278		146	
						epm						36.050776	0	2.393443	38.44421836
						epm%						93.774246	0	6.225754	
GWD-003-NIAD	377043	2678350	30464	44800	7.3	ppm						15336		1464	
						epm						432.60931	0	24	456.6093089
						epm%						94.743865	0	5.256135	
GWD-003-SAA	398013	2663564	450	703	7.7	ppm	145	115	101	4		107		12	
						epm	6.30709004	5.738523	8.3110471	0.102302	20.45896189	3.0183357	0	0.196721	3.215056996
						epm%	30.8280062	28.04894	40.623015	0.500034		93.88125	0	6.11875	
GWD-003-SHIR	379979	2676654	371	580	8	ppm						89		24	
						epm						2.5105783	0	0.393443	2.904020902
						epm%						86.451798	0	13.5482	
GWD-003-SOH	383393	2676020	2897	4260	7.5	ppm	448	36	38	4		781		268	
						epm	19.4867334	1.796407	3.1269286	0.102302	24.51237095	22.03103	0	4.393443	26.42447224
						epm%	79.4975459	7.328574	12.756533	0.417348		83.373584	0	16.62642	
GWD-004-GHAF	389819	2664132	2040	3000	7.8	ppm	441	47	46	138		810		164	
						epm	19.1822532	2.345309	3.7852294	3.529412	28.84220368	22.849083	0	2.688525	25.53760781
						epm%	66.5075851	8.131519	13.123926	12.23697		89.472293	0	10.52771	
GWD-004-MEZ	382484	2659872	901	1344	7.8	ppm									
						epm						0	0	0	0
						epm%						#DIV/0!	#DIV/0!	#DIV/0!	
GWD-004-SHIR	380270	2676506	355	555	8	ppm						182		24	
						epm						5.1339915	0	0.393443	5.52743416
						epm%						92.882003	0	7.117997	
GWD-004-ZAK	365763	2669441	5000	7812	7.6	ppm		669	857			2293		415	
						epm	0	33.38323	70.520469	0	103.9037026	64.682652	0	6.803279	71.48593031
						epm%	0	32.12901	67.870988	0		90.483052	0	9.516948	
GWD-005-AMM	376358	2737325	736	1150	7.8	ppm	156	23				213		31	
						epm	6.78555894	1.147705	0	0	7.933263529	6.0084626	0	0.508197	6.516659345
						epm%	85.5330081	14.46699	0	0		92.201576	0	7.798424	
GWD-005-MEZ	382865	2660223	1178	1758	7.8	ppm						241		244	
						epm						6.7983075	0	4	10.79830748
						epm%						62.957158	0	37.04284	
GWD-005-NIAD	376979	2678268	1632	2400	7.5	ppm						488		67	
						epm						13.765867	0	1.098361	14.86422807
						epm%						92.610712	0	7.389288	
GWD-005-SAA	396081	2662683	441	688	7.7	ppm	145	115	151			107		12	
						epm	6.30709004	5.738523	12.425427	0.102302	24.57334165	3.0183357	0	0.196721	3.215056996
						epm%	25.6663914	23.35264	50.564661	0.416312		93.88125	0	6.11875	
GWD-005-ZAK	365779	2669462	5250	8202.5	7.8	ppm		972	722			1598		183	

						epm	0	48.50299	59.411644	0	107.9146377	45.077574	0	3	48.07757405
						epm%	0	44.9457	55.054296	0		93.760084	0	6.239916	
GWD-006-NIAD	377194	2678050	38420	56500	7.3	ppm						19258		1135	
						epm						543.24401	0	18.60656	561.850563
						epm%						96.688344	0	3.311656	
GWD-007-MEZ	383262	2660530	1476	2216	7.65	ppm	458	69	66			568		317	
						epm	19.9217051	3.443114	5.4309813	0	28.79580014	16.022567	0	5.196721	21.21928831
						epm%	69.1826759	11.957	18.860324	0		75.509446	0	24.49055	
GWD-007-NIAD	377297	2678191	17340	25500	7.3	ppm						8698		864	
						epm						245.35966	0	14.16393	259.5235959
						epm%						94.542333	0	5.457667	
GWD-007-SHIR	379594	2676948	1056	1650	7.8	ppm	212	36	51			373		171	
						epm	9.22140061	1.796407	4.1966674	0	15.21447515	10.521862	0	2.803279	13.32514047
						epm%	60.6093902	11.80722	27.583386	0		78.962483	0	21.03752	
GWD-007-ZAK	365669	2669671	3234	4900	7.5	ppm		626	464			791		244	
						epm	0	31.23752	38.181444	0	69.4189691	22.313117	0	4	26.31311707
						epm%	0	44.99854	55.001457	0		84.798456	0	15.20154	
GWD-008-MAS	372416	2686969	6750	10040	7.5	ppm						3124		1342	
						epm						88.124118	0	22	110.1241185
						epm%						80.022542	0	19.97746	
GWD-008-MEZ	383280	2661055	1000	1562	7.8	ppm						245		73	
						epm						6.9111425	0	1.196721	8.107863766
						epm%						85.239992	0	14.76001	
GWD-008-NIAD	377312	2678189	31280	46000	7.3	ppm						15531		1525	
						epm						438.11001	0	25	463.1100141
						epm%						94.601715	0	5.398285	
GWD-008-SHIR	379440	2676905	419	656	7.8	ppm						181		61	
						epm						5.1057828	0	1	6.105782793
						epm%						83.622084	0	16.37792	
GWD-008-ZAK	365705	2669816	2760	4312	7.4	ppm		421	256			799		110	
						epm	0	21.00798	21.065624	0	42.07360839	22.538787	0	1.803279	24.34206571
						epm%	0	49.9315	50.068499	0		92.591924	0	7.408076	
GWD-009-MEZ	383909	2661063	680	1062	7.8	ppm						114		98	
						epm						3.2157969	0	1.606557	4.822354274
						epm%						66.685206	0	33.31479	
GWD-009-SHIR	379318	2676897	473	736	8	ppm						199		61	
						epm						5.6135402	0	1	6.613540197
						epm%						84.879505	0	15.12049	
GWD-009-ZAK	365512	2669779	2040	3000	7.5	ppm						746		43	
						epm						21.043724	0	0.704918	21.74864159
						epm%						96.758795	0	3.241205	
GWD-010-MEZ	383804	2660490	615	961	7.6	ppm						64		183	
						epm						1.8053597	0	3	4.805359661
						epm%						37.569709	0	62.43029	
GWD-010-NIAD	377057	2678333	928	1450	7.8	ppm	147	46				266		37	
						epm	6.39408438	2.295409	0	0	8.689493566	7.5035261	0	0.606557	8.11008347
						epm%	73.5840856	26.41591	0	0		92.520948	0	7.479052	
GWD-010-ZAK	365878	2669951	4719	6940	7.8	ppm						1931		488	
						epm						54.471086	0	8	62.47108604
						epm%						87.194076	0	12.80592	
GWD-011-MAS	372367	2686347	4765	7220	7.7	ppm						2130		915	
						epm						60.084626	0	15	75.08462623
						epm%						80.022542	0	19.97746	
GWD-011-MEZ	384478	2660534	627	980	7.5	ppm		270	98			170		29	
						epm	0	13.47305	8.0641843	0	21.53723822	4.7954866	0	0.47541	5.270896437
						epm%	0	62.55702	37.442982	0		90.980475	0	9.019525	
GWD-011-NIAD	377113	2678171	16660	24500	7.3	ppm						7810		671	
						epm						220.3103	0	11	231.3102962
						epm%						95.244483	0	4.755517	
GWD-011-SHIR	379375	2676540	410	640	8.2	ppm						106		24	
						epm						2.9901269	0	0.393443	3.383569562
						epm%						88.371966	0	11.62803	
GWD-011-ZAK	365636	2670075	3333	5050	7.7	ppm									
						epm						0	0	0	0

						epm%						#DIV/0!	#DIV/0!	#DIV/0!	
GWD-012-SOH	383410	2676203	670	1000	7.8	ppm									
						epm						0	0	0	0
						epm%						#DIV/0!	#DIV/0!	#DIV/0!	
GWD-012-ZAK	365467	2669964	1822	2690	8.2	ppm						490		220	
						epm						13.822285	0	3.606557	17.42884229
						epm%						79.30696	0	20.69304	
GWD-013-MAS	372852	2686139	4488	6800	7.5	ppm									
						epm						0	0	0	0
						epm%						#DIV/0!	#DIV/0!	#DIV/0!	
GWD-013-NIAD	377305	2678029	23800	35000	7.1	ppm						12815		811	
						epm						361.49506	0	13.29508	374.7901454
						epm%						96.45266	0	3.54734	
GWD-013-ZAK	365797	2670185	5440	8000	7.5	ppm									
						epm						0	0	0	0
						epm%						#DIV/0!	#DIV/0!	#DIV/0!	
GWD-014-MAS	373021	2685685	6732	10200	7.5	ppm									
						epm						0	0	0	0
						epm%						#DIV/0!	#DIV/0!	#DIV/0!	
GWD-014-SHIR	379197	2677015	928	1450	7.9	ppm						266		37	
						epm						7.5035261	0	0.606557	8.11008347
						epm%						92.520948	0	7.479052	
GWD-014-ZAK	365624	2669501	2332	3430	7.6	ppm						852		119	
						epm						24.03385	0	1.95082	25.98467017
						epm%						92.492421	0	7.507579	
GWD-015-MAS	373366	2686032	3828	5800	7.5	ppm									
						epm						0	0	0	0
						epm%						#DIV/0!	#DIV/0!	#DIV/0!	
GWD-015-MEZ	383565	2658370	1750	2740	8.1	ppm						639		24	
						epm						18.025388	0	0.393443	18.41883049
						epm%						97.863911	0	2.136089	
GWD-016-MAS	373376	2686726	3412	5170	7.5	ppm									
						epm						0	0	0	0
						epm%						#DIV/0!	#DIV/0!	#DIV/0!	
GWD-016-MEZ	383854	2658383	835	1290	7.7	ppm						213		37	
						epm						6.0084626	0	0.606557	6.61502
						epm%						90.830604	0	9.169396	
GWD-017-MEZ	383691	2658500	860	1343	7.5	ppm						142		36	
						epm						4.0056417	0	0.590164	4.595805683
						epm%						87.15864	0	12.84136	
GWD-017B-SAA	387796	2660355	458	716	7.5	ppm									
						epm						0	0	0	0
						epm%						#DIV/0!	#DIV/0!	#DIV/0!	
GWD-018-MAS	373271	2686944	3379	5120	7.5	ppm									
						epm						0	0	0	0
						epm%						#DIV/0!	#DIV/0!	#DIV/0!	
GWD-018-MEZ	384062	2658484	804	1260	7.6	ppm						181		18	
						epm						5.1057828	0	0.295082	5.40086476
						epm%						94.536394	0	5.463606	
GWD-019-MAS	373223	2687243	2679	3940	7.6	ppm									
						epm						0	0	0	0
						epm%						#DIV/0!	#DIV/0!	#DIV/0!	
GWD-019-MEZ	383740	2658723	752	1175	8.5	ppm						170		36	
						epm						4.7954866	0	0.590164	5.385650535
						epm%						89.041919	0	10.95808	
GWD-019-SHIR	380199	2676216	244	404	8.5	ppm						89		12	
						epm						2.5105783	0	0.196721	2.707299591
						epm%						92.73367	0	7.26633	
GWD-019B-SAA	389002	2660894	461	720	7.8	ppm									
						epm						0	0	0	0
						epm%						#DIV/0!	#DIV/0!	#DIV/0!	
GWD-020-DAI	351319	2670195	3128	4600	7.7	ppm						1015		317	
						epm						28.631876	0	5.196721	33.82859719
						epm%						84.638082	0	15.36192	

GWD-020-MEZ	384007	2658909	924	1444	7.8	ppm						260		24	
						epm						7.3342736	0	0.393443	7.727716248
						epm%						94.908682	0	5.091318	
GWD-020-SHIR	379957	2676362	704	1100	8	ppm						133		61	
						epm						3.751763	0	1	4.751763047
						epm%						78.95518	0	21.04482	
GWD-021-MAS	373697	2686747	1600	2500	7.7	ppm						443		183	
						epm						12.496474	0	3	15.49647391
						epm%						80.640757	0	19.35924	
GWD-021-MEZ	384188	2659198	983	1445	8	ppm						266		37	
						epm						7.5035261	0	0.606557	8.11008347
						epm%						92.520948	0	7.479052	
GWD-021B-SAA	389020	2660354	386	600	7.7	ppm									
						epm						0	0	0	0
						epm%						#DIV/0!	#DIV/0!	#DIV/0!	
GWD-022-MAS	373975	2687090	2618	3850	7.5	ppm						958		109	
						epm						27.023977	0	1.786885	28.81086268
						epm%						93.797877	0	6.202123	
GWD-022-MEZ	384478	2659088	1032	1613	7.7	ppm						266		24	
						epm						7.5035261	0	0.393443	7.896968716
						epm%						95.017802	0	4.982198	
GWD-028-MEZ	384002	2658189	607	949	7.3	ppm		28	54	5		107		49	
						epm	0	1.397206	4.4435301	0.127877	5.968612965	3.0183357	0	0.803279	3.821614373
						epm%	0	23.40922	74.448287	2.142495		78.980645	0	21.01935	
GWD-029-GHAF	390172	2663774	510	797	7.9	ppm									
						epm						0	0	0	0
						epm%						#DIV/0!	#DIV/0!	#DIV/0!	
GWD-029-MAS	374203	2687185	4440	6530	7.7	ppm	393	540	328	8		1598		458	
						epm	17.0943889	26.94611	26.990331	0.204604	71.23543144	45.077574	0	7.508197	52.58577077
						epm%	23.9970314	37.82683	37.888914	0.287222		85.721999	0	14.278	
GWD-029-SHIR	380568	2676542	651	1017	7.8	ppm	141	23	31	5		142		24	
						epm	6.13310135	1.147705	2.5509154	0.127877	9.959598627	4.0056417	0	0.393443	4.399084372
						epm%	61.5798044	11.5236	25.612633	1.28396		91.056261	0	8.943739	
GWD-030-SHIR	380867	2676542	630	985	7.7	ppm	151	23	32	4		142		24	
						epm	6.56807308	1.147705	2.633203	0.102302	10.4512825	4.0056417	0	0.393443	4.399084372
						epm%	62.8446612	10.98147	25.195023	0.978844		91.056261	0	8.943739	
GWD-031-MAS	373172	2685950				ppm									
						epm						0	0	0	0
						epm%						#DIV/0!	#DIV/0!	#DIV/0!	
GWD-031-MAS	373172	2685950	3978	5850	7.7	ppm	1924	173	150	22		1338		529	
						epm	83.6885602	8.632735	12.343139	0.56266	105.2270939	37.7433	0	8.672131	46.41543157
						epm%	79.5313803	8.203909	11.730001	0.53471		81.316276	0	18.68372	
GWD-032-MAS	373350	2685779	4406	6480	7.8	ppm									
						epm						0	0	0	0
						epm%						#DIV/0!	#DIV/0!	#DIV/0!	
GWD-032-SHIR	380758	2676146	815	1274	7.9	ppm						152		122	
						epm						4.2877292	0	2	6.287729196
						epm%						68.192014	0	31.80799	
GWD-033-SHIR	380452	2676028	539	842	8	ppm	140	37	39			155		49	
						epm	6.08960418	1.846307	3.2092162	0	11.14512777	4.3723554	0	0.803279	5.175634119
						epm%	54.6391598	16.56605	28.794791	0		84.479608	0	15.52039	
GWD-034-MAS	372841	2687280	2803	4380	7.5	ppm	225	792	590	6		1022		329	
						epm	9.78686385	39.52096	48.549681	0.153453	98.01095576	28.829337	0	5.393443	34.22277972
						epm%	9.98547946	40.323	49.534953	0.156567		84.240197	0	15.7598	
GWD-034-SHIR	380217	2676398	410	640	8	ppm	66	27	36			142		49	
						epm	2.8708134	1.347305	2.9623534	0	7.180472212	4.0056417	0	0.803279	4.808920437
						epm%	39.9808441	18.76346	41.255691	0		83.29607	0	16.70393	
GWD-035-SHIR	379811	2676738	443	692	7.8	ppm	82	20	29	3		71		24	
						epm	3.56676816	0.998004	2.3863403	0.076726	7.027838754	2.0028209	0	0.393443	2.396263497
						epm%	50.751992	14.20072	33.955535	1.091749		83.580995	0	16.419	
GWD-035-SOH	384361	2676215	253	395	7.7	ppm	8	14	2			78		12	
						epm	0.34797738	0.698603	0.1645752	0	1.211155366	2.2002821	0	0.196721	2.397003399
						epm%	28.7310275	57.68069	13.588281	0		91.793032	0	8.206968	
GWD-036-GHAF	389792	2663780	461	721	7.5	ppm									

						epm						0	0	0	0
						epm%						#DIV/0!	#DIV/0!	#DIV/0!	
GWD-037-SOH	384860	2676176	253	396	7.7	ppm						74		12	
						epm						2.0874471	0	0.196721	2.28416842
						epm%						91.387618	0	8.612382	
GWD-040-SHIR	379732	2676385	360	563	7.9	ppm	43	18	33	2		53		12	
						epm	1.87037843	0.898204	2.7154906	0.051151	5.535223553	1.4950635	0	0.196721	1.691784781
						epm%	33.7904767	16.22705	49.058373	0.924098		88.371966	0	11.62803	
GWD-041-SHUR	373686	2695555	858	3140	7.6	ppm	149	31	36	69		350		36	
						epm	6.48107873	1.546906	2.9623534	1.764706	12.75504423	9.8730606	0	0.590164	10.46322458
						epm%	50.8118876	12.1278	23.224956	13.83536		94.359636	0	5.640364	
GWD-042-SHIR	379699	2676309	870	1360	7.7	ppm	145	96	39	7		85		49	
						epm	6.30709004	4.790419	3.2092162	0.179028	14.48575354	2.3977433	0	0.803279	3.201021989
						epm%	43.5399513	33.06987	22.154292	1.235891		74.905555	0	25.09444	
GWD-052B-SAA	387634	2659904	530	828	7.6	ppm									
						epm						0	0	0	0
						epm%						#DIV/0!	#DIV/0!	#DIV/0!	
GWD-064-GHAF	389273	2663519	392	612	8.6	ppm									
						epm						0	0	0	0
						epm%						#DIV/0!	#DIV/0!	#DIV/0!	
GWD-065-SAA	392372	2661393	742	1160	7.7	ppm	74	42	69	1		195		92	
						epm	3.21879078	2.095808	5.6778441	0.025575	11.01801867	5.5007052	0	1.508197	7.00890194
						epm%	29.2138802	19.02164	51.532351	0.232124		78.481698	0	21.5183	
GWD-066-SAA	392105	2661724	440	688	7.8	ppm									
						epm						0	0	0	0
						epm%						#DIV/0!	#DIV/0!	#DIV/0!	
GWD-068-SAA	391123	2660983	750	1171	7.7	ppm	120	60	56	4		107		31	
						epm	5.21966072	2.994012	4.6081053	0.102302	12.92407982	3.0183357	0	0.508197	3.526532405
						epm%	40.3870975	23.16615	35.655191	0.79156		85.589336	0	14.41066	
GWD-073-GHAF	388872	2664216	520	813	7.5	ppm									
						epm						0	0	0	0
						epm%						#DIV/0!	#DIV/0!	#DIV/0!	
GWD-075-GHAF	388571	2663527	350	547	7.8	ppm						71		79	
						epm						2.0028209	0	1.295082	3.297902842
						epm%						60.730136	0	39.26986	
GWD-106-GHAF	391791	2663312	479	749	8	ppm						114		24	
						epm						3.2157969	0	0.393443	3.60923952
						epm%						89.099016	0	10.90098	
GWD-107-GHAF	391788	2663059	442	692	7.8	ppm						156		98	
						epm						4.4005642	0	1.606557	6.007121552
						epm%						73.255787	0	26.74421	
GWD-108-GHAF	391960	2663168	401	626	7.5	ppm						100		24	
						epm						2.8208745	0	0.393443	3.214317094
						epm%						87.759682	0	12.24032	
GWD-109-GHAF	392195	2662977	471	736	8.5	ppm						440		24	
						epm						12.411848	0	0.393443	12.8052903
						epm%						96.927499	0	3.072501	
GWD-112-GHAF	392024	2663468	956	1493	7.7	ppm						373		73	
						epm						10.521862	0	1.196721	11.71858309
						epm%						89.787833	0	10.21217	
GWD-149-SAA	392066	2662416	481	752	8	ppm						106		24	
						epm						2.9901269	0	0.393443	3.383569562
						epm%						88.371966	0	11.62803	
GWD-149-SAA	392066	2662416	598	934	7.8	ppm	99	29	46	0		128		73	
						epm	4.3062201	1.447106	3.7852294	0	9.538555261	3.6107193	0	1.196721	4.807440634
						epm%	45.1454123	15.17112	39.683466	0		75.106894	0	24.89311	

ARABIC SUMMARY

ملخص الرسالة

دراسات هيدروجيولوجية وجيوفيزيقية على سهل الجاو- منطقة العين - دولة الإمارات العربية المتحدة

لقد شهدت دولة الإمارات العربية المتحدة فى العقود الأخيرة عمليات تنمية وتطورات واسعة النطاق شملت مناحى عديدة لجوانب الحياة، وتمثل عمليات التنمية السريعة ضغوطا على المصادر الطبيعية و تعتبر المياه فى الطليعة لأى عملية تطور وتنمية. وبالرغم من أن دولة الإمارات العربية المتحدة هى إحدى الدول الواقعة ضمن المناطق القاحلة والتى تتميز بندرة الأمطار وعدم إنتظامها الأمر الذى يهدد تغذية المياه الجوفية إلا أن معدل إستهلاك الشخص للمياه فى دولة الإمارات العربية المتحدة يعتبر من أعلى المعدلات إستهلاكا فى العالم.

وتعتمد دولة الإمارات العربية المتحدة لسد حاجياتها من المياه على مصادر مائية تقليدية ومصادر غير تقليدية. وتعتبر المياه الجوفية واحدة من أهم المصادر المائية التقليدية فى دولة الإمارات العربية المتحدة بوجه عام وفى مدينة العين بوجه خاص.

وتركز هذه الدراسة على منطقة **سهل الجاو** والذى يقع شرق مدينة العين ويحده من الشرق سلسلة جبال عمان ومن الغرب جبل حفيت ويعتبر سهل الجاو من أهم السهول بمدينة العين وتبلغ مساحته حوالى 500 كم^2 .

يعتبر المدى الحيزى والخواص البتروفيزيائية لخزان عصر الرباعى **Quaternary** وكذلك ظروف طبقة الأساس **Bedrock** التى تقع أسفل الخزان الجوفى من العوامل التى تحكم تخزين وحركة المياه الجوفية لذلك فإن المعلومات عن وضع الخزان وإمتداده والمعاملات البتروفيزيائية للخزان وهيدروجيولوجية الخزان وكذلك شبكات أحواض التصريف تعتبر من الأهمية بمكان لفهم نظام سريان المياه وآلية تغذية الخزان وظروف النظام الهيدروجيولوجى.

ولقد كرست هذه الدراسة لإمكانية تواجد المياه ومعرفة نوعيتها وكذلك تعريف المعاملات الهيدروجيولوجية لخزان عصر الرباعى بمنطقة سهل الجاو وتم ذلك من خلال إجراء دراسات هيدروجيولوجية وهيدروكيميائية وإستخدام تقنيات جيوفيزيقية شملت إستخدام طريقة المقاومة الكهربية والطريقة الكهرومغناطسية وبيانات تسجيلات الآبار.

<u>وتتلخص نتائج هذه الدراسة فى عمل تقييم كمى وكيفى لمصادر المياه الجوفية فى منطقة سهل الجاو، توصلت هذه الدراسة إلى مايلى :</u>

1- أن خزان عصر الرباعى بمنطقة سهل الجاو يتميز بسمك صغير نسبيا من صفر متر فى بعض الأماكن خاصة فى أماكن الجبال، بينما يصل إلى 100 متر فى بعض الاماكن الأخرى وهو يتكون من رواسب مختلفة مختلطه بحطام صخرى منحدر من الجبال المحيطة بسهل الجاو.

2- تتم تغذية الخزان بصفة أساسية من الأمطار التى تهطل على سلسلة جبال عمان وجبل حفيت.

3- أن الوضع الهيدروجيولوجى لهذا الخزان متأثر بالوضع التركيبى لمنطقة سهل الجاو حيث يسود فى منطقة سهل الجاو الطيات والفوالق العكسية الدافعة **Thrust Faults**.

4- نظام سريان المياه الجوفية عموما يكون من الشرق إلى الغرب إلا أن هذا النظام قد يحيد فى بعض الأماكن نتيجة وجود بعض الحواجز التحت السطحية كما أظهرت النتائج فى المنطقة الواقعة شرق جبل حفيت.

5- الخرائط الكنتورية التى تم رسمها لمناسيب المياه الجوفية للفترات من عام 1995 وحتى 2002 أوضحت إنخفاض ملحوظ فى مناسيب المياه الجوفية بسبب قلة سقوط الأمطار فى هذه الفترات فضلا عن زيادة معدل السحب من الخزان.

6- كمية الأملاح الكلية الذائبة تزداد قيمتها من الشرق للغرب مع زيادة ملحوظة حول المناطق القريبه من جبل حفيت والتى أعزيت لتدفق المياه شديدة الملوحة من الطبقات التى تقع أسفل خزان الرباعى خلال الكسور التى تعترى طبقات الحجر الجيرى المكونة لجبل حفيت وكذلك وجود السبخات غرب جبل حفيت خاصة وأن مناسيب المياه الجوفية قريبة من السطح فى هذه الأماكن.

7- نتائج المسوحات الجيوفيزيقية أوضحت الوضع الطبقى والتركيبى لمنطقة سهل الجاو والتى لها إنعكاسات مباشرة على الوضع الهيدروجيولوجى لخزان العصر الرباعى. كما أوضحت نتائج الدراسات الكهرومغناطسية تحديد مواقع القنوات القديمة المدفونة والتى تمثل أماكن مناسبة لحفر الآبار للحصول على مياه ذات نوعية جيده حيث يكون فى مجارى هذه القنوات سمك الرواسب كبير وذات مسامية ونفاذية عالية. كذلك بإستخدام بيانات تسجيلات الآبار أمكن تحديد النطاقات ذات المسامية العالية والتى يجب أخذها فى الإعتبار عند تصميم الآبار للإنتاج وكذلك تحديد طبقة الأساس التى تقع أسفل الخزان الرباعى فى منطقة سهل الجاو.

جامعة الإمارات العربية المتحدة
عمـــادة الدراســات العليــا

عنوان الرسالة

دراسات هيدروجيولوجية و جيوفيزيقية على سهل الجاو- منطقة العين دولة لإمارات العربية المتحدة

اسم الباحث

هند سيف النعيمى

المشرفون

م	الاسم	الوظيفة
1	د. أحمد السيد المحمودي	أستاذ الجيوفيزياء المشارك بقسم الجيولوجيا- كلية العلوم- جامعة الإمارات العربية المتحدة
2	أ.د. محسن شريف	أستاذ موارد المياه - كلية الهندسة- جامعة الإمارات العربية المتحدة
3	د. طارق غازى الزبط	أستاذ مساعد الهيدروجيولوجى بقسم الجيولوجيا- كلية العلوم- جامعة الإمارات العربية المتحدة

جامعة الإمارات العربية المتحدة
عمـــــادة الدراســـات العليـــا

دراسات هيدروجيولوجية وجيوفيزيقية على سهل الجاو- منطقة العين-دولة لإمارات العربية المتحدة

إعداد
هند سيف النعيمى

رساله مقدمة إلى
عمادة الدراســـات العليا
جامعة الإمارات العربية المتحدة

لإستكمال متطلبات الحصول على درجة الماجستير فى العلوم فى موارد المياه

عمادة الدراســـات العليا
جامعة الإمارات العربية المتحدة
يونيو 2003